Electric jet assisted production of micro and nano-scale particles as drug delivery carriers

A thesis submitted in partial fulfilment of the requirements for the degree of

Doctor of Philosophy

By

Marjan Enayati

Department of Mechanical Engineering

University College London

Torrington Place, London WC1E 7JE

U.K

September, 2011

Declaration

I, Marjan Enayati, confirm that the work presented in this thesis is my own. Where information has been derived from other sources, I confirm that this has been indicated in the thesis.

………………………………..

Marjan Enayati

Abstract

In this thesis, the capability of the electrohydrodynamic atomization (EHDA) process for preparing drug delivery carriers consisting of biodegradable polymeric particles with different sizes and shapes was explored. The first part of the thesis describes a detailed investigation of how the size, morphology and shape of the particles generated can be controlled through the operating parameters; specifically the flow rate, applied voltage and the properties of the solutions. Diameter and shape of the particles were greatly influenced by viscosity and applied voltage. The mean size of the particles changed from 340 nm to 4.4 μm as the viscosity increased from 2.5 mPa s to 11 mPa s. Also, using more concentrated polymer solution (30 wt%) and higher applied voltage (above 14 kV) were found to be ideal for promoting chain entanglement and shape transition from spherical to oblong to a more needle-like shape. Estradiol-loaded micro and nanoparticles were produced with mean sizes ranging from 100 nm to 4.5 μm with an encapsulation efficiency ranging between 65% to 75%. The *in vitro* drug release profiles of the particles started with an initial short burst phase and followed by a longer period characterised by a lower release rate. Two strategies were developed to tailor these profiles. First, ultrasound was explored as a non-invasive method to stimulate "on demand" drug release from carrier particles. Systematic investigations were carried out to determine the effect of various ultrasound exposure parameters on the release rate in particular output power, duty cycle and exposure time. These three exposure parameters were seen to have a significant enhancing effect upon the drug release rate (up to 14%). The second strategy explored was coating the surface of the particles with chitosan and gelatin. This enabled control and reduction of the prominence 'burst release' phase without affecting other parts of the release profile. Coating the particle surface with 1 wt% chitosan solution considerably reduces the initial release by 62%, 60% and 42% for PLGA 2 wt%, 5 wt% and 10 wt%, respectivly in the first 72 hours This work demonstrates a powerful method of generating micro and nano drug-loaded polymeric particles, with modified release behaviour and with control over the initial release.

Publications

Refereed Journal Papers

- M. Enayati, Z. Ahmad, E. Stride, M. Edirisinghe, (2009), One-step electrohydrodynamic production of drug-loaded micro- and nanoparticles, J. *R. Soc. Interface*, **7**(45), 667–675.

- M. Enayati, Z. Ahmad, E. Stride, M. Edirisinghe, (2009), Preparation of Polymeric Carriers for Drug Delivery with Different Shape and Size Using an Electric Jet, *Curr Pharm Biotechnol*, **10** (6), 600-608.

- M. Enayati, Z. Ahmad, E. Stride, M. Edirisinghe, (2010), Size mapping of electric field-assisted production of polycaprolactone particles. *J. R. Soc. Interface.,* **7** (4), S393-S402.

- Enayati M., Chang M.W., Bragman F., Edirisinghe M., Stride E., (2011), Electrohydrodynamic Preparation of Particles, Capsules and Bubbles for Biomedical Engineering Applications. *Colloid. Surface. A.,* **382** (1-3), 154-164.

- M. Enayati, E. Stride, M. Edirisinghe, W. Bonfield, (2011), Modification of the release characteristics of estradiol encapsulated in PLGA particles, (in preparation).

- M. Enayati, D. Al Mohazey, M. Edirisinghe, E. Stride, (2011), Stimulated release of estradiol from polymeric micro- and nano-particles using low frequency ultrasound, (in preparation).

Conference Presentations

- M. Enayati, Z. Ahmad, E. Stride, M. Edirisinghe, (2009), Electric jet-assisted generation of polymeric drug carriers with different shape and size, PhD forum, Department of Mechanical engineering, UCL, London,UK.

- M. Enayati, Z. Ahmad, E. Stride, M. Edirisinghe. Fabrication of micro- and nano-scale estradiol-loaded particles via co-axial electrohydrodynamic processing, International Conference on Drug Discovery and Therapy, Dubai, UAE, (2010).

- M. Enayati, Z. Ahmad, E. Stride, M. Edirisinghe. Fabrication of biodegradable polymeric drug delivery carrier via electrohydrodynamic atomization process, PhD Forum, Department of Mechanical Engineering, UCL, London, UK, (2010).

Participating in symposia

- Encapsulation for drug delivery and Microbubbling, University College London, UK, June 2008.

- Bubbles and Encapsulation, University College London, UK, April 2010.

Acknowledgements

At the very outset my wholehearted thanks goes to my supervisor Professor Mohan Edirisinghe for first of all accepting me under his wings as a research student at UCL and then for his continuous guidance, constructive criticism, confidence building and valuable support during the period of my study. I am delighted to have realised my ambition of doing this research under his mentorship.

My thanks are equally due to my second supervisor Dr. Eleanor Stride for her trust, guidance, advice and great support throughout this research work. She is extremely patient, and always enthusiastic to teach, and listen to my views. I feel extremely privileged to be jointly supervised by Prof. Edirisinghe and Dr. Stride. I also like to thank UCL (UK) for their funding assistance in carrying out this research study.

Continuous and invaluable support provided by my colleagues, Ms. Chaojie. Luo, Ms. Zeynep Ekemen, Mr. Bhairav. Patel, Mr. Ming-wei. Chang, Ms. Maryam Parhizkar, Dr. Muhammad-Rafique Nangrejo and Dr. Zeeshan Ahmad, is unforgettable and many thanks to them. The lovely memories I have with these peoples will always be cherished. My dream of doing this research study wouldn't have been possible if not for the unparallelled understanding, love and support extended to me and my family.

Last but not least, I would like to give a special thank to my parents, Mr. Hedayat Enayati and Mrs Nahid Lotfizadeh, and my lovely sister, Ms Maryam Enayati for their love, belief, support and help in the past years, without which I would not be brave enough to face this challenge in my life.

Without these important people in my life, I cannot have these achievements.

Thank you all.

DEDICATION

To

My Parents;

Hedayat and Nahid

And

my lovely sister; Maryam

for their sacrifices and supports during the time of this research

Table of Contents

Chapter 1

Introduction and Background

Chapter 3

Experimental details

Chapter 4

Results and discussion

Chapter 6

Conclusions and future work

List of figures

List of tables

Glossary of abbreviations

ABS	Absorbance
BSA	Bovine serum albumin
CEHDA	Co-axial electrohydrodynamic atomization
CD	Collecting distance
DMAC	Dimethylacetamide
DC	Duty cycle
EHDA	Electrohydrodynamic atomization
EAP	Electrostatic atomization printing
ELPs	Elastin-like polypeptides
EB	Evans blue
EA	Ethyl acetate
FDA	Food and Drug Administration
FIB	Focused Ion beam microscopy
FTIR	Fourier Transform Infrared
IM	Intramuscular
IV	Intravenous
M_n	Molecular weight
MAbs	Monoclonal antibodies
NC	Nanocrystals
O/W	Oil-in-water
PI	Polydispersivity index
PLA	Poly (lactic acid)
PGA	Poly (glycolic acid)
PCL	Poly (ε-caprolactone)
PLGA	Poly (lactic acid-co-glycolid acid)
PFH	Perfluorohexane

PDLA	poly-D-lactic acid
PLLA	poly-L-lactic acid
PMSQ	Polymethylsilsesquioxane
SEM	Scanning electron microscopy
SC	subcutaneous
TPP	tripolyphosphate
SBF	simulated body fluid
W/O/W	water-in-oil-in-water
W/O	water-in-oil

Chapter 1

Introduction and Background

1.1 Background

The first microencapsulation procedure was published by Bungenburg de Jong and Kaas1 in 1931 which deals with the preparation of gelatin microspheres [Bungenburg de Jong and Kaas 1931]. In the late 1940s and 1950s, Green *et al.* of National Cash register Co., Dayton, Ohio, developed a microencapsulated dye for the manufacture of carbonless copying paper which eventually lead to several patents and made microencapsulation more common [US Pat. 2712507, US Patent 2800457]. Since then, and particularly since the mid 1970s, microencapsulation has become more and more popular in the pharmaceutical industry as well as for many other products and processes in daily use. Encapsulated products now available include liquid crystals, adhesives, perfumes and fragrances, cosmetics, insecticides, algaecides, fertilizers, washing powders, animal feed stocks, tissue mimicking materials , medicinal products, insulation materials, etc [Arshady 1990, Schmidt and Roessling 2006]. Such particles normally have diameters between 50 nm and 1 mm with a solid, liquid, or gaseous core. The wall material can be made from polymers, surfactants, glasses, oxide ceramics, mixed oxides or even metals [Bertling *et al.* 2004, Gaponik *et al.* 2004]. The main motivating factors for encapsulation are as follows: taste and odor masking, separation of incompatible components, protection from immediate environment, modification of impact strength, alteration of colloidal and surface properties, prolonged action or sustained release, targeted release, improved biocompatibility [Arshady 1989].

In medical and pharmaceutical applications, there is rapidly growing interest in the use of particles as drug delivery systems and in the synthesis of artificial cell structures [Bertling *et al.* 2004, Botchwey *et al.* 2004]. Both micro and nano particles are used therapeutically. For example, particles loaded with an entrapped therapeutic agent can transport the substance through blood vessels and release their load at a target site [Panyam and Labhasetwar 2003]. The preparation of effective drug delivery systems, however, still represents a significant on-going challenge in medicine [Mathiowitz *et al.* 1997]. The goal in designing an ideal drug carrier is to obtain sustained and controlled release which can decrease the fluctuation and variation of drug dosage and keep drug concentration constant over the designated treatment period to maximise the effectiveness of the therapeutic agent [Luan *et al.* 2006, Yang *et al.* 2001]. In particular, the aims in designing a drug delivery system are to minimize drug degradation and loss, to prevent harmful side-effects and to maximise drug bioavailability and the percentage of the drug accumulated in the required zone. Therefore, various preparation techniques have been studied with a view to generating drug carriers or vehicles which can be tailored to achieve these aims [Freitas *et al.* 2005, Yang *et al.* 2001].

Techniques used to produce micro- and nano-particles of different sizes for biological uses, include single and double emulsification, phase separation, spray drying, coacervation, and electrohydrodynamic atomization (EHDA) [Mitragotri and Lahann 2009]. Several of these methods suffer from the fact that protein denaturation and unsteadiness during encapsulation and release process may occur. For example, the double emulsion method involves exposing the active pharmaceutical ingredients to organic solvents, high shear stresses, and aqueous-organic interfaces. Spray drying requires high temperatures and is thus not suitable for highly thermally sensitive materials. Furthermore, particle size cannot be easily controlled using this technique. In the coacervation method, residual solvents and coacervating agents can cause frequent damage to the coacervation. Of these techniques, EHDA has recently attracted the attention of many researchers for generating drug delivery vehicles. It is an attractive process based on the formation, control and breaking up of jet under the influence of a high electrical field. The process involved in this technique is referred to by a number of different terms in the

literature. In this thesis, 'EHDA' processing or 'electrospraying' will be used. In this method a single needle or a co-axial series of needles can be used. In the latter, two different liquids or suspensions are pumped through two concentrically aligned needles, which are subjected to an applied voltage. The co-flowing liquids are capable of experiencing various modes of atomization. Among these modes, the 'cone jet' mode is normally the most desirable mode. In this mode, the liquid(s) issuing from the capillary are in the form of a regular, axisymmetric cone with a thin jet at its apex. The jet can break-up eventually which results in near monodisperse compound particles with the outer material surrounding or encapsulating the inner one. This phenomenon has particular importance for encapsulation of targeted drug delivery and material processing [Loscertales *et al.* 2002]. The EHDA method has many advantageous over conventional methods, which are discussed below:

• It is a method capable of producing fine and near monodisperse particles. Monodisperse particles have the advantage of possessing more regular and predictable drug release profiles.

• Particles are produced at ambient temperature and pressure, and without the need for additives other than normal polymer solvents, thus overcoming the problems associated with defunctionalisation of drugs under harsh processing conditions.

• It is a technique that can be scaled up easily for mass production with multiple electrospraying needles being used in parallel or if it is miniaturised into a portable device for *in situ* particle fabrication [Deng *et al.* 2006 and Regele *et al.* 2002].

• This method is very flexible and different surfactants can be added to adjust the encapsulation efficiency (EE) and to control the release profile.

• It is a cost-effective and convenient method which provides a means of directly encapsulating a drug inside a polymeric carrier of pre-determined size in a single step, unlike many existing methods which require two or more steps to achieve an encapsulated product.

• The EHDA process can be halted at anytime simply to check the quality of the produced particles. Whereas, single and double emulsification methods are multi-steps methods, therefore, all steps of the fabrication should be completed in order to be able to check quality of the production. The option of terminating the process at anytime to check the quality and characteristic of the fabricated particles is often very desirable.

• The electrosprayed solution could be a mixed solution, an emulsion, even a solid particle dispersion. Also, during the fabrication process different polymers can be employed.

The above-mentioned advantages make EHDA an attractive method for the production of drug delivery vehicles.

Biodegradability is another key feature of drug delivery devices [Burton *et al.* 2000]. The elimination of an inactive material by a natural process is preferred over surgical removal of a drug delivery system, which may leave non-degradable foreign debris in the body for an indefinite period of time. Biodegradable polymeric materials are the most promising materials that can be used for encapsulating drugs in developing drug delivery systems (DDS) for sustained and controlled release of drugs. These DDS are used to provide a predetermined amount of drug at an appropriate time and at a targeted site over the duration of several minutes to several years [Kawaguchi 2000, Pareta and Edirisinghe 2006]. There are several types of biodegradable polymers but only relatively few have been approved by the US Food and Drug

Administration [Sinha and Trehan 2003]. Amongst them are polycaprolactone (PCL), poly (L-lactic acid) and poly (DL-lactic acid) (PLA), poly(glycolic acid) (PGA), and their copolymers such as poly(DL-lactic-co-glycolic acid) (PLGA). PLGA is a good candidate as a biodegradable and biocompatible polymer. It degrades via hydrolysis in the body and produces the monomers, lactic acid and glycolic acid. These two monomers are by-products of different metabolic pathways in various bio-processes under normal physiological conditions. PLGA has been used to fabricate micro- and nano-scale particles for controlled release systems [Okada and Toguchi 1995]. PCL also degrades via hydrolysis at its ester linkages under physiological conditions in the human body [Armani and Liu 2000].

The drug release characteristics of polymeric carriers encapsulating various hydrophobic drugs have been studied [Avgoustakis 2004]. However, there have been relatively few attempts to modulate and manipulate the drug release profile. There are two features of a polymeric drug delivery system which require particular attention. First, eliminating or controlling the initial undesirable 'burst release' phase. This is the rapid release of drug during the first 24 hours after administration, which typically accounts for 20 to 80% loss of the total encapsulated drug. Second, the ability to modify the release profile *in situ*, e.g. in order to achieve pulsatile release. One method for achieving this type of profile is control drug release through external stimuli, for example exposure to light, electrical or magnetic fields or ultrasound.

Ultrasound has many applications in medicine. Its most common one is in diagnostic imaging [Moore and Promes 2004]. However, there are other more recent applications relating to drug delivery and stimulating drug release processes [Mitragotri *et al.* 1995]. In ultrasonically stimulated systems, ultrasonic waves increase the degradation of the polymeric carrier so stimulating the drug release. For instance, in a study by Miyazaki *et al.*, it was found that using ultrasound in an insulin loaded ethylenevinyl alcohol copolymer system, caused a sharp drop in blood glucose levels right after ultrasonic waves were administered [Miyazaki *et al.* 1988].

Drug delivery systems are an intricate system from the vehicles where the drugs are entrapped to the way the drug is released into its physiological environment. Developing such a system requires certain objectives to be able to produce a product that can delivery controllable release of drugs, which are mentioned in the next section.

1.2 Objectives of the research
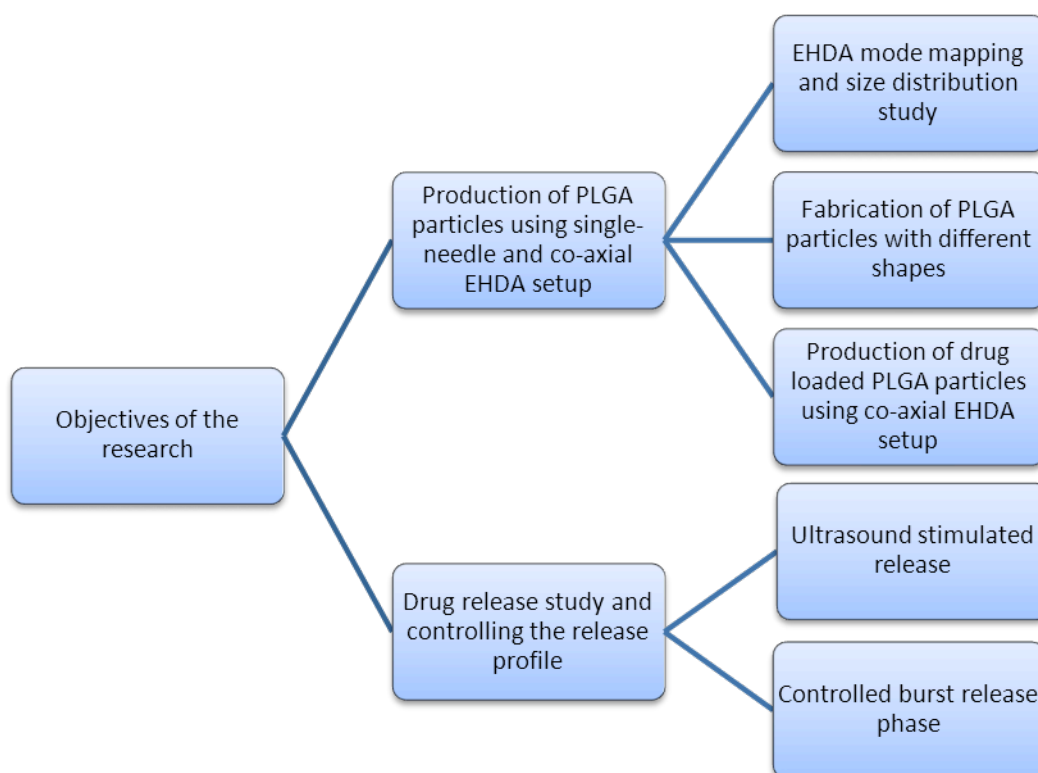
Figure 1.1 Objectives of the research presented in this thesis

The flow chart in **Fig. 1.1** sets out the key objectives of this study. The detail of each objective is discussed below.

1.2.1 Production of PLGA particles using single-needle and co-axial EHDA setup

The **first main objective** of this work was to demonstrate whether single-needle and co-axial electrohydrodynamic processing could successfully produce polymeric nanometre and micrometre scale particles via a single step process which provides

control over particle size, size distribution and shape under ambient conditions. To meet this objective, several studies were necessary which were arranged into different stages as follows:

1.2.1.1 EHDA mode mapping and size distribution study

The first aim was to investigate the fundamentals of single-needle EHDA processing for the preparation of polymeric carriers. It was determined how the size and size distribution of the particles generated can be systematically controlled through the range of operating parameters: polymer solution flow rate, applied voltage and the inherent properties of the solution such as viscosity and electrical conductivity during particle generation. It was shown how changes in these parameters affect the mode of jetting and the desirable stable 'cone-jet' mode window. In this part of investigation, the biodegradable polymer polycaprolactone was used and a particle range of 300 nm – 4.5 μm in diameter were prepared. After these extensive studies the ideal set of processing parameters for obtaining PCL particles with different size ranges were determined.

1.2.1.2 Fabrication of PLGA particles with different shapes

The second aim was to find a simple method for generating PLGA and PCL biodegradable particles with both different sizes and shapes based on EHDA processing. Most work on drug-delivery carriers has focused on spherical particles because size has been considered to be the most significant, if not the only parameter of interest. In addition, non-spherical particles have often proved difficult to fabricate. However, there is increasing evidence that particle shape may play a significant role in the effectiveness of drug delivery and other biomedical interventions, for example shape-related phagocytosis by macrophages [Champion and Mitragotri 2006] and the rate of cellular internalisation of particles based on their shape [Gratton *et al.* 2007]. Thus, further understanding the shape related phenomena is essential for enhancing future prospects. This requires examination of the potential of non-spherical particles as suitable carriers for drug delivery and in order to do this, more convenient preparation methods are essential. A second aspect of this part of the research was to demonstrate that the length and width of the non

spherical particles and hence the aspect ratio can be controlled to reduce the particle shape from the micro to the nano scale.

1.2.1.3 Production of drug loaded PLGA particles using co-axial EHDA setup

Production of particles and capsules with a narrow size distribution is of tremendous interest in biomedical engineering [Zhu *et al.* 2000, Kissel *et al.* 1995, Vonarbourg *et al.* 2009]. In particular, research into the encapsulation of various therapeutic materials by efficient methods is important for the preparation of advanced particles with different cores, targeting behaviour, and release profiles [Luan *et al.* 2006]. Since the single needle EHDA process has been shown to be a promising technique for fabricating drug delivery carriers with a given size and size distribution, the next objective was to encapsulate a therapeutic material into the PLGA polymeric particles via co-axial EHDA processing.

To fulfil these objectives, first, evans blue dye was chosen as a model encapsulated material, to show the feasibility of the encapsulation process. In the next step, a real drug, estradiol, was used instead of evans blue dye as the encapsulated agent. The structure and size of these drug-loaded PLGA particles were also characterised. This study confirmed that EHDA co-axial processing has considerable potential as a technique for producing drug-loaded particles.

1.2.2 Drug release study and controlling the release profile

As discussed before, the first main objective was the fabrication of polymeric drug loaded carriers via both single and co-axial EHDA processing. **The second main objective** was an in-depth study of the release profiles for these carriers and the effect of different parameters on the release characteristics, which have not been well documented in previous EHDA studies. The overall aim was to achieve a regulated and controllable drug release profile.

1.2.2.1 Ultrasound stimulated release

The **final objective** was to tailor and control the drug release profiles. In one set of experiments, ultrasound was used to stimulate *in vitro* drug release. Ultrasound responsive drug delivery systems have great potential for applications requiring stimulated release *in vivo* with a high degree of control over spatial and temporal location. Systematic investigations were carried out to determine the effect of various ultrasound exposure parameters, in particular: output power, duty cycle and exposure time, on the release rate of a model drug (estradiol), encapsulated in PLGA particles of different sizes prepared using EHDA.

1.2.2.2 Controlled burst release phase

In another set of experiments, the aim was to control the 'burst release' phase of the drug release profiles. Burst release is a very fast release phase during the first day of release typically accounting for 20 to 80% loss of the total drug which can cause many severe toxicity effects. This reduces the effective lifetime of the therapeutic system. Therefore, an optimized coating technique was used to tailor the *in vitro* drug release profiles for a system of PLGA particles encapsulating the hydrophobic drug, estradiol. It was shown that coating the particles with different materials can significantly reduce the initial burst without affecting the subsquent parts of the release profile. This part of work demonstrates a powerful method of generating drug-loaded polymeric particles, with modified release behaviour with a controlled burst release phase. The surface modified particles have great application in controlled therapeutic delivery systems with less undesirable side effects and the reducing potential loss of drug during the initial lifecycle of the vehicle.

1.3 The structure of the thesis

The organisation of this thesis is given in this section. This **Chapter 1** provides background information about the research project and gives an overview about the basics of electrohydrodynamic atomization and other related techniques that are used for micro and nano encapsulation. The objectives of the research are stated and the organisation of this thesis and scope of the research outlined.

Chapter 2 presents a detailed literature survey. Since the aim of the research is to prepare micro and nano particles through EHDA to be used as drug delivery vehicles, an extensive collection of literature has been surveyed to understand the principles of electrohydrodynamic atomization, the procedure and its uses, as well as the materials and the methods used for the preparation of polymeric particles. Also, a literature survey has been presented on micro and nano particulate drug delivery systems and conventional encapsulation methods in comparison with the electrohydrodynamic atomization.

Chapter 3 describes the experimental setup, materials used, experiments and characterisation procedures carried out, and a detailed description of the experimental tools employed.

In **Chapter 4**, results obtained during the experiment using single needle and co-axial EHDA processing are discussed in conjunction with existing literature. This chapter is split into three sections; in **Section 4.1**, PCL solutions with different concentrations were used to show the feasibility of fabrication of polymeric particles via EHDA. Different modes of EHDA processing were studied and classified. The effect of different parameters such as; applied voltage, flow rate, viscosity and drug loading were studied on size, size distribution, polydispersivity index and morphology of the PCL particles.

In **Section 4.2**; a method to fabricate PLGA and PCL drug carriers with different shapes and sizes was established. The effect of different parameters, such as collecting distance, on the morphology, size and size distribution of the PLGA particles was studied. The next part of the chapter was concerned with the fabrication of non-spherical PCL particles using a viscous solution and investigating the effect of polymer concentration, applied voltage and flow rate on the shape and size of the particles.

Section 4.3 discusses how co-axial electrohydrodynamic atomization can be used for encapsulating a second material inside the polymeric matrix with a controlled mean size and size distribution. The production of evans blue and estradiol loaded PLGA particles of various sizes was investigated.

Chapter 5 studies the release profiles of the drug loaded PLGA particles and discusses how to tailor and control the release profiles. This chapter has three sections. **Section 5.1** focuses on the *in vitro* release study via two techniques, the colorimetric and the UV spectroscopy methods. The next parts of the chapter are focused on tailoring and controlling the drug release profiles. A detailed description is given in **Section 5.2** about the ultrasound stimulated drug release from PLGA nano and micro particles. An extensive study was conducted to determine the effect of various ultrasound parameters such as out-put power, duty cycle and ultrasound timing on the release profile and on microstructure and biodegradation of the particles. **Section 5.3** discusses the charactecterisation and modification of the release pattern of estradiol from PLGA micro and nano particles with improved initial release characterisation. A coating technique was used to tailor the *in vitro* drug release profiles for a system of PLGA particles encapsulating a hydrophobic drug, estradiol. The three most important factors affecting drug release were identified as: particle size, type and concentration of the coating agent.

Chapter 6 is divided into two sections. **Section 6.1** summarizes the experimental results and presents the conclusions of the work. **Section 6.2** discusses some recommendations for future work, employing EHDA processing and beyond, to continue the research presented in this thesis in new directions. Finally, the literature referred to throughout the thesis is listed in the **References** section.

Chapter 2

Literature review

2. 1 Introduction

The objective underlying the research described in this thesis is to investigate electrohydrodynamic atomization as a technique for preparing micro and nano particles that can satisfy the requirements for particles that are used primarily in medical engineering, targeted drug delivery and controlled released systems.

In order to fulfil this objective, first the relevant literature will be reviewed as follows:

- **Fundamental concepts of drug delivery systems, routes of drug delivery and the mechanism of drug release:** the goals of drug delivery systems, various routes of drug administration and the mechanisms that control the drug release including degradation and erosion of the polymeric carrier are presented. Furthermore, a detailed description of various particulate drug carriers with different structures will be given.

- **Techniques for polymeric particle preparation:** different methods for the fabrication of drug loaded polymeric carriers such as: emulsion-solvent evaporation, coaccervation phase separation and spray drying are discussed and they are compared with electrohydrodynamic atomization processing which is used in this study.

- **Electrohydrodynamic atomization processing:** previous work on the processing methods based on electrohydrodynamic atomization (EHDA) and the theory of this processing technique are reviewed. Various modes of electrohydrodynamic atomization and all the parameters such as processing parameters (applied voltage and flow rate) and liquid properties (surface tension, viscosity, electrical conductivity, relative permittivity and density) involved in this process is well explained. Also, the application of single needle and co-axial electrohydrodynamic atomization method in preparation of various drug carriers such as particles, capsules, aerosols, porous structures and microbubbles, are reviewed in order to understand how these techniques offer opportunities for further research.

- **Polymer based drug delivery systems:** polymers have been extensively used for the preparation of drug delivery carriers. In this section, a detailed examination of synthetic polymers such as poly (lactic acid) (PLA), poly (glycolic acid) (PGA), poly (ε-caprolactone) (PCL) and poly (lactic acid-co-glycolid acid) (PLGA) will be made.

- **Controlling the drug release profile:** the ultimate aim in a drug delivery system is to have a regulated release profile from the drug loaded carrier. In this study, two approaches were investigated to fulfil this aim including ultrasound stimulated drug release and controlling the burst release phase using a coating technique. Ultrasound responsive drug delivery systems have great potential for applications requiring stimulated release *in vivo* with a high degree of control over spatial and temporal location. The role of ultrasound in biomedical engineering especially in drug delivery and drug release will be explained. In the last part of this chapter previous studies on the effects of burst release in drug delivery, the mechanism of the initial release and the control of this phenomenon were reviewed.

2.2 The drug delivery concept and goal of drug delivery systems

Successful therapy with any agent requires the drug to reach the site of action in adequate amounts and over an appropriate length of time. The aim of many controlled drug delivery systems is to have a delivery profile that will yield a high drug concentration level in the blood over a long period of time. An effective drug delivery system must thus: a) allow the drug to be released in the correct place, in the correct quantity, and in the correct time window, i.e. demonstrate appropriate "bioavailability" and/or b) minimise adverse reactions or side-effects of the drug, whilst not introducing any new ones [Gregoriadis 1977].

In conventional drug delivery systems, such as tablets or injections, the concentration level of the therapeutic agent decreases significantly after its administration. It is difficult to keep the drug concentration in the blood stream at a therapeutic level for extended periods of time, and multiple administrations are usually required to obtain the desired therapeutic effect [Cohen *et al.* 1991]. In these systems, high drug concentrations may induce adverse toxic effects, because in such systems, delivering the therapeutic agent is only dependent on diffusion or partition from the blood stream to the action site. The only real advantage of these systems over controlled release systems is their low processing and administration cost. **Fig. 2.1a** shows a typical release profile and drug concentration level for a conventional drug delivery system. The drug level in the blood rises after each administration of the drug and then decreases until the next administration. The concentration of any therapeutic agent has two limits in blood; the upper limit (the toxic level of the therapeutic agent) and the lower limit (the effective therapeutic level). The key point with traditional drug administration is that the drug level of the agent should remain between these limits [Park *et al.* 1998].

In contemporary drug delivery systems which can release drugs over long periods of time, the concentration level of the drug in the blood follows the profile shown in **Fig. 2.1b**, remaining constant between the toxic and effective level of the therapeutic agent for a specific time [Brannon-Peppas 1997]. For example, in treatment of the

imbalance in biological homeostasis, the drug may be released only when it is needed (**Fig. 2.1c**). This type of release profile is typically called "pulsatile release". Highly localised drug release can also be achieved by various targeting strategies (**Fig. 2.1d**). Release is restricted to a target site at a high local concentration for an extended time. Therapeutic efficiency in these systems is very high while side effects are significantly reduced.
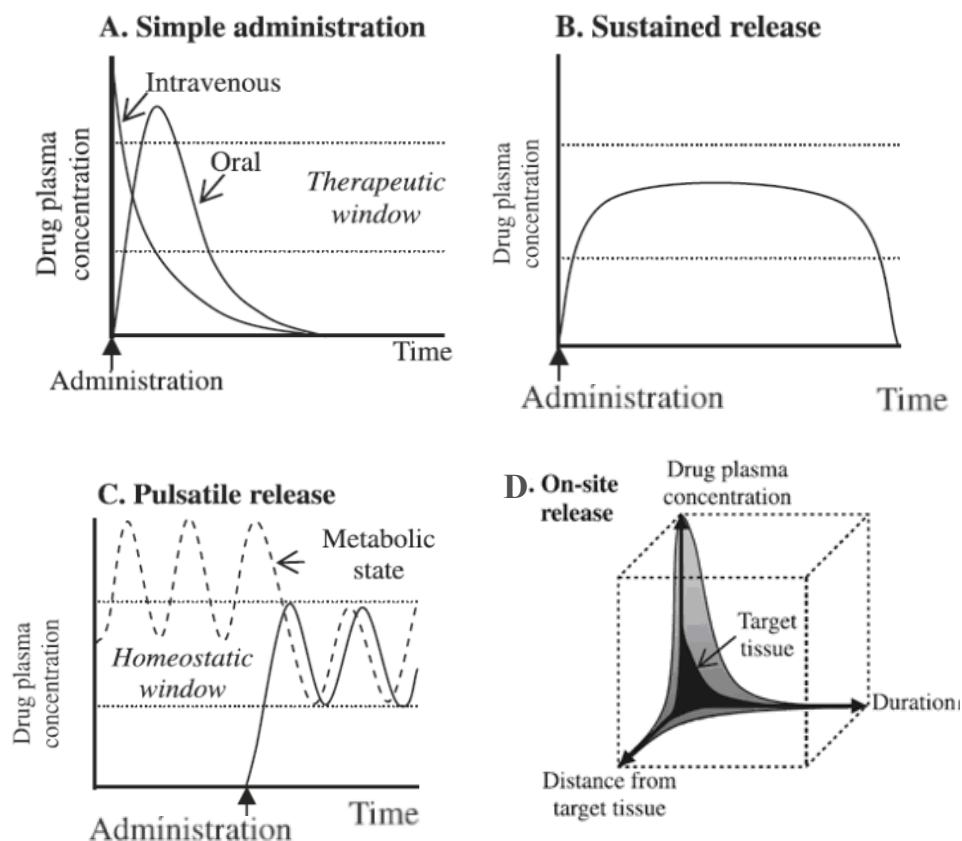
Figure 2.1 Different types of controlled release systems characteristics. (a) Drug delivery based on simple diffusion and partition. (b) Sustained release to prolong the therapeutic period. (c) Pulsatile release to tightly maintain homeostasis. (d) On-site release to maximize therapeutic efficiency and to minimize side effect [Kim *et al.* 2009].

In summary, drug delivery and targeting systems (DDTS) aim to overcome the limitations of conventional drug administration methods and thus improve drug performance. Ideal DDTS should:

- Specifically direct the drug to target cells or target tissue and ensure minimal drug leakage during transit to target,

- Keep the drug out of non-target organs, cells or tissue,

- Protect the associated drug from metabolism,

- Protect the associated drug from clearance,

- Retain the drug at the target site for the desired period of time,

- Facilitate transport of the drug into the target tissues and cells,

- Be biocompatible, biodegradable and non-antigenic

In certain situations, some of these requirements may be inappropriate. For example, the drug may work outside the cell, thus cell penetration may not be necessary [Brocchini and Duncan 1999].

2.3 Routes of drug delivery using micro and nano particles

There are many potential routes of administration for drug loaded micro- and nano-particles, ranging from parenteral, i.e. intramuscular and subcutaneous, to nasal, pulmonary, oral, ophthalmic, transdermal etc. In this section a short description of the most popular drug delivery routes is given.

Oral drug delivery: This is the most common method of drug delivery as it is convenient and can be controlled by the patient. There are, however, some disadvantages associated with this route. For instance, the oral route is very variable, so that there is noticeable potential for bio-inequivalence between orally administered drugs [Zhang *et al.* 2002].

Parenteral drug delivery: Parenteral therapy is used if drugs cannot be given by the oral route, this could be because of two reasons; first, poor absorption properties of the drug, second, propensity to degrade in the gastrointestinal tract. Drugs can be delivered by injection to carry the drug to target sites in the body. Routine parenteral administration by injection serves to deliver drugs to specific body tissues. The most

common ways of administering the drugs are intramuscular (IM), intravenous (IV) and subcutaneous (SC) [Sinha and Trehan 2005].

Pulmonary drug delivery: Therapeutic agents that have an effect on the respiratory system can be delivered by inhalation [Clark 1995] and delivering therapeutic agents to lungs is one of the most significant local therapeutic systems. The physical characteristics of the drug carriers are crucial for successful pulmonary drug delivery. For instance, the desirable particle size should be in the range of 1–5μm [Grossman 1994, Schreier *et al.* 1993]. Inhalation treatment can often benefit from a sustained release of the drug, by the aid of biodegradable polymeric materials [Kawashima 1998]. Gradual release from an inhaled drug loaded particle can extend the residence of the drug in the airways and can decrease the percentage of the therapeutic agents in the bloodstream. Also, this would be more convenient for the patient due to the reduction in the dosage frequency [Schreier *et al.* 1993].

Transdermal drug delivery: This method typically utilises an adhesive patch containing drugs, which passively diffuse through the skin. Although the skin acts as a potent barrier against external damage, transdermal delivery systems have been developed to overcome this resistance and now many drugs are delivered transdermally such as contraceptives, nicotine and estrogen [Singh and Roberts 1989, Prausnitz *et al.* 2004].

In all of the above drug delivery routes, polymeric particulate carriers encapsulating therapeutic agents are used with various sizes ranging from nano to micro size.

2.4 Particulate drug carriers

The development of drug delivery carriers is a relatively new area of science, as the technology to work at atomic, molecular and supramolecular levels has only become widely available in recent years. Particulate drug carriers include different types of structures such as micro/nanospheres, micro/nano particles, liposomes, vesicles, micelles and dendrimers (**Fig. 2.2**). **Microspheres** are small spherical units,

composed of various abut natural and synthetic materials with diameters in the micrometre range. The therapeutics agents can be dispersed or dissolved in the matrix. **Nanospheres** are spherical nano-scale structures, where active compounds can also be firmly adsorbed at their surface, entrapped or dissolved in the matrix. **Nanocapsules** have a polymeric shell and an inner core. In this case, the active substances are dissolved in the core [Mainardes *et al.* 2006].
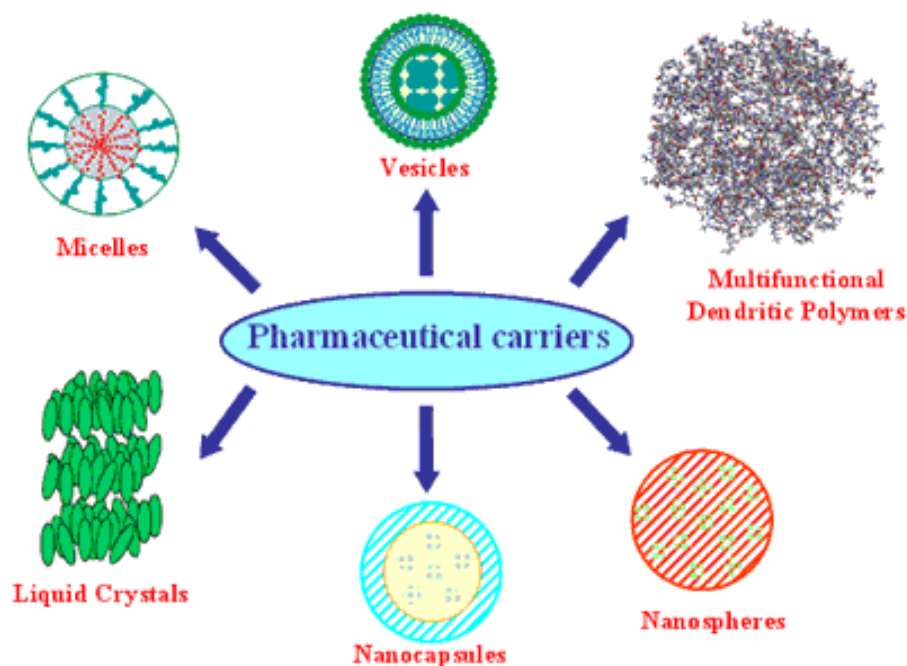
Figure 2.2 Pharmaceutical carriers [Kaparissides *et al*. 2006].

Liposomes consist of a lipid bilayer surrounding an aqueous core. They can be produced in sub-micron size, and they can carry drugs in their lipid bilayer or aqueous core [Bangham *et al.* 1965]. **Micelles** are a collection of amphiphilic surfactant molecules that spontaneously aggregate in water into a spherical vesicle. The centre of the micelle is hydrophobic and therefore can sequester hydrophobic drugs until they are released by some drug delivery mechanism. Usually, micelles are formed from small molecules that have a hydrophilic or polar or charged "head" group and a hydrophobic "tail", often composed of the hydrocarbon portion of long fatty acids. The molecular size and other geometrical features of the surfactants determine the size of the micelle [Nishiyama and Kataoka 2003, Savic *et al.* 2003]. A **dendrimer** is generally described as a macromolecule, which is characterised by

its highly branched 3D structure that provides a high degree of surface functionality and versatility. Dendrimers have often been referred to as the "Polymers of the 21st century" [Pushkar *et al.* 2006, Lee *et al.* 2005]. The unique architectural design of dendrimers, high degree of branching, multivalency, globular architecture and well-defined molecular weight, clearly distinguishes these structures as unique nanocarriers in medical applications such as drug delivery, gene transfection, tumor therapy, diagnostics, etc. Synthetic approaches lead to a dendritic architecture with properties amenable to modifications of shape, size, polarity, surface properties and internal structure [Boas and Heegaard 2004].

2.5 Mechanisms of drug release

Drug release from synthetic degradable polymeric carriers involves a series of steps: diffusion, chemical reaction and solvent activation. A convenient classification of controlled-release systems is based on the mechanism that controls the drug release which requires dissolution of the drugs followed by diffusion through the polymeric particle's structure to reach the release medium. Two types of diffusion-controlled systems have been developed; the first is a reservoir device and the second is a matrix device [Huang and Brazel 2001].

In a reservoir device, the drug is physically entrapped inside a polymeric vehicle that can then be injected or implanted in the body. The drug diffuses through the polymer membrane, which protects and surrounds the drug from the environment **(Fig. 2.3a)**. Early forms of these systems involved non-degradable polymers such as silicone rubber, which could release low molecular mass lipophilic drugs over extremely long time periods [Folkman and Long 1964]. This type of approach led to the development of Norplant, small silicone capsules containing contraceptives that are slowly released by diffusion through the polymer for 5 years.

The process of diffusion is generally described by a series of equations governed by Fick's first law of diffusion:

$$J = -D \frac{\partial c}{\partial x}$$

$\qquad\qquad$ (2.1)

Where **J** (the flux density) is the amount of drug crossing a certain area (the membrane) per unit time and is typically expressed in units such as moles of particles per m^2 per second. **D** is the diffusion coefficient of the drug in the membrane. This reflects a drug molecule's ability to diffuse through the polymeric matrix and is dependent on factors such as molecular size and charge. $\partial c/\partial x$**:** represents the rate of change in concentration **c** relative to a distance **x** in the membrane.

In matrix systems, drugs are physically embedded and distributed in a polymeric carrier (**Fig. 2.3b**) through which the drug subsequently diffuses out [Langer and Folkman 1976, Langer 1990]. Matrix devices are probably the most common of the devices for controlling the release of drugs. This is possibly because they are relatively easy to fabricate, compared to reservoir devices, and there is less danger of an accidental high dosage that could result from the rupture of the membrane of a reservoir device.

The release properties of matrix devices may be dependent upon the solubility of the drug in the polymer matrix or, in the case of porous matrixes, the solubility in the sink solution within the particle's pore network, and also the tortuosity of the network [Huang and Brazel 2001].

In some other drug delivery systems, the mechanism of the drug release is based on a combination of diffusion and degradation processes. In these systems, biodegradable (or bioerodible, see below) polymers are used for fabrication of drug carriers. The rationale for using bioerodible systems is that the bioerodible devices are eventually absorbed by the body and thus need not be removed surgically.

Polymer bioerosion can be defined as the conversion of a material that is insoluble in water into one that is water-soluble. In a bioerodible system **(Fig. 2.3c)**, the drug is

ideally distributed uniformly throughout a polymer in the same way as in monolithic systems. As the polymer surrounding the drug is eroded, the drug escapes.
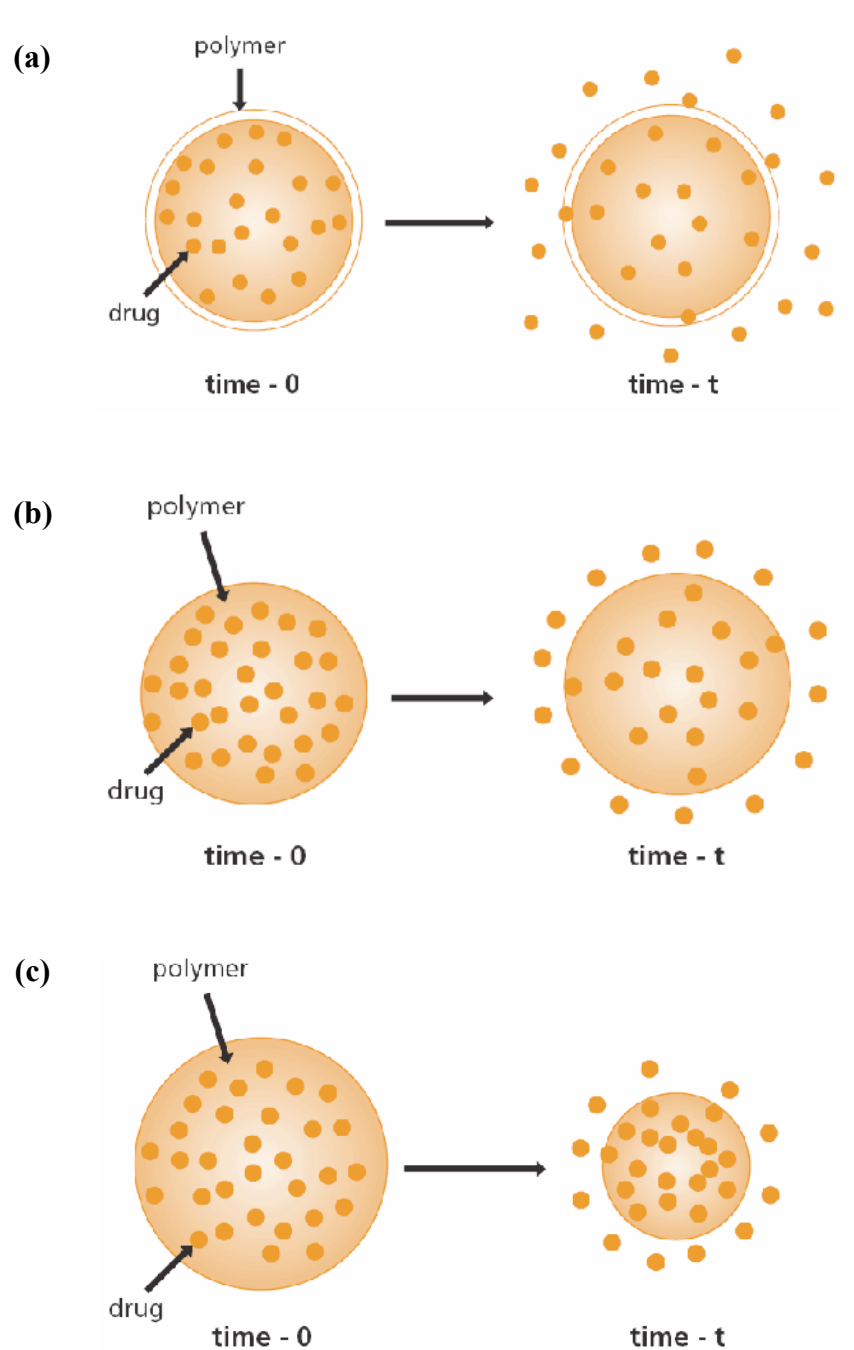
Figure 2.3 Schematic representation of (a) reservoir diffusion controlled (b) monolithic (matrix) diffusion controlled and (c) biodegradable (bioerodible) drug delivery devices.

2.6 Polymer degradation and erosion

Classification of the biopolymers used in drug delivery systems can be difficult due to the inherent diversity of structures. However, it is useful to categorise them because it can emphasise common properties within groups of polymers. There are many descriptions of degradation and erosion in the literature [Vert *et al.* 1992]. However, the following definitions are used in this thesis: degradation is based on a chemical process and specifically refers to bond cleavage and the chain scission process during which polymer chains are cleaved to form oligomers and monomers. Erosion is basically a physical phenomenon dependent on dissolution and diffusion processes leading to depletion of material [Tamada and Langer 1990].

Polymer degradation: degradation is one of the significant processes leading to drug release. Therefore it needs to be studied more extensively. Depending on the mode of degradation, polymeric biomaterials can be further classified into hydrolytically degradable polymers and enzymatically degradable polymers. Enzymatic degradation, mainly occurs in natural biopolymers like proteins (gelatin and collagen), polysaccharides and poly (β-hydroxy acids), where appropriate enzymes are available [Huang and Brazel 2001].

Hydrolytic degradation is the main type of degradation especially for synthetic polymers. There are various factors that influence this process: the type of chemical bond, pH, copolymer composition and water uptake are the most important. Some of these factors can have a significant effect on the degradation process. One of the most important parameters for monitoring degradation is molecular weight. Besides loss of molecular weight, other parameters have been proposed as a measure of degradation, including: loss of mechanical strength, complete degradation into monomers or monomer release [Huang and Brazel 2001].

Polymer erosion: polymer erosion can have two different mechanisms, first; surface erosion, second; bulk erosion [Gopferich 1996]. Surface eroding polymers lose material from the surface only (**Fig. 2.4a**). They get smaller but keep their original geometric shape. In other words, surface erosion occurs when the rate of erosion exceeds the rate of water permeation into the bulk of the polymer. This is often

considered to be a desirable mechanism of erosion in drug delivery because of the kinetics of erosion, and hence the rate of drug release, are highly reproducible and predictable. Furthermore, the magnitude of the rate of the erosion may be changed by simply changing the surface area of the drug delivery device. The slow rate of water permeation into surface eroding devices has the further beneficial effect of protecting water labile drugs up to the time of drug release [Gopferich 1996]. Examples of surface eroding polymers are the poly (anhydrides) and the poly (ortho esters). Both of these classes of biodegradable polymers possess highly labile groups that ensure rapid hydrolysis of polymer chains encountering water molecules. Water permeation is retarded by designing the polymers with hydrophobic monomer units. Alternatively, hydrophobic excipients can be added to stabilise the polymer bulk [Lee *et al.* 2004, Modi *et al.* 2005]. In ideal surface erosion, the erosion rate is directly proportional to external surface area. Surface erosion can lead to zero-order drug release (a steady amount of drug is released over time) provided that diffusional release is limited and the overall shape remains constant.
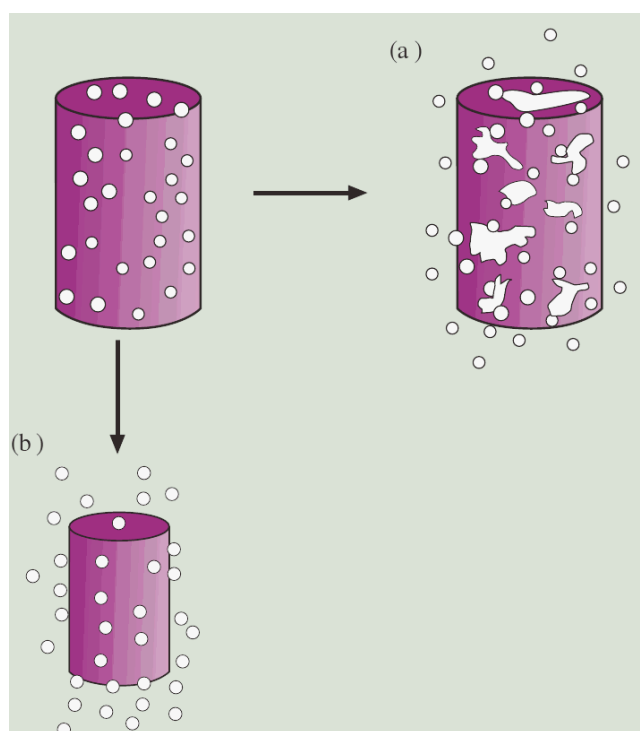
Figure 2.4 Schematic illustration of the biodegradation of a polymeric drug delivery system(a) bulk erosion and (b) surface erosion.

For bulk eroding polymers, degradation and erosion are not confined to the surface of the device. Therefore, the size of a device may remain constant for a considerable portion of time during its application (**Fig. 2.4a**). In this case, bulk erosion occurs when the rate of water permeation into the bulk of the polymer exceeds the rate of erosion. As a consequence, polymer molecules in the bulk may be hydrolyzed and the kinetics of polymer degradation/erosion are more complex than for surface eroding polymers. The majority of biodegradable polymers used in controlled drug delivery undergo bulk erosion, including the very important poly (ester) materials [Lee *et al.* 2004].

For most biodegradable polymers, both surface and bulk erosion mechanisms will occur, but the relative extent of the mechanisms varies radically with the chemical structure of the polymer backbone. Polymer erosion is much more complicated than degradation, because it depends on many other processes, including degradation, swelling, the dissolution and diffusion of oligomers and monomers, and morphological changes. Even more parameters apply to some special types of polymers such as electrically erodible materials [Kwon *et al.* 1991].

2.7 Techniques of micro and nano polymeric particle preparation

There are several methods for micro and nano encapsulation of therapeutic agents such as the emulsion solvent evaporation/extraction method, spray drying, coaccervation phase separation and elctrohydrodynamic atomization. All techniques have their own advantages and disadvantages. Using a specific method depends on the polymer, the drug, the site of the drug action, and the duration of the therapy [Jain *et al.* 2000, Fukushima *et al.* 2000, Okada and Toguchi 1995]. Generally, several requirements need to be met for successful and effective preparation of polymeric particles such as:

- The chemical stability and biological activity of the therapeutic agent should be preserved during the whole process.

• The encapsulation efficiency and the yield of the process should be high enough for mass production.

• Particles should be in a certain size range and they should be almost monodisperse.

• Particles should have a controlled release profile without high initial burst release.

2.7.1 Emulsion-solvent evaporation/extraction methods

2.7.1.1 Single emulsion method

This technique is used to load hydrophobic drugs via an oil-in-water (o/w) emulsification method. In the first step the polymer is dissolved in a water-immiscible solvent and subsequently the drug is dissolved into the polymer solution. At the end, the resulting solution is emulsified in water using an emulsifier [Jain *et al.* 2000, Hombreiro *et al.* 2000]. Usually, the amount of solvent in the emulsion is reduced by increasing the temperature to evaporate the residual solvent [Arshady 1991]. This technique is only suitable for hydrophobic drugs. The encapsulation efficiencies for hydrophilic drugs are very low since drugs may diffuse out or partition from the dispersed oil phase into the aqueous phase [Hombreiro *et al.* 2000, Arshady 1991].

2.7.1.2 Double emulsion method

Most water-soluble drugs are encapsulated by the water-in-oil-in-water (w/o/w) method [Crotts and Park 1998, Okochi and Nakano 2000]. In this technique, the polymer is dissolved in an organic solvent and then the aqueous solution of the drug is emulsified in to form a water-in-oil (w/o) emulsion. Subsequently, a w/o/w emulsion is formed by adding the w/o emulsion into an excess amount of water containing an emulsifier under vigorous stirring (**Fig. 2.5**). The residual solvent is removed by evaporation or another extraction method. The advantage of this method to the single emulsion technique is its high encapsulation efficiency for hydrophilic drugs [Crotts and Park 1998, Okochi and Nakano 2000].
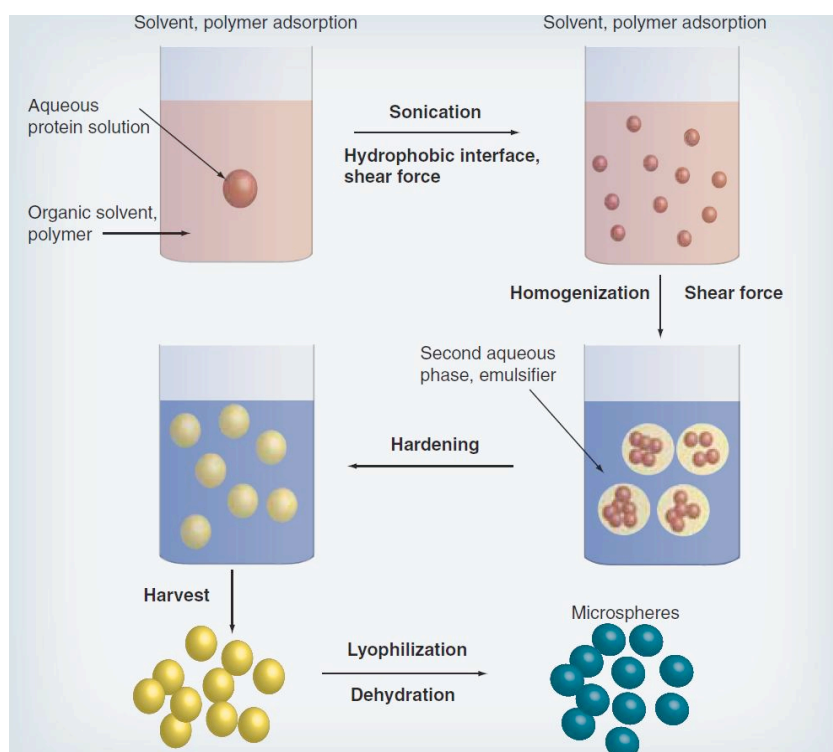
Figure 2.5 Processing scheme for microsphere preparation by double emulsion technique [Chiellini *et al.* 2008].

2.7.2 Coacervation phase separation

The term coacervation is derived from the Latin acervus, meaning aggregation, and the prefix 'co' to indicate union of colloidal particles. The process of three steps is carried out under continuous agitation: first, formation of three immiscible chemical phases, second, deposition of the coating, and third, rigidization of the coating [Carrasquillo *et al.* 2001, Mallarde *et al.* 2003] (**Fig. 2.6**).

Formation of three immiscible chemical phases: the three phases are a liquid vehicle phase, core material phase and coating material phase. The three phases are formed by dispersing the core material in a solution of coating polymer, the vehicle phase is used as a solvent for the polymer. For the coating material phase, an immiscible polymer in liquid state is formed by: (i) changing temperature of polymer solution, (ii) addition of salt, (iii) addition of nonsolvent, or (iv) addition of incompatible polymer to the polymer solution [Madan 1978].

Deposition of the coating: this involves depositing the liquid polymer coating upon the core material. This happens if the polymer adsorbs at the interface formed between the core material and liquid vehicle phase, and this adsorption phenomenon is a prerequisite to effective coating.

Rigidization of the coating: The continued deposition of the coating material is promoted by a reduction in the total free interfacial energy of the system by rigidization of the coating. This can be carried out using thermal cross linking or desolvation techniques.

(a)

(b)

(d)

(c)
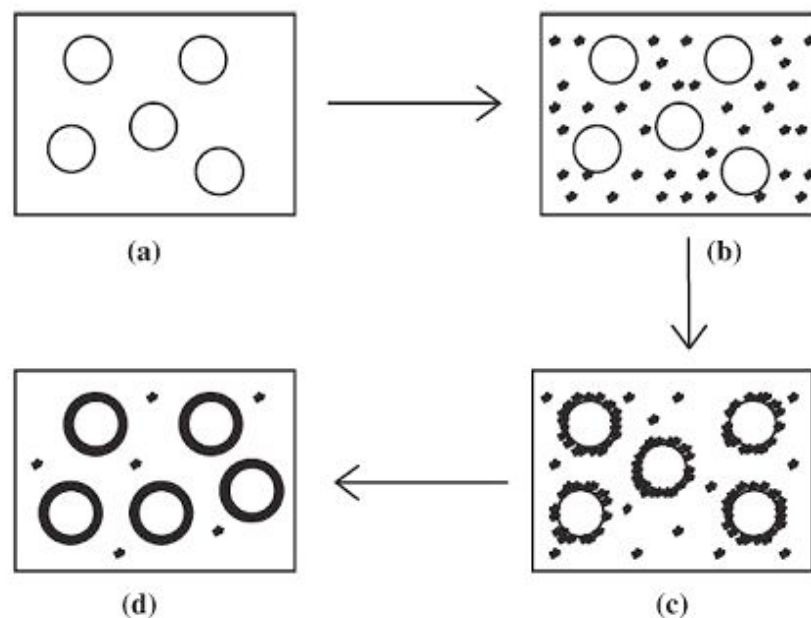
Figure 2.6 Schematic representation of the coacervation process. (a) Core material dispersion in a solution of the shell polymer, (b) separation of coacervate from solution, (c) coating of core material by microdroplets of coacervate, (d) coalescence of coacervate to form continuous shells around the core particles.

The processing setup for this method is relatively simple. It contains mainly of jacketed tanks with changeable speed agitators. The significant disadvantage of this method is that the droplets formed stick to each other prior to the completion of the process and produce large aggregates.

2.7.3 Suspension cross-linking

Preparation of polymeric particles by suspension cross-linking involves the formation of a stable droplet suspension of the polymer solution (or melt) in an immiscible liquid, gradual hardening of the droplets by covalent cross-linking and, finally, recovery of the resulting cross-linked polymer particles. For the preparation of particles, the core material remains completely within the droplets. This means that the core material (dispersed or dissolved) should have a substantially higher affinity for the droplet phase than the suspension medium. The average size of the droplets must be about one order of magnitude larger than that of the core particles to ensure complete encapsulation [Arshady 1989].

2.7.4 Spray drying
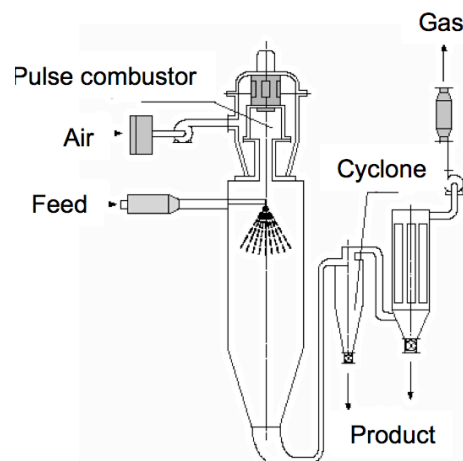
Figure 2.7 Processing scheme for microsphere preparation by spray drying [Zbicinski *et al*. 2000].

The spray drying method offers several advantages in comparison with the methods described above. It has improved reproducibility and processing conditions are relatively mild which helps to control the particle size; but the two main disadvantages of this technique are: loss of a large number of particles due to products sticking to the wall of the spray-drier, and production of large aggregates before the complete removal of the solvent [Murillo *et al*. 2002, Blanco-Prieto *et al*. 2004, Burke *et al*. 2004]. The schematic process is shown in **Fig. 2.7**.

2.7.5 Electrohydrodynamic atomization

This is the method used in all of the experiments discussed in this thesis. Electrohydrodynamic atomization (EHDA) is an attractive method for generating particles suitable for use as drug delivery vehicles [Ding *et al.* 2005, Pareta and Edirisinghe 2006]. As mentioned above, different fabrication methods such as single and double emulsification are commonly deployed to fabricate drug-loaded polymeric particles [Yang *et al.* 2001, Zhu *et al.* 2000, Zhang *et al.* 2008]. However, there are inevitably certain disadvantages associated with these methods. For example, conventional emulsification methods result in a broad particle size distribution [Kissel *et al.* 1995]. Also, some non-degradable additives such as surfactants or polymers are commonly used as emulsifiers [Freitas *et al.* 2005] and the separation of particles from the solvent can be time-consuming and expensive but needs to be carried out to reduce the amount of residual solvent to a safe level. Most importantly, the biofunctionality of drugs, especially in the case of biomacromolecules can be greatly reduced during processing due to exposure to certain condition, e.g., elevated temperatures and high shear stresses [Rasiel *et al.* 2002, Kohane *et al.* 2006].
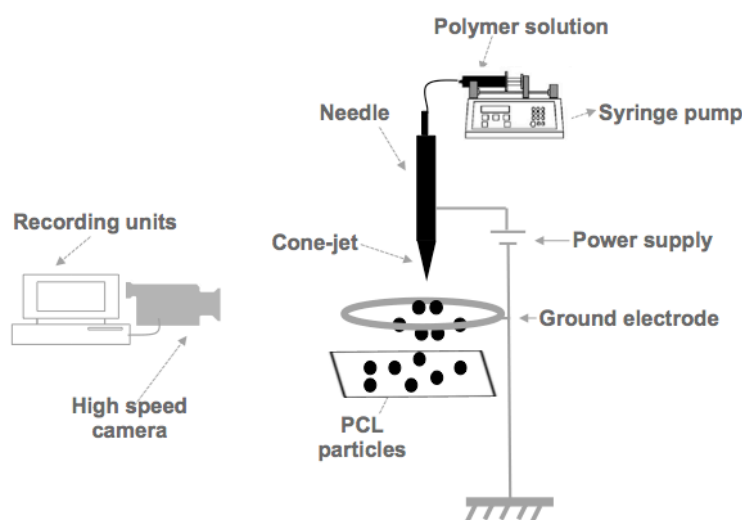
Figure 2.8 Schematic representation of the single needle EHDA set up used in this work using polycaprolactone (PCL) as a polymeric carrier.

In EHDA, particles are produced at the ambient temperature and pressure, thus overcoming the problems associated with defunctionalisation of drugs under extreme processing conditions. Also this method is capable of generating particles with a

narrow size distribution, and a mean diameter which can be varied between hundreds of micrometres and tens of nanometres by controlling the processing parameters, e.g. flow rate(s), needle diameter(s) and applied voltage [Samarasinghe *et al.* 2008, Xie *et al.* 2008, Ahmad *et al.* 2008].

EHDA is a phenomenon which occurs when a liquid is passed at a controlled flow rate through a capillary needle maintained at several kilovolts relative to a ground electrode few centimetres away. The schematic representation of a single EHDA setup is shown in **Fig. 2.8**.

2.8 Principles and theoretical aspects of electrohydrodynamic atomization processing
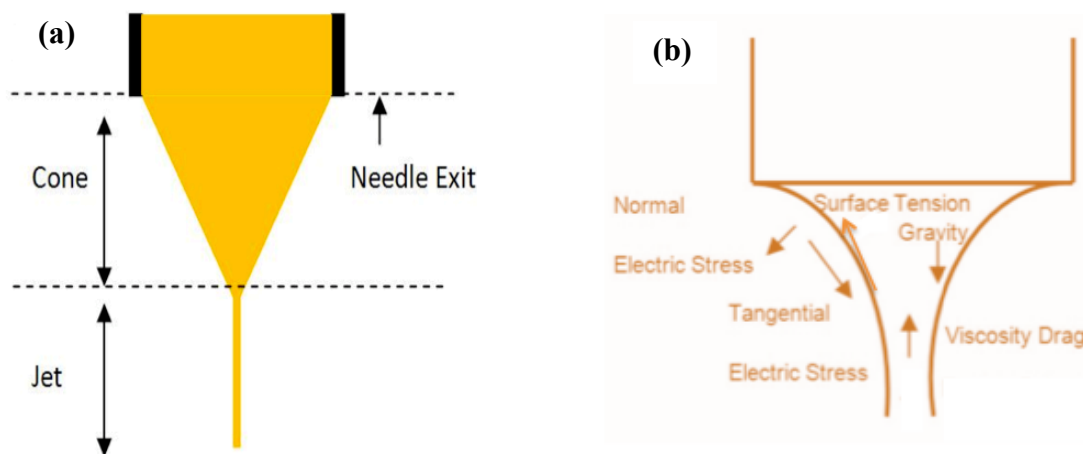
Figure 2.9 Schematic representation of cone-jet mode, (a) Forces acting on a cone-jet, (b) An axisymmetric liquid cone with a thin jet at its apex [Hartman *et al.* 1999].

The influence of an applied electrical field on a conducting liquid was described in 1600 when William Gilbert reported that electrostatically charged amber, could produce a jet of liquid to be emitted from a droplet [Gilbert 1600]. Electrohydrodynamic research was first presented in the technical literature by Lord Rayleigh, who also studied the effect of an electric field on liquid drops. He concluded that the stability of a drop suspended from a capillary is dependent upon a balance of forces such as the electrical stresses due to the presence of an electric

field and the surface tension forces [Rayleigh 1882]. In particular he observed that the deformed liquid can take on a conical shape and a thin jet evolve from the tip of a cone. Taylor subsequently explained the conical shape through a mathetmatical description of the balance between electrostatic stresses and surface tension [Taylor 1964].

This "cone-jet mode" is the most desirable mode for producing fine particles. In the cone-jet mode the liquid issues from the capillary in the form of a regular, symmetric cone with a thin jet at its apex (**Fig. 2.9a**), stretching along the capillary axis and breaking up into fine droplets. To achieve this, liquid is pumped through a nozzle at a low flow rate and a droplet is formed at the tip of this nozzle. An electric field is applied which induces a surface charge to the droplet. As a result of the electric stress, the droplet is transformed into a conical shape. The liquid acceleration and the shape of the liquid cone results from the balance of several forces involved. These are: liquid pressure, liquid surface tension, gravity and electric strengths in the liquid surface. The conical shape is sometimes referred to as a 'Taylor cone' which forms when the outward stress due to an applied electric field balances the inward stress due to the liquid surface tension. The forces that are involved in the formation of a cone jet are illustrated in **Fig. 2.9b** [Hartman *et al.* 1999]. The applied electric field accelerates the surface charge towards the cone apex. This jet breaks up into a number of primary or main droplets and a number of secondary droplets and satellites [Jaworek and Krupa 1999a and 1999b].

Most theoretical studies are devoted to the cone-jet mode. Zeleny (1917) was the first to study this mode. Taylor successfully examined the cone profile and angle based on the liquid in the cone. By assuming that the jet is much thinner than the capillary tube for a liquid with relatively high conductivity, Mora and Loscertales (1994) reported scaling laws of droplets sizes and spray current (two ratios below) related to the flow rate and liquid properties [Mora and Loscertales 1994, Zeleny 1917]:

$$r^* \sim (\varepsilon \varepsilon_0 Q/K)^{1/3} \tag{2.1}$$

$$I \sim f(\varepsilon)(rQK/\varepsilon)^{1/2} \tag{2.2}$$

where **r*** is the scaled jet radius, ε_0 is the vacuum permittivity, ε is the liquid to vacuum permittivity ratio, **K** is the liquid conductivity, **Q** is the flow rate, **I** is the spray current, and **f(ε)** is a dimensionless function of ε and γ, with γ being the surface tension of the liquid.

However, the use of scaling laws for the prediction of resultant relics is still somewhat controversial, because experimental errors in the reported measurements do not allow adequate distinction between different relics [Ganan-Calvo 1997a and 1997b]. In addition, there is a range of combinations where EHDA is stable for different properties of injected liquids. For example, Mei and Chen (2007) showed that increased flow rate of the inner liquid results in an increase in capsule size for a certain value of inner liquid flow rate [Mei and Chen 2007]. However, over a certain range of material combinations and processing parameters, capsule diameter decreases with an increase in the magnitude of the following processing parameters: voltage, electrical conductivity, and surface tension of the sprayed solution. In contrast, an increase in particle diameter can also be obtained by means of increasing flow rate, density, and viscosity of the sprayed solution [Zhang *et al.* 2006].

2.8.1 Modes of electrohydrodynamic atomization

The geometrical features of the jet and the various types encountered as a function of the operating parameters have been classified previously by Jaworek and Krupa (1999a and 1999b). Different parameters such as the physical properties of the liquid (e.g. surface tension, density, electrical conductivity and viscosity) and processing parameters (e.g. flow rate and electric field strength) have significant influences on generating EHDA modes [Paine *et al.* 2007]. At a low voltage only fragments of the pumped solution are jetted, creating various modes such as dripping, microdripping, rapid microdripping, unstable cone-jet modes. At higher applied voltages, different modes involving a sustained and a continuous jet can be formed; these are stable cone-jet, multi-jet, and irregular instable jet modes (**Fig. 2.10**). In these modes, under the action of high voltage, the jet usually breaks up into particles a few millimetres

from the needle orifice. The meniscus and the jet can be stable or spin around the needle axis or rotate irregularly [Cloupeau and Prunet-Foch, 1994, Hayati *et al.* 1987a, Hayati *et al.* 1987b].
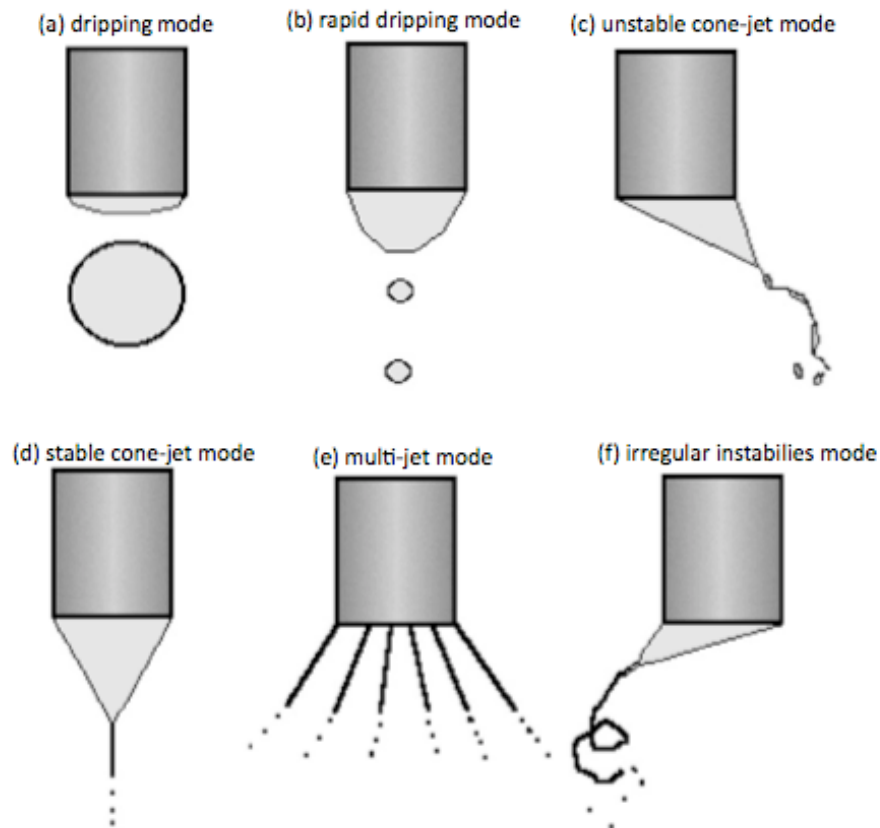
Figure 2.10 Various modes of electrospraying, (a) dripping mode; (b) rapid dripping mode; (c) unstable cone-jet mode; (d) stable cone-jet mode; and (e) multi-jet mode; and (f) irregular instabilies mode [Jaworek and Sobczyk 2008].

2.8.2 Effect of liquid flow rate on cone-jet mode

The size distribution of particles produced by electrohydrodynamic atomization in the cone-jet mode depends on the diameter of the jet, and on the break-up of this jet into droplets. Every liquid has a minimum flow rate, below which a stable cone-jet mode cannot exist for a given voltage. At this minimum flow rate the jet breaks up due to asymmetric instabilities. These instabilities are also called varicose instabilities [Hartman *et al.* 2000]. At higher flow rates, the current through the liquid cone increases. With increasing current, the surface charge on the jet increases. Above a certain surface charge the jet break-up will also be influenced by lateral or azimuthal instabilities of the jet. These instabilities are also called kink instabilities.

When the influence of these 'kink' instabilities increases, then the size distribution of main droplets also become wider [Hartman *et al.* 2000].

2.8.3 Effect of applied voltage on the cone-jet mode

The electric field between the capillary and the ground electrode is an important parameter in controlling the process of electrohydrodynamic atomization. This is determined mainly by the applied voltage and other factors such as the configuration of the ground electrode. Within a well defined voltage range, the meniscus of liquid becomes conical and stationary. Below this voltage range, the spray always operates in pulsating mode [Ganan-Calvo *et al.* 1997a and 1997b]. With a given inter-electrode spacing, different modes of atomization can be observed if the voltage is gradually increased from low values to high values. Applied voltage is a key variable in establishing the cone-jet mode and the cone-jet mode can prevail within a range of applied voltages [Tang and Gomez 1994]. Within this range, droplet size reduces with increasing applied voltage. Thus, it is necessary to select the highest possible value of applied voltage and the lowest possible value of flow rate (within the stable jet range) to achieve the minimum droplet size [Jayasinghe and Edirisinghe 2004]. For highly conducting and viscous liquids, the sizes of the droplets produced in the cone-jet mode are found to be relatively insensitive to the applied voltage [Ku and Kim 2002].

2.8.4 Liquid properties

The modes of electrohydrodynamic atomization are also influenced by the liquid properties such as surface tension, viscosity, electrical conductivity, relative permittivity, and density [Ganan-Calvo *et al.* 1997a and 1997b, Hartman *et al.* 1999]. Each of these properties is discussed briefly below.

2.8.4.1 Surface tension

In order to form a stable cone-jet, the surface tension has to be overcome by the electric stresses. The higher the surface tension the greater the electric field strength required. According to the experimental results obtained by Smith (1986) the

threshold voltage for the stable cone-jet will increase with the liquid surface tension [Smith 1986] but if the liquid surface tension is very large, a stable jet may not be established because the field required exceeds that for the electric break down in the gas surrounding the cone. Tang and Gomez (1995) used gases with higher electrical breakdown strength as a surrounding fluid instead of air to obtain the stable cone-jet mode for water.

2.8.4.2 Viscosity

Viscosity is another vital liquid property which plays a significant role in the jet break-up process and influences the size of the particles produced [Lopez-Herrera *et al.* 2003]. According to Weber (1931) an increase in viscosity will lead to an increase of droplet size in electrohydrodynamic processing [Weber 1931]. Jayasinghe and Edirisinghe (2002) studied the effect of viscosity on the size of relics produced by electrohydrodynamic processing. They found that an increase in viscosity over three orders of magnitude had a dramatic effect on the size of particles obtained.

2.8.4.3 Electrical conductivity

Liquid conductivity is the most important property for electrospraying in the cone-jet mode. Sufficient electrical conductivity is necessary for the liquid droplet at the capillary exit to be transformed into a conical shape. On the other hand, if the electrical conductivity is too high, electrohydrodynamic processing will be impossible due to corona discharge occurring before the required applied voltage for the stable cone-jet mode is obtained. Liquids with low conductivity (insulators), e.g., olive oil, cannot be subjected to electrohydrodynamic atomization, although they can be electrosprayed in cone-jet mode by artificially increasing their conductivities with additives such as ethanol [Lopez-Herrera *et al.* 2003]. The value of liquid conductivity influences the morphology of the liquid issued in the stable cone-jet mode. As conductivity increases, the filament width, length, flow rate for the cone-jet mode and droplet size all decrease [Ganan-Calvo *et al.* 1997a and 1997b].

2.8.4.4 Relative permittivity

Relative permittivity or dielectric constant is a measure of the polarisability of a material in an electric field. Polarisation reduces the magnitude of the electric field inside the liquid. Relative permittivity along with the vacuum permittivity and conductivity determines the electrical relaxation time, $t_e = \beta \varepsilon_0 / K$. Electrical relaxation time is the time required to smooth a perturbation in the electric charge; β being the relative permittivity, ε_0 and K are the vacuum permittivity and electrical conductivity, respectively [Ganan-Calvo *et al.* 1997a and 1997b].

2.8.4.5 Density

The density of the liquid plays an important role in determining the jet characteristics in the cone-jet mode. When the viscosity and the conductivity of the liquid are large enough, the electrical charge is efficiently transmitted across the jet section by viscous forces. However, the viscous force depends on the density of the liquid [Ganan-Calvo *et al.* 1997a and 1997b]. Also, the liquid density is of some importance due to the influence of gravity on the cone shape. For large capillaries, diameters larger than 1mm, gravity influences the shape of the cone strongly [Hartman *et al.* 1998].

2.8.4.6 Needle size and electrode configuration

With regard to needle size, there is a difference of opinion among researchers. Cloupeau and Prunet-Foch (1990) showed that, for a given liquid, the range of flow rates varies with the change of needle size [Cloupeau and Prunet-Foch 1990]. Tang and Gomez (1996) found that the droplet size is independent of the needle size. However, they showed that the needle size significantly affected the stable cone-jet domain of electrospraying. The maximum liquid flow rate needed for the stable cone-jet electrospray decreases dramatically as the needle diameter increases. This shows that in the voltage-flow rate graph, the stable cone-jet domain of the electrospray becomes narrower as the needle size increases [Tang and Gomez 1996].

Jayasinghe *et al.* (2002) showed that the droplet trajectories depend on the configuration of the ground electrode. For a point like ground electrode, the smaller

the radius of the point, the higher the concentration of the droplets produced in the spraying pattern. They pioneered the use of a point-like ground electrode. This configuration of the ground electrode was the key to their innovation of electrostatic atomization printing (EAP) [Jayasinghe *et al.* 2002].

2.9 Co-axial electrohydrodynamic atomization (CEHDA)

Co-axial electrohydrodynamic atomization (CEHDA) is a further development of EHDA. The technique uses electrohydrodynamic forces to generate co-axial jets of immiscible liquids or suspensions. A schematic of the basic experimental setup for CEHDA is given in **Fig. 2.11**. Two immiscible liquids or suspensions (T1 Outer Liquid, T2 Inner Liquid) are passed through two concentrically arranged capillaries. The outer and inner needles are connected to the same electrical potential of several kilovolts relative to an earthed ring electrode
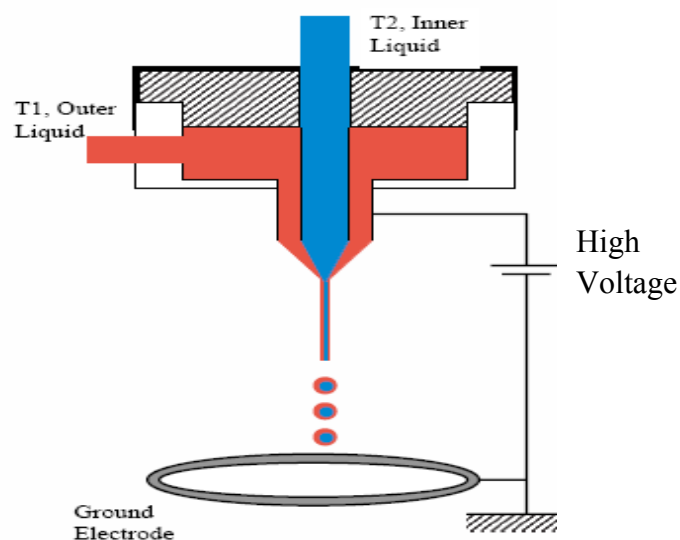
Figure 2.11 Schematic representation of the CEHDA setup [Loscertales *et al.* 2002].

2.9.1 The mechanism of co-axial electrohydrodynamic atomization
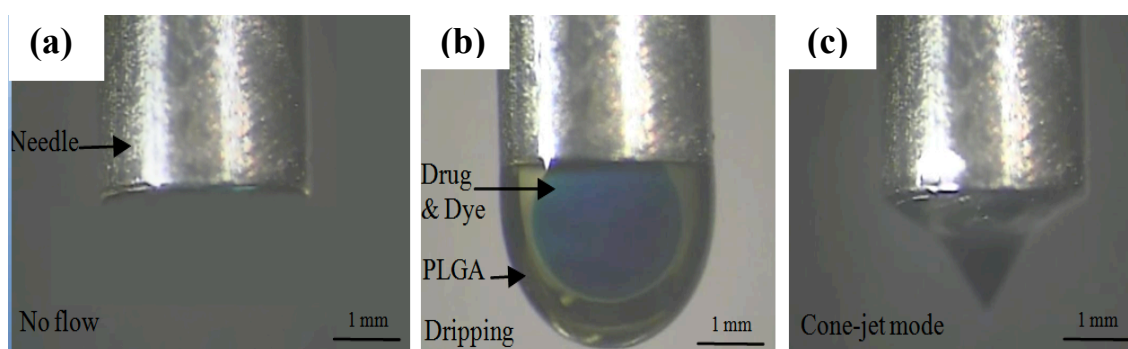
Figure 2.12 Formation of a cone-jet in CEHDA with outer meniscus surrounding the inner one, (a) no flow; (b) dripping mode demonstrating immiscibility; and (c) Formation of a compound cone-jet in CEHDA.

For a certain range of values of the applied voltages and flow rates, a cone-jet is formed at the exit of the needles with an outer meniscus surrounding the inner one. A liquid thread is issued from the vertex of each one of the two menisci, giving rise to a compound jet of two co-flowing liquids or suspensions (**Fig. 2.12**) [Loscertales *et al.* 2002].

2.9.2 The driving liquid concept

To obtain a structured cone-jet, electrohydrodynamic forces must act on at least one liquid, although they may act on both. The liquid upon which electrohydrodynamic forces act predominantly to form a cone-jet is called the driving liquid. The driving character of one of the liquids can be determined by comparing their electrical relaxation times. The electrical relaxation time, $t_e = \beta\varepsilon_o/K$ is the time required to smooth a perturbation in the electric charge. The driving character of one of the liquids can be lost in favour of the other if the electrical conductivity of the latter is enhanced sufficiently by adding a suitable additive to it [Lopez-Herrera *et al.* 2003]. When charges are located at the outer interface, the tangential electrical stresses which point towards the vertex of the conical interface must be efficiently transmitted throughout the liquid bulk by viscous diffusion. This requires that the viscosity of the outer liquid be high enough to play an important role in the liquid

motion. Moreover, the use of a less viscous liquid outside would give rise to intense re-circulations in the electrified meniscus and these re-circulatory motions are incompatible with steady compound jets. However, liquids with lower viscosity can be used as drivers when they are used inside, even when a non conducting liquid such as olive oil is used outside. This is also one way of electrospraying liquid insulators [Loscertales *et al.* 2002].

2.10 Applications of single needle and co-axial EHDA methods in preparation of various drug carriers

The versatility of electrohydrodynamic atomization has been demonstrated through several published results in the pharmaceutical field. Current challenges in the field of drug delivery lie in the development of drug-encapsulation carriers on the micrometre or nanometre scale. In this section, various techniques are discussed in the context of potential biomedical applications of the different products, specifically drug delivery vehicles, which were produced using single needle and co-axial EHDA methods.

2.10.1 The application of single needle EHDA processing

In single needle EHDA processing, a therapeutic agent is incorporated in the particles, e.g. dispersed in a polymeric matrix [Ciach 2007]. The processing parameters and physical properties of the solutions used play an important role in determining the characteristics of the carrier. It has been shown that adjusting the processing parameters (i.e. needle size, working distance, flow rate and applied voltage) enables carriers to be obtained with different size, shape, and morphology for different applications [Xie *et al.* 2006a and 2006b, Berkland *et al.* 2004]. The first part of the experimental work in this thesis will concentrate on this (Chapter 4); with extensive studies on controlling the size of the fabricated particles via the processing parameters. In the next section, a detailed description of various structures such as particles, aerosols, and porous structures made via single needle EHDA will be given.

2.10.1.1 Particles

The fabrication of drug loaded particles with high encapsulation efficiency and a well defined and controllable size distribution is one of the most significant challenges in current pharmaceutical and medical research [Langer 1998]. Wu *et al.* used an EHDA technique to produce nanoparticles (300−400 nm in diameter) which were composed from genetically engineered elastin-like polypeptides (ELPs), a biodegradable and bioresponsive polymer. They successfully loaded doxorubicin into the particles and the loading of this drug at 20 w/w% did not influence particle morphology. The particle diameter, polydispersity (ratio of standard deviation to mean size) and morphology, were significantly influenced by solvent concentration, spraying voltage, and polymer molecular weight. Release of the drug was influenced by the pH and solubility of the ELPs [Wu *et al.* 2009a]. Xu *et al.* similarly prepared bovine serum albumin (BSA)-loaded tripolyphosphate (TPP) cross-linked chitosan particles whose size was found to be strongly influenced by the flow rate [Xu and Hanna 2007]. In another study, BSA was loaded into particles by electrospraying an emulsion of BSA in a poly(lactide) (PLA) solution and spherical particles in the range of 0.8 to 4 μm with smooth surfaces were produced [Xu *et al.* 2006]. The encapsulation efficiency and the yield of the process were between 22 to 80% and 64 to 80%, respectively. However, the release profile of the drug did not reach a steady state within the time of observation due to PLA erosion.

It has been shown that EHDA processing can be used for preparing polymeric nanoparticles incorporating both hydrophilic and hydrophobic drugs [Valo *et al.* 2009, Pareta *et al.* 2005], that the biofunctionality of the drug is unaffected and that high encapsulation efficiencies can be achieved. For example, Xie *et al.* fabricated particles by EHDA processing for sustained delivery of the anticancer drug paclitaxel to treat C6 glioma with an encapsulation efficiency of ~80% [Xie *et al.* 2006a]. Similar values were reported for the case of Ampicillin loaded chitosan micro/nanoparticles with a size of 520 nm [Arya *et al.* 2009] and by Ding *et al.* for taxol-loaded polycaprolactone (PCL) particles which exhibited excellent sustained release profiles over a month [Ding *et al.* 2005].

Furthermore, changing the properties of the solvents and solutions used in EHDA also provides a means of tailoring the morphology and structure of the particles [Farook *et al.* 2009a]. Berkland *et al.* showed that specific structural types, such as tapered shapes, porous surfaces, and blood cell-shaped particles, could be achieved by varying the properties of the polymer solvent used [Berkland *et al.* 2004]. The size of the fabricated particles has also been shown to decrease with increasing conductivity of the polymer solution. Furthermore, the morphology of the fabricated particles can be significantly altered by using different combinations of polymers (e.g. poly (ε-caprolactone) (PCL), poly (lactic acid-co-glycolid acid) (PLGA), poly-D-lactic acid (PDLA) and poly-L-lactic acid (PLLA)) and solvents [Yao *et al.* 2008].

2.10.1.2 Aerosols

Aerosols are another type of pharmaceutical carrier, which can be produced using single needle EHDA. Aerosol-based pulmonary disease therapy emerged in 1990. An inhaled drug delivery system should have some critical characteristics. For instance, for effective delivery of the aerosol down to the lower airways, the final aerodynamic size of the particles should be between 2-5μm, and they should also be monodisperse [Ijsebaert *et al.* 1999]. EHDA processing was shown to meet these requirements for the production of aerosols. The resulting droplets were nearly monodisperse, and the droplet size could be easily varied by the voltage and flow rate. Zimlich *et al.* (2000) developed a hand-held prototype of pulmonary drug delivery nebulizer using EHDA principles. Here 78% of the aerosol with a droplet size of 1-6μm were found in the respiratory tract, which was approximately four times higher than that achieved using some other commercially tested devices [Zimlich *et al.* 2000].

2.10.1.3 Porous particles

Porous structures have attracted much attention because of their specific morphology and high surface area to volume ratio. The bioactive agents can be arranged in a specific order to make this structure have a unique architecture for biomedical applications [Jiang *et al.* 1999]. Wu and Clark (2007) electrosprayed porous PCL particles by jetting into a water bath using various solutions of different PCL

concentrations in chloroform solvent. Solvent evaporation and phase separation are the two main mechanisms for the formation of pores. They showed that solvents with low boiling points make pores with irregular morphologies and large dimensions. Moreover, Wu and Clark demonstrated that rapid solvent evaporation mechanism has a key role in forming porous particles via EHDA processing [Wu and Clark 2007].

2.10.2 Co-axial EHDA processing and its application

As mentioned in **Section 2.6**, the co-axial EHDA processing provides a powerful technique for the production of capsules in both the micrometre and nanometre size range. It facilitates encapsulation of sensitive core materials, for example, cells, enzymes or drugs in a protective shell. A range of polymeric materials including polyurethanes, polysiloxanes, polylactides (PLA), polyglycolides (PGA), poly(lactide-co-glycolides) (PLGA), are employed as shell materials for capsule/ bubble production because of their desirable physical properties, such as elasticity, insulating ability, physical strength, toughness, and freedom from leachable impurities. Many of these polymers are designed to degrade within the body [Langer 1998, Brannon-Peppas 1997], in particular polylactide (PLA), polyglycolides (PGA), and poly(lactide-co-glycolides) (PLGA). These biodegradable polymeric carriers have been extensively investigated as they have shown no adverse tissue reactions when carrying bio-active agents and, as above, can be hydrolyzed in the body to form products that can be easily eliminated, sparing the need to remove these implants by surgery. Another versatile application of co-axial EHDA is the production of microbubbles, which have shown great promise in therapeutic applications such as targeted drug delivery, diagnostic imaging, thrombolysis, gene therapy, and focused ultrasound surgery [Mizushige *et al.* 1999, Poliachik *et al.* 1999, Schmidt and Roessling 2006, Unger *et al.* 2001].

2.10.2.1 Capsules

Micro/nano encapsulation via co-axial EHDA is of particular importance for drug delivery [Barisci *et al.* 2000, Xie *et al.* 2008], food industry [Yoshii *et al.* 2001], and specific material processing [Burlak *et al.* 2001, Lee *et al.* 2001]. Lopez- Herrera *et*

al. investigated the electrified co-axial jets of two solutions evolved from a structured cone jet [Lopez-Herrera *et al.* 2003]. The group introduced the driving-liquid concept and studied the linear scaling law for predicting jet diameters as described in **Section 2.5**. However, their work did not specify the criteria that determine the structure of the capsules. Loscertales *et al.* demonstrated the production and control of monodisperse capsules in different size ranges from 0.15 to 10 micrometres [Loscertales *et al.* 2002]. They also showed that the diameter of capsules was influenced by several parameters including the operational parameters such as the applied flow rates and voltage, the physical properties of solutions, and the interaction between inner and outer solutions during the spray. Chen *et al.* investigated co-axial jet electrospraying using an ethanol/ glycerol/TWEEN mixture and cooking oil as the two solutions and found that the properties of the outer liquid, which was very viscous and electrically conductive, played a key role in controlling the process [Chen *et al.* 2005].

Many studies have focused on the encapsulation of bioactive agents. Paclitaxel (a hydrophobic anticancer drug) has been encapsulated in biodegradable polymeric particles by electrospraying, with particle sizes in the range 1 to 15 μm [Ding *et al.* 2005]. Pareta and Edirisinghe (2006) demonstrated the preparation of polymer-coated starch/bovine serum albumin (BSA) microspheres using a co-axial system. The mean diameter was 5–6μm and 75% of the BSA was released over a 7 day period [Pareta and Edirisinghe 2006]. In addition, co-axial jetting producing oligodeoxynucleotide encapsulated lipoplex nanoparticles for either intravenous injection or potential pulmonary delivery, has been demonstrated [Wu *et al.* 2009b]. The diameter of the particles was about 190 nm and the particles provided an efficient medium for gene delivery. Capsules with micro- and nanoscale anisotropy have received increasing interest for their ability to simultaneously present different physical and chemical properties. In a study, it was demonstrated that gold nanocrystals (NC) could be selectively incorporated into one compartment of anisotropic polymer particles. Stable bicompartmental particles were prepared via electrohydrodynamic co-jetting of aqueous nanoparticle suspensions followed by thermal cross-linking [Lim *et al.* 2010]. Bicompartmental particle populations with different NC densities were obtained by varying the NC concentration in the jetting suspension. This study delineates a new approach for preparation of

inorganic/organic composite particles with precisely engineered, anisotropic nanoparticle distributions and may contribute to further developments in emerging scientific areas, such as smart materials or particle-based diagnostics.

2.10.2.2 Microbubbles

The co-axial EHDA principle can be used to prepare microbubbles with a near monodisperse size distribution [Farook *et al.* 2007a]. Preparation of microbubbles is an area of significant interest in a range of biomedical application areas, from use as contrast agents for ultrasound imaging to drug delivery; and the EHDA method can offer unique advantages compared with e.g. microfluidic devices and simple agitation [Pancholi *et al.* 2007]. Farook *et al*. were the first to demonstrate that suspensions containing bubbles less than 10 μm in diameter with a narrow size distribution can be prepared by EHDA. In this process, glycerol was injected through the outer needle of the two needle set arrangement while air flowed through the inner needle at the same time [Farook *et al.* 2007a]. The process was then adapted to prepare phospholipid-coated microbubbles with a high yield (10^9 bubbles min^{-1}) [Farook *et al.* 2009b]. EHDA bubbling shows three characteristic spray modes: bubble dripping, coning and continuous bubbling; the latter mode being the most suitable for the preparation of microbubbles for biomedical applications.
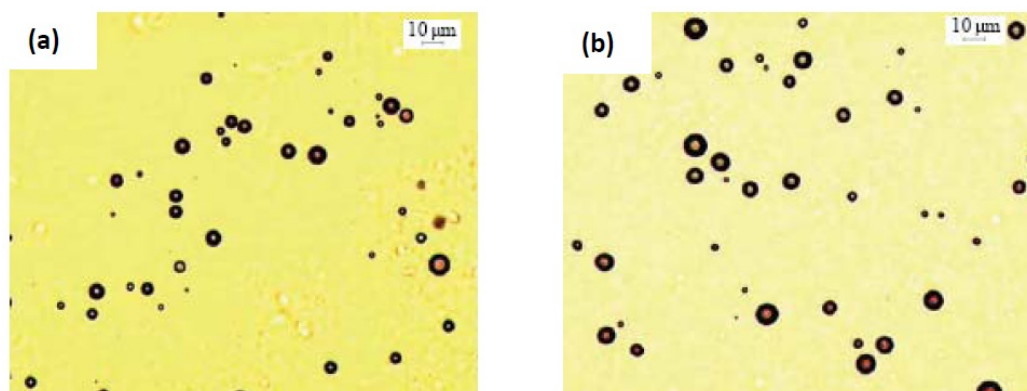
Figure 2.13 Optical micrographs of lipid-coated microbubbles collected at ambient temperature at a flow rate combination of (a) 5 μl s^{-1} : 5 μl s^{-1} and (B) 10μl s^{-1}: 5μl s^{-1} [Farook *et al.* 2009b].

Fig. 2.13 shows phospholipid-coated microbubble suspensions with a mean diameter of 6.6 μm and a standard deviation of 2.5 μm. These bubbles were found to be very stable at ambient temperature, while at human body temperature (37°C), the mean bubble diameter fell rapidly initially and stabilized at 1–2 μm after 20 min [Farook *et al.* 2009a]. The stability of the microbubbles prepared by EHDA can be further improved and the polydispersivity index controlled be adding a dispersant such as Tween to the phospholipid [Farook *et al.* 2009a].

2.10.2.3 Hollow spheres

Chang *et al.* (2009) demonstrated that using a volatile liquid (perfluorohexane PFH) instead of air, polymer (polymethylsilsesquioxane, PMSQ) capsules could be generated using co-axial EHDA with an even higher degree of control over their characteristics. It provides a means of controlling the content of the capsules via heating the suspension to the boiling point of the PFH (**Fig. 2.14**).
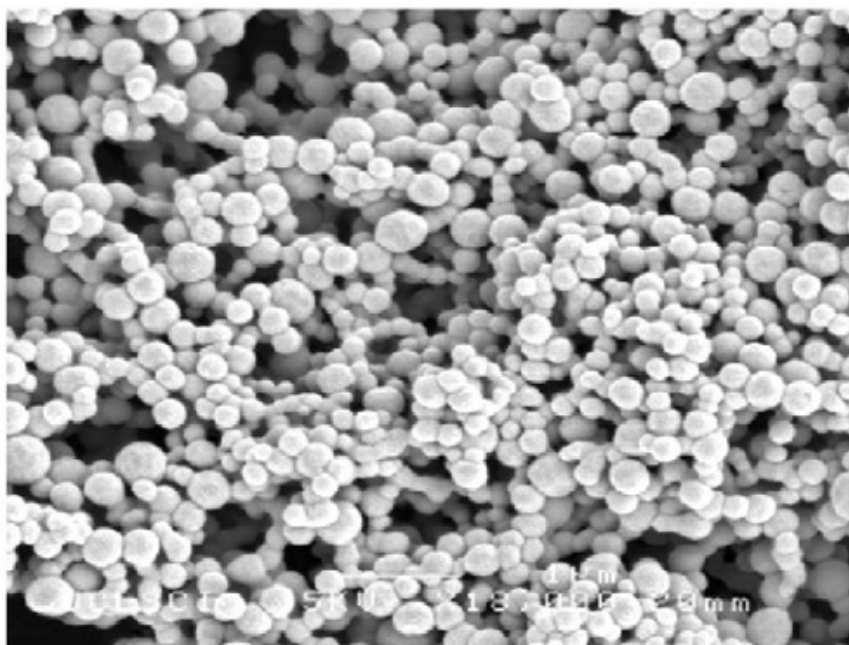
Figure 2.14 SEM micrograph of PFH encapsulated in PMSQ after 48 hrs drying [Chang *et al.* 2009].

Core-shell particles were obtained in a single step, which is clearly preferable compared with multistep processes such as emulsification. Dye encapsulation was

achieved by evaporation of the PFH core to enable inward diffusion of the liquid [Chang *et al.* 2009]. This method has been further developed for the preparation of monoporous hollow microspheres [Chang *et al.* 2010] which provide high effective diffusivity [Guan *et al.* 2007]. Chang *et al.* showed that the geometry and the porosity of these microspheres with or without a single surface pore can again be controlled by varying the process control parameters of the co-axial system. Among these, the flow rate plays a significant role in the final structure which can be varied to control the pore size of the hollow microsphere.
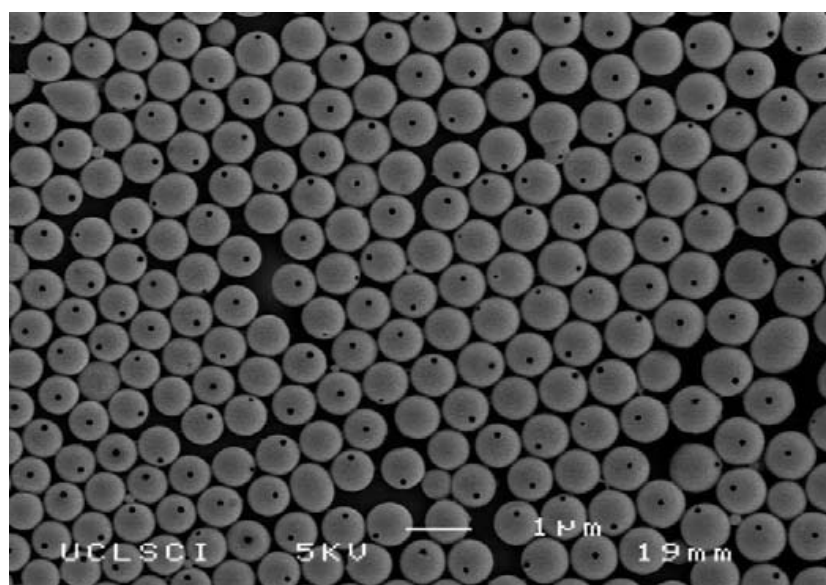
Figure 2.15 SEM image of the one-hole microspheres (PMSQ flow rates at 600 μl min^{-1} and PFH was fixed at 300 μl min^{-1}) [Chang *et al.* 2010].

The formation of the surface pore occurs during the spraying process and may be attributed to evaporation flux of the perfluorohexane solvent (**Fig. 2.15**). This method overcomes several processing challenges associated with the existing methods of fabricating this type of structure; for example, requirement for highly specialised equipment, presence of highly controlled processing environment and the use of surfactants and other additives [Guan *et al.* 2007]. The size of the prepared monoporous hollow spheres ranged from 275 to 860 nm with the pore size of 35 to 135 nm. The ability to tune the pore size of the monoporous hollow sphere through the co-axial EHDA system is of interest for applications in the areas of drug/gene delivery vehicles, targeting, and catalysis.

2.10.3 The application of multi-capillary EHDA

Different combinations of needles provide versatile capabilities of encapsulation. Ahmad *et al*. (2008) showed the flexibility of using three co-axially arranged needles to form a variety of novel morphologies (**Fig. 2.16**).
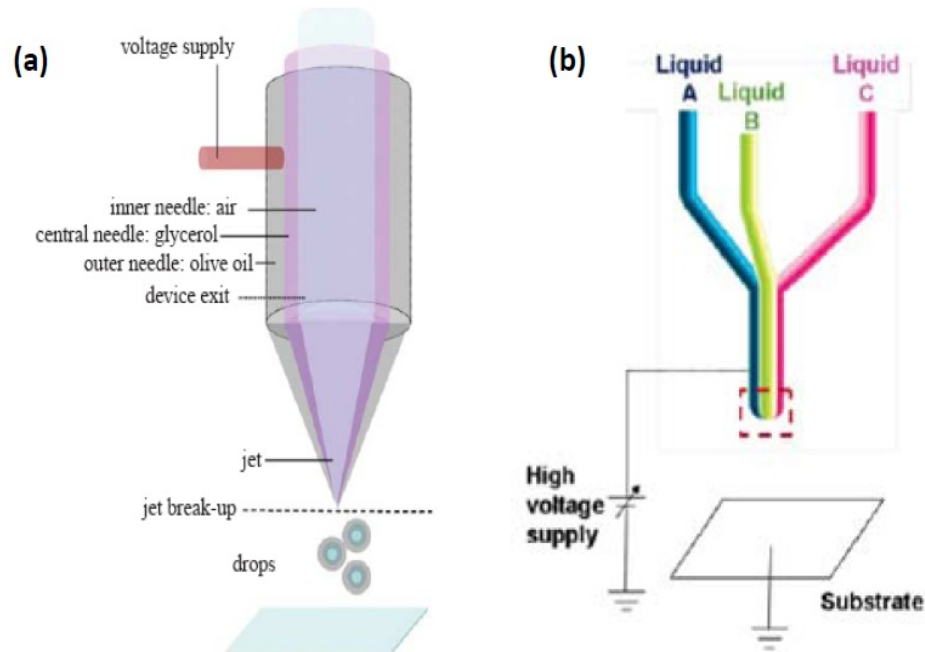
Figure 2.16 Schematic representation of the experimental set-up used for three needles set of (a) concentric arrangement and (b) co-planar arrangement [Ahmad *et al.* 2008, Roh *et al.* 2006].

The resulting electrohydrodynamic flow enables the preparation of: double-layered bubbles, porous encapsulated threads and nanocapsules containing three layers (**Fig. 2.17**). The ability to process multilayered structures can provide multistage controlled release [Ahmad *et al.* 2008], and *in situ* encapsulation of nanoparticles, liquids and/or gases [Ahmad *et al.* 2008, Kalra *et al.* 2009]. However, it is not necessary to arrange the needles concentrically. Langer and Yamate (1969) used two droplets with opposite charges emitted from two separate capillaries and demonstrated that microcapsules can be obtained due to Coulomb attraction [Langer and Yamate 1969]. Borra *et al.* (1997) utilized this idea to develop a chemical reactor for different reacting compounds [Borra *et al.* 1997].
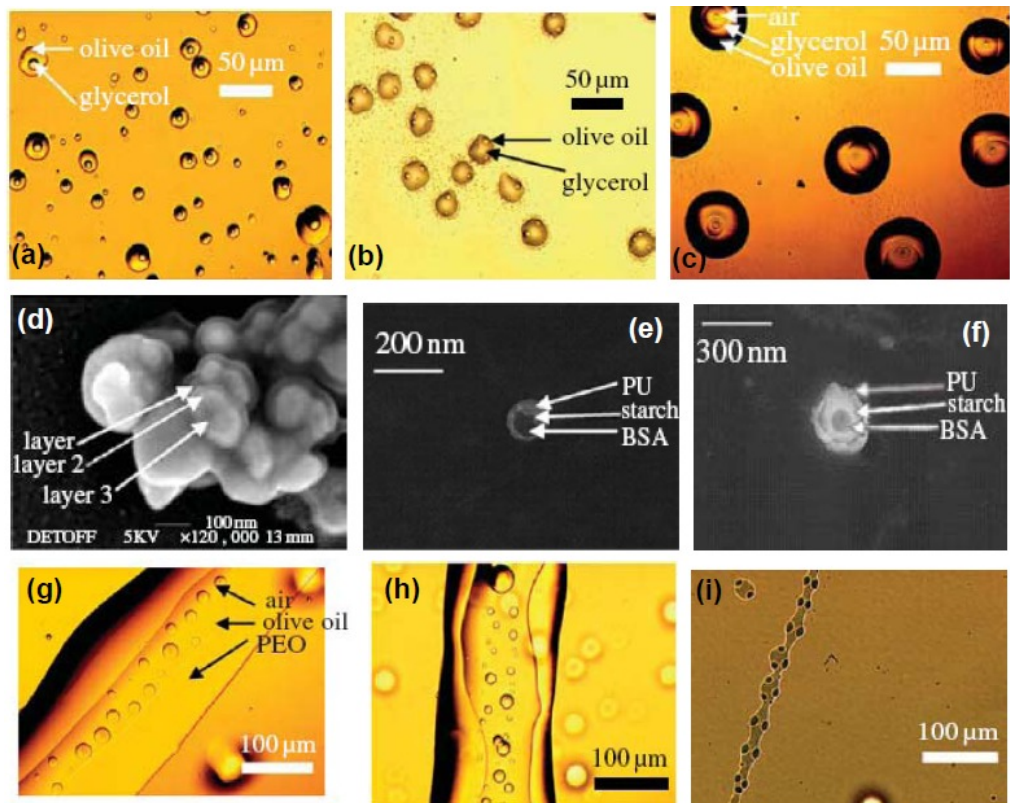
Figure 2.17 Droplet, nanocapsule and thread formation using two- and three-needle co-axial devices. (a) co-axial two needle product with olive oil and glycerol; (b) non-concentric co-axial two-needle encapsulation; (c) co-axial tri-needle encapsulation with air, glycerol and olive oil; (d) high magnification scanning electron micrograph of nanocapsules showing different regions (densities); (e) transmission electron micrograph of nanocapsule with non-concentric multiple layers; (f) transmission electron micrograph of nanocapsule with concentric multiple layers; (g) air encapsulation in twin-layered thread with olive oil and PEO solution; (h) instabilities during thread formation; and (i) two-needle (third needle switched off) co-axial non-concentric thread encapsulation using olive oil and PEO solution [Ahmad *et al.* 2008].

Furthermore, by reducing the coplanar distance of two needles, biphasic nanocolloids can be used as anisotropic imaging probes with short-term biocompatibility [Yoshida *et al.* 2007]. The concept of electrified co-jetting was further extended by Roh *et al.* (2006) and triphasic nanocolloids with three distinct compartments were obtained by simultaneous injection of three distinct liquid flows [Roh *et al.* 2006] (**Fig. 2.16b**).

2.11 Polymers and drug delivery systems

Polymers, the most versatile class of materials, have been widely used in drug delivery systems [Li and Vert 1999]. Polymers can be degradable or non-degradable. The use of biodegradable and biocompatible polymers for the administration of therapeutic agents has been increased rapidly. Biodegradable polymers can be either natural or synthetic. In general, synthetic polymers have several advantages over natural polymers as their properties can be tailored and they have lower toxicity. An important point to consider when choosing a drug carrier is to match the degradation rate to the needs of the application [Uhrich *et al.* 1999].

As mentioned above, the synthetic polymers used for drug encapsulation often include esters such as poly (lactic acid) (PLA), poly (glycolic acid) (PGA), the copolymer poly (lactic-co-glycolic acid) (PLGA) and poly (ε-caprolactone) (PCL). These are considered as aliphatic polyesters which have attracted much interest as drug carriers due to their biocompatibility and biodegradability. This class of polymers degrade via the hydrolytic cleavage of the ester bonds in their backbone [Fu *et al.* 2000, Sinha and Trehan 2003]. More details about PLA, PGA and the PLGA and PCL copolymers (two copolymers used in this research) are given below.

2.11.1 Poly (lactic acid) (PLA)

The basic monomeric unit of poly (lactide) or poly (lactic acid) (PLA) is lactic acid. PLA can be synthesised by ring-opening polymerization of the cyclic dimer lactide in a moisture-free atmosphere under heat (105-185 °C) and with the use of a catalyst (**Fig. 2.18**).
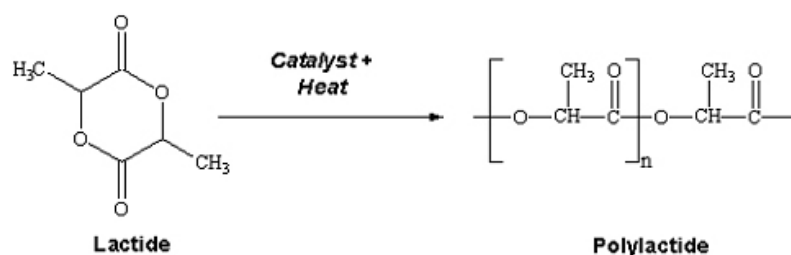
Figure 2.18 Synthesis of poly (lactide) or poly(lactic acid) (PLA).

PLA degrades into water-soluble monomers of lactic acid via hydrolysis of the ester linkage, and also undergoes enzymatic hydrolysis when its molecular weight becomes lower than~10,000 g/ml. The lactic acid eventually becomes incorporated in the tricarboxylic acid cycle (Kerbs cycle) and is excreted by the lungs as carbon dioxide and water. The degradation rate is progressively reduced with an increase in molecular size [Li and Vert 1999, Jalil and Nixon 1990].

2.11.2 Poly (glycolic acid) (PGA)

The synthetic monomeric unit of poly (glycolide) or poly(glycolic acid) (PGA) or glycolic acid, PGA is synthesised from the ring-opening polymerisation of the cyclic dimmer glycolide in a moisture-free process under heat and with the use of a catalyst (**Fig. 2.19**). PGA is semi-crystalline (45-55%) with a high T_m (220-225 °C) and a T_g just below or around body temperature (35-40 °C). Unlike PLA and other polyesters, PGA is not soluble in most common organic solvents due to its high degree of crystallinity, except in highly fluorinated organic solvents. Sutures of PGA lose about 50% of their strength after two weeks and 100% at four weeks. The degradation time for full resorption of PGA could be between 6 and 12 months [Li and Vert 1999, Jalil and Nixon 1990].
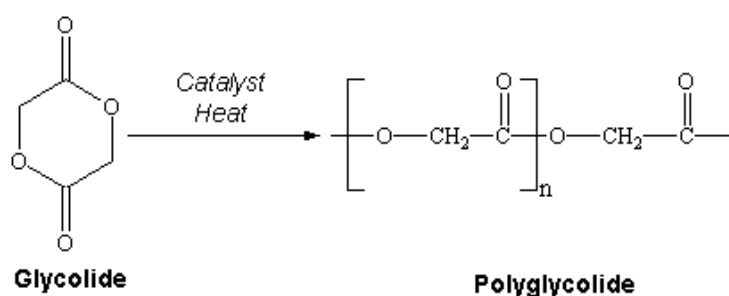
Figure 2.19 Synthesis of poly(glycolide) or poly(glycolide acid) (PGA).

Apart from hydrolytic degradation, PGA is additionally broken down by nonspecific esterases and carboxy peptidase *in vivo* to produce water-soluble glycolic acid. This can then be excreted in the urine or undergo further enzymatic conversion and reaction before eventually entering the tricarboxylic acid cycle (Krebs cycle).

2.11.3 Poly (lactic acid-co-glycolic acid) (PLGA)

Lactic acid is more hydrophobic than glycolic acid and hence lactide-rich PLGA copolymers are less hydrophilic, absorb less water, and subsequently degrade more slowly [Witschi and Doelker 1998]. The physical properties such as the molecular weight and the polydispersity index affect the mechanical strength of the polymer and its ability to be formulated as a drug delivery device. Also these properties may control the polymer biodegradation rate and hydrolysis. PLGA is synthesised by means of random ring-opening co-polymerisation of two glycolic acid and lactic acid monomers. During polymerisation, successive monomeric units (of glycolic or lactic acid) are linked together in PLGA by ester linkages, thus yielding linear, aliphatic polyester as a product (**Fig. 2.20**). The commercially available PLGA polymers are usually characterised in terms of intrinsic viscosity, which is directly related to their molecular weights. The mechanical strength, swelling behavior, capacity to undergo hydrolysis, and subsequently the biodegradation rate are directly influenced by the crystallinity of the PLGA polymer. The resultant crystallinity of the PLGA copolymer is dependent on the type and the molar ratio of the individual monomer components (lactide and glycolide) in the copolymer chain [Jalil and Nixon 1990]. PLGA polymers containing 50:50 ratio of lactic and glycolic acids are hydrolysed much faster than those containing higher proportion of either of the two monomers [Sinha and Trehan 2005].

The T_g (glass transition temperatures) of the PLGA copolymers are above the physiological temperature of 37°C and hence they are glassy in nature. Thus, they have a fairly rigid chain structure which gives them sufficient mechanical strength to be utilised in drug delivery devices. Jamshidi *et al.* have reported that the T_g of PLGAs decreases with decreasing content of lactide in the copolymer composition and decreasing molecular weight [Jamshidi *et al.* 1988].

A three-phase mechanism for the PLGA biodegradation has been reported [Cai *et al.* 2000]:

1. Random chain scission process. The molecular weight of the polymer decreases significantly, but there is no appreciable weight loss and no soluble monomer products formed.

2. In the middle phase a decrease in molecular weight is accompanied by rapid loss of mass and soluble oligomeric and monomer products are formed.

3. Soluble monomer products are formed from soluble oligomeric fragments. This phase corresponds to complete polymer solubilisation.

Lactide   Glycolide   PLGA: poly(lactide-*co*-glycolide)
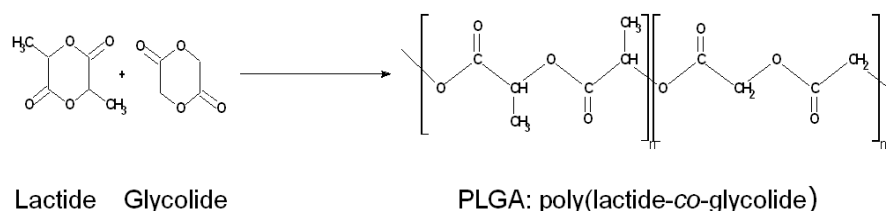
Figure 2.20 Synthesis of poly(lactide-co-Glycolide) or poly(lactic acid-co-glycolic acid) (PLGA).

2.11.4 Poly(ε-caprolactone)

Poly (ε-caprolactone) (PCL) is an aliphatic polyester which is synthesised by the ring-opening polymerization of the cyclic monomer ε-caprolactone (**Fig. 2.21**) [Benoit *et al.* 1999].

ε-Caprolactone   PolyCaprolactone
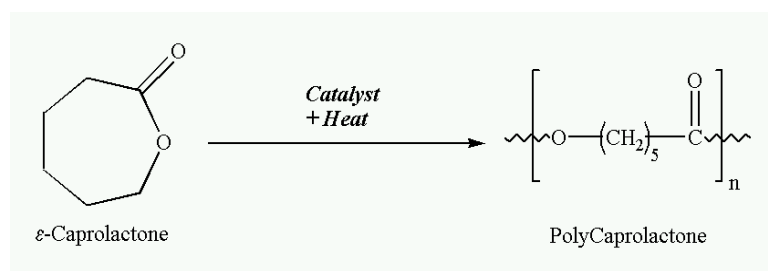
Figure 2.21 Synthesis of poly (ε-caprolactone).

There are various mechanisms which affect the polymerization of PCL and these are categorised as anionic, cationic, co-ordination and radical. Each mechanism is affected by the molecular weight (M_n), molecular weight distribution, end group composition and chemical structure of the copolymers. PCL is a semi-crystalline polymer having a glass transition temperature of −60°C and a melting point ranging between 59 and 64°C, depending upon its crystallinity. The number average molecular weight of PCL samples may vary from 10,000 to 42,500 and it is graded

according to the molecular weight (M_n). PCL is soluble in chloroform, dichloromethane, carbon tetrachloride, benzene, toluene, cyclohexanone and 2-nitropropane at room temperature. It has low solubility in acetone, 2-butanone, ethyl acetate, dimethylformamide and acetonitrile and is insoluble in alcohol, petroleum ether and diethyl ether. PCL can be blended with other polymers to improve stress crack resistance, dyeability and adhesion. Polycaprolactone is used in combination with polymers such as cellulose propionate, cellulose acetate butyrate, polylactic acid and polylactic acid-co-glycolic acid for manipulating the rate of drug release from microcapsules [Chang *et al.* 1986].

2.12 Controlling and regulating drug release profiles

Polymer based controlled release systems are used to reduce the amount of drug required to acheive a given therapeutic effect in patients. The main goal of these systems is to deliver the drug at the target site and to release it at a specified rate over a defined period of time. One strategy to achieve this aim and to increase the efficiency of the system is to control the burst release phase, which is the period of high release rate during the 24 hours following administration. Another strategy is to use external stimuli to non-invasively promote release from carrier particles "on demand". This type of release profile regulation is applicable in pulsatile drug delivery systems. In this thesis, ultrasound is investigated as the external stimulus on account of its excellent track record in medical imaging and various therapeutic applications. The existing literature relevant to both strategies will be discussed in the following sections.

2.12.1 Significance of the burst release in drug delivery systems

It was mentioned earlier **(Section 2.2)** that drug-loaded biodegradable polymer particles have been investigated extensively for their potential to release bioactive agents in a sustained way. However, these particles still suffer from a key technical problem, the 'burst release' **(Fig. 2.22).** It normally occurs over a short time

compared to the whole release profile [Huang and Brazel 2001, Wang *et al.* 2002, Zhang *et al.* 2005, O'Donnell and Mcginity 1997].
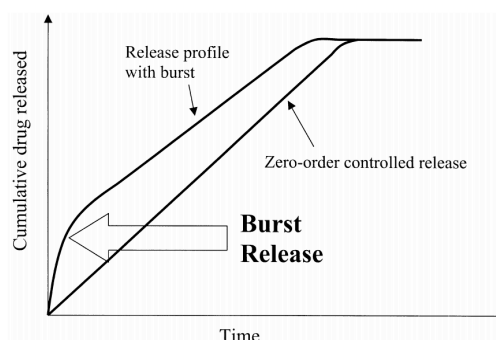
Figure 2.22 The burst release effect in drug delivery systems with a zero-order release pattern [Huang and Brazel 2001].

Table 2.1 Desirable application and negative effects of burst release.

Positive burst release situations	Negative burst release effects
Wound treatment (burst release followed by a diminishing need for drug)	Local or systemic toxicity (from high drug concentrations) and short half-life of drugs
Targeted delivery (triggered burst release)	Economically and therapeutically wasteful of drug
Pulsatile release	Shortened release profile; requires more frequent dosing

This phenomenon can be associated with toxicity and reduces the lifetime of the therapeutic system, making it a major obstacle in the utilisation of these types of delivery system. Hence, burst release is often regarded as an undesirable and negative phenomenon. There are certain situations however, in which rapid initial release may be desirable (**Table 2.1**). For instance, in many pulsatile delivery systems, repeated burst release is one of the objectives, so that the active agent can be delivered rapidly at a specific time. Also, there are some therapeutic agents that need to be administered at different rates. For example, the drugs used at the first

stage of wound treatment, need to have high initial release rates to provide instant pain relief followed by a sustained and prolonged release to help gradual healing [Setterstrom *et al.* 1984]. Few studies have focused on the mechanism of the initial release and the control of this phenomenon. Burst release may be attributed to two causes. First, the heterogeneous distribution of the drug in the polymeric particles. Second, morphology of the drug loaded particles, as the drugs can escape from the polymeric particles through the porous structure that forms during the fabrication process [Huang and Brazel 2001, Yang *et al.* 2001].

However, in most of the previous studies, surface-associated drugs have been identified as the key factor determining the burst release phase [Cohen *et al.* 1991]. This phenomenon mainly occurs due to rapid water intake by the particle surface, which subsequently causes swelling of polymer chains close to the surface and tremendously enhances the diffusion process of the therapeutic agent molecules dispersed in this region. Another reason for the presence of drug on the surface of the drug carrier could be the fact that some drugs become trapped on the surface of the polymer matrix during the fabrication process [Batycky *et al.* 1997]. This happens particularly if the drug loading is too high [Brazel and Peppas 1999]. Also, the diffusion and migration of drugs during drying and storage steps may result in a heterogeneous distribution of drug. For example, as water moves to the particles' surfaces and evaporates, drugs may diffuse by convection with the water, leaving an uneven drug distribution across the particles, with higher concentrations at the surface (**Fig. 2.23**) [Kishida *et al.* 1998, Mallapragada *et al.* 1997].
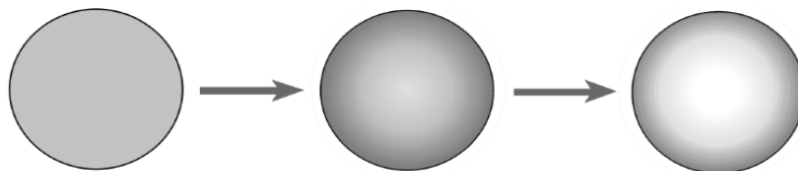
Figure 2.23 Potential drug redistribution due to convection during the drying process.

2.12.1.2 Controlling the burst release phase

Several strategies can be applied for controlling the burst release such as:

Reducing the rate of water intake, this can be performed by increasing the hydrophobicity of the carrier,

Increasing the diffusional resistance to the drug by increasing the length of the diffusion pathways to the drug molecules,

Prevention of drug on the surface of the particles,

These three strategies can be made effective by increasing polymer concentration, manipulating particle size and surface modification [Yamaguchi *et al.* 2002, Huang and Brazel 2001, Ravivarapu *et al.* 2000]. There are various surface modification methods such as:

Surface extraction, this method is effective at reducing burst phase because the drug is removed from the outer layers of controlled release devices, but one important issue is the cost of extraction and the reduction in the effective use of (often expensive) drugs.

Surface modification via chemical couplings, this is a complex procedure which involves two steps: surface activations and coupling reaction.

Surface modification via co-incorporation of surface modifying agents into the particles, in this process, surface modifying agents are co-incorporated into the particle matrix during the particle formulation protocol. This technique involves over night stirring, ultracentrifugation and in some cases elevated temperature which may cause defunctionalisation of the active agent.

Overall, of the suggestions that have been given to prevent burst, many involve additional costly steps, which also result in reduced drug loading percentages and reduced efficiency of the drug delivery system. However, there is other method which is **surface modification via additional coating** which is an effective means of executing all three of the aforementioned strategies, by providing an outer drug-

free layer. This is a cost effective and more efficient method compare to the methods mentioned above. In this coated particulate drug release system, the amount of drug release is controlled by the dissolution or erosion of the outer coat which is applied to the drug loaded polymeric particles (**Fig. 2.24**). Time dependent release of the active ingredient can be obtained by optimising the thickness of the outer coat. However the processing parameters such as the type of the coating agent, the coating method and the concentration of the coating materials should be optimised carefully.
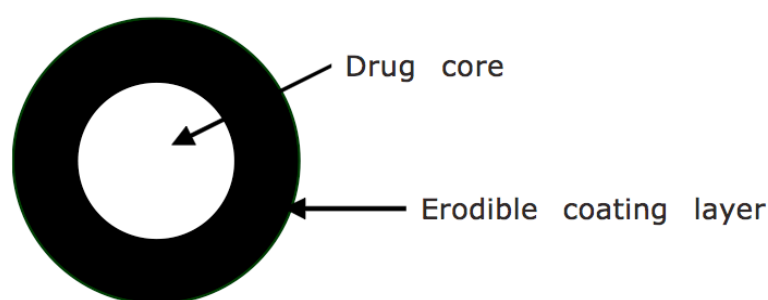
Figure 2.24 Schematic diagram of a delivery system with erodible coating layer.

Because of the important role of the burst release, the final section of this thesis is mainly focused on the study of this phenomenon and how to control it. One of the most important questions in developing controlled release devices is how to control release and to quantify it in advance.

2.12.2 Ultrasound stimulated drug release

Ultrasound is a subsection of acoustics that relates to vibratory or stress waves at frequencies which are higher than the human hearing range i.e., >20 kHz [Wu and Nyborg 2008]. Ultrasound has been used for over 30 years in diagnostic imaging of the body and has been used for other therapeutic applications such as: nerve regeneration [Paik *et al.* 2002, Lazar *et al.* 2001], thrombolysis, fracture healing enhancement [Dalecki 2004, Warden 2003], collagen repair promotion [Demir *et al.* 2004] and drug delivery enhancement including facilitating the delivery of drugs across the skin and delivering chemotherapeutic drugs into tumours.

In ultrasound stimulated pulsatile systems, ultrasonic waves promote the erosion of the polymeric matrix thereby modulating drug release. Miyazaki *et al.* studied the influence of ultrasound (at a frequency of 1 MHz) on the release rates of bovine insulin from ethylenevinyl alcohol copolymer drug delivery systems. They found that insulin release was enhanced by exposure to ultrasound, giving rise to a dramatic reduction in blood glucose level [Miyazaki *et al.* 1988]. Also, Kost *et al.* studied the effect of ultrasound on the degradation of biodegradable polymers (polyanhydrides, polyglycolides and polylactides) and the release rate of the molecules incorporated within those polymers. Up to 20-fold increases in the release rate of the molecules incorporated were observed and the feasibility of ultrasonically augmenting of polymer degradation and drug release were demonstrated [Kost *et al.* 1989].

Table 2.2 Diseases that require pulsatile drug delivery systems.

Disease	Chronological behaviour	Drugs used
Peptic ulcer	Acid secretion is high in the afternoon and at night	H_2 blockers
Asthma	Precipitation of attacks during night or at early morning hour	β_2 agonist, Antihistaminics
Cardiovascular diseases	Blood presure is at its lowest during the sleep cycle and rises steeply during the early morning awakening period	Nitroglycerin, Calcium channel blocker
Arthritis	Pain in the morning and more pain at night	NSAIDs, Glucocorticoids
Diabetes mellitus	Increase in the blood sugar level after meal	Sulfonylurea, Insulin
Attention deficit syndrome	Increase in DOPA level in afternoon	Methylphenidate
Hypercholesterolemia	Cholesterol synthesis is generally higher during night than during day time	HMG CoA reductase inhibitors

A further application of ultrasound is the stimulation of drug release in pulsatile systems. As above, pulsatile drug delivery systems have attracted the attention of many researchers for their treatment of various diseases in which the drug release is required at different time intervals. **Table 2.2** shows some diseases, which need to use pulsatile drug delivery systems.

2.12.2.1 The physiological effects of ultrasound

Ultrasound has two main types of physiological effect upon tissue: thermal and non-thermal. When thermal effects of ultrasound are desired, non-thermal effects will also occur, but via variation of the exposure parameters, non-thermal effects can be obtained in the absence of thermal effects.

Thermal bioeffects of ultrasound: Thermal effects occur with an increase in tissue temperature to 40-45 ^{o}C for more than 5 minutes which can produce a number of responses including: blood flow enhancement, muscle spasm reduction and improved extensibility of collagen fibers [Barnett *et al.* 1994]. Higher temperature rises can lead to protein denaturation and tissue ablation.

Non-thermal bioeffects of ultrasound: Non-thermal effects of ultrasound exposure are predominanly based on two processes: cavitation and acoustic streaming. The former in particular can play significant role in delivering a therapeutic agent to the targeted tissue and is of primary interest in this thesis.

Cavitation is the formation and subsequent oscillation of gas and/or vapour filled bubbles that expand and compress due to ultrasonically induced pressure changes in a medium exposed to ultrasound [Barnett *et al.* 1994]. Although it is still a somewhat contentious area of research, conventionally, two different types of cavitation are defined: ''stable'' or ''non-inertial'' cavitation and ''transient'', ''inertial'' or ''collapse'' cavitation. In stable cavitation, the induced pressure in the medium produces a fairly stable oscillation in bubble size [Marmottant and Hilgenfeldt 2003]. This oscillation produces a circulating fluid flow, called 'acoustic

microstreaming', around the bubbles. In other words, it is the unidirectional movement of fluids along cell membranes. The amplitude of the oscillation controls the velocities and shear rates of microstreaming. For instance, microstreaming is capable of shearing open red cells [Rooney 1970] as well as drug carriers such as liposomes [Marmottant and Hilgenfeldt 2003] at high amplitudes. If the shear stress exceeds the strength of the vesicle, it will rupture and spill its contents.

The other type of cavitation, inertial or collapse cavitation occurs when the ultrasonic intensity increases. For a given bubble size and ultrasound frequency there is a critical pressure above which the inertia of the surrounding fluid cannot be supported by the pressure of the gas inside the bubble during compression [Brennen 1995]. Consequently the bubble collapses violently, producing shock waves and also very high temperatures and pressures (and free radicals due to these conditions) inside the bubble. The collapse process can thus inflict significant damage upon both cells and drug carriers. Smaller bubbles may also be produced by fragmentation of the original bubble during collapse. This then acts as a further cavitation nucleus, growing by absorbing gas from the surroundings, so the process is repeated [Brennen 1995]. In the case of a bubble collapsing near a solid surface, asymmetrical collapse will occur which may produce a high speed fluid jet towards the solid surface [Jenne 2001]. The jet may be strong enough to pierce the surface e.g in the case of a relatively rigid drug carrier. **Figure 2.25** illustrates this type of collapse.
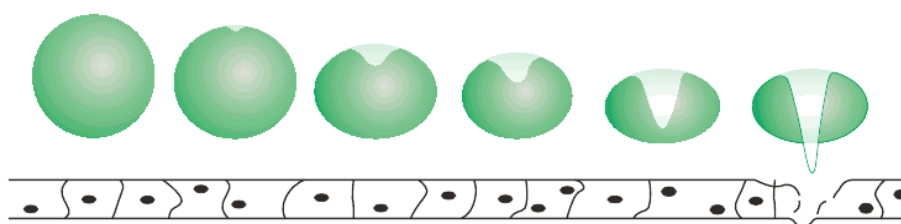
Figure 2.25 Illustration of an asymmetric collapse of a bubble near a surface, producing a jet of liquid towards the surface [Pitt *et al.* 2004].

In addition, the acoustic shock wave caused by collapsed cavitation may enhance drug release rate by damaging the surface of the carrier. Recently, it has been shown

that ultrasound can effectively control drug release from liposomes and micelles by inducing both thermal and non-thermal effects. For instance, the existence of cavitation near the liposomes and micelles was found to enhance drug and gene delivery substantially [Ferrara 2008, Suzuki *et al.* 2007, Unger *et al.* 2001].

The basic mechanism of ultrasound and microbubbles in drug delivery could be summarised as follows: upon exposure of the particles to ultrasound, microbubbles form due to increased temperature and decreased pressure caused by the ultrasound, these microbubbles undergo cavitation, leading to the formation of pores on the surface of the particles, causing the drug to be released to the surrounding medium. The second step is the enhanced permeability of the cellular membrane, most likely as a result of microstreaming, leading to enhanced penetration of the drug into the cells [Lentacker *et al.* 2010].

To conclude, an ideal drug delivery system would be one in which the drug is sequestered inside a carrier until it can be released at the targeted point in space and time. The subsequent chapters in this thesis will describe the investigations conducted with a view to developing a drug delivery system prepared using EHDA consisting of drug loaded particles, whose release profile can be controlled through either an external stimulus (ultrasound) or through a particulate coating.

Chapter 3

Experimental details

3.1 Introduction

This chapter describes the materials and procedures used for the experiments subsequently detailed in this Thesis. The materials used, corresponding suppliers and product details are given. The methods used to characterise the materials and solutions are described. A detailed description of the equipment used in the single and co-axial electrohydrodynamic processing is also given. Finally, the experiments conducted for *in vitro* characterisation of the drug loaded particles are also discussed.

3.2 Materials

The main materials used in the experiments were poly (lactic-*co*-glycolic acid) (PLGA), polycaprolactone (PCL), estradiol and dimethylacetamide (DMAC). Other subsidiary materials used were ethanol, evans blue dye (EB), gelatin, chitosan, ethyl acetate (EA) and simulated body fluid (SBF). Evans blue was used as a model drug and chitosan and gelatin were used as the coating agents.

3.2.1 Poly (lactic-*co*-glycolic acid) (PLGA)

Poly (lactic-*co*-glycolic acid) is a copolymer of glycolic and lactic acid which has been approved by the Food and Drug Administration (FDA) for uses in therapeutic devices because of its biodegradability and biocompatibility. Depending on the ratio of lactide to glycolide used for the polymerisation, different forms of PLGA can be

obtained: these are usually identified in terms of the monomer ratio used. In this research the PLGA copolymer 50:50 Resomer RG503H (Boehringer Ingelheim, Germany) was used with the molecular weight 33000 kDa composed of 50% lactic and 50% glycolic acid.

3.2.2 Polycaprolactone (PCL)

Polycaprolactone (PCL) is an important polymer due to its mechanical properties, miscibility with a large range of other polymers and biodegradability. It has a low melting point of around 60°C and a glass transition temperature of about −60°C. The molecular weight of polycaprolactone used in this work was 14000 kDa and was purchased from Sigma Aldrich (Poole, UK).

3.2.3 Dimethylacetamide (DMAC)

Dimethylacetamide is a colourless, water miscible, high boiling point liquid compound (formula : C_4H_9NO ,molecular weight : 87.12 g/mol, density 0.937 g/cm^3, Sigma Aldrich, Poole, UK) which was used as a solvent in the study.

3.2.4 Ethanol

General purpose research grade ethanol (C_2H_5OH 99%, density 790 kg m^{-3}, molecular weight 46, viscosity 1.3 mPa s, Sigma Aldrich, Poole, UK) was used in this research. The particle collecting slides were covered by a thin film of ethanol as described below in **Section 3.5.2**. In addition, ethanol was also used for the calibration of the characterisation apparatus and for the cleaning of capillary needles which were essential components of the experimental set-up.

3.2.5 Evans blue (EB)

Evans blue, (6,6_-[(3,3_-dimethyl-[1,1_-biphenyl]-4,4_-diyl)bis(azo)]bis[4-amino-5-hydroxy-1,3-naphthalenedisulfonic acid]), is a compound dye. It is usually used as a

diagnostic tool for estimating blood volume. The dye is injected into the bloodstream and after a sufficient period of time samples of the blood are taken to determine the degree of dilution of the dye. However, in the experiments, it was used in the preliminary encapsulation and *in vitro* release studies as the inner encapsulated material. It provided a means of visualising the encapsulation process and detecting the blue inner solution surrounded by the outer polymer solution in different EHDA modes. Also, it fluoresces with excitation peaks at 470 and 540 nm and an emission peak at 680 nm [Hed *et al.* 1983] making it detectable in the *in vitro* release study. It was purchased from Sigma Aldrich (Poole, UK).

3.2.6 Estradiol

Estradiol (linear formula: $C_{18}H_{24}O_2$ and molecular weight of 272.38) was used as a model drug in this research and was also purchased from Sigma Aldrich (Poole, UK). It is the most potent female sexual hormone and represents the major estrogen in humans. Estrogen deficiency due to loss of ovarian function at menopause is mainly responsible for the development of various metabolic abnormalities and such conditions can be made reversible with estrogen replacement therapy. Numerous epidemiological studies suggested that postmenopausal estradiol treatment reduces the risk of cardiovascular disease by up to 50%. This is a significant drug which is used in estrogen replacement therapy for conditions such as female hypogonadism, ovariectomy, or primary ovarian failure, and in treatment of abnormal uterine bleeding, vasomotor menopausal symptoms (such as hot flashes, and vaginal dryness, burning, and irritation) and postmenopausal osteoporosis. Estradiol is sometimes used as part of cancer treatment in advanced breast or prostatic carcinomas [Mittal *et al.* 2007]**.**

Estradiol's primary function is the control of sexual characteristics, but it is also of great importance in the regulation of brain development. Long-term estrogen replacement therapy has proved to be beneficial in the prevention of Alzheimer's disease and in the therapy of schizophrenia [Valles *et al.* 2010].

3.2.7 Gelatin

Gelatin is a natural polymer that is derived from collagen found in animals. It has many applications in the pharmaceutical and medical fields due to its biocompatibility and biodegradability in physiological environments [Ikada and Tabata 1998, Yamamoto *et al.* 2001, Yao *et al.* 2004]. Gelatin has been used widely as an ingredient in drug formulations and as a sealant for vascular prostheses, due to these characteristics [Kuijpers *et al.* 2000a and 2000b]. In this study gelatin from porcine skin (type A) was purchased from Sigma Aldrich (Poole, UK). It was used as a coating agent in the experiments. The manufactured/fabricated PLGA particles were coated with gelatin to investigate its effect upon the burst release phase in the drug release profile.

3.2.8 Chitosan

Chitosan is also a natural polymer with numerous potential biomedical and pharmaceutical applications because of its biodegradability, biocompatibility and non-toxicity. It is a natural linear biopolyaminosaccharide which is derived by alkaline deacetylation of chitin. It is the second most abundant polysaccharide after cellulose. Chitin is the main constituent of defensive cuticles of crustaceans such as, prawns, shrimps, crabs, and lobsters [Felt *et al.* 1998]. In this study, chitosan (75-85% deacetylated) was purchased from Sigma Aldrich (Poole, UK). It was also used as a coating agent because of its biodegradation characteristics. The produced PLGA particles were coated with chitosan solutions with different concentrations again with a view to controlling the burst release phase.

3.2.9 Ethyl acetate (EA)

Ethyl acetate ($C_4H_8O_2$, Molar mass: 88.105 g/mol, density: 0.897 g/cm^3, Sigma Aldrich (Poole, UK)) was used as a solvent in this study. Ethyl acetate is generally recognized as safe by the FDA as a synthetic flavoring substance or adjuvant for food (21 CFR 182.60). EPA's oral reference dose (daily oral exposure likely to be without an appreciable risk of deleterious effects during a lifetime) of ethyl acetate is 0.9 mg/kg/day [Coopman *et al.* 2005 and Pohanish 2002].

3.2.10 Simulated body fluid (SBF)

SBF is a combination of various chemicals that when combined have a similar composition to human blood plasma [Swain and Pattanayak 2008, Oyane *et al.* 2003]. Reagent grade chemicals such as NaCl, KCl, $CaCl_2 \cdot 2H_2O$, $MgCl_2 \cdot 6H_2O$, $NaHCO_3$, K_2HPO_4, $Na_2SO_4 \cdot 10H_2O$, tris buffer (tris-hydroxymethyl-aminomethane, $H_2NC(CH_2OH)_3$) and 1M HCl were used for SBF preparation. The total ion concentrations in SBF are presented in **Table 3.1** [Kokubo *et al.* 1990]. All of these reagents were purchased from Sigma Aldrich (Poole, UK) with analytical grades. Also, the pH of the solution was adjusted to 7.4 using 1M HCl. The preparation procedure is described below.

500 ml of deionised water was put into a one litre polyethylene bottle and covered with a transparent glass lid. The reagents were dissolved one by one in the order given in **Table 3.2** with constant stirring. The temperature of the solution in the bottle was maintained at 36.5°C by being placed in a water bath, and the pH of the solution was adjusted to 7.4 by titration with 1M HCl solution. The total volume of the solution was made up to 1L by adding deionised water.

Table 3.1 Ion concentrations (mM) of SBF and Human blood plasma [Kokubo *et al.* 1990 and Ohtsuki *et al.* 1995].

Ion	SBF	Blood plasma
Na^+	142.0	142.0
K^+	5.0	5.0
Mg^{2+}	1.5	1.5
Ca^{2+}	2.5	2.5
Cl^-	148.8	103.0
HCO^{3-}	4.2	27.0
HPO_4^{2-}	1.0	1.0
SO_4^{2-}	0.5	0.5

Table 3.2 Reagents for preparing SBF [Kokubo *et al.* 1990 and Ohtsuki *et al.* 1995].

Order	Reagent	Amount
1	NaCl	7.996 g
2	$NaHCO_3$	0.350 g
3	KCl	0.224 g
4	$K_2HPO_4 \cdot 3H_2O$	0.228 g
5	$MgCl_2 \cdot 6H_2O$	0.305 g
6	1M-HCl	40 mL
7	$CaCl_2$	0.278 g
8	Na_2SO_4	0.071 g
9	$(CH_2OH)_3CNH_2$	6.057 g

3.3 Characterisation of the solutions

3.3.1 Density

The density of the liquids/solutions used was measured using a 25 ml standard density bottle (VWR International, Lutterworth, UK). The mass of the empty bottle and the mass of the bottle filled with liquid/solution were obtained using an electronic balance (AND HF-1200G A&D Instruments Ltd., Japan). The density (ρ) was calculated as follows:

The mass of the empty density bottle = W_1 g   (3.1)

The mass of the density bottle filled with liquid /solution = W_2 g   (3.2)

Therefore, the mass of liquid/suspension/solution only = (W_2-W_1) g   (3.3)

Therefore, the density of liquid /solution = $(W_2-W_1)/25$ g cm^{-3} (3.4)

The mean value of five such consecutive calculations was taken as the density of liquid/solution and reported in this thesis. Measurements were taken at the ambient temperature (~25 °C) and pressure.

3.3.2 Viscosity

The dynamic viscosities of the solutions were determined using a U-tube viscometer (BS/U type, Schott Instruments GmbH, Germany). A calibrated U-tube (size C, nominal constant 0.03) was used. The time taken for a standard volume of solution to pass through the capillary of the U-tube was noted for five passes and the mean value of the time was calculated. Then, the kinematic viscosity (v) was obtained by multiplying the nominal constant (C) by the time (t):

$$v = Ct \qquad\qquad (3.5)$$

The dynamic viscosity (η) was then calculated by multiplying the kinematic viscosity by the density (ρ) of the solution:

$$\eta = v\rho \qquad\qquad (3.6)$$

If equations (3.5) and (3.6) are combined,

$$\eta = Ct\rho \qquad\qquad (3.7)$$

Ethanol was used to calibrate the viscometer. The mean value of five readings was taken as the dynamic viscosity of the sample. For U-tube viscometers that are not calibrated by manufacturers, use of a calibrating liquid is essential as the viscosity value cannot be calculated without comparing with another liquid.

3.3.3 Surface tension

The surface tension of the solutions was measured using a Kruss Tensiometer K9 (Standard Wilhelmy's plate method). The plate was hung from the hook and the beaker containing the sample was placed on the platform. The plate was completely immersed into the sample whose surface tension was to be measured. The plate was

then gradually lifted and the surface tension value was directly read when the plate was just about to detach from the liquid surface. In order to minimize errors, the plate was cleaned thoroughly with ethanol and dried in a drier before each measurement. The mean values of five readings were taken as the surface tension of the sample.

3.3.4 Electrical Conductivity

Electrical conductivity was measured using a HI-8733 (Hanna Instrument, USA) conductivity probe. The electrode was always cleaned with distilled water and dried before measurements. The electrode was kept immersed in the solution up to the point marked on the electrode for 10 min and the reading shown on the meter was recorded. The mean value of five consecutive readings was taken as the electrical conductivity of the sample.

3.4 Preparation of solutions

3.4.1 Preparation of PLGA solutions

PLGA solutions of different concentrations (2 wt%, 5 wt% and 10 wt%) were prepared by combining appropriate amounts of PLGA polymer and DMAC and mechanically stirring for 900s to obtain clear solutions indicating the total dissolution of the PLGA. 5 wt% PLGA:EA was also prepared for the study described in **Chapter 4**.

3.4.2 Preparation of drug-dye and drug solutions

10 wt% estradiol was dissolved in methanol. To assist visualisation in the preliminary experiments, evans blue dye (0.01g) was dissolved in distilled water (5 ml) and then added to the methanol solution and thoroughly mixed to prepare a drug-dye solution. This was used to determine the feasibility of encapsulating this solution and whether the cone-jet mode was achievable using both the polymer and drug solutions. Subsequently, the drug solution was used without dye.

3.4.3 Preparation of PCL solutions

Appropriate quantities of PCL were dissolved in DMAC. The weight ratio of the polymer to the solvent was 30:70. The polymeric solution was stirred mechanically at the ambient temperature (25 °C) to ensure the polymer had completely dissolved (~15 min).

3.5 Characterisation of generated particles

3.5.1 Optical microscopy

Particles were collected on glass slides covered by a thin film of ethanol for preliminary structural study. An optical microscope (Nikon Eclipse ME 600, Nikon, Japan) was extensively used for all the investigations described in **Chapters 4** and **5**. The measurements were carried out by means of 'Acquis' digital imaging software (Synoptics Ltd., Cambridge, UK).

3.5.2 Scanning electron microscopy (SEM)

The morphology and structure of the prepared particles were determined using a scanning electron microscope (JEOL JSM-6301F field emission SEM). It was equipped with an emitter that can achieve a resolution of ~ 1.5 nm. The accelerating voltage was set at 6 kV and the working distance between the emitter and the sample was 20 mm.

Particles were collected on glass slides covered by a thin film of ethanol for the morphology and structural study but for the degradation studies, particles were kept in SBF and at fixed time points 0.05 ml samples of the solution were taken out and allowed to dry under ambient conditions for 2 h. After that, the glass slides were placed inside a desiccator for further drying for at least two days under ambient conditions before SEM examination.

Since the polymer used for the preparation of particles is nonconductive, the SEM sample was gold coated for 2 min using a sputtering machine (Edwards sputter coater S 1 50B) to enable conduction of the sample surface and avoid charging which can cause damage when gold is used to make surface conductive. The sample was then placed on an aluminium stub with a carbon sticker upon it and was placed in the SEM chamber. The diameter of the particles was measured from the SEM images using the image-processing program UTHSCSA Image Tool (Image Tool Version 2, University of Texas, USA).

3.5.3 Focused ion beam microscopy (FIB)
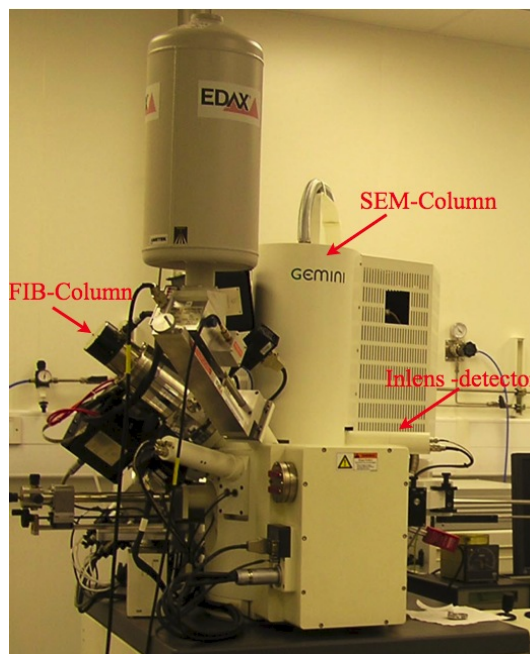
Figure 3.1 Carl Zeiss 1540 XB cross-beam Focused Ion Beam.

The internal structure of the particles was also studied using SEM, in combination with a focussed-ion-beam (FIB) microscope for sectioning the particles (Carl Zeiss XB1540 "Cross-Beam") as shown in **Fig. 3.1**. This system was comprised of a field emission SEM system of top-down Gemini SEM column from Carl Zeiss and an add-on focused ion beam (FIB) system of Orsay Physics Canion 31 FIB column, 54 deg related to the SEM column. Both columns can operate at up to 30 kV. For the FIB studies, particles were collected on glass microscope slides and dried under

ambient conditions (25°C) in a desiccator. Prior to the FIB studies, dried samples were sputter coated with gold for 60 s. The accelerating voltage ranged from 5 to 10 kV during scanning.

3.5.4 Fourier Transform Infrared (FTIR) spectroscopy

Fourier Transform Infrared (FTIR) spectroscopy was used to show the presence of different functional groups of chitosan and gelatin on the surface of the particles. A Perkin-Elmer Spectrum 2000 spectrophotometer was used. A resolution of 4 cm^{-1} and 32 scans were chosen. FTIR spectra were obtained by the KBr disk method. In this method, 200 mg of dried, spectrophotometric-grade KBr powder was used to make each KBr disk. The KBr powder is fused into a transparent disk using a hydraulic press. KBr disks were dried overnight at 110° C and then stored in a desiccator to eliminate moisture interference. After preparation of the KBr disks, the particles were directly electrosprayed for 2 seconds on to the surface of the KBr disks. The samples were kept in a desiccator for 24 hours prior to FTIR spectroscopy.

3.6 *In vitro* release measurement

The release of the encapsulated materials (the dye or the estradiol) from the polymeric particles was determined via two methods: colorimetry and UV spectroscopy. Samples collected in glass vials, containing SBF, were kept at 37°C with continuous stirring. In both studies, at discrete time intervals they were centrifuged for 45 min at 4300 rpm and the entire supernatant was extracted and its absorbance was measured by colorimeter and UV spectroscopy. Fresh SBF solution was added immediately after the solution to be measured was removed. Samples without EB dye and the therapeutic agent were also monitored so that any contributions to the measured absorbance from the polymer could be evaluated. All the measurements were repeated four times.

3.6.1 Colorimetry

EB dye release profile was monitored using a colorimeter (Biochrom Fisher, model 45, operating at an optical wavelength of 580 nm). This instrument measures in absorbance and percentage transmission mode, enabling changes in absorbance over time and reaction rates to be determined. It can be used in the 400 – 700 nm wavelength range as it has an integral, colour coded rotating wheel containing filters at 440, 470, 490, 520, 550, 580, 590 and 680nm.

3.6.2 UV spectroscopy

Estradiol release profiles were also measured using an UV spectrophotometer. In this section a brief description is given about how UV absorption spectra can be used to identify compounds and to measure the concentrations of it in a solution. In UV spectroscopy, light in the ultra-violet wavelength range is transmitted through a sample such as a drug solution. Different components in the sample may absorb certain wavelengths of the light. The amount (intensity) of light absorbed at a given wavelength will thus be related to the concentration of the component in the sample. At sufficiently low concentrations of the absorbing component in the sample, a linear relationship exists between absorbance and concentration of material. This is expressed by the Beer-Lambert law [Mitschele 1996 and Calloway 1997]:

$$A = \log_{10} \frac{I_o}{I} \tag{3.8}$$

$$\log_{10} \frac{I_o}{I} = \varepsilon \, l \, c \tag{3.9}$$

$$A = \varepsilon \, l \, c \tag{3.10}$$

where A is the absorbance, I is the intensity of transmitted light, I_o is the incident intensity, ε is the extinction coefficient of the material (compound in the sample), L is the path length through the sample, and C is the concentration of the species under consideration (mol/ml).

A calibration curve of the amount of light absorbed by a solution versus solution concentration must be prepared and then used to find the concentration of an unknown solution. In order to plot a calibration curve, a number of standard solutions with different known concentrations of the drug compound need to be prepared [Thompson *et al.* 2005, Iglesias *et al.* 2003, Cavrini *et al.* 1989]. A sample of an UV calibration curve is given in **Fig. 3.2**.
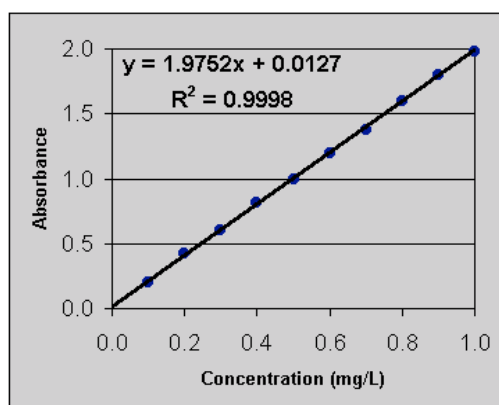
Figure 3.2 A sample of an UV calibration curve.

As previously mentioned, estradiol release profiles were measured using an UV spectrophotometer (UV-2401PC spectrophotometer, Shimadzu). The specifications of the system were as follows: optical system: double-beam, spectral bandwidth: 0.1, 0.2, 0.5, 1, 2 and 5nm, wavelength range: 190 to 900nm, accuracy: ±0.3nm, repeatability: ±0.1nm, photometric readout: absorbance, % transmittance, % reflectance. The first step in calculating drug release and encapsulation efficiency was determining the calibration curve and the second step was finding out the linear range for the relationship between estradiol concentration and the corresponding absorbance. These two steps will be described further in the next sections.

3.6.3 Measuring estradiol encapsulation

The amount of estradiol encapsulated during PLGA-estradiol and PCL-estradiol particle synthesis was determined as follows. Estradiol absorbs light with a wavelength of 280 nm. Different samples with a known concentration of estradiol were dissolved in 50:50 SBF: ethanol (v/v) and the absorbance of each sample was

measured with UV spectroscopy (**Table 3.3**). All the measurements were repeated in triplicate. The spectra of each sample are shown in **Fig. 3.3**.

Table 3.3 Light absorbance (Abs) of estradiol in 50:50 SBF:ethanol with various known concentrations.

Estradiol concentration (mg/ml)	Abs#1	Abs#2	Abs#3	Average Of Abs
0.01	0.733	0.746	0.741	0.740
0.02	1.359	1.311	1.301	1.323
0.04	2.511	2.522	2.518	2.517
0.06	4.013	4.011	4.011	4.011
0.08	5	4.98	4.99	4.99
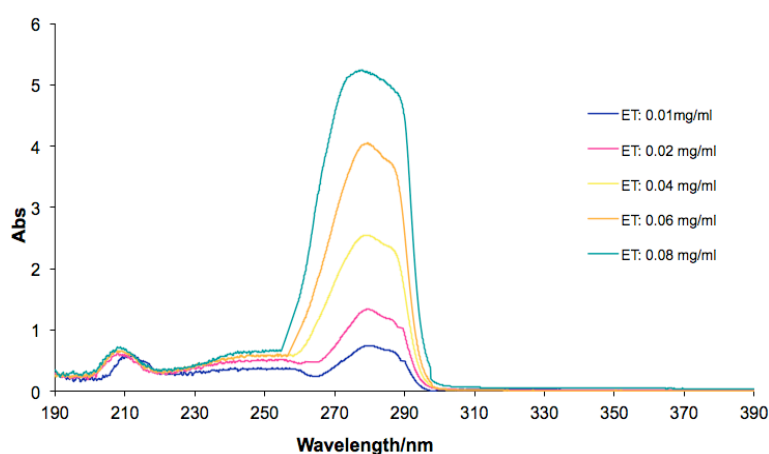
Figure 3.3 UV spectra of SBF:ethanol 50:50 media with different known estradiol concentration.

50:50 SBF:ethanol (v/v) solution was chosen because of the low solubility of estradiol in water or buffered solutions. It was important that the solubility of estradiol was high enough in the release solution so that it would be the rate of drug

release due to polymer degradation and release that was measured, not the rate of estradiol dissolution. The calibration curve for the quantification of estradiol was linear over the range of standard concentrations of estradiol at 0-0.12 mg/ml with a correlation coefficient of R2=0.9963 at light absorbance of 280 nm. The linear relation between estradiol concentration and absorbance is shown in **Fig. 3.4**. The equation between the concentration of estradiol and the absorbance was determined as follows:

$$Abs = 61.296C + 0.1017 \qquad (R2 = 0.9963) \qquad (3.8)$$
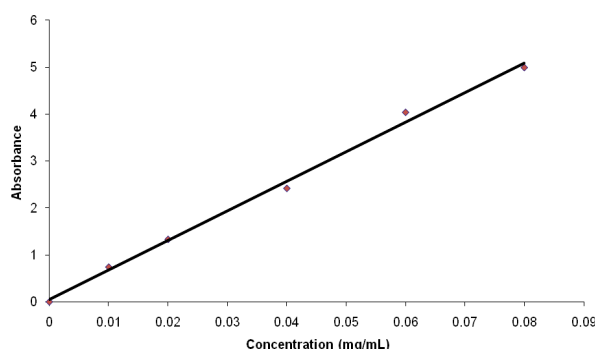
 Figure 3.4 The linear relation between estradiol concentration and absorbance at 280 nm

The amount of unencapsulated drug in the supernatant was measured to determine the encapsulation efficiency. 10 mg of particles were collected in 10 ml release medium and then immediately centrifuged for 45 min at 4300 rpm. The supernatant was drawn out carefully and the concentration of the unencapsulated estradiol in the supernatant was measured using UV spectrometry. The encapsulation efficiency was calculated as the mass ratio between the amount of estradiol incorporated into the particles and that which was used in the particle preparation.

3.7 Ultrasound exposure setup

The effect of ultrasound exposure on the drug release profile was investigated. First, a preliminary study was carried out to study the influence of ultrasound exposure time on the release profile of PLGA particles fabricated via co-axial

electrohydrodynamic processing. PLGA solution of three different concentrations (2 wt%, 5 wt% and 10 wt %) and estradiol were used as the polymeric coating material and encapsulated drug, respectively. The prepared particles were exposed to ultrasound using an ultrasonic cell disruptor (XL2000 Misonix Inc. Farmingdale, NY, USA; probe diameter 3 mm, operating centre frequency 22.5 kHz). Particles were collected in 10 cc SBF:ethanol (50:50) and then gently poured into a waterproof elastic rubber (latex) tube which is relatively transparent to ultrasound at kHz frequencies [Fatemi and Greenleaf 1998]. The tube and the ultrasound probe were immersed in a beaker of water with an estimated distance of 40 mm between them. The probe was held at an angle of approximately 45° to the vertical so that the particles were not directly in line with the probe axis and thus exposed to relatively low intensity ultrasound[1]. Continuous wave ultrasound was applied for either 15 or 30 s, after which the sample was returned to the vial and UV spectroscopy measurements were carried out. Control measurements were carried out to ensure there was no change in the UV spectroscopy readings due to transfer of the particles between the vial and the tube.

---
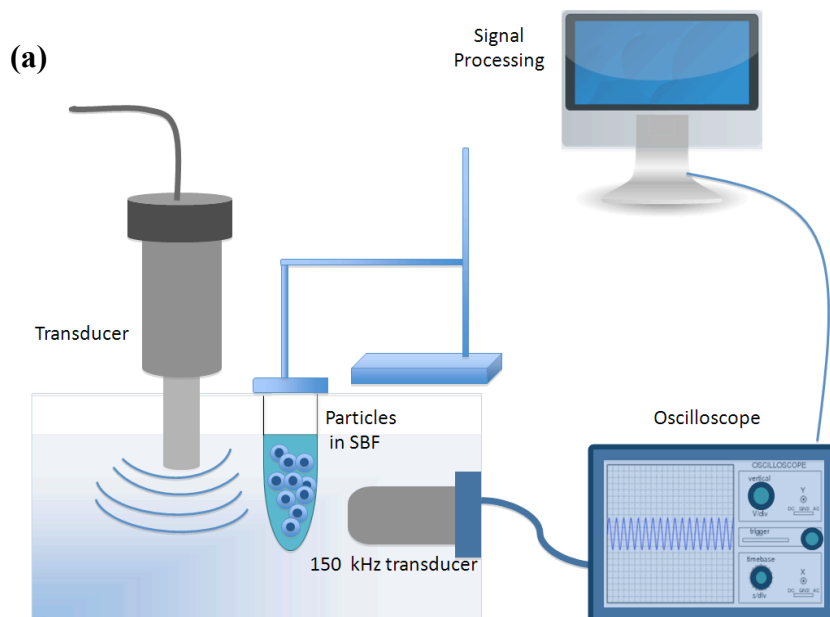
[1] With the available apparatus it was not possible to determine the intensity of the ultrasound to

Figure 3.5 (a) Schematic and (b) real apparatus used for ultrasound exposure and acoustic emission measurements.

After preliminary study, a better understanding of the phenomena involved was required to facilitate a reliable measure of control over the release process. Therefore, more thorough investigations were carried out to elucidate the effects of different ultrasound parameters (duty cycle, intensity and exposure time) on the release profile. For this study, the prepared estradiol-loaded PLGA particles were exposed to ultrasound using a programmable sonicator (Branson Sonifier S250A, Branson Hartford, CT; probe diameter 10 mm, nominal operating centre frequency 20 kHz). The real and schematic experimental set up used in the investigation is shown in **Fig. 3.5a** and **3.5b**. The particle suspensions were gently poured into a waterproof elastic rubber (latex) tube. The tip of the sonicator probe was immersed approximately 1 cm below the water surface. The particles were not directly in line with the probe axis and thus exposed to relatively low intensity ultrasound[2]. Following exposure, the samples were returned to the vial for further spectroscopy measurements. In each case the estradiol concentration in the solution was measured immediately before and after ultrasound exposure. The combinations of exposure

---

[2] Due to the low frequency and intensity of the sound field even at the lowest power setting it was not possible to accurately map the sound field incident upon the particles due to lack of availability of a suitable hydrophone. Hence only relative measurements of the effect of increasing sonicator output power could be made as described below.

conditions (sonicator output power, duty cycle and exposure time) and number of samples per set of conditions are detailed in **Section 5.2**.

3.7.1 Acoustic emissions

In this study, the acoustic emissions from the samples produced during ultrasound exposure were recorded using a broadband unfocussed transducer (Harisonic, Olympus NDT, nominal centre frequency 150 kHz). This transducer was selected so as to measure the non-linear emissions from the microbubbles (3rd harmonic and above) which would be indicative of cavitation activity rather than simply scattering of the sonicator field. The initial experiments indicated that broadband emissions were generated under each set of conditions tested. The transducer was positioned with its axis perpendicular to that of the sample holder and at approximately 45 degrees to that of the sonicator probe. The water in the bath was sonicated several times prior to the start of the experiments so that its dissolved gas content would be much lower than that of the samples and hence the majority of the cavitation activity would originate from these.

The emissions were sampled randomly[3] over the course of each exposure via a digital oscilloscope (LeCroy 9310M Dual 300 MHz) controlled through a computer via a GPIB interface (software written in LabVIEW, National Instruments Corp. Austin, TX, 2007). The signals were subsequently processed using MATLAB (version 7.8.0 (R2009a)) as follows: (i) the frequency spectrum for each captured signal was obtained via Fast Fourier Transform (after normalising each trace with respect to its mean); (ii) signal integration was performed over the frequency range for which the sensitivity of the receiving transducer was constant (for this reason convolution with the transfer function was not performed); (iii) the average and standard deviation emitted energy for each set of conditions (n = 4).

---

[3] Ideally the emissions would have been recorded throughout the exposure with a much higher sampling rate, but this was not possible using the available system. The authors recognise this as a shortcoming of this aspect of the experimental work, the implications of which will be discussed later

3.8 Co-axial and single needle EHDA setup

Needle set-up: In the co-axial EHDA setup, a three-needle stainless steel co-axial device was coupled to a high power voltage supply (Glassman Europe Ltd., Tadley, UK). In this case, the central needle and outer needles were used and the inner needle was disabled. The central needle carried the drug solution, the outer needle was perfused with a given PLGA solution to produce the polymeric carrier. The external and internal diameters of the central needle were 1.5 mm and 0.9 mm and those of the outer needle were 2.8 mm and 1.9 mm, respectively. The tip of the inner needle was held 0.5 mm inside and above the tip of the outer needle. The schematic of the needle configuration is given in **Figure 3.6**. However, in the single needle EHDA setup, the internal diameter of a single stainless steel needle was 600 μm.
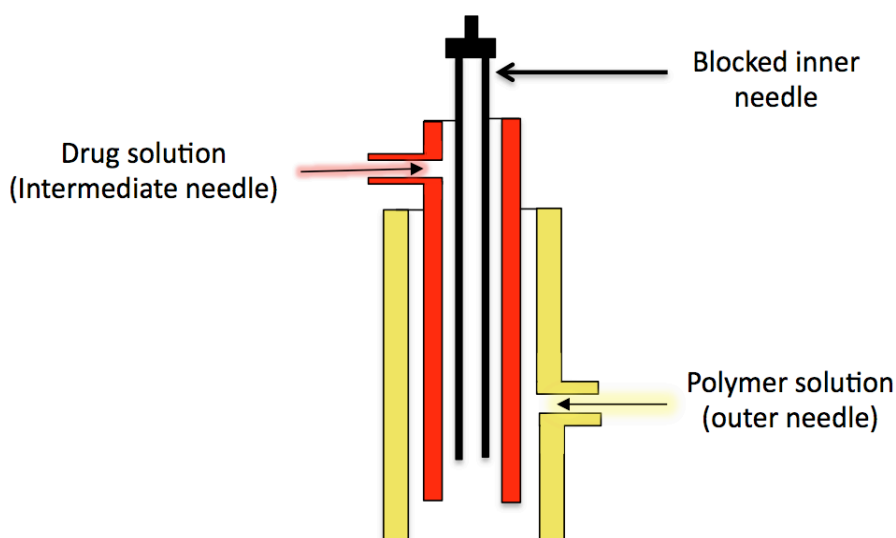
Figure 3.6 Schematic of the needle configuration of co-axial EHDA set-up.

Ground electrode: A ring (inner diameter 15 mm and outer diameter 20 mm) electrode was placed ~30 mm below the tip of the outer needle as shown in **Figures 3.7a** and **3.8b.** The electrical stress is determined by the strength of the electric field between the needle and the ground electrode.

Syringe pumps: The needles were connected by silicone tubing to plastic syringes (BD Plastic™, VWR, Lutterworth, UK) containing the solutions. The flow rates of

the solution through the needles were controlled by high precision Harvard syringe pumps (Infuse/Withdraw PHD 4400 Hpsi programmable syringe pump, Harvard Apparatus Ltd., Edenbridge, UK). The capacity of the syringes used for the solutions were 5 ml. The pumps were calibrated frequently using ethanol. In the co-axial setup, the two liquids were introduced simultaneously into the device using the precision syringe pumps at appropriate at inner and outer needle flow rates of 2 μl/min and 10 μl/min, respectively. This combination of flow rates was determined empirically to provide a suitable compromise between jet stability and the required range of particle sizes.

High voltage power supply: The needles and the ground electrode were connected to a high voltage DC power supply unit (FC30 P4 12w, Glassman Europe Limited, Bramley, UK) using a high voltage power cable. The output voltage range of the unit was 0-30 kV and the output current range was 0-4 mA. At an applied voltage of between 6 and 7 kV between the needles and a ground ring electrode; a stable cone-jet was obtained, with fine encapsulated droplets emerging from the cone apex.

Data recording unit: The jet and droplet formation process was monitored using a LEICA S6D JVC-colour video camera attached to a zoom lens and a data DVD video recorder MP- 600 using CDV Recorder/Editor DN-100 with a video screen for real time monitoring.

The experimental setup used for all the investigations is shown in **Figures 3.7a** and **3.7b**. In co-axial processing, the droplets were collected at a working distance of 20 mm below the device exit directly into glass vials containing 50% simulated body fluid (SBF) and 50% ethanol. Samples were collected for 600 s and were used for the *in vitro* release studies. Specimen samples were also collected on glass slides covered by a thin film of ethanol for microscopy as above. The single needle EHDA setup was similar to the co-axial set up (**Fig. 3.7b**). However, the apparatus consists of a single stainless steel needle which is coupled to a high voltage power supply. The introduction and subsequent flow rate of individual polymeric solutions in the needle were controlled by the high precision syringe pump PHD4400.
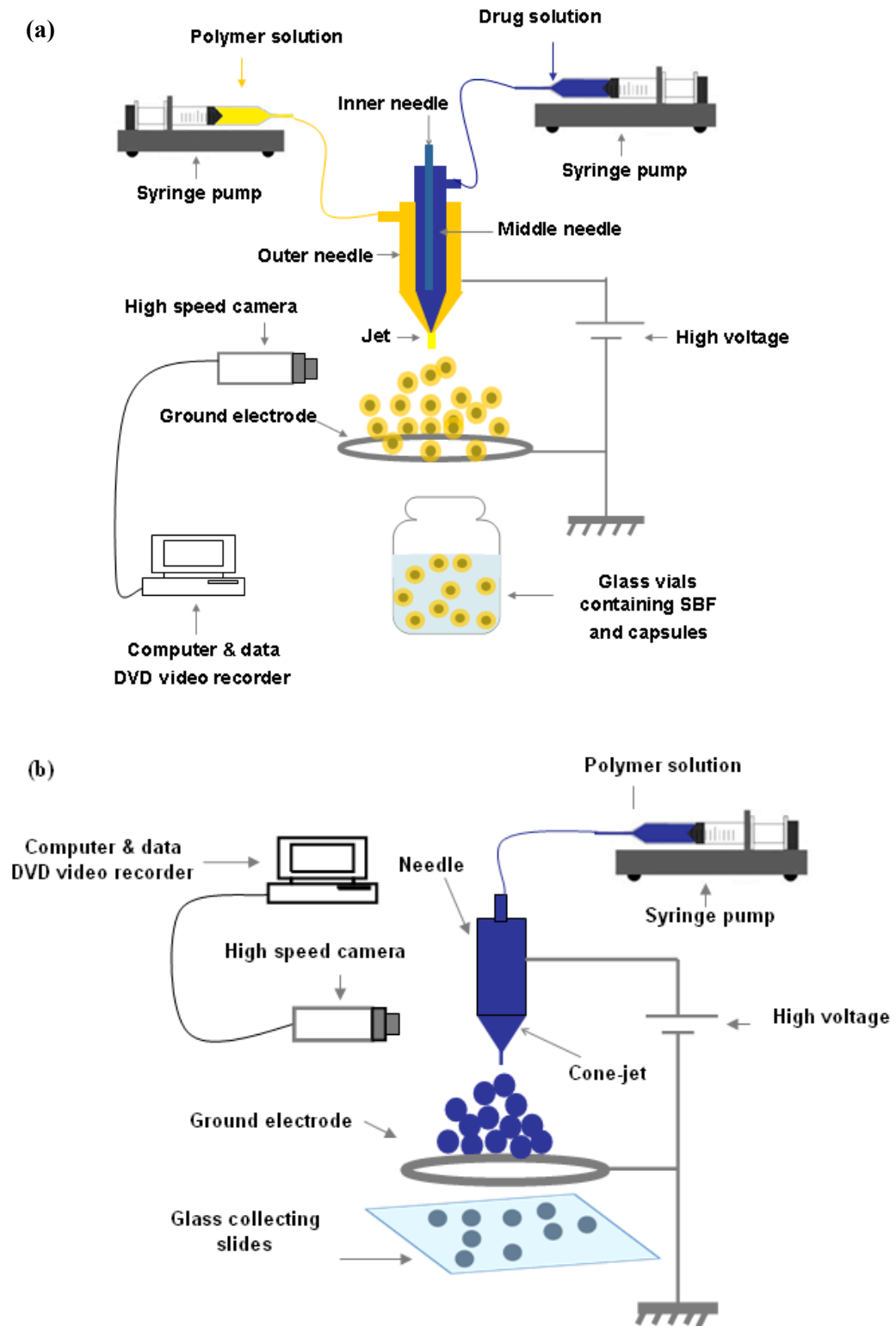
Figure 3.7 Experimental set up used for the production micro and nanoparticles (a) co-axial setup (b) single needle setup.

Chapter 4

Results and discussion

Production of polymeric drug carriers via single needle and co-axial EHDA processing

Overview

Methods for producing particles with a predictable narrow size distribution are in high demand for a wide range of biomedical applications. Therefore, various preparation techniques have been studied with a view to generating drug-carriers with the required size distribution. In this chapter, single needle and co-axial EHDA processing methods were used to explore their capability for preparing polymeric drug carriers with different sizes. In the first set of experiments (**Section 4.1**), the aim was to optimise the combination of several key processing parameters in order to obtain a stable 'cone jet' and subsequently produce polymeric particles with a narrow size distribution. The next set of experiments (**Section 4.2**), investigated the capability of using single needle EHDA processing for the fabrication of polymeric particles with various surface morphologies and shapes. The final set of experiments (**section 4.3**), involved using a co-axial EHDA method to incorporate secondary materials into the polymeric particles and to study the encapsulation process.

4.1 EHDA mode mapping and controlling the size of the fabricated particles via systematic processing parameter variation

4.1.1 Introduction

One of the most important characteristics of drug delivery systems is the size of the constituent particles [Panyam and Ladhasetwar 2003]. This has a significant effect upon different *in vivo* functions of drug carriers such as: circulation time, extravasation, targeting, immunogenicity, internalization, intracellular trafficking, degradation, flow properties, clearance and uptake mechanisms [Mitragotri and Lahann 2009]. For instance, micrometre size particles are important in passive drug targeting such as in pulmonary drug delivery. Nano-size particles have also certain unique applications in drug delivery [Monsky *et al.* 1999] in that they can penetrate small capillaries, allowing enhanced accumulation of nanoparticles at target sites [Lanza *et al.* 2002].

Polycaprolactone was used as a polymer in this study due to its suitability for drug delivery and its biocompatibility and non-toxicity [Murthy 1997]. It was dissolved in DMAC (solvent) and the weight ratios of the polymer to the solvent were as follows; (PCL:DMAC) 2:98, 5:95 and 10:90. A systematic investigation of the effects of several key processing parameters specifically: voltage, flow rate, solution properties (such as viscosity and electric conductivity) and polymer concentration on the modes of EHDA processing was carried out and a range of operating parameters were identified for the ideal processing window of stable jetting (cone-jet). Also, it was determined how the size and size distribution of the particles generated can be controlled by systematically varying the polymer concentration in the solution (and thereby its viscosity and electrical conductivity). In the final section, 15 wt% estradiol was also added to the individual solutions. Estradiol is the drug which was used in all the experiments in this thesis. As mentioned in **Section 3.2.6**, it is one of the main estrogens in human body that has several applications in the treatment of different diseases. Estradiol loaded PCL particles were produced and the effect of estradiol loading on particle size and morphology was studied.

4.1.2 Characteristic of PCL solutions with various concentrations

The electrohydrodynamic process by which the particles are produced is governed by the physical properties of the solutions (such as surface tension, viscosity, density and electrical conductivity), and also on the processing parameters (flow rate and applied voltage). Different combinations of these variables enable the generation of different jetting modes [Cloupeau and Prunetfoch, 1990]. Therefore, the first step was to characterise the properties of the solutions used (**Table 4.1**).

Table 4.1 Properties of the solutions and solvents used in this study.

Sample	Density (kg m^{-3})	Viscosity (mPa s)	Surface tension (mN m^{-1})	Electrical conductivity (μS m^{-1})
DMAC	940	2.0	29	5.6
PCL:DMAC 2:98	946	2.6	29	3.4
PCL:DMAC 5:95	951	4.6	29	1.8
PCL:DMAC 10:90	958	11.1	32	0.8
PCL:DMAC 2:98 + 15% ET	947	2.6	29	4.1
PCL:DMAC 5:95+15% ET	951	4.6	29	2.5
PCL:DMAC 10:90+ 15% ET	958	11.2	32	1.1

The electrical conductivity of the solutions decreased more than four times as the concentration of the polymer increased up to 10 wt% from 2 wt% due to the insulating characteristics of PCL. Polymer solutions which were further mixed with estradiol demonstrated a slight increase in their electrical conductivities when compared to their parent solutions, suggesting that estradiol causes an increase in the

electrical conductivity, while PCL reduces the electrical conductivity. The density of the solutions did not change significantly in samples with different polymer concentrations but the viscosity increased significantly as a function of this concentration.

4.1.3 Classification of EHDA jetting modes of the PCL polymeric solutions
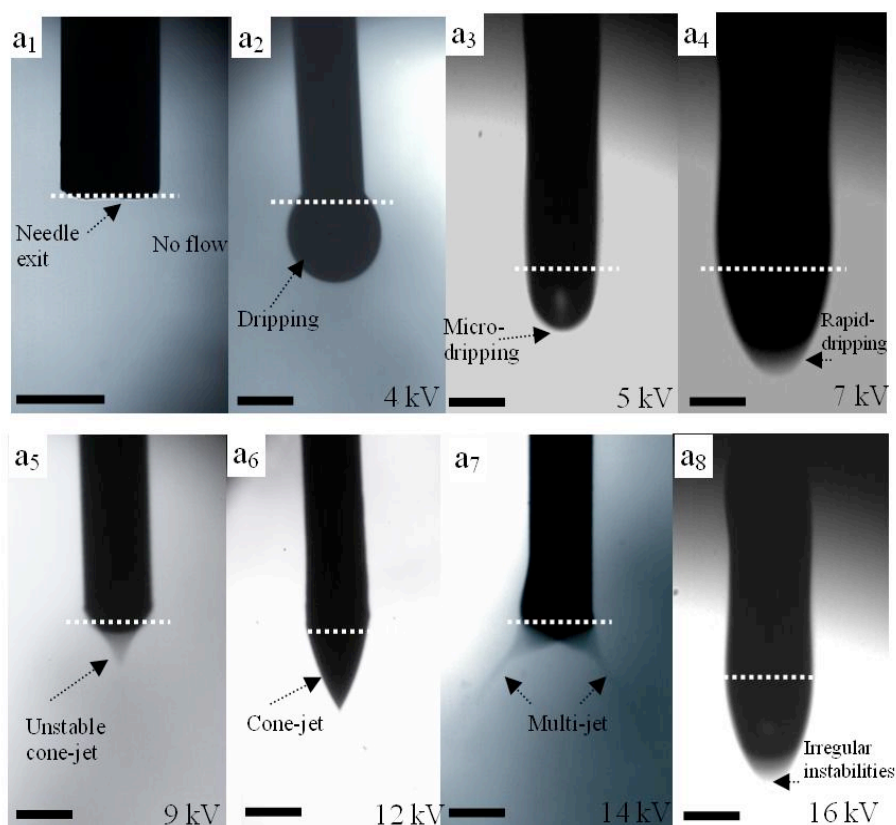
Figure 4.1 Flow of 5 wt% PCL solution under an electric field showing with flow rate set at 10 µl/min, (a_1) no flow (a_2) dripping mode (a_3) micro-dripping mode (a_4) rapid dripping mode (a_5) unstable cone-jet mode (a_6) stable cone-jet mode and (a_7) multi-jet mode (a_8) irregular instabilities mode. Scale bar= 600 µm.

The geometrical features of the jet and the various types encountered as a function of operating parameters, including the electric field, have been classified into various modes [Jaworek and Krupa 1999a]. These include dripping, microdripping, rapid microdripping, unstable cone-jet, stable cone-jet, multijet and irregular instability modes (5 wt% PCL and flow rate: 10 µl/min) (**Fig. 4.1**).

The cone-jet is the most stable and the most used mode, as it generates a near uniform particle size distribution [Cloupeau and Prunetfoch, 1990]. In this study, the 'dripping mode' (0-4 kV) did not differ significantly from dripping under electrically neutral conditions. The drops took the shape of regular spheres detaching from the capillary as the gravitational force (and the small electric force) overcame surface tension (**Fig. 4.1a$_2$**). An increase in the voltage stabilised and shaped the 'cone-jet' (9.5 -12.5 kV) (**Fig. 4.1a$_6$**) which results as a balance of liquid pressure, liquid surface tension, gravity, electric stresses at the liquid surface, the liquid inertia and the liquid viscosity [Hartman *et al.*, 2000]. Further increasing the voltage (13-15 kV) caused 'multijet modes' to evolve. When irregular instabilities are encountered, one possible form the jet can take is shown in **Fig 4.1a$_8$**, where intermittent droplet formation occurs. Although the images may look similar there is a considerable difference in the stability in real time compared with rapid dripping (**Fig 4.1a$_4$**), (due to technical shortage, the high speed camera was not able to capture many frames per second; therefore it was harder to frame the irregular instability mode).

4.1.4 Parametric mode maps of applied voltage *vs.* flow rate for three different polymer concentrations

EHDA modes were investigated in detail for three different polymer concentrations. The most appropriate processing parameters to obtain the desired cone-jet were also determined. The findings are presented as maps in the parametric space of applied voltage vs. flow rate (**Fig. 4.2**). Mode mapping of these solutions showed that in more viscous solutions the upper and lower limits of the voltage required for forming the stable cone-jet increased. For instance, at a flow rate of 2 µl/min, the lower limit of the applied voltage for the least viscous solution (2.6 mPa s) was 7.5 kV, whereas that for the most viscous solution (11.1 mPa s) was 11 kV (**Fig. 4.2d**). This is due to the lower conductivity and higher surface tension of the more viscous solutions. Therefore, a stronger and dominant electric field (voltage) needed to be applied to overcome the surface tension and liquid viscosity to form a cone jet [Li and Yin 2006].
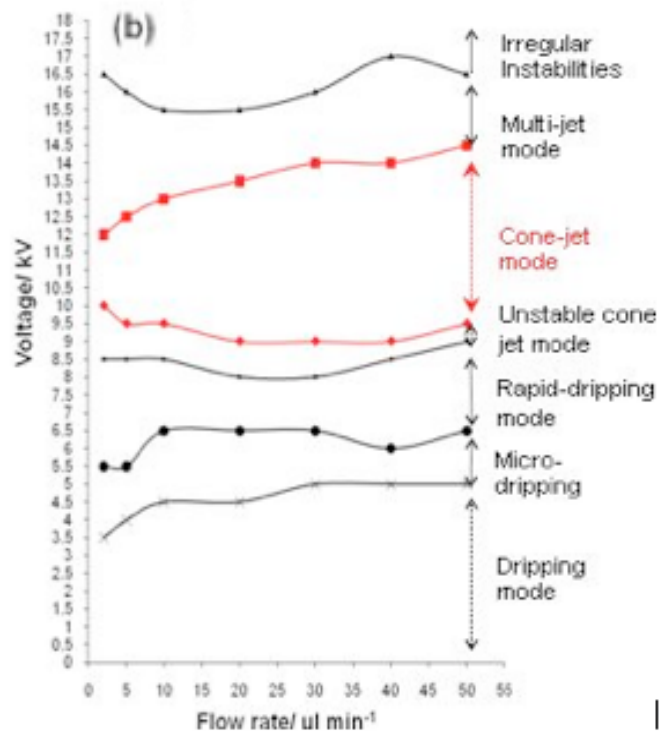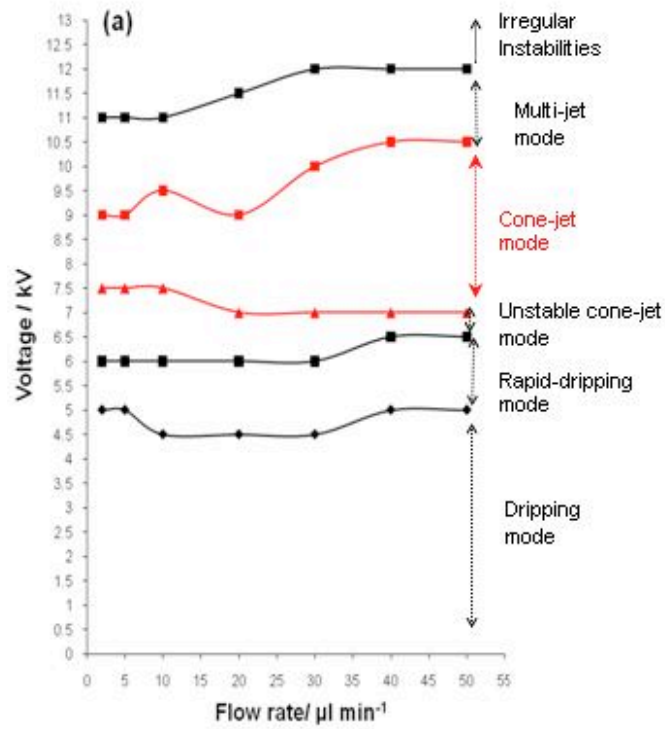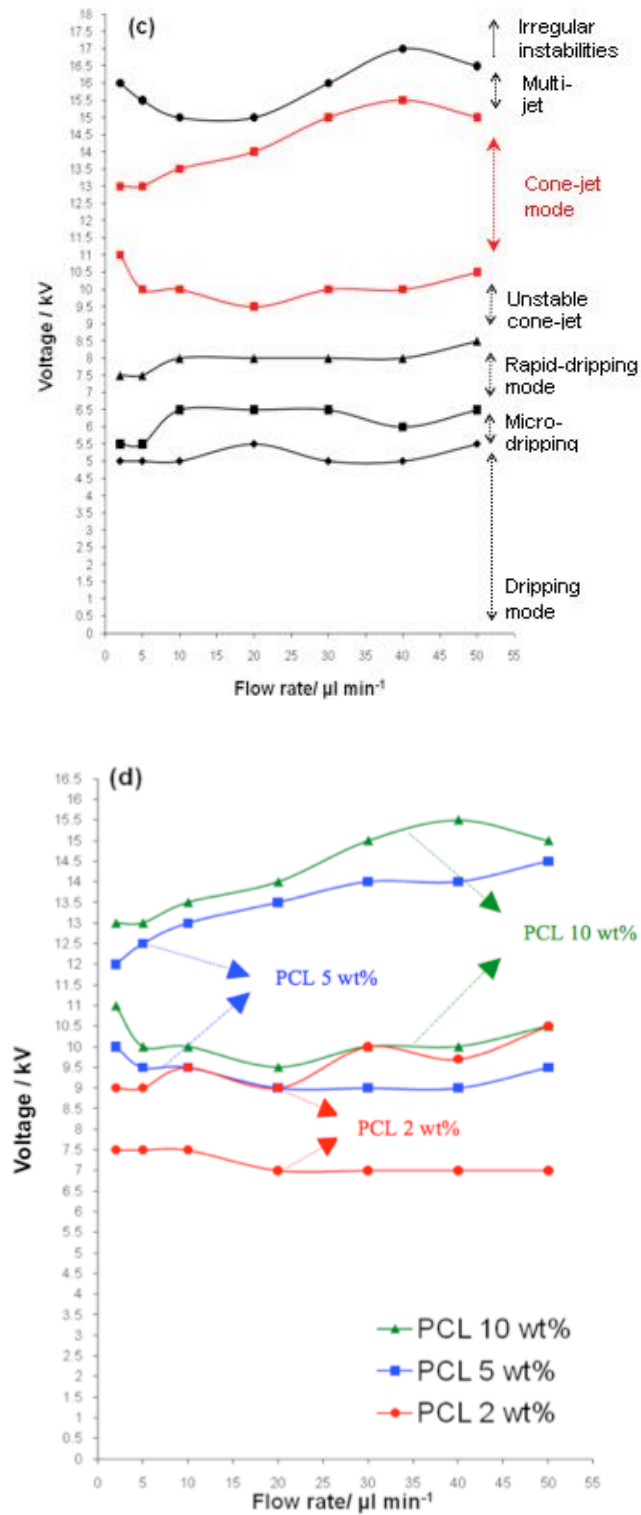
Figure 4.2 Operating ranges in order to obtain different spraying modes (a) PCL:DMAC 2:98 (wt%) (b) PCL:DMAC 5:95 (wt%) (c) PCL:DMAC 10:90 (wt%). (d) Comparison of the cone-jet mode region of different solutions.

In less viscous solutions the regions for different jetting modes occupied a smaller area in the parametric space and transition between modes occurred more quickly as the applied voltage is increased (**Fig. 4.2a, 4.2b** and **4.2c**). The cone jet area increased as the flow rate increased, and this could be due to the presence of a greater volume of liquid which maintains the balance between the surface tension and electrical forces.

4.1.5 Effect of applied voltage and flow rate on the mean size of the particles
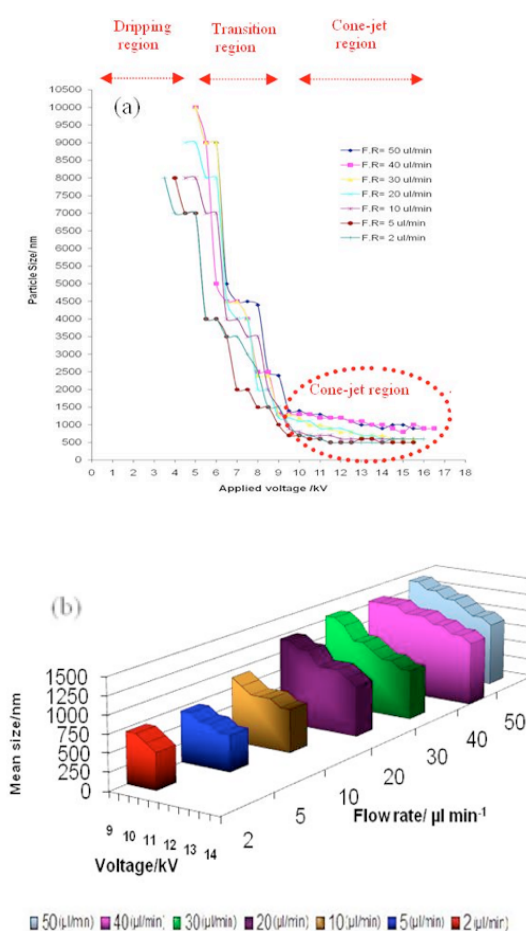
Figure 4.3 Variation of mean particle size obtained as (a) a function of applied voltage and flow rate and (b) highlighting the cone-jet region for PCL:DMAC 5:95 wt% solution.

In this section, the effect of applied voltage and flow rate on the mean size of the particles was studied (**Fig. 4.3a**). Prior to the attainment of the stable cone-jet region,

the reduction in droplet size was enhanced by increasing the voltage as the mode of jetting changed from dripping to unstable cone-jet. The size of droplets electrosprayed from the stable-cone jet was found to decrease as the applied voltage increased but this phenomenon was more noticeable at higher flow rates, for instance the mean size of particles produced from PCL 5 wt% decreased from 700 nm to 500 nm at 2 μl/min flow rate as the voltage increased (10 kV to 12 kV), whereas at 50 μl/min flow rate, the mean size reduced from 1400 nm to 900 nm (**Fig. 4.3b**). This is because at a lower flow rate insufficient solution was available to affect the electrohydrodynamic forces on the droplet, [Pancholi *et al.* 2008] thus the appropriate range of applied voltages for forming the cone-jet was narrow and as a result, the influence of applied voltage on particle size was relatively small.

4.1.6 Effect of viscosity on size, size distribution and polydispersivity index

Droplet diameter is known to be greatly influenced by the processed solution viscosity [Jayasinghe and Edirisinghe 2002]. The mean size of the particles obtained with solutions with different viscosities (PCL:DMAC 2:98 (2.6 mPa s), PCL:DMAC 5:95 (4.6 mPa s), PCL:DMAC 10:90 (11.1 mPa s)) is shown in **Fig. 4.4**.
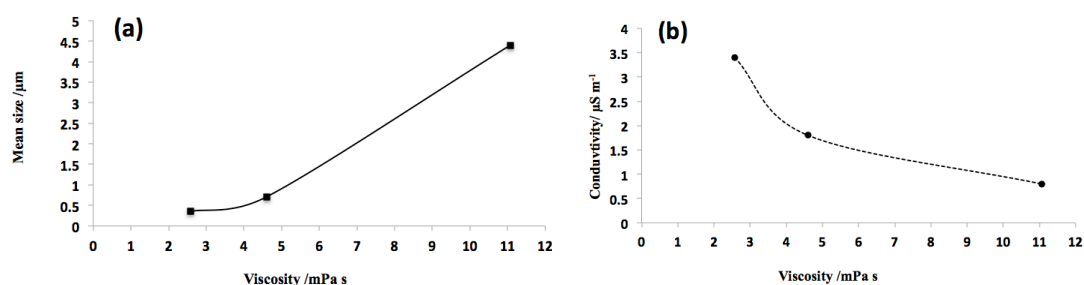
Figure 4.4 Relationship between mean particle size generated, the electrical conductivity with the viscosity of the PCL solutions used (flow rate: 10 μl/min, applied voltage: 10 kV).

As the concentration of PCL was varied from 2 to 10 wt%, the viscosity and the electrical conductivity of the PCL solutions changed from 2.6 (mPa s) to 11 (mPa s) and from 3.4 ($\mu S\ m^{-1}$) to 0.8 ($\mu S\ m^{-1}$), respectively. This also results in an increase in mean particle size from 300 nm to 4.5 μm. This is due to the local shear viscosity

decreasing sufficiently and resulting in the formation of smaller droplets under the action of electrohydrodynamic forces [Jaworek and Krupa 1999b]. The particle size distributions are shown in **Fig. 4.5**. All the samples displayed monomodal size distributions; however, the more viscous solutions generated a narrower distribution.
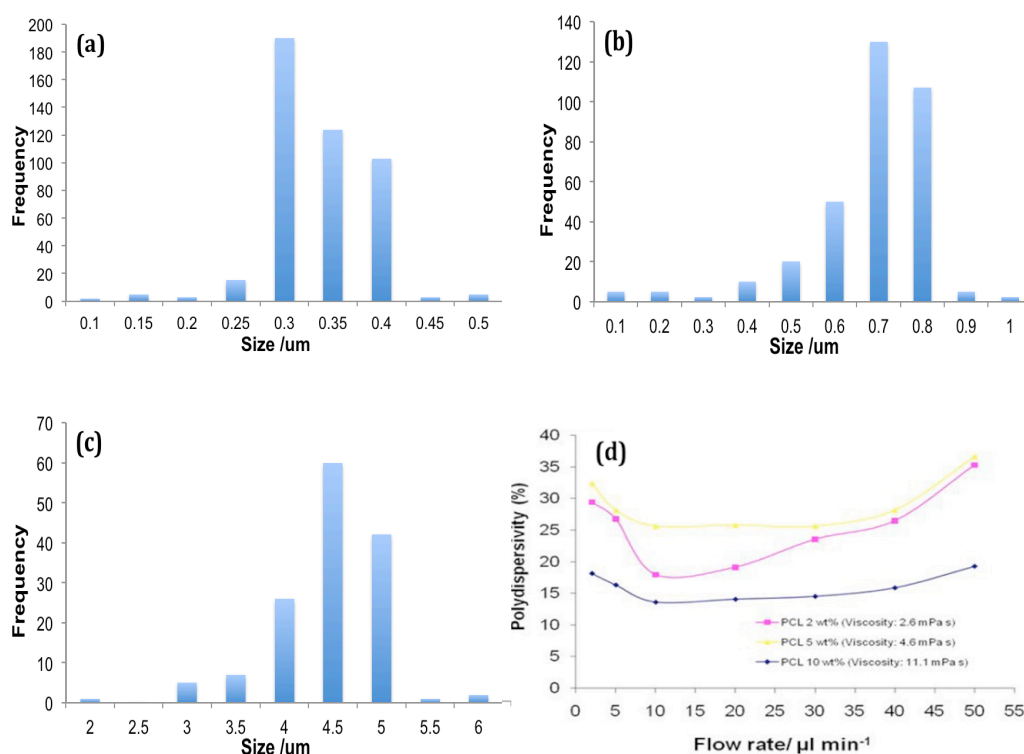
Figure 4.5 Size distribution of PCL particles produced using different concentrations of PCL solution (a) PCL 2wt%, (b) PCL 5wt%, (c) PCL 10wt%, (flow rate: 10 μl/min, applied voltage: 10 kV), (d) Polydispersivity index of particles produced in the cone-jet region as a function of flow rate (applied voltage: 10 kV).

Further investigations were carried out to determine the impact of viscosity and flow rate on the polydispersivity of the samples. It was observed that the polydispersivity index increased at the upper and lower limits of flow rate for the stable cone-jet region and this influence was more noticeable at lower viscosities (**Fig. 4.5d**). This may be attributed to the reduced stability of the cone-jet in these zones which can dictate the size distribution of the generated morphologies. With the increase in flow rate, the charge on the liquid jet increases, and the repulsion force due to the electric charge competes with the surface tension of the liquid. With much higher surface charge, the repulsion force of the charge becomes stronger, resulting in jet oscillation

which produces satellites droplets [Hartman *et al.* 2000]. Therefore, the number of satellite droplets and secondary droplets depends on the liquid flow rate and their quantity will increase at higher flow rates, which in turn results in a higher polydispersivity index [Hartman *et al.* 2000].

4.1.7 Effect of drug loading on the size and morphology of the particles
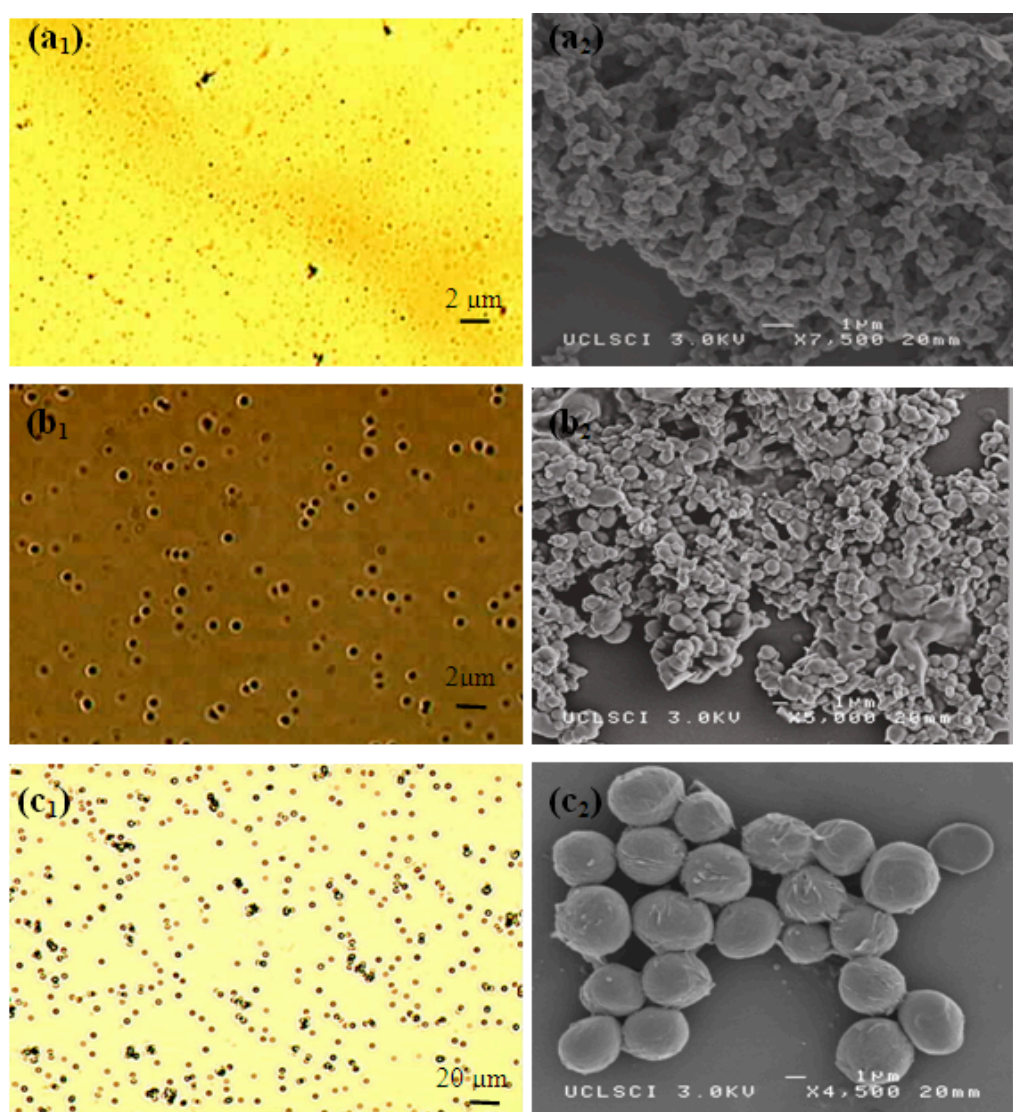
Figure 4.6 Optical micrographs (a_1, b_1 & c_1) and SEM images (a_2, b_2 & c_2) of particles prepared at different polymer concentrations. (a: 2 wt% PCL, b: 5 wt% PCL & c: 10 wt% PCL), flow rate = 10 µl/min, collecting distance = 150 mm, voltage ~ 10 kV.
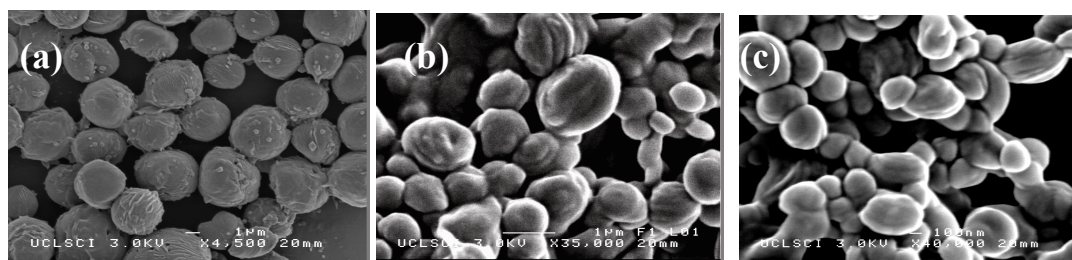
Figure 4.7 Scanning electron micrographs of PCL particles incorporating estradiol a: 10 wt% PCL, b: 5 wt% PCL & c: 2 wt% PCL) with each contains 15 wt% estradiol, flow rate = 10 µl/min, collecting distance = 150 mm, voltage ~ 10 Kv.

Table 4.2 Size of "blank" and drug loaded particles at various polymer concentrations.

Sample (weight ratio)	Mean size of the blank particles /µm	Mean size of the particles loaded with 15 wt% estradiol /µm
PCL:DMAC 2:98	0.31	0.34
PCL:DMAC 5:95	0.71	0.8
PCL:DMAC 10:90	4.4	4.6

4.2 Single needle elctrohydrodynamic atomization and fabrication of drug carriers with different shape and size

4.2.1 Introduction

Recently, it has been shown that shape is another important characteristic of drug delivery systems and there is increasing evidence that suggests shape can play a significant role in the effectiveness of drug delivery and other biological processes [Mitragotri and Lahann 2009]. This includes, for example, shape-related phagocytosis by macrophages [Champion and Mitragotri 2006] and varying the rate of cellular internalisation of particles based on their shape [Gratton *et al.* 2007]. With these findings, the need to further understand shape and size related drug delivery behaviour is essential. This requires comparison of the potential of spherical and non-spherical particles with different sizes as suitable carriers for drug delivery and in order to do this a convenient means of preparation for these is essential.

In this study, the capability of single needle EHDA processing for producing biodegradable particles of different shapes and sizes was investigated. Poly (lactic-co-glycolic acid) (PLGA) and polycaprolactone (PCL) were used. The weight ratios of the polymers to solvents were as follows; PLGA:EA 5:95 and PCL:DMAC 30:70 and particles were produced using the method described in **Section 3.6**. The effect of different parameters such as applied voltage, collecting distance, flow rate and polymer concentration on inducing shape and size differences for these particles was studied.

4.2.2 Effect of collecting distance on the morphology and size of the PLGA particles

The 5 wt% PLGA solution was used to investigate the role of collecting distance on the shape and size of the particles. The solution was introduced into the processing needle and maintained at a flow rate of 20 μl/min, with stable cone-jet generation at 8 kV. Three collecting distances were selected and the glass slides were placed under

the cone-jet at these distances. Optical and scanning micrographs of the particles are shown in **Fig. 4.8**.
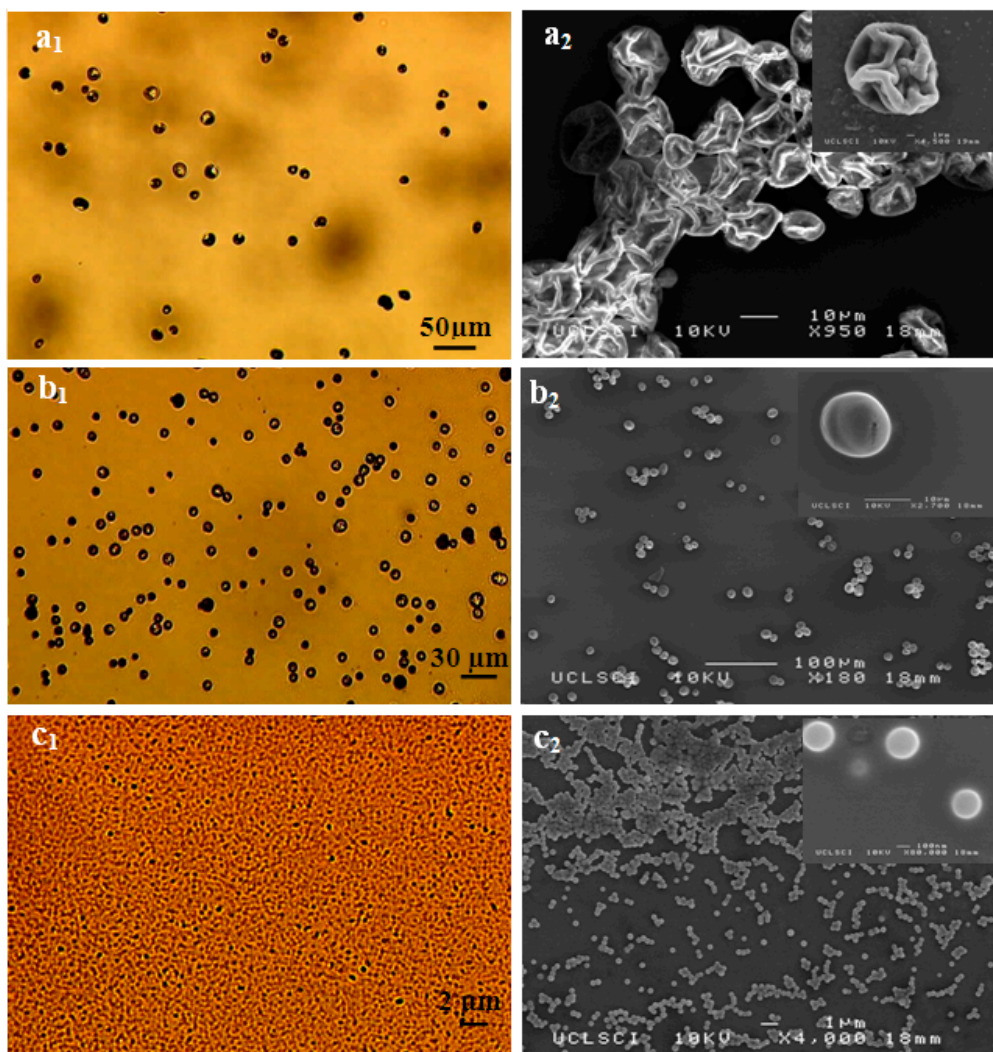
Figure 4.8 SEM images of particles fabricated at different collecting distance (CD), flow rate = 20 µl/ml, voltage~ 7 kV, polymer solution = PLGA:EA (5:95 wt. ratio). (a) CD = 100 mm, (b) CD = 150 mm, (c) CD = 400 mm.

It was observed that as the collecting distance increased, the size of the particles significantly decreased from tens of micrometres to hundreds of nanometres. **Fig. 4.8a₁** shows an optical image of particles collected at a working distance of 100 mm from the needle outlet. A closer examination of the surface of these structures shows the particles contained corrugated features. In comparison, samples collected at a working distance of 150 mm, display a slightly reduced particle size (**Fig. 4.8b₁**) and

have smoother surfaces as shown in **Fig. 4.8b$_2$**. The difference in size and surface morphology can be attributed to excess residual solvent on collection. When the collection distance is increased, more solvent is lost as vapour and as a consequence there is reduced solvent mixing with the thin film of the ethanol during collection on the substrate. When the collection distance is increased significantly (400 mm) the production of nano-particles is achieved (**Fig. 4.8c$_1$**). The relative drying time (directly proportional to deposition distance) for these particles is far greater than for the previous two samples and the surfaces of these particles (**Fig. 4.8c$_2$**) are also smooth.
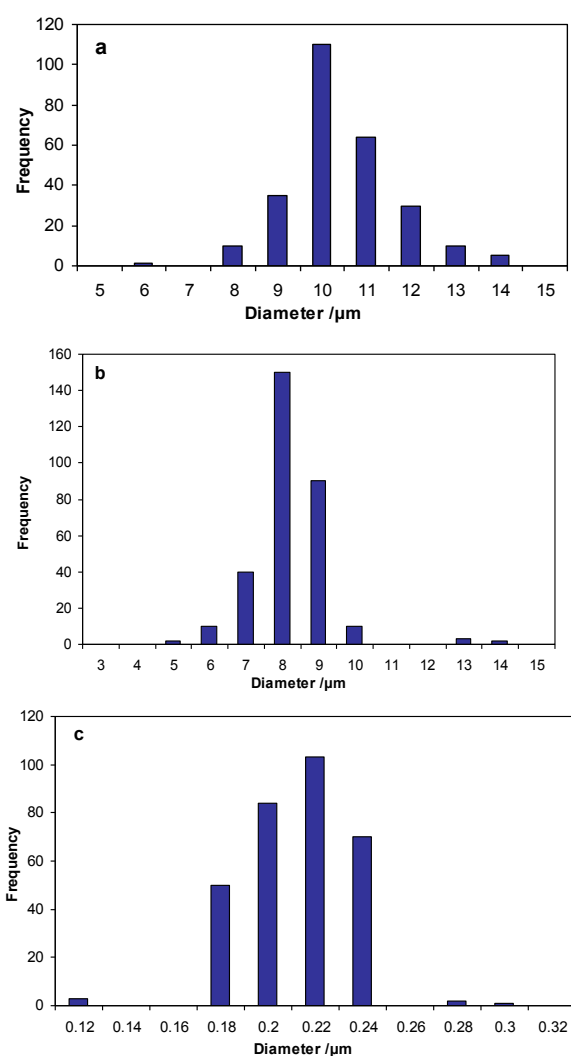
Figure 4.9 Size distribution of the PLGA particles, (a) CD = 100 mm,(b) CD = 150 mm, (c) CD = 400 mm.

The results show that both nano- and micro-scale particles can be prepared using this method, which addresses a key demand of the pharmaceutical industry [Panyam and Labhasetwar 2003, Pilcer *et al.* 2009]. The surface features are also an important factor for interaction with living systems and the ability to produce structural variations is desirable in assessing particle-cellular interactions for drug delivery [Mitragotri and Lahann 2009].

The size distribution of the PLGA particles for the different collecting distances is shown in **Fig. 4.9**. The differences in the particle size, as a function of the collecting distance, is clearly a feature which can be used to control particle size, and the surface morphology can also be changed simultaneously from smooth to textured. All the samples had narrow monomodal size-distributions. The mean size and the polydispersivity index of the particles collected at 100 mm (sample a) were 10 μm and 12% respectively, whilst the mean size of particles collected at 400 mm (sample c) was five times smaller, but the polydispersivity index was almost the same. The key values are shown in **Table 4.3**.

Table 4.3 Size distribution data for different spherical particles generated.

Sample	Number of particles studied	Mean size (μm)	Standard deviation	Polydispersivity (%)
a	265	10	1.22	12
b	307	8	1.08	13
c	313	0.2	0.02	11

4.2.3 Effect of polymer concentration, applied voltage and flow rate

The effect of concentration of PCL in solution on the size and size distribution of the carrier particles was studied using concentrations of 2, 5 and 10 wt%. The particles generated were spherical in shape and the mean sizes for 2, 5 and 10 wt% were 0.3,

0.7 and 4.4 μm, respectively. As the concentration increases, the viscosity of the solution increases, resulting in the production of larger polymer particles, as discussed above.

It is a well established principle in electrohydrodynamic processing that by increasing the viscosity of a medium the transition from spraying droplets to spinning fibres can be realised [Morota *et al.* 2004]. Therefore, to explore and demonstrate the variations in the shape of the particles generated by this process, requires the use of a much higher polymer concentration. The polymer solution used for this was again PCL (being the most economical) and its concentration in solution was 30 wt%. In contrast to the low concentration polymer solutions used to generate particles, the more concentrated PCL polymer solution is ideal for undergoing chain entanglement, thereby considerably increasing the viscosity of the solution, which is crucial in order to obtain shape changes.

The influence of the applied voltage and flow rate on the structure of the particles was investigated with the collection distance fixed at 150 mm. In the electrospinning process, the fibres generated undergo a whipping motion as a result of the applied electric field [Jaworek *et al.* 2008], which also leads to drying and thinning of the fibres emitted prior to collection. By increasing the applied voltage, this effect can be increased and may result in the breakdown of fibres into smaller constituents. **Fig. 4.10** shows scanning electron micrographs of structures obtained as a result of variations in the applied electric field, with a fixed flow rate of 5 μl/min and a collecting distance of 150 mm. At an applied voltage of 6 kV, polymeric micro-particles were generated with diameters ranging from 1-3μm, with smooth outer surfaces (**Fig. 4.10a**). When the applied voltage was increased to 8 kV, the particle size distribution became narrower, with the size range between 100nm and 1μm (**Fig. 4.10b**). As the voltage was increased further to 14 kV, the particle shape began to change as a direct consequence of the increased electric field. This resulted in needle like structures (**Fig. 4.10c**) with a constant width of 100nm and length varying between 1-3 μm. Similar structures were formed when the applied voltage was increased to 16 kV (**Fig. 4.10d**). The formation of such structures could be due

to one of two reasons. The first is due to intermediary fibre formation, where the transition between droplets to fibres is not complete. The second could be due to the whipping effect, where fibre generation has been achieved but the mechanical strength of the fibres is weak, causing them to break up during whipping and subsequent ejection. Other experiments have demonstrated structural changes as a function of the applied voltage, which can lead to bead formation in fibres using electrospinning [Zhang *et al.* 2006]. The jet and fibre size have also been shown to reduce as the applied voltage is increased during processing [Pham *et al.* 2006].

The exact applied voltage needed for a change in shape depends on the polymer concentration and properties of the solution such as viscosity and conductivity. The shape change is a transition from spherical to oblong to a more needle-like shape, and mapping the transition as a function of applied voltage is currently being investigated. A further area of interest is the identification and characterisation of the different particle shapes. Optical and electron microscopy clearly provide means of determining and quantifying variation in particle shape and size but these require careful sample preparation.

Such structural changes from spherical to needle-shape have potential application for drug delivery and in particular, in understanding how biological systems respond to shape orientated micro- and nano- scale particles. "Worm-shaped" drug delivery particles have been shown to inhibit phagocytosis compared with spherical particles of equal volume, indicating that the high curvature of spherical particles may play a role in inducing phagocytosis. Needle-like structures like those shown in **Fig. 4.10c** and **4.10d** have a much lower curvature compared with those prepared in **Fig. 4.10a** and hence have increased potential as drug delivery carriers [Champion and Mitragotri 2006]. Furthermore, cylindrical particles which are geometrically similar to the fabricated needle-like particles in this work (**Fig. 4.10** and **Fig. 4.11**) have been shown to internalise into cells without causing any toxicity [Gratton *et al.* 2007].
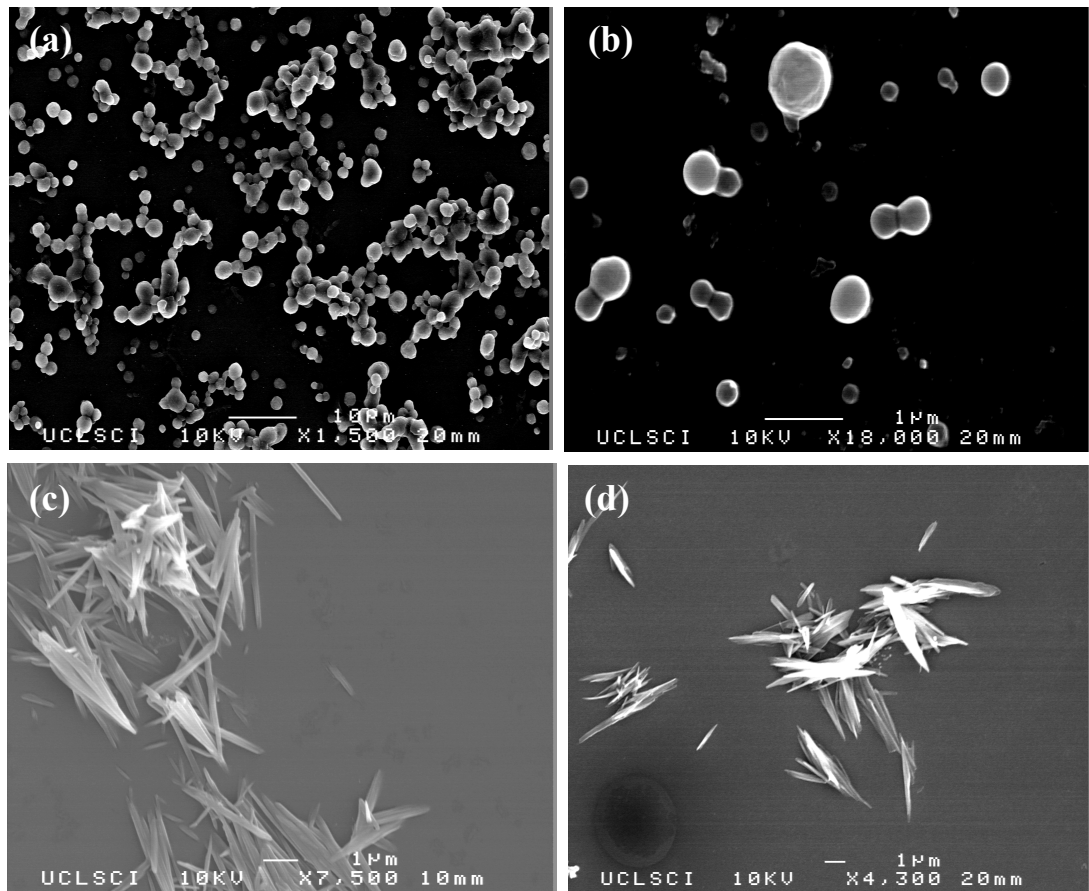
Figure 4.10 SEM images of particles fabricated at different applied voltages, flow rate= 5 μl/ml, CD = 150 mm, polymer solution= PCL:DMAC(30:70 wt. ratio) (a) voltage=6 kV, (b) voltage= 8 kV, (c) voltage= 14 kV, (d) voltage= 16 kV.

Another important parameter in electrohydrodynamic particle processing is the solution flow rate and this is perhaps the most important factor influencing the size of the structures generated [Ganan-Calvo *et al.* 1997a and 1997b]. The relationship between droplet size and processing variables has been expressed by the following scaling laws in the cone-jet model [Hartman *et al.* 1999, Hartman *et al.* 2000]:

$$d \propto (\frac{\rho Q^4}{I^2})^{1/6} \qquad\qquad (4.1)$$

Where d is the droplet diameter, Q is the liquid flow rate, ρ is the liquid density, and I is the current. The equation shows that the droplet size decreases with a reduction in the flow rate of the medium, in this case the polymer solution. In the present study, the size of the particles was found to decrease with decreasing polymer solution flow rate as shown in **Fig. 4.11**. Here, the flow rate of the 30 wt% PCL solution was changed from 5 μl/min to 2 μl/min and the same conditions were applied as before with the gradual changes to the applied voltage. The characteristics of the products were similar in terms of shape, but with regards to size there is a marked reduction.
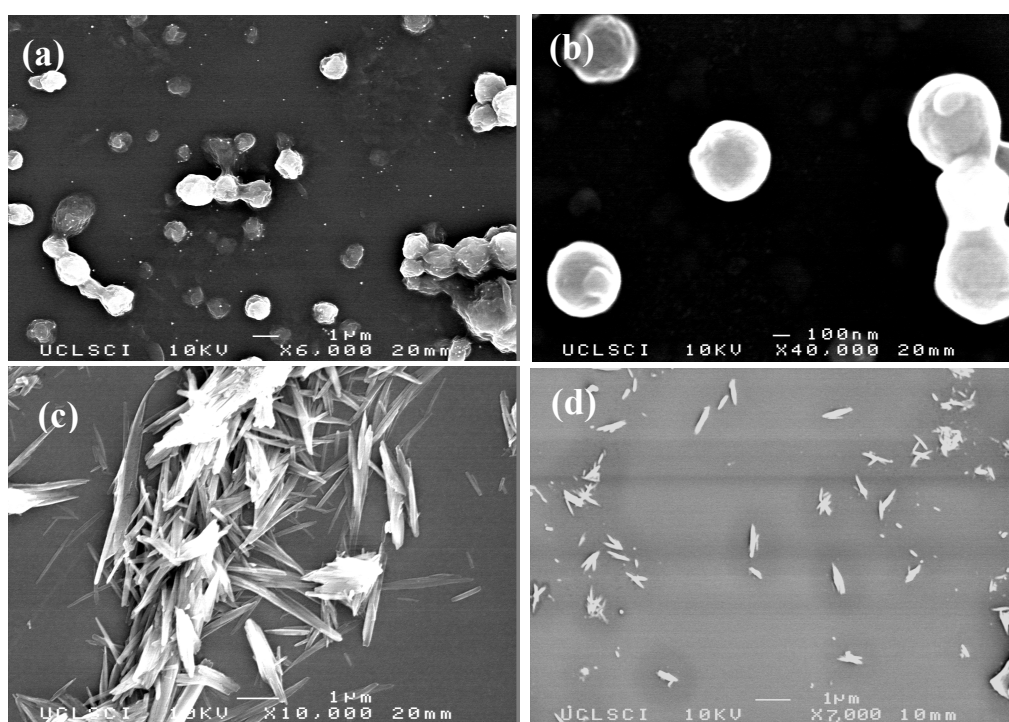
Figure 4.11 SEM images of particles fabricated in different applied voltage, flow rate = 2 μl/ml, CD = 150 mm, polymer solution = PCL:DMAC (30:70 wt. ratio), (a) voltage= 6 kV, (b) voltage= 8 kV, (c) voltage= 14 kV, (d) voltage= 16 kV.

A flow rate of 2 μl/min and an applied voltage of 6kV resulted in spherical particles with a mean size of 1μm (**Fig. 4.11a**). When the electric field was increased by increasing the voltage to 8kV the particles were smaller with a mean size of 300 nm. When the applied voltage was increased to ≥14kV the formation of needle like structures was evident again (**Fig. 4.11c**) although the aspect ratio was reduced when compared to those generated using a flow rate of 5μl/min as there was a reduction in

the particle length. Finally, this ratio was reduced further by increasing the applied voltage to 16 kV and preparation of rod like particles is achieved with a particle length ≥ 1μm (**Fig. 4.11d**). Controlling the aspect ratio of rod and needle morphologies is another important feature in drug delivery systems. It has been shown that using cylindrical particles, the aspect ratio of particles can influence the rate of internalisation within cells [Gratton *et al*. 2007].

In summary, it was shown that a variety of structures can be prepared via single needle electrohydrodynamic processing. Also, the length and width of the particles and hence the aspect ratio can be controlled. The structures and morphologies of different generated carriers were shown in **Fig. 4.12.** These include the common spherical particles to more needle like structures. The aspect ratio of these particles can also be controlled to reduce the particle shape from the micro to the nano scale.
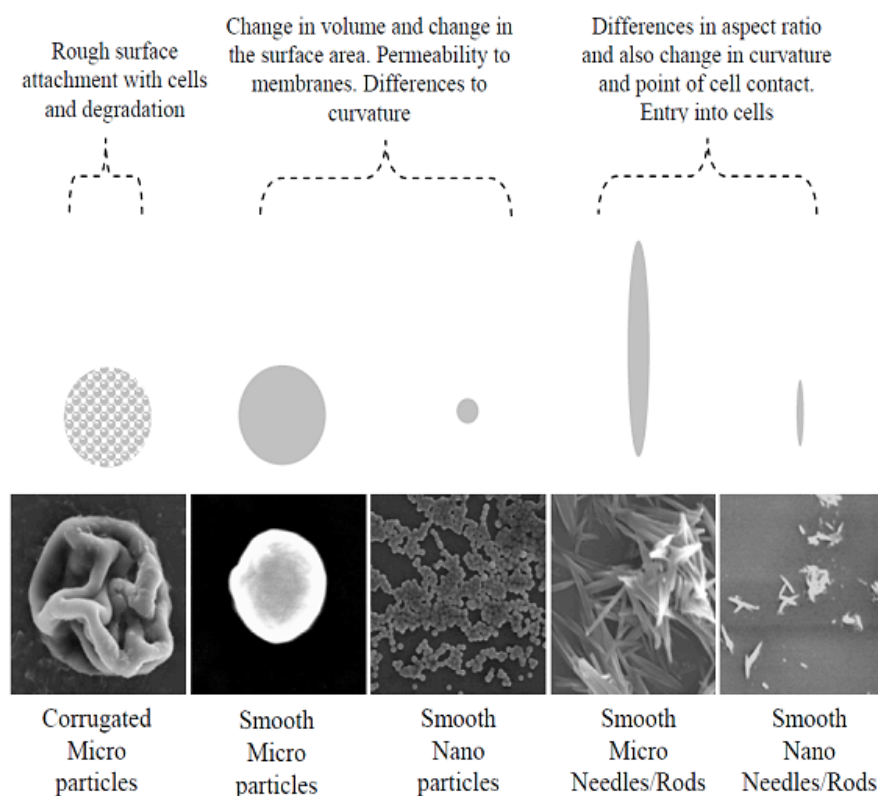
Figure 4.12 Morphologies of drug-delivery carriers generated in this study.

4.3 Co-axial electrohydrodynamic production of drug-loaded micro- and nano-particles

4.3.1 Introduction

One of the limitations in using single needle method is that the sprayed solution should have an electrical conductivity within a suitable range. The requirement is often achieved by dissolving additives in spray solutions. For some applications, suitable additives are very difficult to identify. For instance, some biomedical materials are very sensitive to the solution pH, and a small amount of acid additive will cause denaturalisation. This problem can be solved by using the co-axial EHDA method which proposes to coat more electrical charges on particles by sheathing the biomaterial suspension (in the inner capillary) with highly conductive and volatile liquid in the outer capillary during the spraying process.

However, it was shown that single needle EHDA process had great potential in producing polymeric particles with various sizes and shapes, the next step is to study the capability of co-axial EHDA process in encapsulation of a therapeutic agent in the polymeric carriers and fabrication of drug-loaded nanometre and micrometre scale particles as a drug delivery system. Thereafter, the influence of processing parameters, specifically the polymer concentration and applied voltage on size and size distribution of the drug-loaded particles were studied.

Biodegradable and biocompatible polylactic-coglycolic acid (PLGA 50:50) was used as the polymeric carrier material. Estradiol and evans blue dye (EB) were used as the encapsulated materials. The polymeric solution and the drug solution were pumped individually through the outer and inner needle of the co-axial setup, respectively. The characteristics of PLGA and estradiol drug were discussed in **Chapter 3** (**Section 3.2.1** and **3.2.6**).

4.3.2 Encapsulation process and particle formation

In this study, co-axial EHDA was used to prepare polymeric drug-loaded particles with different size ranges. PLGA solutions of different concentrations (2 wt%, 5

wt% and 10 wt%) and the drug-dye solution were prepared as described in **Section 3.4.1** and **3.4.2**. The central needle carried the drug/EB solution, the outer needle was perfused with a given PLGA solution to produce the polymeric coating. All characteristics of the co-axial setup were as explained in **Section 3.8**.
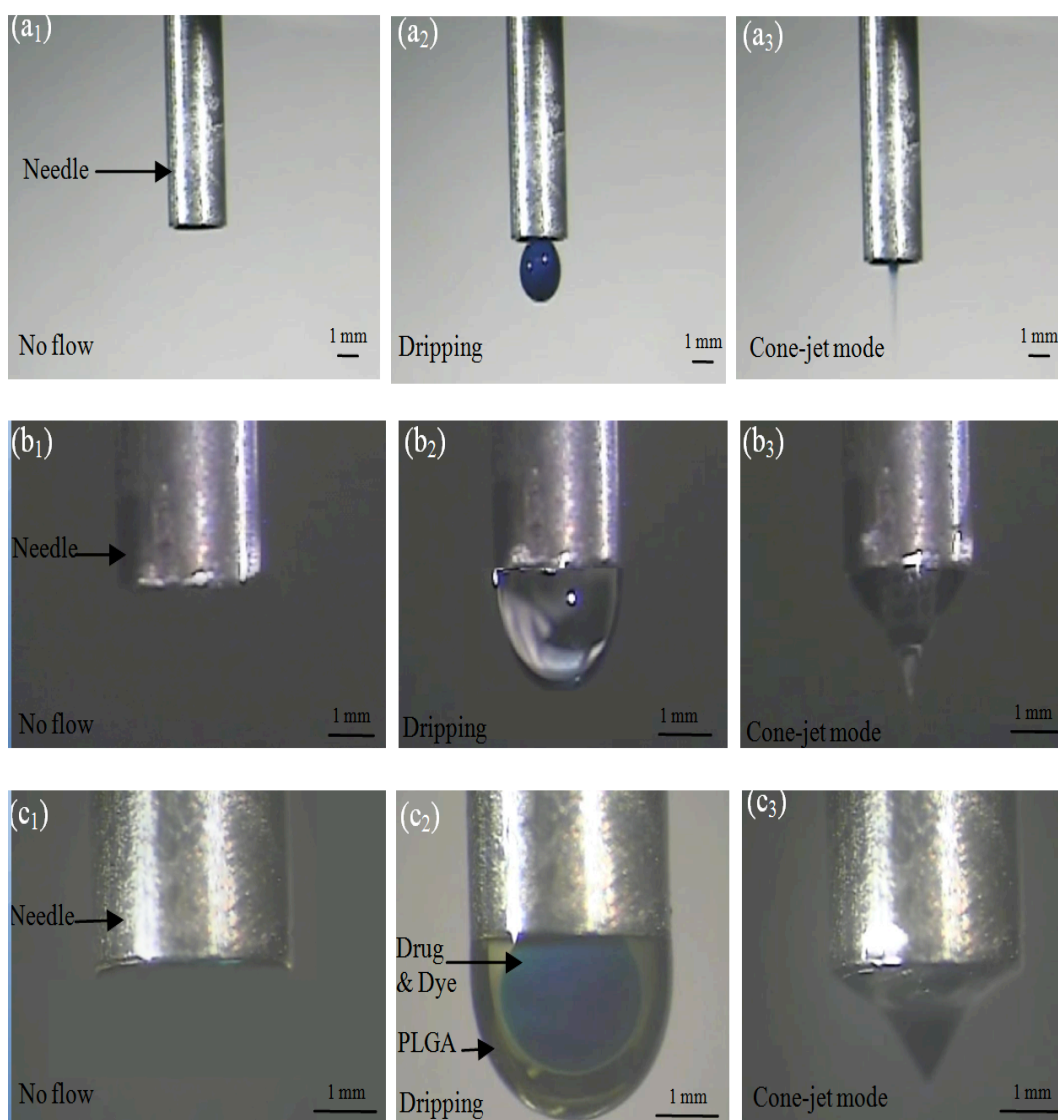
Figure 4.13 Flow of liquid under an electric field using a single (central) needle showing (a₁) no flow (a₂) dripping mode and (a₃) cone jet mode. Single needle (outer needle) showing (b₁) no flow (b₂) dripping mode and (b₃) cone jet mode. Co-flowing solutions showing (c₁) no flow (c₂) dripping mode demonstrating immiscibility and (c₃) cone jet for encapsulation.

The jetting modes generated for flowing liquids under the influence of an electric field are functions of the applied voltage, the working distance between the needle outlet and the collecting plane, the flow rate of the liquid, needle diameter and the properties of the flowing liquids [Jaworek and Krupa 1999a]. As the applied electric field strength increases due to either an increase in the applied voltage or by reducing the working distance, the atomisation mode can be transformed from the dripping to the cone-jet mode. The cone-jet mode is the preferred atomisation mode because it can produce uniform, stable and continuous particle generation with a controllable jet size [Amsden and Gossen 1997]. A stable cone-jet can be obtained for liquids satisfying the condition $\sigma_i > \sigma_o$ where σ is the liquid-dielectric atmosphere surface tension and subscripts i and o refer to the inner and outer solution, respectively [Ku and Kim 2002]. Another factor influencing the stability of the cone-jet is the ability of the electric field to be able to interact with at least one of the solutions, which is sometimes referred to as the driving medium, and must be selected carefully to satisfy the requirements for electrical conductivity and surface tension [Lopez-Herrera *et al.* 2003].

As shown in **Fig. 4.13**, stable cone-jet generation was found to be easily achievable for both the inner and outer solutions used in this study; separately (**Fig. 4.13a$_3$** and **4.13b$_3$**) and under simultaneous flow (**Fig. 4.13c$_3$**). The inner blue coloured solution (drug with dye added to enable visualisation), was clearly encapsulated by the outer straw-yellow coloured polymeric solution. As the applied voltage was increased, the desired co-axial cone-jet formed (**Fig. 4.13c$_3$**).

4.3.3 Particle Characteristics

4.3.3.1 Structural characterization of PLGA particles loaded with EB dye

A preliminary morphological and structural study was carried out on the fabricated PLGA particles loaded only with EB. (**Fig4.14**). It was observed that the jet broke up to form fine droplets and particles with various size ranges (nano to micro) with 3 different polymer concentrations. The mean diameters of the particles fabricated from 2, 5 and 10wt% polymer solutions were 110, 120 and 2500 nm, respectively.
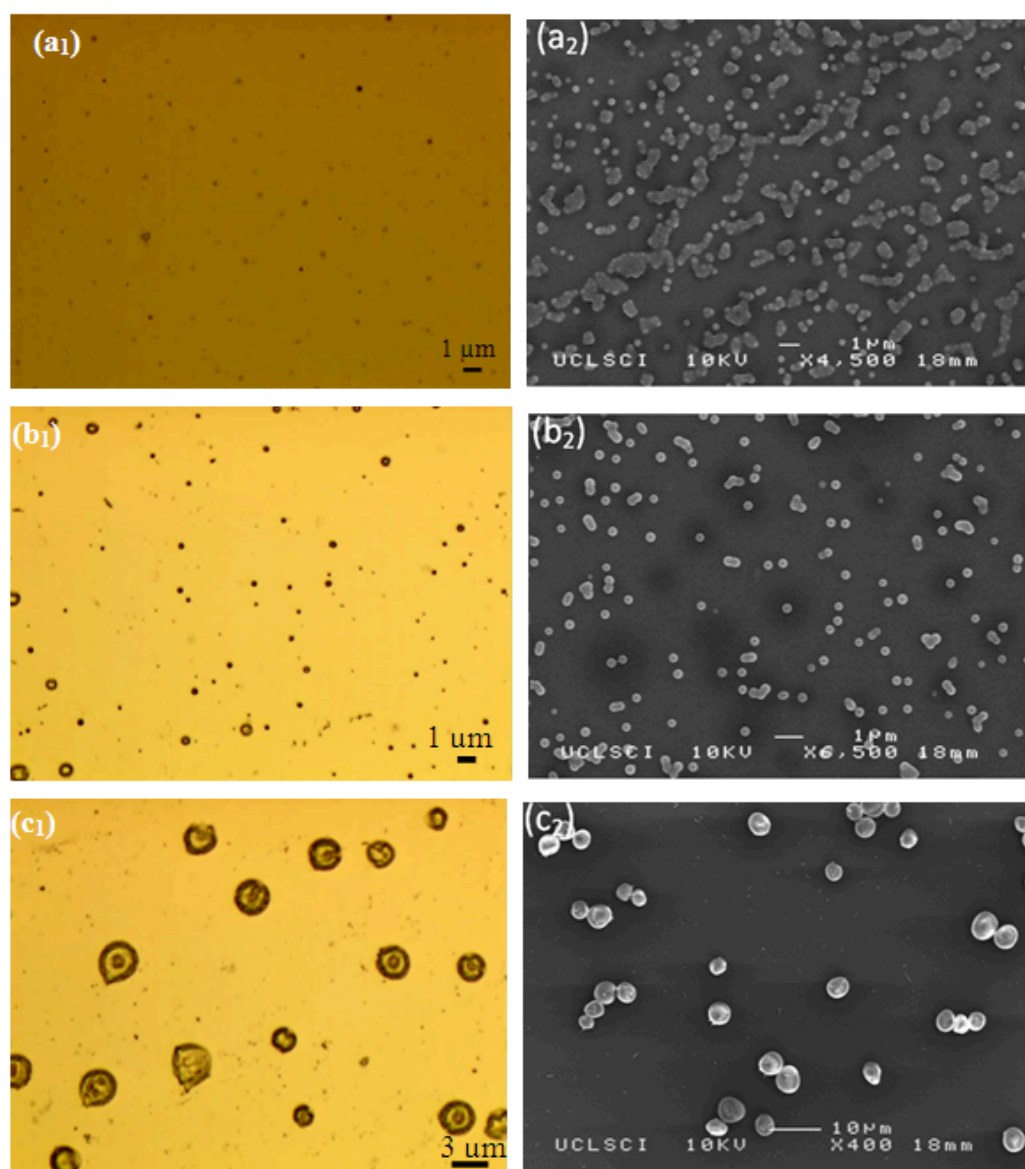
Figure 4.14 Optical microscopy (a$_1$, b$_1$ & c$_1$) and SEM images (a$_2$, b$_2$, c$_2$) of particles prepared with different polymer concentrations. (a: 2 wt% PLGA, b: 5 wt% PLGA & c: 10 wt% PLGA) loaded with EB dye.

4.3.3.2 Structural characterization of PLGA particles loaded with estradiol

Further morphological and structural characterisation was carried out on PLGA particles loaded with estradiol which was the main model drug in our study. The optical images (**Fig. 4.15a$_1$, 4.15b$_1$ & 4.15c$_1$**) demonstrate that very small particles were obtained when polymer concentrations of 2 wt% and 5 wt% were used.

Detailed analysis using SEM showed that all particles were spherical with a smooth outer surface (**Fig. 4.15a$_2$, 4.15b$_2$ & 4.15c$_2$**).
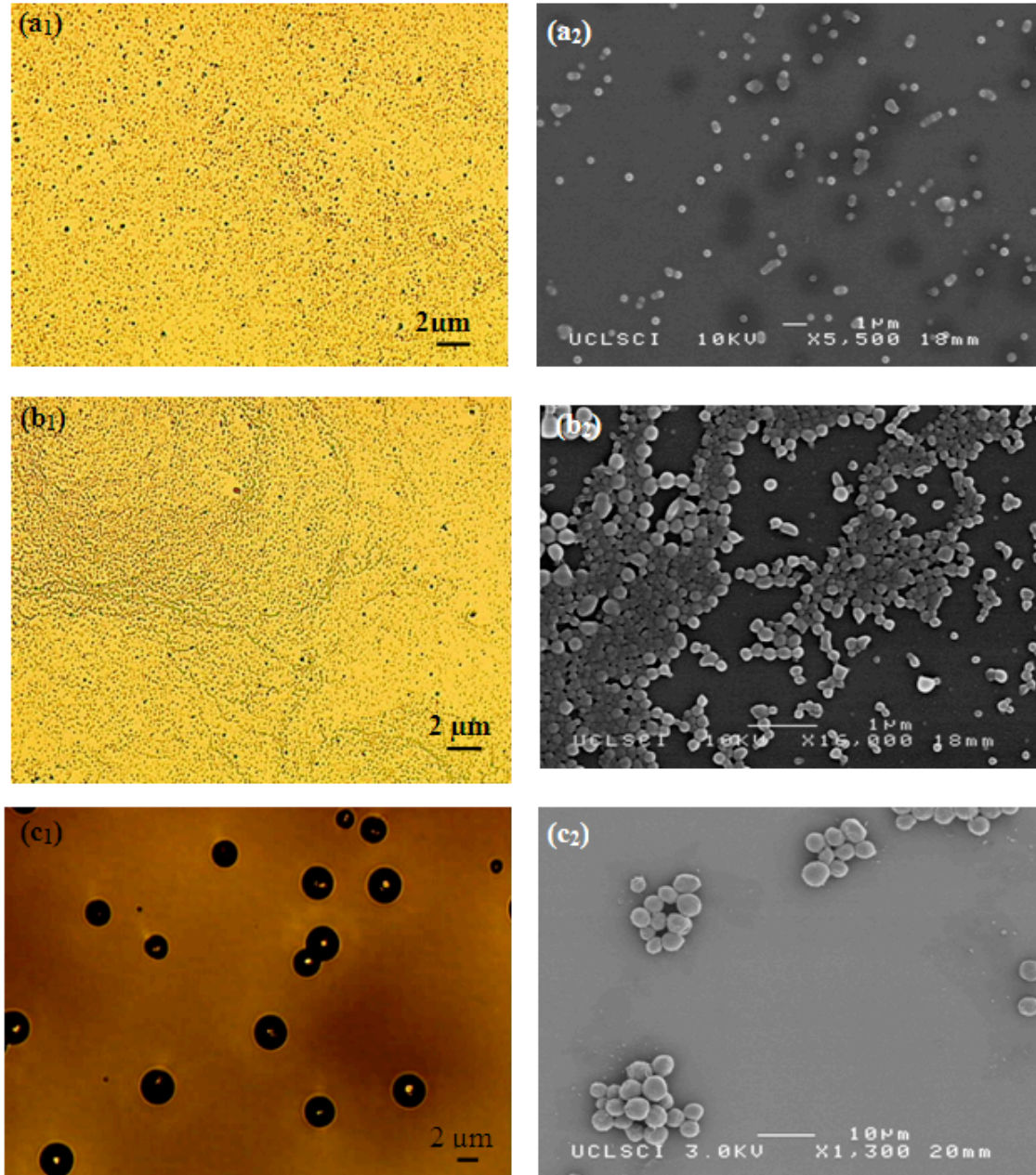
Figure 4.15 Optical microscopy (a$_1$, b$_1$ & c$_1$) and SEM images (a$_2$, b$_2$, c$_2$) of particles prepared with different polymer concentrations. (a: 2 wt% PLGA, b: 5 wt% PLGA & c: 10 wt% PLGA).
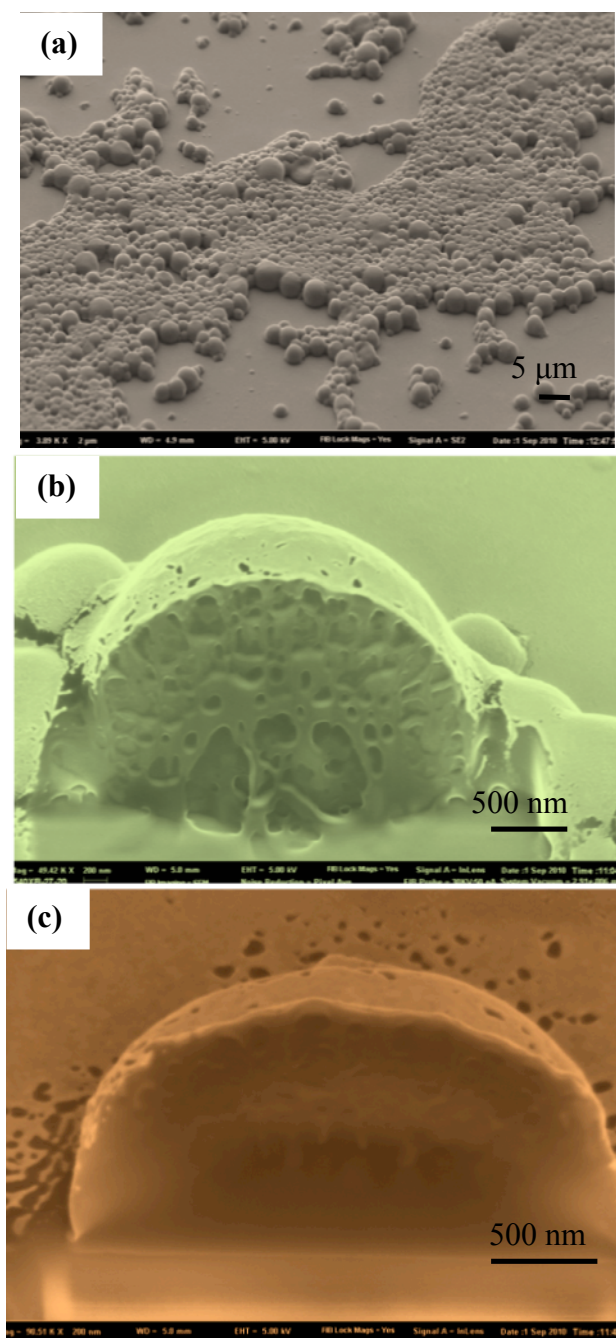
Figure 4.16 External and Internal morphology of the particles fabricated from 10 wt% PLGA solution using dual beam FIB-SEM. (a) prior to FIB sectioning (b,c) 2 particles following FIB sectioning.

It was also observed that the mean particle diameter decreased as the polymer concentration was reduced. Particles with a diameter of 120 nm were produced using 2 and 5 wt% polymer solution. Particles prepared from the higher polymer concentration (10 wt %) agglomerated due to the presence of residual solvent during drying. The higher polymer concentration leads to larger particles being produced

and thus reduces the degree to which the solvent can diffuse out of the particles over the fixed working distance. These results, as expected from previous studies [Xie *et al.* 2006a and 2006b], confirmed that the concentration of polymer in the liquid has a significant impact on the size of the particles produced. In this study FIB was also used to examine cross-sections of the PLGA particles using a dual beam FIB-SEM instrument. This showed that the particles had a porous internal structure with certain degree of vacuolation (**Fig. 4.16b & 4.16c**).
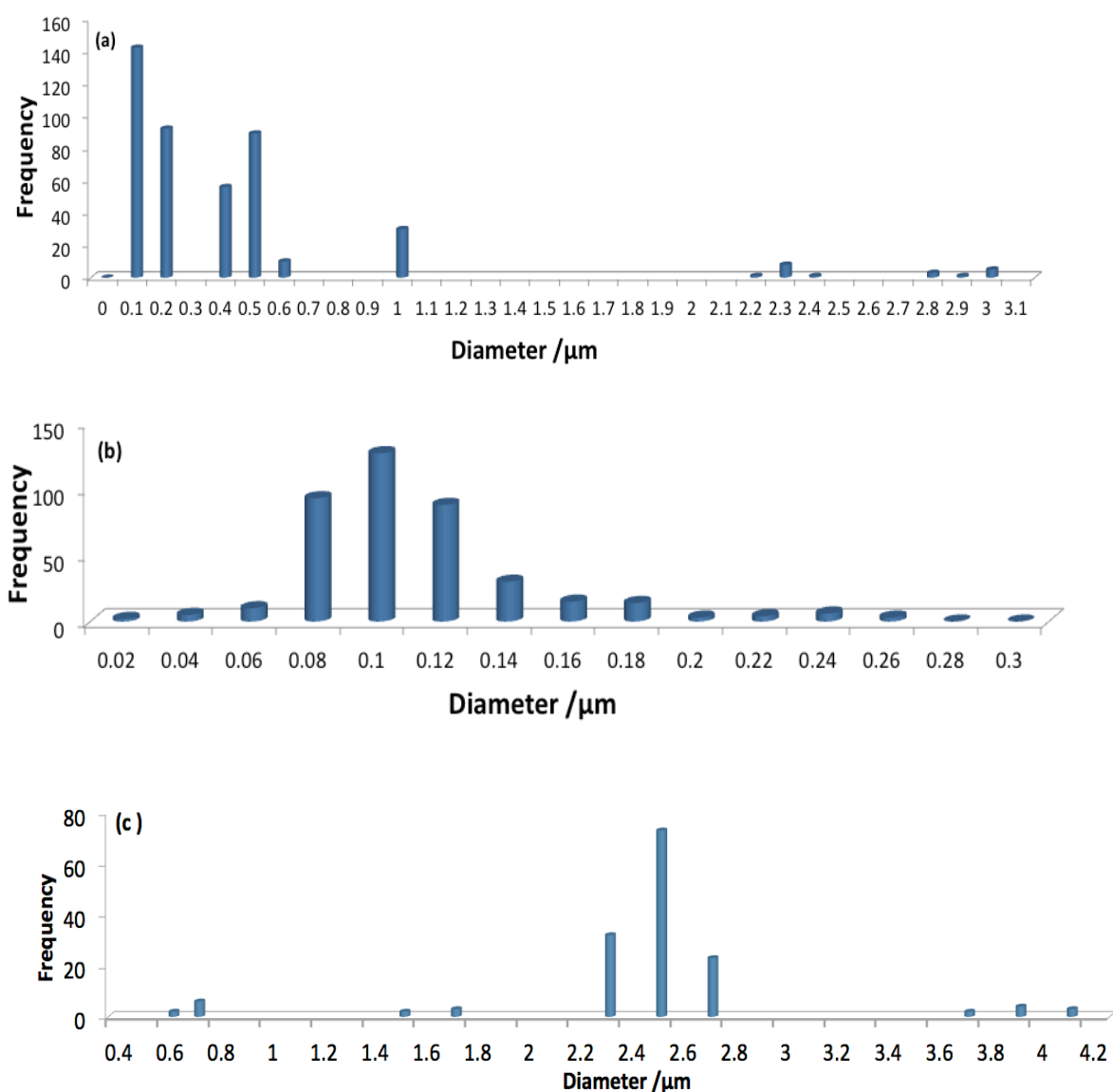
Figure 4.17 Size distribution of particles prepared (a: 2 wt% PLGA, b: 5 wt% PLGA & c: 10 wt% PLGA).

The diameters of the particles were measured from the SEM images using the image-processing program UTHSCSA (Image Tool Version 2, University of Texas, USA). Particles prepared from 2 wt% PLGA had a bimodal size distribution with two peaks. 70 % of the particles were <120 nm in diameter and 20 % of them were >500 nm (**Fig. 4.17a**). In this case the wider variation in particle size can be attributed to the generation of different types of droplets ("primary" and "satellite") during the processing [Hartman *et al.* 2000, Tang and Gomez 1994 and 1995]. More than 90% of the particles prepared using 5 wt% PLGA were <120 nm in diameter (**Fig. 4.17b**). The particles produced from the 10 wt% PLGA, 95% had diameters >2 μm (**Fig. 4.17c**).The polydispersivity index of the 5 wt% PLGA was the lowest (**Table 4.4**). These results confirmed that the concentration of polymer in the liquid has a significant impact on size of the particles produced and this is caused primarily by the increase in viscosity with polymer concentration which results in larger droplets being formed [Jayasinghe and Edirisinghe 2002].

Table 4.4 Size characteristics of the prepared particles.

Sample	Number of particles studied	Mean size (nm)	Standard deviation (nm)	Polydispersivity (%)
PLGA 2 wt%	300	250	100	38
PLGA 5 wt%	300	100	10	11
PLGA 10 wt%	150	2500	400	16

Although production of the polymeric particles via both single and co-axial EHDA was simple to perform, attaining exactly the desired particle size, size distribution, and morphology might be challenging. The right parameters have to be experimentally found for every case and the correct instrumentation set-up used. The results showed that smaller particle size was achieved via co-axial method. The size range for PCL particles produced via single needle EHDA was from 310 nm to 4.4 μm, whereas the PLGA particles produced via co-axial EHDA was from 100 nm to 2.5 μm.

Summary

This study demonstrates the successful preparation of micro and nano scale polymeric carriers using both single needle and co-axial electrohydrodynamic atomization methods. These methods overcome some of the disadvantages of other conventional methods for producing polymeric drug carriers, such as the need for elevated temperatures, multiple processing steps, and the use of surfactants and other additives.

First, the key processing parameters such as flow rate, applied voltage and the properties of the solutions were optimised to obtain a stable cone jet. The cone-jet mode was of particular interest, as this resulted in a near-uniform distribution of particles upon jet break-up. The flow rate and applied voltage were varied from 2-50 µl/min and 0-15 kV, respectively. It was shown that the particle sizes were reduced at higher applied voltages and this effect was more noticeable at higher flow rates. The size distribution of all samples was monomodal but it was found that the polydispersivity index of the particles increased at the upper limit and lower limit of flow rates in the cone-jet region. Furthermore, the effect of these parameters on the size and polydispersivity of the particles were determined. For instance, the size range of generated particles from PCL solutions with different concentrations were varied from 310 nm to 4.4 µm (flow rate = 10 µl/min, voltage ~ 10 kV).

Second, it was shown that the polymer concentration (PLGA and PCL solutions), the flow rate and the collecting distance can control the particle size, shape and morphology. Specifically the collecting distance not only has a great effect on the mean size of the particles but also it has a key role in changing the surface morphology of the produced PLGA particles from a crinkled surface to a smooth surface. Furthermore, it was elucidated that in the case of using viscous PCL polymer solution (30 wt%), there is a transition between electrospraying and electrospinning, in which the needle-like shape particles is generated.

Third, it was shown that the co-axial EHDA method has a great potential for encapsulating a therapeutic agent inside a polymeric carrier. The structures, size and size distribution of the particles were investigated. The mean size of the estardiol loaded PLGA particles were varied from 100 nm to 2.5 µm.

Chapter 5

Results and discussion

In vitro release study: controlling and regulating the release profile

Overview

The main objective of a delivery system is to release therapeutics at the desired anatomical site and to maintain the drug concentration within a therapeutic band for a desired duration. Therefore, in the first set of experiments (**Section 5.1**), the capability of the drug-loaded PLGA particles produced in providing controlled release of the estradiol in a sustainable dose over extended periods was studied. Advanced treatment of diseases requires particles that can deliver their payload in a highly regulated manner to achieve the desired therapeutic effect. Therefore, in the next sets of experiments (**Section 5.2**), the effect of ultrasound exposure upon the estradiol release profiles was studied. In addition, "burst release" is one of the major challenges to overcome in drug encapsulated particle systems. In most cases, the burst release is an ineffective form of drug usage from both therapeutic and economic standpoints. For this reason, the final goal in the development of the estradiol loaded PLGA particles was to reduce the initial burst and achieve a controlled drug released thereafter. Therefore, in the last sets of experiments (**Section 5.3**), the aim was to modify the release profile via a coating method in order to minimize the burst release phase.

5.1 *In vitro* release study of micro- and nano-particles produced via co-axial electrohydrodynamic processing

5.1.1 Introduction

In this section, further *in vitro* investigations were carried out on the evans blue and estradiol loaded PLGA particles, which were produced in **Section 4.3**. The aims were to study the efficiency of the encapsulation process, to determine the capability of the polymeric particles designed for releasing their payload and to measure the amount of drug released over an extended period.

In the first part of this study, the evans blue release profile was investigated using a simple and qualitative colorimetric method. Subsequently, estradiol was used as the encapsulated drug. The encapsulation efficiency and drug release profile were measured using the UV spectrophotometer method which is a more accurate and a quantitative method.

5.1.2 Evans blue dye and estradiol release studies

Drug release from polymeric particles can take place by several mechanisms including diffusion, surface and bulk erosion, desorption and disintegration. From PLGA particles it occurs initially by diffusion from the polymer matrix, whereas during the later phases the release is mediated through both drug diffusion and degradation of the polymer matrix itself. PLGA degrades by means of hydrolysis [Schliecker *et al.* 2003]. The inwards diffusion of the aqueous phase causes degradation of the polymer chains, which in turn facilitates outwards diffusion of the entrapped drug [Zhang *et al.* 2008].

In the first step of the *in vitro* release study, a colorimetric method was used to measure the EB dye release profile. The aim was to study the feasibility of EB encapsulation in the PLGA particles and to study whether these PLGA carriers are able to release the loaded EB dye.

The colour change of the solutions in the vial over time (t) was measured. These colour changes were apparent to the naked eye over prolonged periods as shown in **Fig. 5.1**, where $t_1 < t_2 < t_3$.
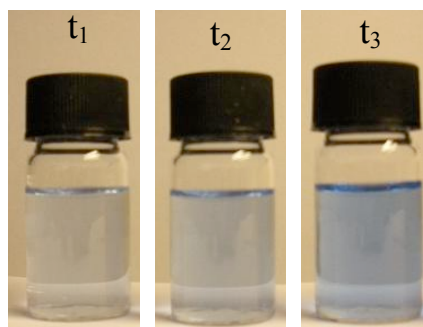
Figure 5.1 Changing the colour of the medium as function of time $t_1 < t_2 < t_3$.

However, more subtle colour changes over a 10 day period were assessed at fixed time intervals using a colorimeter. The release profile obtained using the colorimeter is shown in **Fig. 5.2a**. The results show that the optical absorption increased in all samples and the profiles had two different stages: initial burst release in the first 8 to 10 hours followed by a slow increase as the EB dye diffused out of polymer matrix. The release rate for the particles produced from the more concentrated solution (PLGA:DMAC 10 wt%) was lower than that for those produced from the less concentrated solutions (PLGA:DMAC 2 & 5 wt%). The colorimeter could detect the released EB dye up to 5, 7 and 10 days in PLGA 2 wt%, PLGA 5 wt% and PLGA 10 wt% samples, respectively. This method is applicable for showing the feasibility of encapsulation by qualitatively measuring the colour change of the solution in the vial over time (t).

The next step of the *in vitro* release study was to investigate the behaviour of the drug (estradiol) release from the PLGA particles using UV spectroscopy. Clear absorbance peaks were achieved at the expected wave length for estradiol (280 nm) indicating that the drug was not damaged during the encapsulation process (**Fig. 5.2b**). It was observed that estradiol release was time-dependent and all the drug-

loaded nano and micro particulate formulations showed a biphasic release pattern (as for the results from colorimetric release study) wherein there is a burst release followed by a period of sustained release (**Fig. 5.2b**).
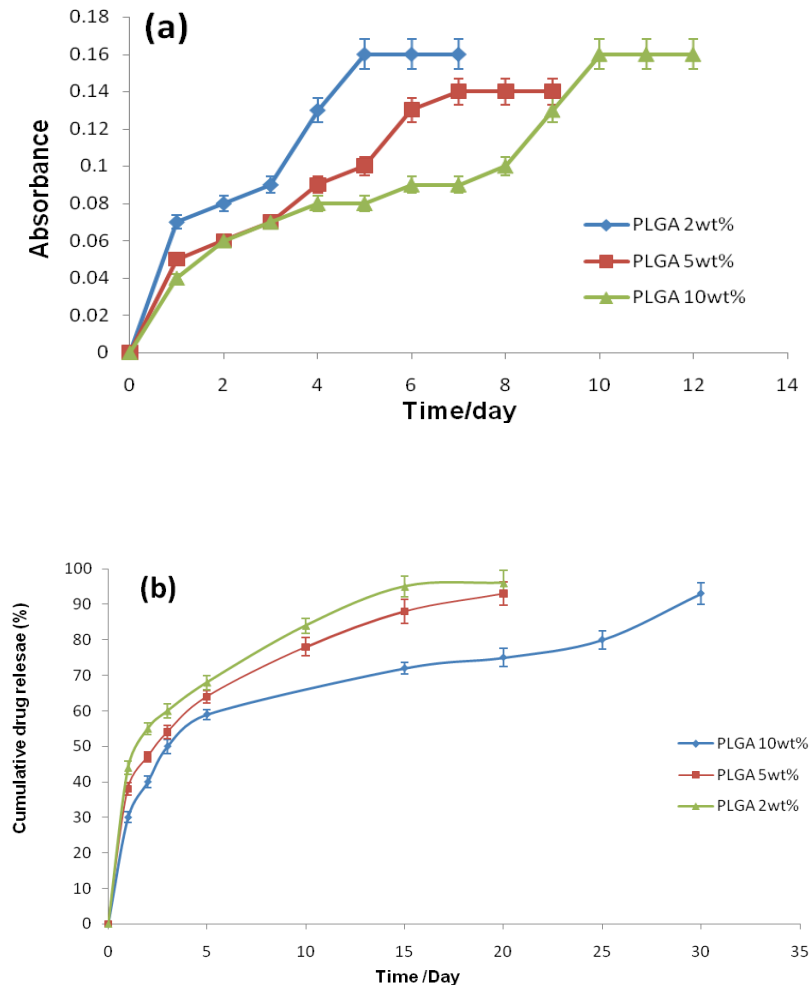
Figure 5.2 Release profile of PLGA particles prepared from different concentrations (a) PLGA particle loaded with EB dye (using colorimetry method) (b) PLGA particles loaded with estradiol (using UV spectroscopy method).

The release rate for the particles produced from the more concentrated solution (PLGA:DMAC 10 wt%) was lower than that for those produced from the less concentrated solutions (PLGA:DMAC 2 & 5 wt%). This could be explained by the fact that the particles fabricated from the more dilute solutions were smaller in size and, with a decrease in particle size, the surface area to volume ratio increases leading to increased buffer penetration and faster drug diffusion. In the last stage, the

release rate for PLGA 10 wt% sample increased significantly, as degradative hydrolysis of the polymer particles took place and the region, which would be expected to contain a higher concentration of drug, was exposed. The encapsulation efficiencies for the particles prepared from 2 wt%, 5 wt% and 10 wt% polymer solution were 65%, 68% and 75%, respectively. This slight increase with polymer concentration may be due simply to the fact that an increase in the polymer concentration would result in higher resistance to outwards drug diffusion during processing.

Generally, it was shown that colorimetric method is a fast, simple, and qualitative method indicating the feasibility of the encapsulation and the UV method is a sensitive, accurate and quantitative method showing the release behaviour of the encapsulated materials over time. It was observed that the estradiol release rate was time-dependant. All samples with various size ranges (from 100 nm to 2.5 μm) showed controlled release profiles with no fluctuations. However, all release profiles had burst release phase in the beginning.

5.2 Effect of ultrasound exposure on the release profile of PLGA nano and micro particles

5.2.1 Introduction

In this chapter, further investigation was carried out on the particles which were fabricated in **Section 4.3**. As mentioned in **Section 1.2**, the final objective of this study was to tailor and control the drug release profile to produce a more efficient system. As mentioned in **Section 2.12.2**, one way to stimulate the drug release is to expose the particles to ultrasound. First, some preliminary experiments were carried out using an ultrasonic cell disruptor, in order to test the feasibility of this technique. Continuous wave ultrasound was applied for either 15 or 30 s, after which the sample was returned to the vial and UV spectroscopy measurements were carried out.

After, demonstrating an enhanced drug release rate, a better understanding of the phenomena involved was required to facilitate a reliable measure of control over the release process. Therefore, systematic investigations were carried out to determine the effect of various ultrasound exposure parameters, in particular: output power, duty cycle and exposure time, on the release rate. For this study, the prepared estradiol-loaded PLGA particles were exposed to ultrasound using a programmable sonicator (Branson Sonifier S250A).

5.2.2 Preliminary study on the effect of ultrasound exposure on the drug release profile

The release profiles for prepared particles with different sizes (100 nm to 2.5 μm) were clearly affected by exposing the particles to ultrasound. Ultrasound has been used in various drug delivery applications to enhance the release of pharmaceuticals in target tissues [Mitragotri 2005]. As discussed in **Chapter 2**, the main mechanism for increased release is thought to be related to acoustic cavitation, which is the formation and/or activity of gas or vapour-filled bubbles in the medium exposed to ultrasound [Larina *et al.* 2005].
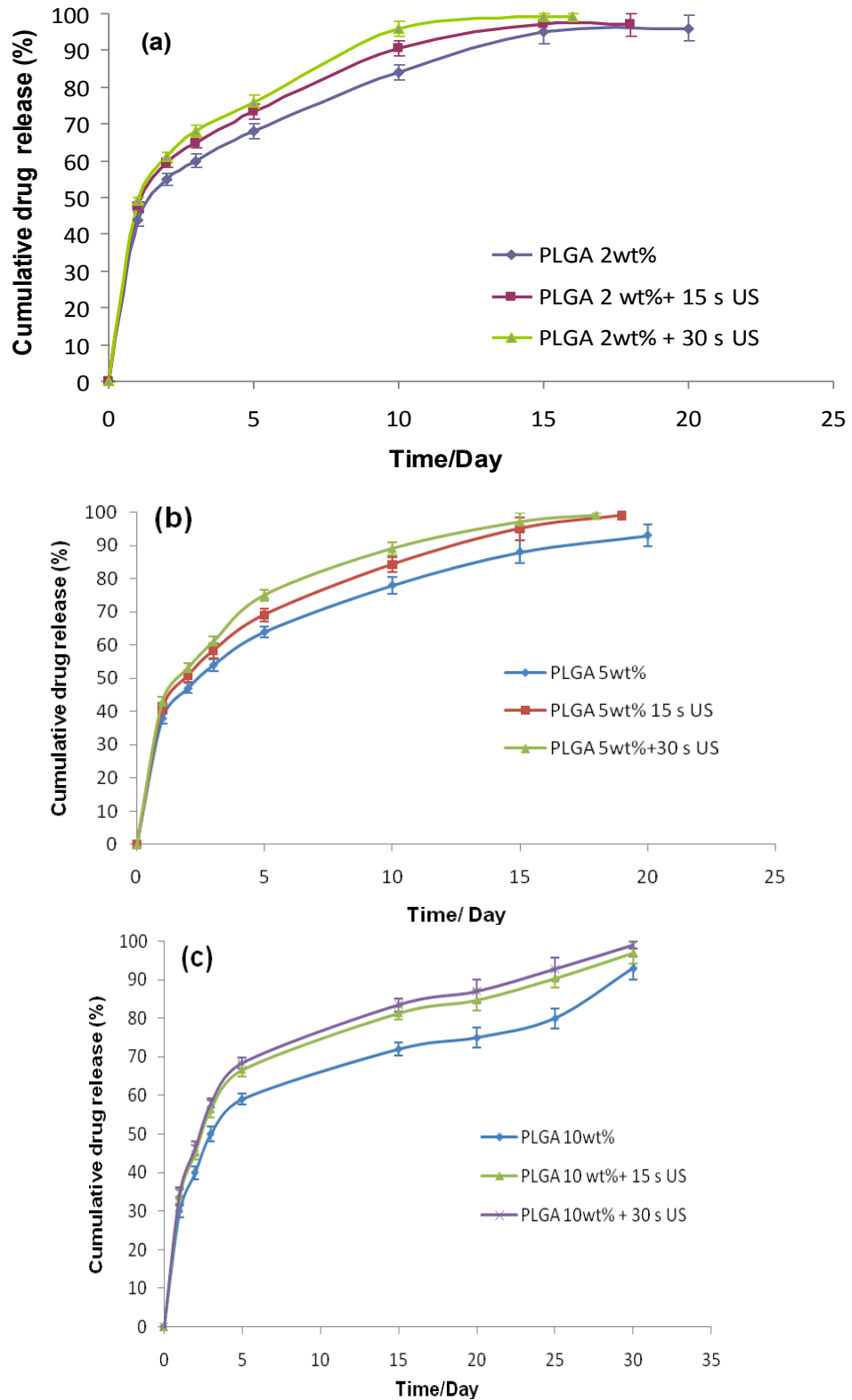
Figure 5.3 Estradiol release profile for PLGA particles following exposure to ultrasound (15 and 30 s). (a) PLGA:DMAC 2:98, (b) PLGA:DMAC 5:95 and (c) PLGA:DMAC 10:90.

In this study, an increase in the amount of drug released was observed for all the samples exposed to ultrasound (**Fig. 5.3** and **Table 5.1**) with a greater increase obtained for longer exposures as would be expected. It was found that ultrasound had a slightly greater effect on larger particles. This may be due to the higher probability of gas entrapment in or on the particles' surface, or simply of a particle encountering a bubble due to its larger size.

Table 5.1 Release characteristics of particles exposed to ultrasound.

Sample	Drug released difference after 15s US (%)	Drug released difference after 30s US (%)
PLGA 2wt%	+3.5	+5.7
PLGA 5wt%	+4.4	+6.8
PLGA 10wt%	+6.3	+7.8

5.2.3 Preliminary study on degradation

Although PLGA is insoluble in water, it is hydrolytically unstable and degrades by hydrolytic attack of its ester bonds. Through this hydrolytic attack, random chain scission occurs, causing it to degrade into lactic and glycolic acids.

One interesting feature of the surface of particles during degradative hydrolysis was the variation in porosity as a function of time. The quantity and the size of pores have been observed to increase for PLGA based implantable devices over prolonged periods *in vivo* [Schliecker *et al.* 2003]. The surface morphology of 10 wt% PLGA particles incubated in deionised water was studied over 30 days. The surface of the particles became porous (**Fig. 5.4**), a characteristic of PLGA degradation, which would explain the drug release patterns in **Table 5.1**.
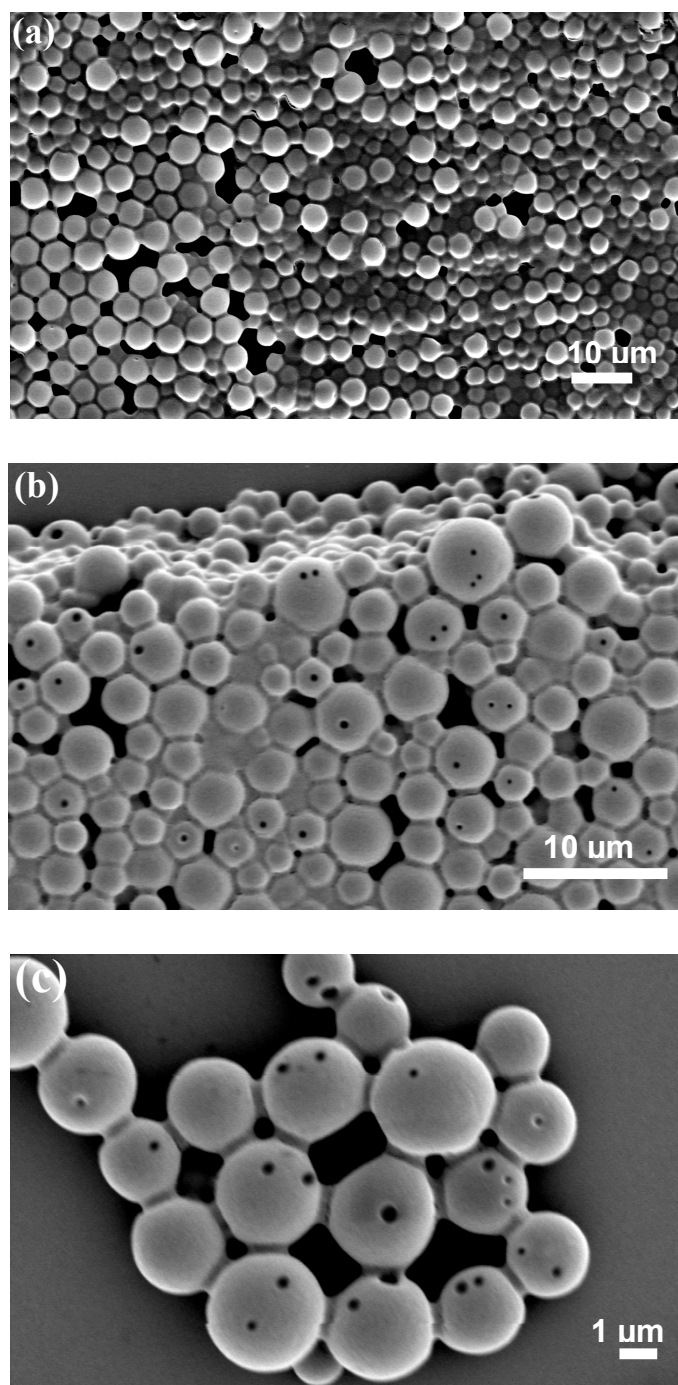
Figure 5.4 Surface morphology of the capsule prepared from 10 wt% PLGA as a function of time, a: t = 0, b: t = 15 days, c: t = 30 days, (all samples were incubated in deionised water during the experiments).

Structural study was also carried on particles exposed to ultrasound. It was observed that the surfaces of the particles exposed to ultrasound were rougher and contained more pores in comparison with the samples which were not exposed to ultrasound (**Fig. 5.5**). This may have been due to both mechanical damage (e.g. formation of

liquid jets from collapsing bubbles) and also faster polymer degradation as a result of increased agitation of the surrounding liquid due to the motion of the bubbles. Also, the internal pores closer to the surface (**Fig. 4.16**) may become broken due to the agitation, revealing pores upon the surface.
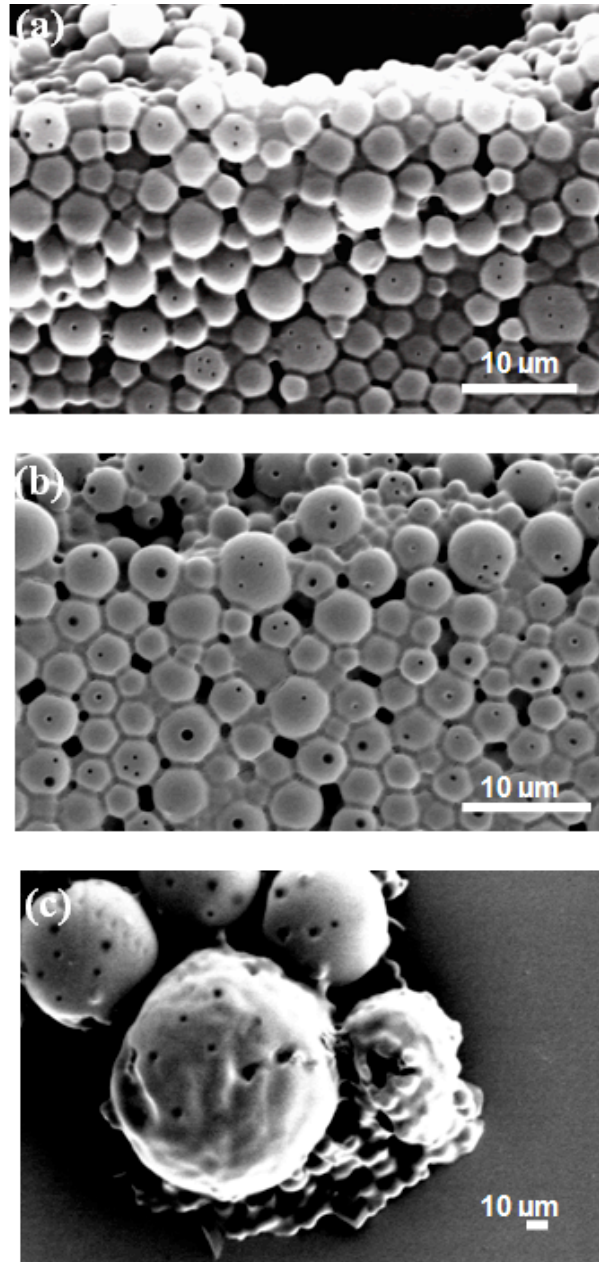
Figure 5.5 Surface morphology of the microcapsules exposed to ultrasound as a function of time, a:t=0, b: t=15 days, c: t=30 days, (all samples were incubated in deionised water during the experiments).

5.2.4 Effect of sonicator output power on the release profile
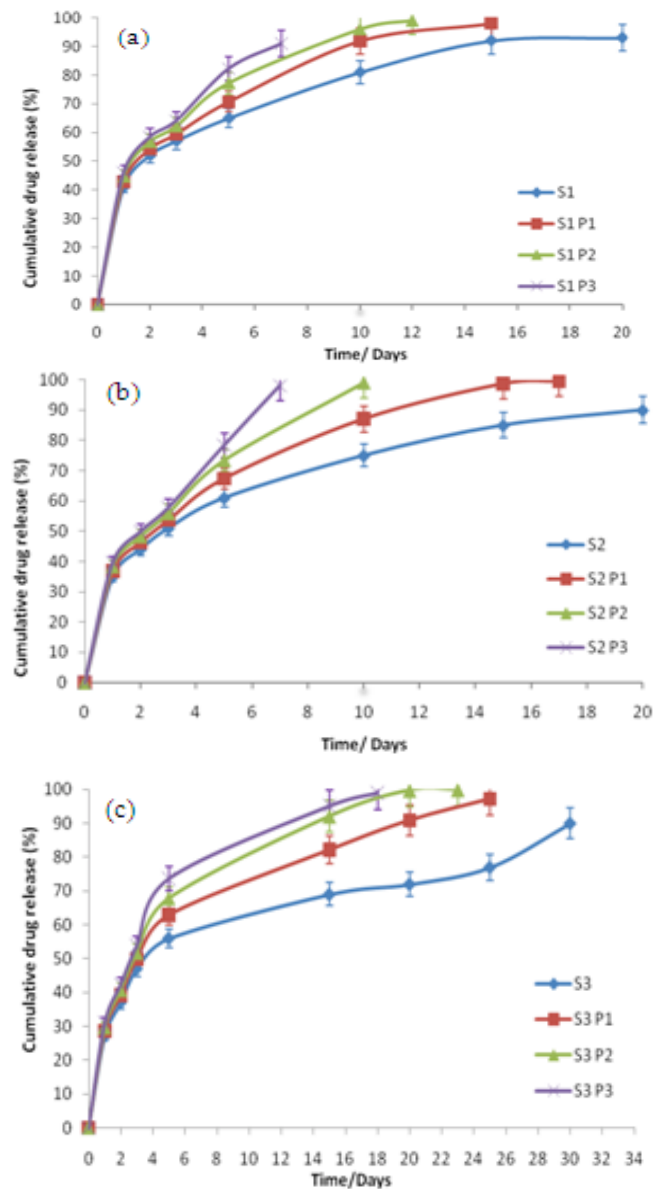
Figure 5.6 Estradiol release profiles for PLGA micro and nano particles following ultrasound exposure at various output powers (P_1, P_2 & P_3) (a) sample S_1 with particles containing PLGA 2wt%, (b) sample S_2 with particles containing PLGA 5 wt%, (c) sample S_3 with particles containing PLGA 10 wt% (error bars represent the standard deviations, $n \geq 4$); The cumulative drug release was calculated by measuring the percentage drug released at each specific time plus the entire drug which released before that specific time. Please note the longer timescale in (c) results from the fact that the mean particle size was larger and hence the degradation rate lower.

After the preliminary experiments, more extensive studies were carried out on ultrasound mediated drug release. First, the *in vitro* release behaviour of the control samples which were not exposed to ultrasound was determined. These profiles (the blue curves **Fig. 5.6**) showed burst release followed by a period of sustained release. The encapsulation efficiencies for the particles prepared from 2 wt%, 5 wt% and 10 wt% polymer solutions were 65%, 68% and 75%, respectively. This slight increase with polymer concentration may simply be due to the fact that an increase in the polymer concentration would result in a higher resistance to outwards drug diffusion during fabrication. Next, the effect on the release profile of varying the sonicator output power[4] was investigated. Three different power settings on the sonicator (P_1, P_2 & P_3 corresponding to settings 2, 4 & 6) were used with a fixed duty cycle and exposure time. Each sample was exposed to ultrasound three times during the period over which the release profile was measured, to ensure the effect could be distinguished from other factors (e.g. disintegration of the particles).

It was also observed, as would be expected, that the active-period of the drug carriers (i.e. the duration over which the drug delivery system can effectively release the loaded therapeutic agent) was shortened as the power of the ultrasound increased. The results for the particles with different polymer concentrations were qualitatively similar. The frequency spectra for the corresponding acoustic emissions were obtained and their mean energy calculated as described befor in section 3.7.1. The mean energy increased with increasing output power as would be expected, since there would be a higher probability of bubble formation and the oscillations of those bubbles would be of larger amplitude.

The correlation between mean energy and drug release enhancement was examined and the relationship was found to be linear again as would be expected based on the linear relation between sonicator power setting and output. Visual observations in a

---

[4] It would be preferable to investigate the effect of ultrasound intensity, but as indicated befor it was not feasible to measure this directly. An attempt was made to use laser vibrometry to indirectly quantify the intensity by measuring the motion of the sonicator probe tip, but this was not possible in water due to the scattering of the light by bubbles. Measurements in air were performed and whilst these could not provide an accurate measure of intensity in water they did indicate a linear progression in probe tip displacement and velocity (and hence intensity) with the sonicator power setting.

water bath containing freshly drawn water confirmed that bubble formation occurred under all conditions i.e. the threshold for bubble formation in terms of acoustic pressure was always exceeded. This was also indicated by the appearance of the exposed particles as discussed in **Section 5.2.3**.

5.2.5 Effect of duty cycle and exposure time on the release profile

The effects on the release profile of varying the duty cycle (30%, 60% & 90%) and the exposure time (15 s, 45 s & 90 s) were also investigated at each output power setting. Both were found to be positively correlated with the drug release rate (c.f. **Table 5.2**), e.g., for an exposure time of 45s, increasing the duty cycle from 30% to 90% increased the release rate enhancement from 6.9% to 13.5%. No significant changes or trends were observed, in either the frequency content or the mean energy of the acoustic emissions (**Table 5.2**). This might seem to be somewhat unexpected given that higher duty cycles and longer exposure times would correspond to higher energy input. Total energy input does not, however, always correspond to greater cavitation activity and reports in literature have been correspondingly contradictory on the effect of the duty cycle on cavitation activity. An extensive review is given by Hodnett *et al.* 2004. This is due to the fact that there are a number of competing processes. If the pressure amplitude of the incident field is sufficiently high, bubbles will form during the negative portion of the cycle in [Hodnett *et al.* 2004]. Over subsequent cycles they may grow through rectified diffusion and will oscillate and may undergo violent collapse, again depending on the pressure amplitude. If the duty cycle is too low, the bubbles will dissolve back into the liquid before they have grown to sufficient size and/or had sufficient time to produce any effect upon the particles. If the duty cycle is too high, on the other hand, then the bubbles will collapse and fragment very rapidly and only a small proportion may interact with the particles. Moreover, for a given temperature and pressure there will be a finite amount of gas dissolved in the liquid which will progressively be driven out of the solution during sonication, so prolonging the exposure time or increasing the duty cycle will not increase the number of bubbles.

Table 5.2 Drug release enhancement and change in energy of measured acoustic emissions for different ultrasound exposure times and duty cycles (output power P2)

Samples	Ultrasound exposure Time (s)	Duty cycle (%)	Drug release rate enhancement (%)	Difference of ultrasound energy in each set (%)
S$_1$:PLGA 2 wt%	45	30	6.9	
	45	60	9	4.7
	45	90	11.7	
S$_2$:PLGA 5 wt%	45	30	7.3	
	45	60	9.7	3.8
	45	90	12.7	
S$_3$:PLGA 10 wt%	45	30	7.4	
	45	60	10.1	2.2
	45	90	13.5	
S$_1$:PLGA 2 wt%	15	60	7.3	
	45	60	9	3.2
	90	60	9.8	
S$_2$:PLGA 5 wt%	15	60	7.8	
	45	60	9.7	2.5
	90	60	10.5	
S$_3$:PLGA 10 wt%	15	60	8.2	
	45	60	10.1	1.1
	90	60	11.3	

5.2.6 Effect of ultrasound exposure on particle microstructure and degradation

PLGA is well known to be highly hygroscopic and to undergo degradation in an aqueous environment. The degradation of PLGA normally involves four stages: hydration, initial degradation, further degradation, and solubilisation [Cai *et al.* 2000, Loo *et al.* 2005] the last of these normally occurring at a lower rate [Cohen *et al.* 1991, Loo *et al.* 2005]. It has been observed in previous studies that during ultrasound exposure, the rate of erosion of the polymeric matrix and hence release of the drug is increased [Miyazaki *et al.* 1988]. Similarly, in this study a clear difference was observed between exposed and unexposed particles (**Fig. 5.7 & 5.8**). In terms of the effect of specific exposure parameters: it was observed that when the duty cycle or the exposure time increased, there was a slight increase in the apparent roughness of the particles. The ultrasound output power also had an effect on the particle morphology with an increasing number of surface pores becoming visible (**Fig. 5.8**).

It is interesting to consider these observations in relation to the measurements of the release profile and the acoustic emissions. As discussed above, duty cycle, exposure time and output power all had significant effects on the release rate enhancement (**Fig. 5.6 & Table 5.2**). Only output power, however, had a noticeable effect upon the acoustic emissions and the particle morphology. The presence of the surface pores may be attributed to bubbles collapsing in close proximity to the particles (microjetting), the probability of which would be expected to increase with increasing ultrasonic power. The resulting increase in surface diffusivity and rate of particle degradation would in turn account for the enhanced drug release rate. The fact that there was no increase in pore formation observed with increasing duty cycle or exposure time is consistent with the lack of increase in acoustic emissions and would seem to indicate that there may be more than one mechanism determining the drug release rate. It may be hypothesised that, unlike cavitation-mediated particle degradation, these other mechanisms are directly related to the energy of the ultrasound field and may be associated with diffusion enhancement as a result of agitation of the liquid and/or a temperature rise (although as noted above this would be expected to be small).
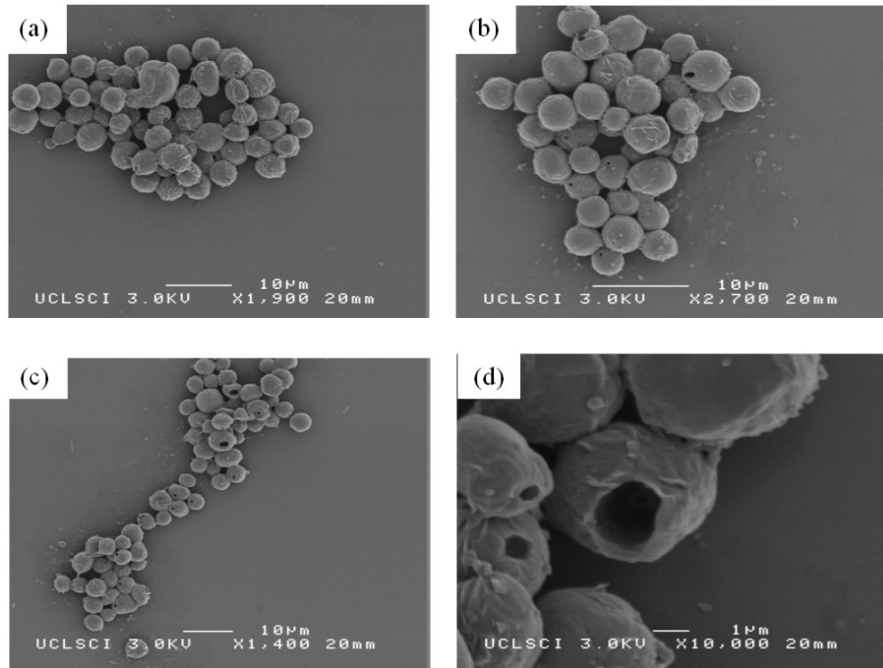
Figure 5.7 Effect of ultrasound duty cycle (DC) on the morphology of the particles produced from PLGA 10 wt% (a) without ultrasound exposure (b) DC: 30 % (c) DC: 60% (d) DC: 90%, (exposure time: 45s and ultrasound out-put power: 4).
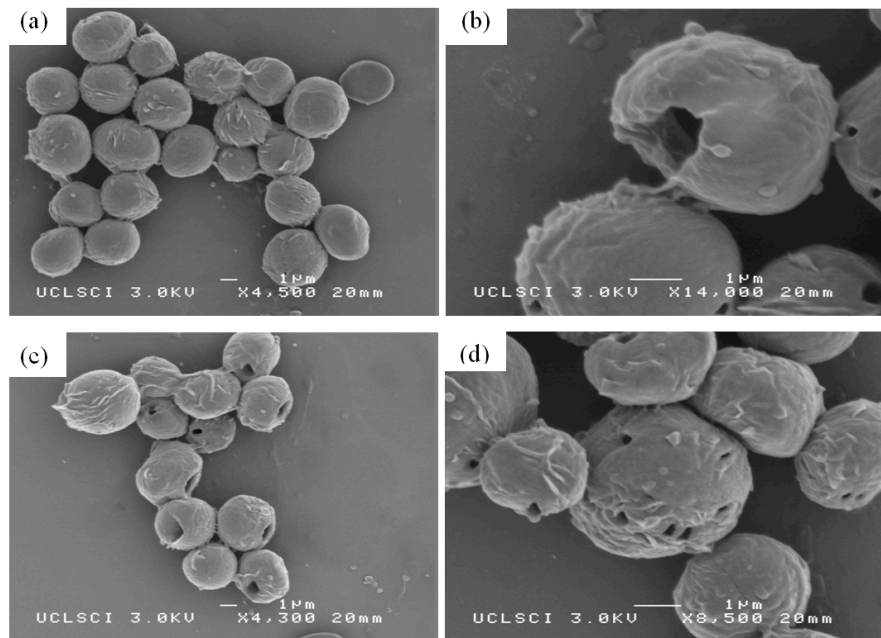
Figure 5.8 Effect of output power of ultrasound on the morphology of the particles produced from 10 wt% PLGA (a) without ultrasound exposure (b) P_1: 2 (c) P_2:4 (d) P_3:6, (ultrasound exposure time: 45s, ultrasound duty cycle: 60 %).

5.3 Characterization and modification of release pattern for estradiol from PLGA particles with improved burst release characteristics

5.3.1 Introduction

As discussed earlier, the objective in engineering many drug delivery systems is to achieve a drug release profile with the desired characteristics in terms of time and rate of drug release. Understanding of the burst effect during controlled release is still limited but knowledge continues to grow as researchers realise both the economic and therapeutic importance of the burst period. Controlling the release requires controlling the properties affecting release, including particle size, size distribution, polymer properties, and surface properties. In this part of the work, a coating method was used to tailor the *in vitro* drug release profiles by changing the surface properties of the PLGA carriers. The influence of coating the particles and the concentration of the coating agent on the release profile were investigated. Also, the size and size distribution of the particles generated were controlled by systematically varying the polymer concentration in the processed solution and their influences on the burst release phase were studied. In this study, the 'burst release' phase is defined as the amount of drug released between 0-24 hours. And, the amount of drug released in between 0 to 72 hours is defined hereafter as the 'initial release' phase.

In order to modify the surface properties, first, the coating technique was optimised by examining the effect of coating on the morphology of the particles. The next part of the study then focused on tailoring the release profiles to achieve minimum initial release and investigating the effects of different coating materials on the *in vitro* release profile of the drug-loaded carriers. The challenging part was finding a simple coating method which can provide a homogenous outer layer on the surface of the particles without having the agglomeration problem. Also, this method should be engineered in such a way that it is capable of controlling the burst release phase without affecting the rest of the release profile. The strong point of this manuscript was optimizing all the involved parameters such as type and concentration of the coating agent. This made it possible to have an effective coating that does not

dissolve quickly (before passing the burst release phase) or slowly (lasts after the burst release phase and slows down the rest of release profile). Therefore, this part of the study needs to find out a smart strategy which can meet all the criteria mentioned above. In all experiments, PLGA solutions with different concentrations (1 wt%, 2 wt%. 5 wt%, 10 wt% and 15 wt%) were used in order to study the effect of particle size on the burst release phase. Again, estradiol was used as a model drug.

5.3.2 Particle characteristics

The most significant solution properties that affect the generation of polymer particles by the EHDA method are density, electrical conductivity, surface tension, viscosity, and polymer concentration. Specifically, the size of the fabricated particles is controlled mainly by the electrical conductivity and viscosity of the solutions [Hartman *et al.* 2000, Cloupeau and Foch 1990]. The viscosity increased and electrical conductivity decreased as the concentration of PLGA increased from 1 wt% to 15 wt% (**Table 5.3**). Also, PLGA concentration was found to affect the surface tension of the polymer solutions, with an increase of the concentration from 1 wt% to 15 wt%, the surface tension increased from ~33 to 41 m Nm^{-1}.

Table 5.3 Properties of the solutions and the solvent used in this study.

Sample	Density (kg m^{-3})	Viscosity (mPa s)	Surface tension (mN m^{-1})	Electrical conductivity (µS m^{-1})
DMAC	940	2.0	29	5.6
PLGA:DMAC 1:99	948	0.6	33	4.7
PLGA:DMAC 2:98	950	0.8	33	4.7
PLGA:DMAC 5:95	958	1.7	34	3.1
PLGA:DMAC 10:90	970	4.9	39	1.5
PLGA:DMAC 15:85	990	11.7	41	0.9
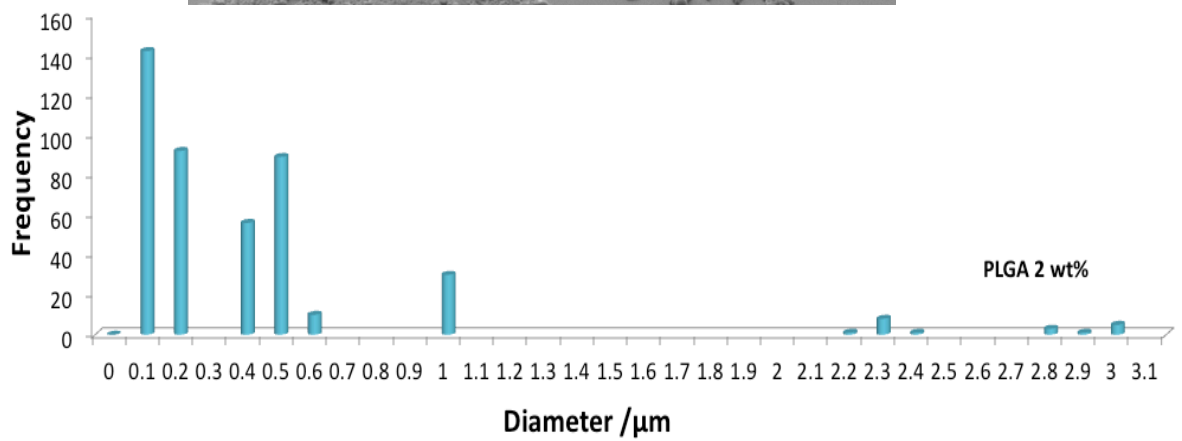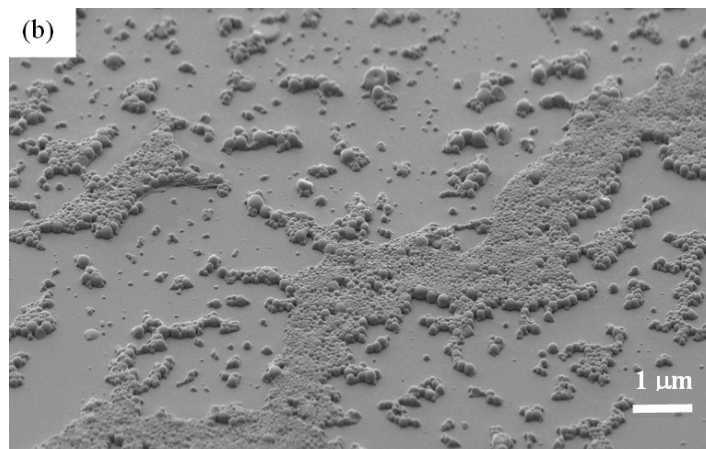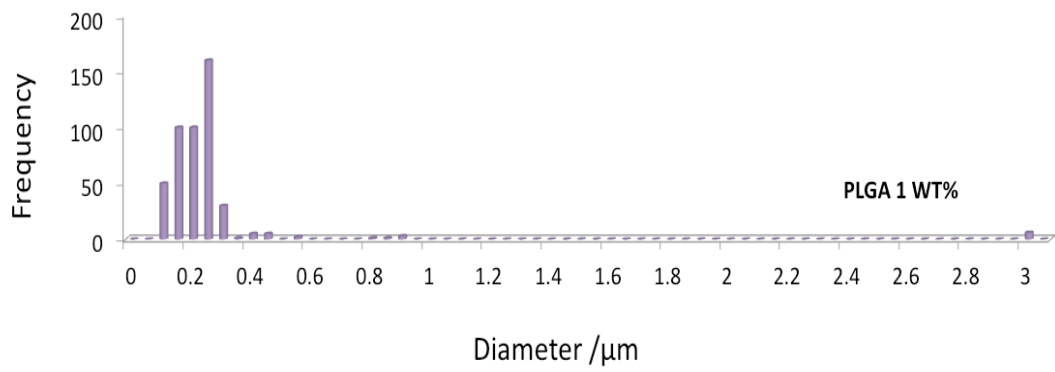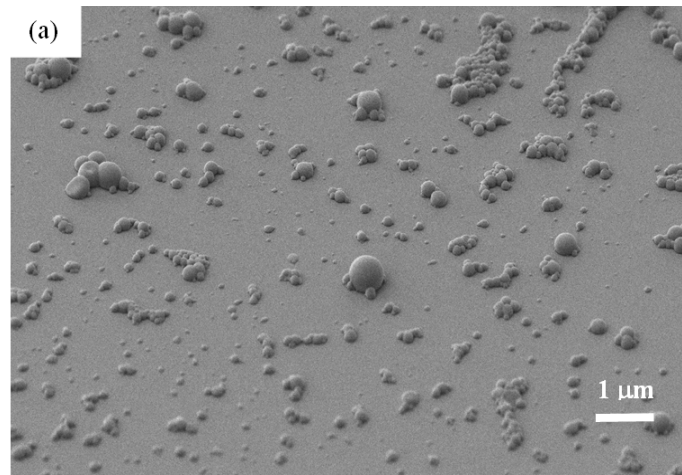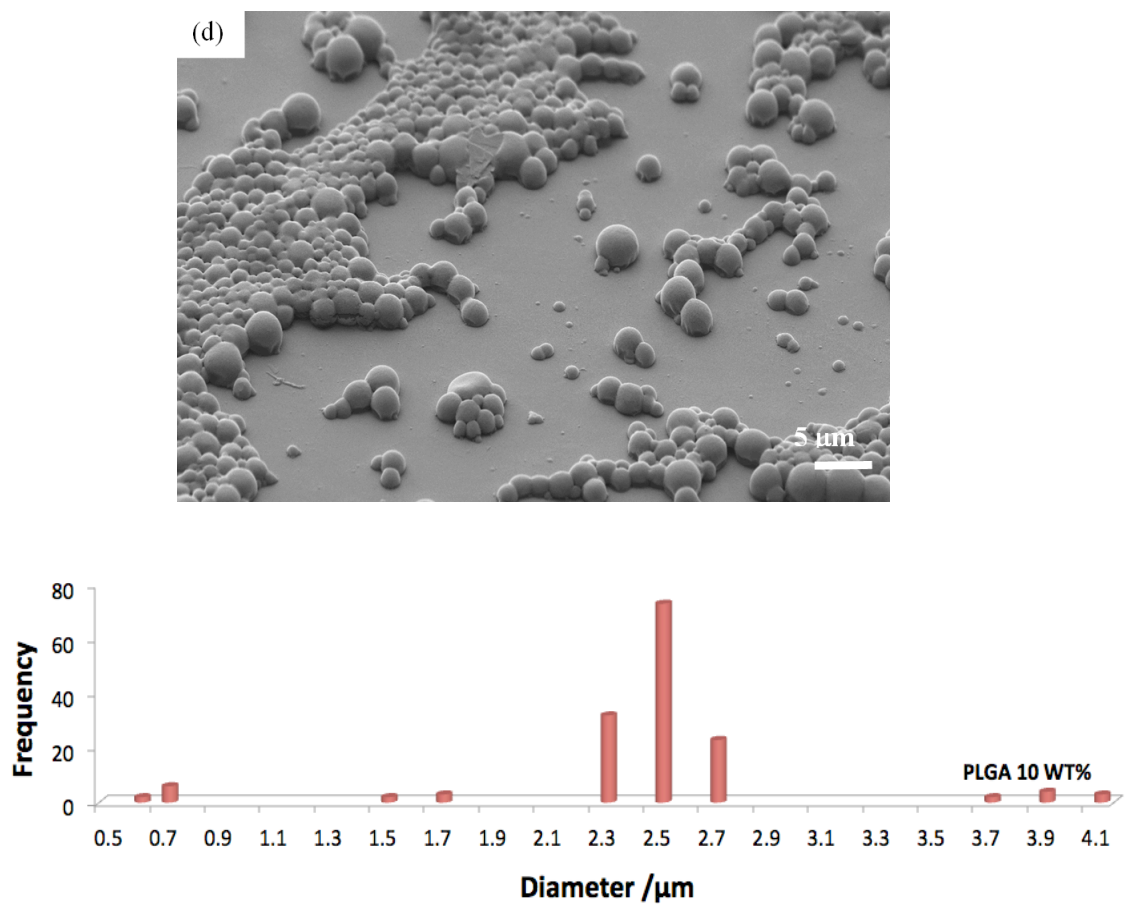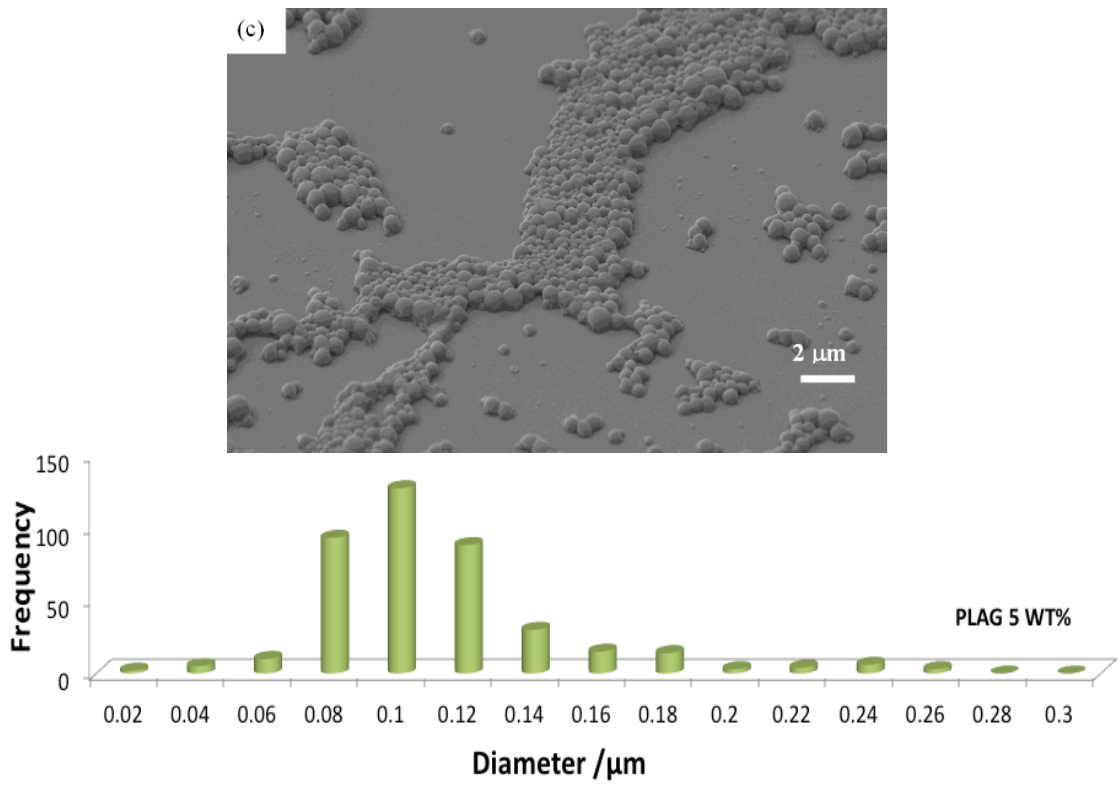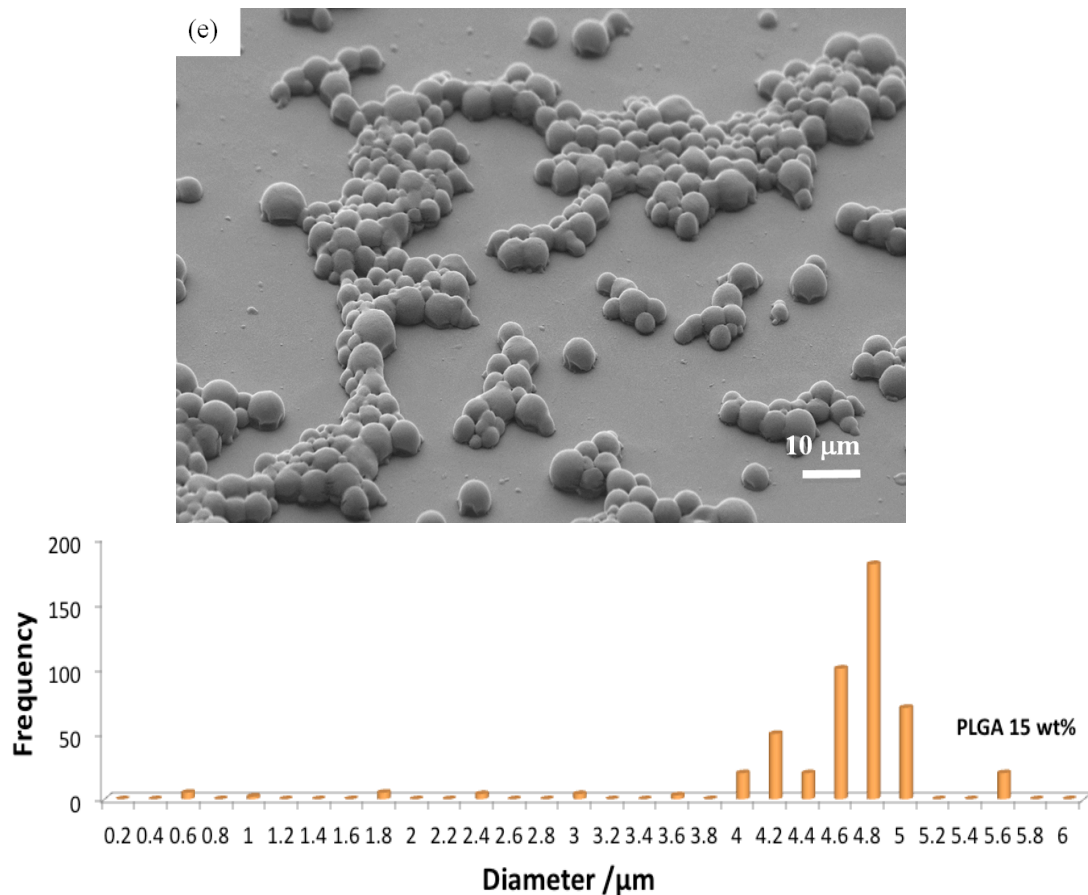
Figure 5.9 SEM micrograph and size distribution of PLGA particles fabricated with 5 different concentrations: (a) 1 wt% PLGA (b) 2 wt% PLGA (c) 5 wt% PLGA (d) 10wt% PLGA (e) 15 wt% PLGA.

The structure and size of the particles were determined prior to investigating the effect of particle size on burst release phase. Representative SEM micrographs and size distributions plots for PLGA particles prepared using various polymer concentrations are shown in **Fig. 5.9**. As can be seen, the majority of the particles were spherical with smooth surfaces and without visible pores. This may be attributable to the fact that the high boiling point (164-166°C) of the dimethylacetamide slowed the evaporation rate during jetting, thus decreasing formation of pores. Particles prepared from the highest polymer concentration (15 wt%) were slightly agglomerated due to the presence of residual solvent during drying. The mean size of the particles was calculated by measuring the diameter of ~300 particles using Image Tool. The mean size of the fabricated particles ranged from 100 nm to 4.5 μm.

In the size distribution study, most of the samples had monomodal size distributions, and particles made from the more viscous solutions had narrower size distributions. More than 90% of the particles prepared using 5 wt% PLGA were <120 nm in diameter (**Fig. 5.9c**). For the particles produced from the 10 wt% PLGA solution, 95% had diameters >2 μm (**Fig. 5.9d**). Particles prepared from 15 wt% PLGA had a narrow bimodal size distribution, and the mean size of the particles was 4.5μm (**Fig. 5.9e**). The polydispersivity index (PI=standard deviation/mean size) of the particles made from 15 wt% solutions was slightly higher than (< 2%) the PI of the particles made from 10 wt% solution. This was due to the presence of some particles with diameters larger than the mean size, which shifted the monomodal size distribution to a bimodal one.

However, particles prepared from 1 wt% and 2 wt% PLGA solutions, had bimodal size distributions. The mean size of these particles was also higher than that made from the 5 wt% solution. This wider variation in particle size can be attributed to the generation of different types of droplets ("primary" and "satellite") during the processing [Hartman *et al.* 2000, Tang and Gomez 1994 and 1995]. The presence of some larger particles at the higher range of the size distribution graph, (see second peak in **Fig 5.9a** and **5.9b**) was clear. These few but significantly larger particles among the small particles made from 1 wt% and 2wt% solutions had a significant role in mathematical size distribution analysis which causes a noticeable increase in both mean size, polydispersivity and standard deviation of the particles (**Fig. 5.10**).

The increase in PI for the 1 wt% and 2wt% samples is attributed to the stability of the cone-jet which can dictate the size of the generated droplets and their particle relics. The concentration of the solutions in these two samples was below the critical range to achieve a stable cone-jet. The apex of the cone-jet shifts away from the centre of the cone, which is no longer symmetrical and takes the form of an "off-centered" jet which may alter the balance of interacting forces. Therefore, a symmetrical cone-jet could not be established and this results in oscillation and

instability which produces some large droplets, which in turn results in a higher polydispersivity index.
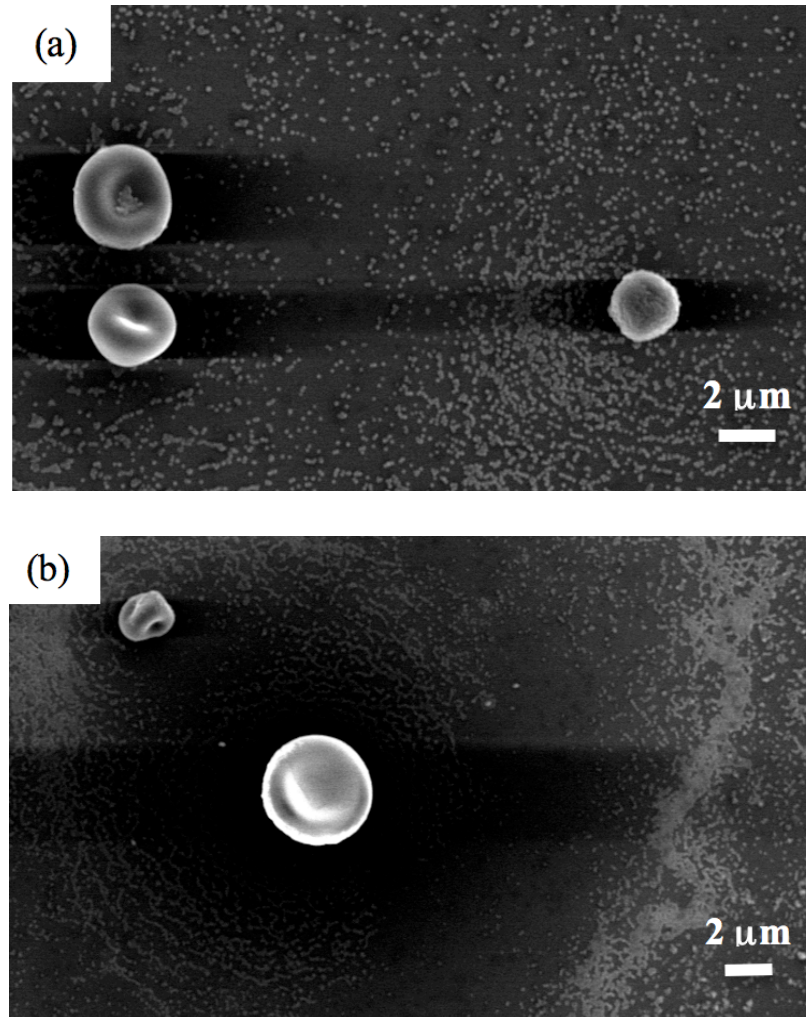
Figure 5.10 SEM images of particles prepared with (a) 1 wt% and (b) 2 wt% polymer concentrations, the evidence of the presence of large particles.

The polydispersivity index of the particles made from the 5 wt% PLGA solution was the lowest (**Table 5.4**). These results confirmed that the concentration of polymer in the liquid has a significant impact on the size of the particles produced and this is caused primarily by the increase in viscosity with polymer concentration, which results in larger droplets being formed [Edwards *et al.* 1997].

Table 5.4 Particle size characteristics of the prepared polymeric carriers.

Sample	Mean size (nm)	Polydispersivity (%)	Standard deviation (nm)	Number of particles studied
PLGA 1wt%	250	50	130	464
PLGA 2wt%	250	38	100	300
PLGA 5wt%	100	11	11	300
PLGA 10 wt%	2500	16	400	150
PLGA 15 wt%	4500	18	800	483

5.3.3 Effect of particle size on burst release phase

The main goal of designing sustained and controlled delivery systems is to reduce the frequency of dosing and provide uniform drug release. The total amount of estradiol used in the release study was the same for all formulations, and the PLGA formulations were prepared under the same processing conditions. One factor affecting the drug release kinetics is the particle dimension [Gaumet *et al.* 2007] as particles with different dimensions, have different surface areas, and thus, have different total surface areas available for drug release. **Figure 5.11** compares the estradiol release profiles from PLGA particles with different diameters. The burst release is commonly attributed to the release of drug located close to the surface of particles [Pitt 1990, Cohen *et al.* 1991]. Also, it is related to the porosity of the particles. A high surface porosity correlates with a large surface area and rapid penetration of the release medium and consequently a very significant burst release [Musante *et al.* 2002].The release profile of particles made from PLGA solutions with concentrations of 5 wt% was more biphasic (**Fig. 5.11**). The release pattern consisted of a burst release followed by zero-order like release phase where a steady amount of drug is released over time. The release profiles of microparticles made from PLGA solutions with concentrations of 10 wt% and 15 wt% were triphasic; a

burst release phase followed by a slow release phase and then a second, more rapid release phase. The release profiles of PLGA 1 wt% and PLGA 2wt% samples showed that the few large particles which increased the mean size did not have a significant effect on the overall release profile.
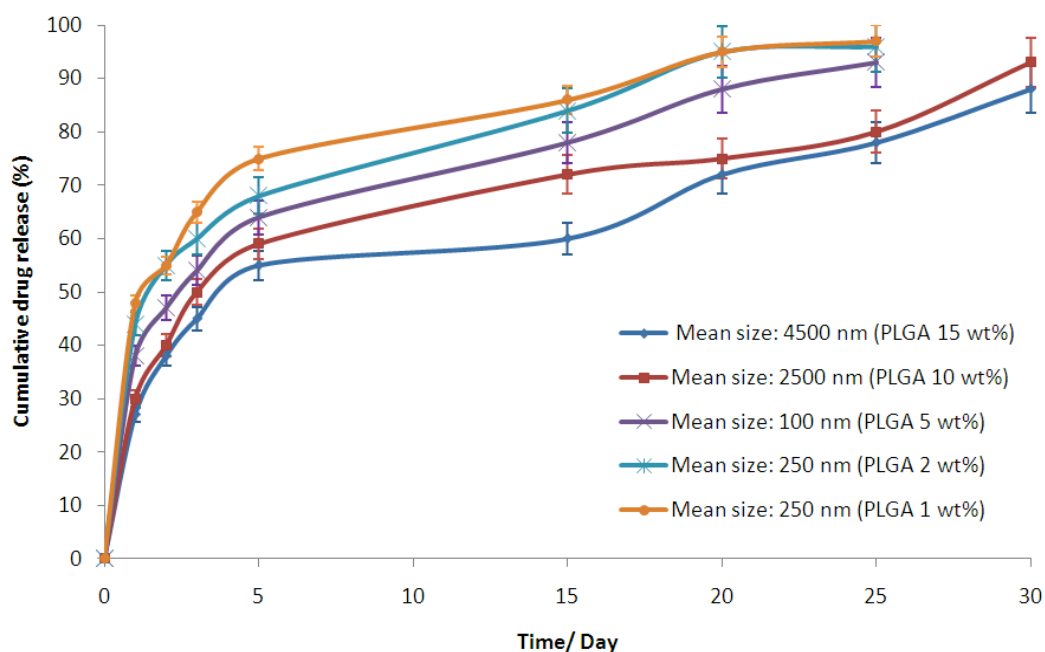
Figure 5.11 Estradiol release profile from PLGA particles produced with various solution concentrations.

These results also showed that the burst release was lower for the larger particles. This is most likely to be because the total surface area of a constant total volume of particles decreases when the size of the particles increase. In addition, increasing the size of the particles, increases the length of diffusion pathways for the estradiol molecules. Thus, these molecules have to traverse a longer distance within the polymer matrix to reach the surface. However, the products of polymer degradation also have to travel a longer distance before they can dissolve in the release medium. The trapped products change the localised pH within the polymer matrix (especially in the bigger particles), which accelerates the polymer degradation due to autocatalysis. This accelerates the rate of loss of molecular weight within the matrix leading to faster drug diffusion in the final fast release phase. However, in the

smaller particles (<300 nm), autocatalysis is insignificant [Shive and Anderson 1997]. The overall significant impact of increasing the diffusion pathways (by increasing the particle diameter) is reducing the burst release phase. This result indicates that the burst release is a diffusion-based process, which is influenced by the morphology of the particles while the subsequent release is a function of the polymer degradation.

5.3.4 Coating particles

5.3.4.1 Feasibility of method

As mentioned in **Section 2.12.1.2,** burst release could be minimized by: first, inducing a reduction in water intake, second, providing longer diffusion pathways to the drug molecules, and third, eliminating the amount of drug on the surface of the carriers. Therefore, the above mentioned parameters that effect on initial burst can be fulfilled by surface modification by additional coating steps to provide an outer layer with no drug. For instance, in a study where alginate beads were coated three times with a polycation, either poly(L-lysine HBr) or poly(vinyl amine), to avoid the burst release of biomacromolecules including proteins and dextrans [Wheatley *et al.* 1991]. It was discovered that increasing the polycation concentration decreased the burst release, and caused the release profile to be more sustained.

Three PLGA concentrations; 2 wt%, 5 wt% and 10 wt% were chosen for further investigation since they had desirable size distributions (both in nano and micro scale) and estradiol release characteristics. The particles were coated with chitosan and gelatin coating agents, however, the viability of the coating method was studied for just chitosan coated particles. Coating the particles with a thin layer of material such as chitosan and gelatin, means the therapeutic molecules have to pass through an additional layer increasing the diffusional resistance. Therefore, slowing down the release process and, in particular, reducing the initial release phase. The release profiles of chitosan coated particles showed a noticeable reduction in the initial release rate between 0 to 72 hours.

(a) Un-coated particles

(b) Dip-coating
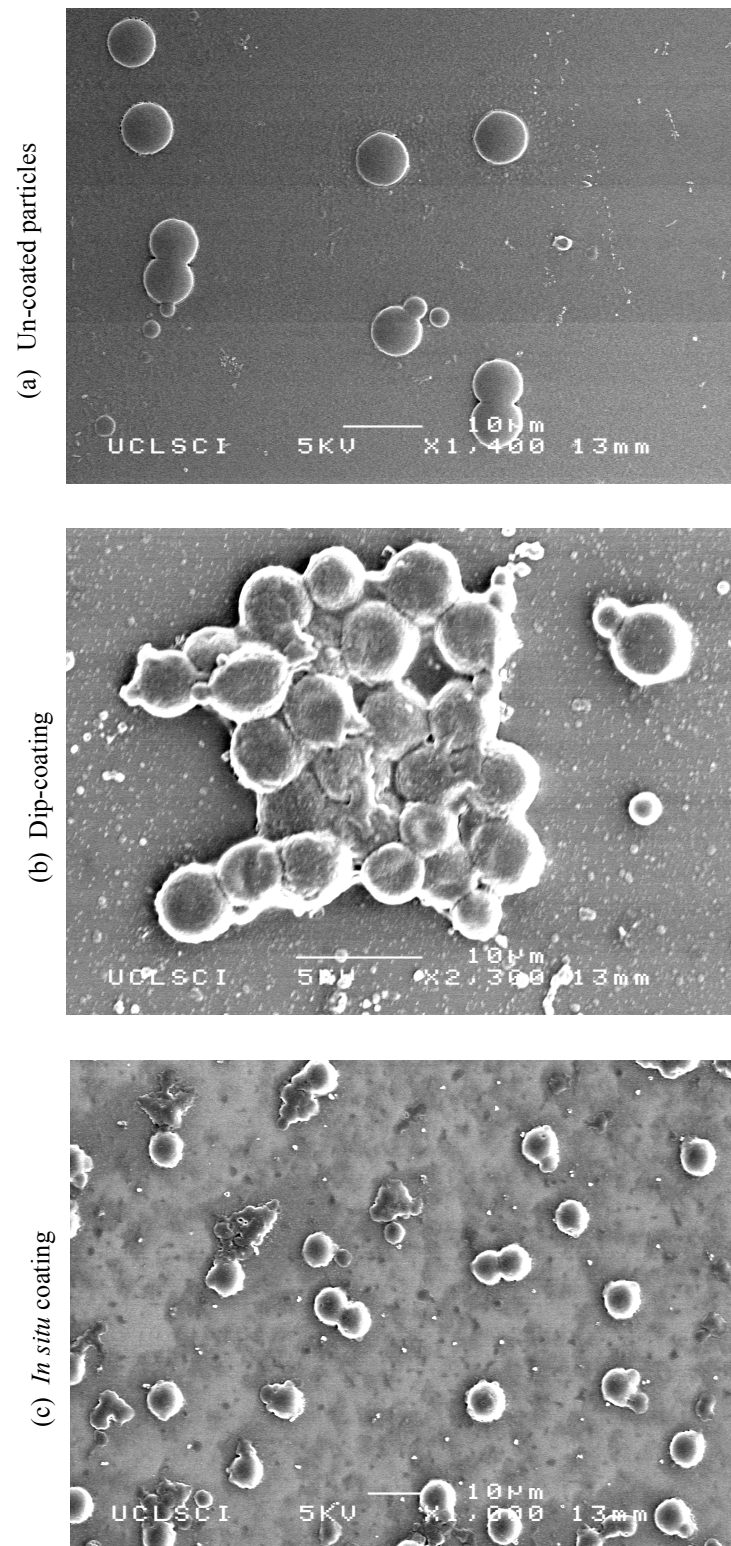
(c) *In situ* coating

Figure 5.12 Influence of coating method on surface morphology of chitosan coated PLGA particles. (a) uncoated (b) dipped (c) *in situ.*

Two physical coating methods, dip-coating and *in situ* coating, were used. In the former method, coating was achieved by carefully spreading a drop of solution of chitosan on the surface of the particles following preparation and then mixing it to ensure that the particles were coated evenly. The coating protocol was later modified to an *in situ* coating method. Here electrosprayed PLGA particles were collected in an aqueous solution. Then, chitosan was added to the particulate suspension straight after collection to form chitosan solutions with specific concentrations while mechanically stirring for 300s. The coated particles were centrifuged and were separated from the solutions. This technique promotes uniform chitosan coating on the particle surface and prevents agglomeration of the particles (**Fig. 5.12**). As shown in **Fig. 5.12**, chitosan-coated PLGA particles which were coated using the *in situ* method were spherical and uniform (**Fig. 5.12b**) while the other particles coated via dipping were agglomerated and clustered (**Fig. 5.12c**). Therefore, the *in situ* coating technique was chosen for further investigation in this work (**Section 5.3.4.2 and 5.3.5**).

Figure 5.13 FTIR spectroscopy of uncoated PLGA particles, chitosan solution and PLGA particles coated with chitosan solution of three different concentrations.

The presence or absence of the chitosan coating was confirmed via FTIR spectroscopy to show the presence of different functional groups and to study the feasibility of the coating process. The chemical structure of pure PLGA particles, chitosan solution and chitosan-coated PLGA particles is shown in **Fig. 5.13**. The interpretation of infrared spectra involves the correlation of absorption bands in the spectrum of an unknown compound with the known absorption frequencies for different types of bond. The FTIR spectrum of chitosan solution has some characteristic absorption bands at about 3422 cm^{-1} (N-H and O-H), 1652 cm^{-1} (-CONH-) and 1076 cm^{-1} (C-O-C) [Wu *et al.* 2005]. The spectrum for the chitosan-coated particles was compared with the spectrum of chitosan solution and pure PLGA particles (**Fig. 5.13**). The existence of the chitosan moiety in the chitosan-coated sample was proved by two peaks around 3422 cm^{-1} and 1652 cm^{-1}, which are the particular peaks assigned for N-H/O-H and –CONH- groups. C–O–C group belongs to both PLGA and chitosan. The C–O–C peak was observed around 1090 cm^{-1} and 1080 cm^{-1} in the pure PLGA particles and chitosan samples, respectively. The strong shift of the C–O–C peak about 1089 cm^{-1} was observed in the coated sample, which also confirms the presence of chitosan, which attached to PLGA. These results showed that the coating process of the PLGA particles was successful.

The effect of the chitosan concentration on the coating process was also studied using FTIR spectroscopy. All the particles were physically coated and the coating process is solely due to physical adsorption or electrostatic interactions between the polymer chains and the coating material. **Figure 5.13**, presents the FTIR spectra of the PLGA particles made from 10 wt% solutions which were coated with chitosan of three different concentrations (0.5 wt%, 1 wt% and 1.5 wt%). The transmission intensities of chitosan bands at 3422 cm^{-1} (N-H and O-H) and 1652 cm^{-1} (-CONH-) increased with the chitosan concentration. These results suggest that when a more viscous solution is used, more coating material covers the surface of the particles. These results were also confirmed with cross-section study of the particles. The cross-section and the coating thickness were elucidated using FIB and SEM microscopy. It was found that the particles had porous inner microstructures (**Fig. 5.14**), while the surface of the particles were not porous (the inset figure in **Fig. 5.14c**).
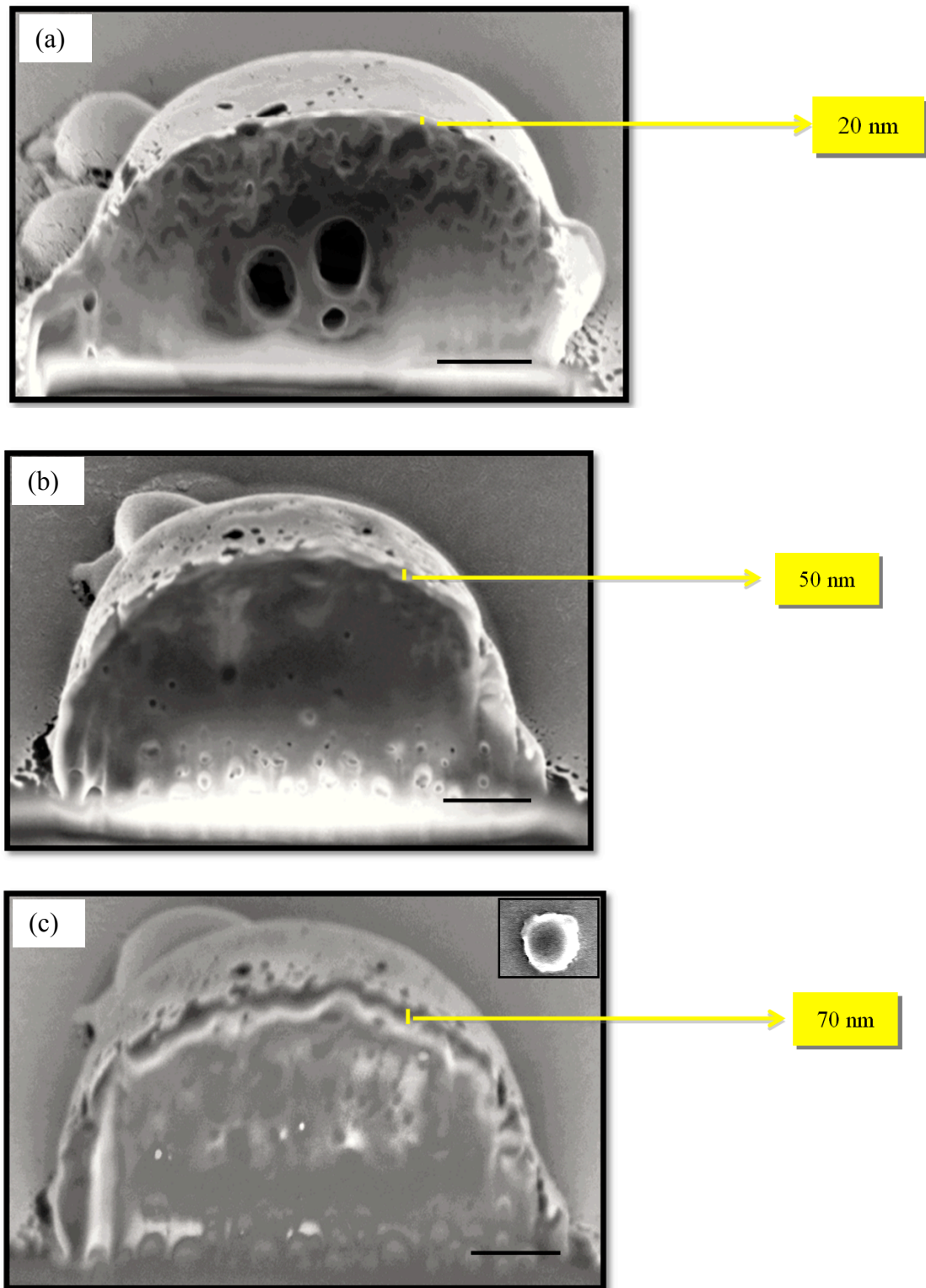
Figure 5.14 Cross section structure of the PLGA 10 wt% particles and the thickness of the coating (a: coated with 0.5 wt% chitosan solution, b: coated with 1 wt% chitosan solution, c: coated with 1.5 wt% chitosan solution), scale bar: 500 nm.

The additional coating layer was observable in the FIB micrographs. For the more viscous chitosan solutions (1 wt% and 1.5 wt%) the coating layers were more clearly observable. The thickness of the chitosan coating was increased from 20 nm to 70 nm as the concentration of the chitosan increased from 0.5 wt% to 1.5 wt%.

5.3.4.2 Stability

For further investigation, PLGA particles were *in situ* coated with either chitosan or gelatin. The stability of both chitosan and gelatin on the surface of PLGA particles was again studied using FTIR (**Fig. 5.15**). According to **Fig. 5.15a**, FTIR spectroscopy of chitosan coated PLGA particles at 0, 24, 48 and 72 hours of release showed similar trend with various intensities. The peaks at 3422, 1649 and 1076 cm^{-1} were due to the stretching of O-H/N-H, -CONH-, and C-O-C, respectively. The intensity of the FTIR spectrum of the chitosan coated PLGA particles was decreased as a function of time, which indicated that ionic desorption between chitosan and PLGA ions was started after 24 h of the release test. These results showed that the coating lasts for up to 72 hours on the surface of the particles. Also, the *in vitro* release studies showed that the coated particles had a less pronounced initial release phase between 0 to 72 hours. The evidence suggests that chitosan can be used successfully as a coating material which limits the burst release phase.
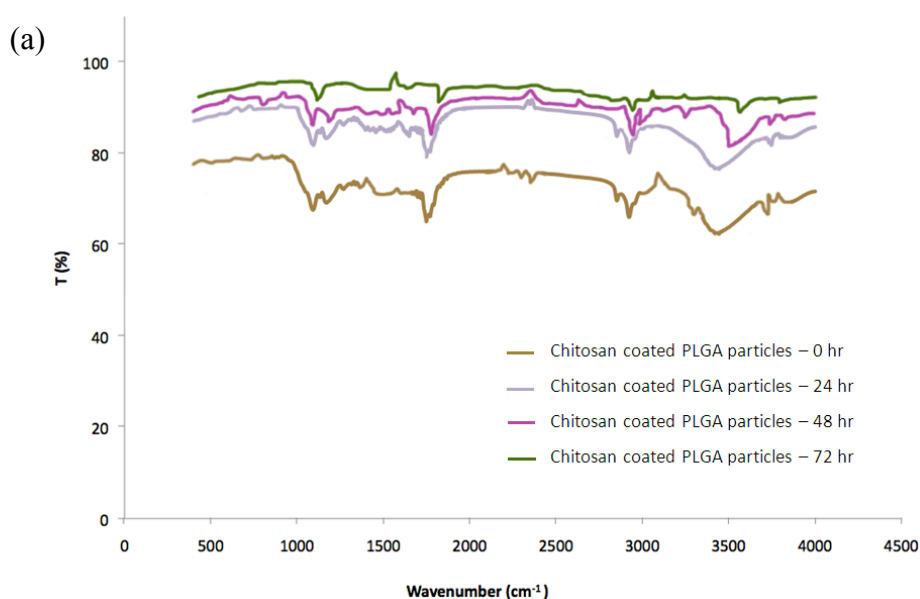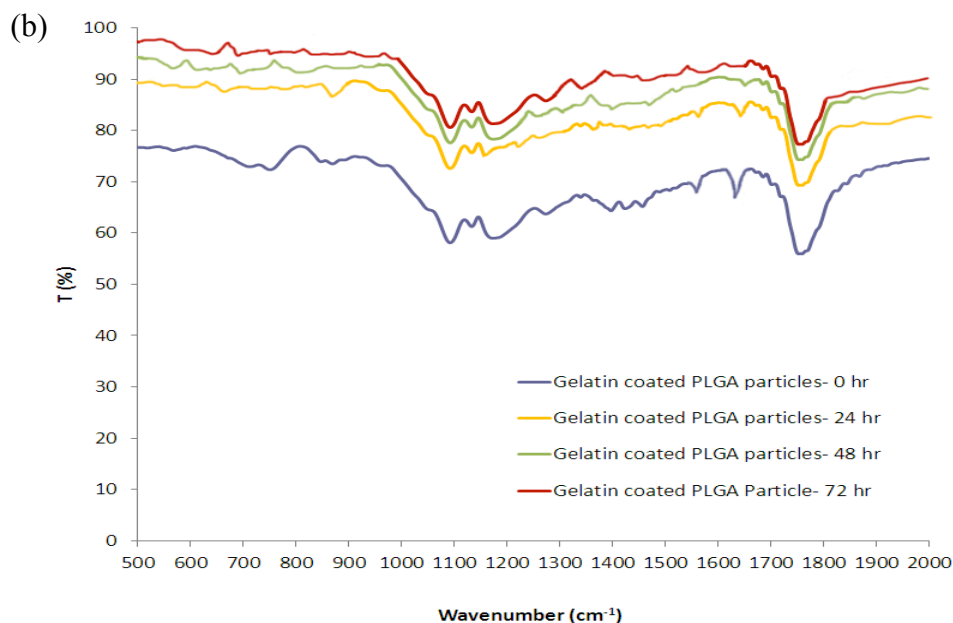
Figure 5.15 FTIR spectra of coated PLGA particles with 1 wt% solution at 0, 24, 48 and 72 hours of release testing, (a) chitosan coated (b) gelatin coated.

The FTIR spectroscopy of the gelatin molecules on the surface of PLGA particles is shown in **Fig. 5.15b**. The C–O–C peak of the PLGA particles was observed around 1090 cm^{-1} and 1080 cm^{-1} in the gelatin coated PLGA particles. Gelatin has two intense bands at 1641 and 1557 cm^{-1} assigned to amide bonds (amide I and amide II modes, respectively). These two peaks were clearly seen in the FTIR spectrum of the gelatin coated samples straight after the coating process. But, after keeping the sample in the release medium, the intensity of the band was significantly reduced after 24 hours. These results suggest that the stability of gelatin on the surface of the PLGA particles was less than the stability of chitosan. This is likely to be due to the fact that gelatin is more hydrophilic and can dissolve/degrade in the aqueous release medium faster than chitosan.

5.3.5 Effect of coating on release profile

The release profiles of estradiol from both chitosan and gelatin coated PLGA particles fabricated from various PLGA, chitosan and gelatin concentrations are shown in **Fig. 5.16** and **5.17** (the uncoated release profiles are given as references).
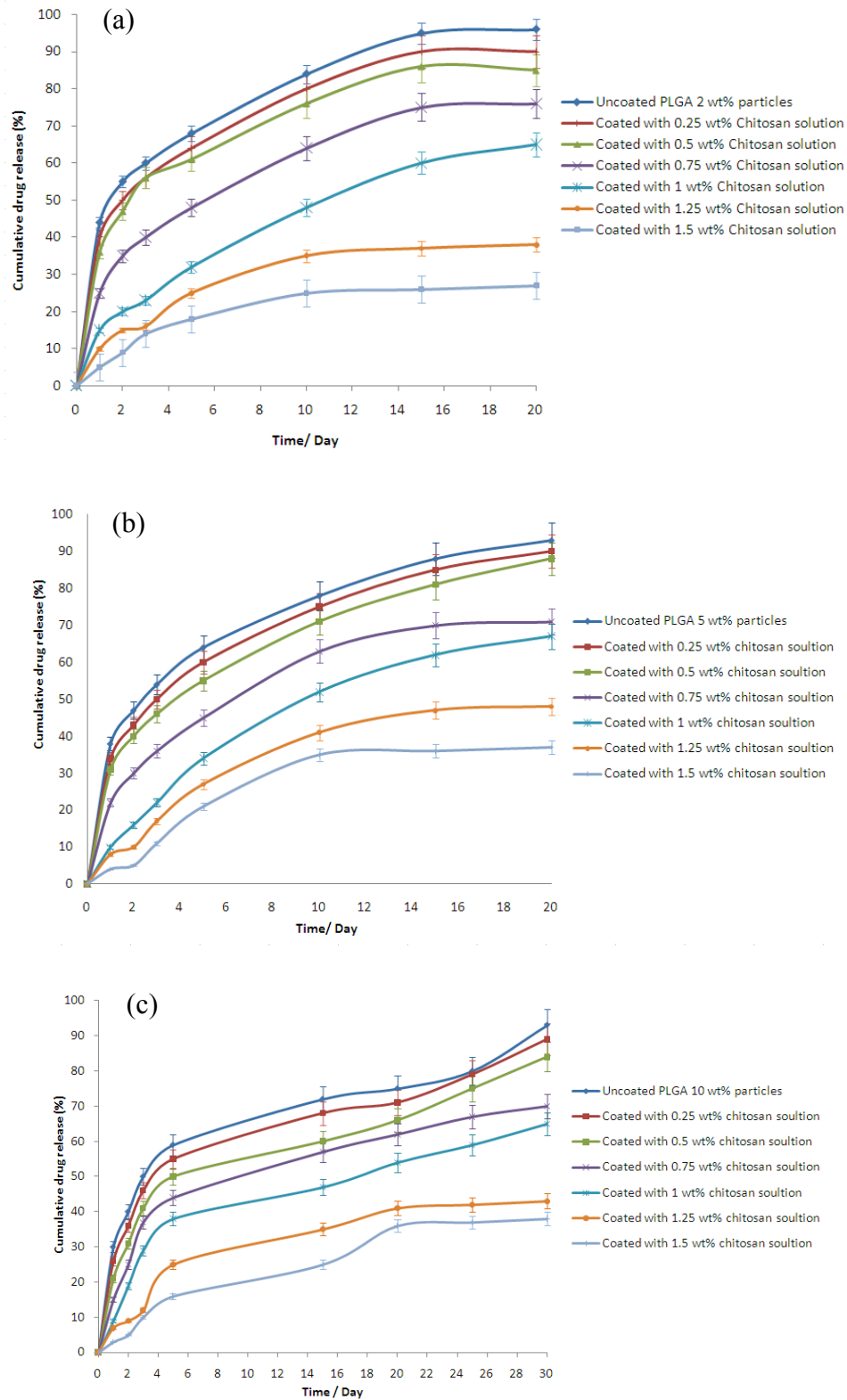
Figure 5.16 Estradiol release from different PLGA particles coated of chitosan solution of various concentrations (a) PLGA 2 wt%, (b) PLGA 5 wt%, (c) PLGA 10 wt%.

The initial release might be attributed to the fact that estradiol macromolecules were loosely bound onto PLGA particles by ionic interaction, which could be easily desorbed in an ionic environment [Pitt 1990, Cohen *et al.* 1991]. As depicted in **Fig. 5.16a**, in PLGA particles made using the 2 wt% polymer solution, 44 % of the drug was released in the first 24 hours followed by 60% release after 72 hours.

Table 5.5 Estradiol release data for chitosan coated PLGA particles and the effect of coating on burst and initial release[5].

Sample	Burst release % (released between 0 to 24)	Initial release % (released between 0 to 72)	Drug released reduction in 72 hr (%)	Encapsulation efficiency (%)
Uncoated PLGA 2wt%	44	60	---------------	65
PLGA 2 wt% + chitosan 0.25 wt%	40	56	4	65
PLGA 2 wt% + chitosan 0. 5 wt%	36	56	4	65
PLGA 2 wt% + chitosan 0.75 wt%	25	40	20	65
PLGA 2 wt% + chitosan 1 wt%	15	23	37	65
PLGA 2 wt% + chitosan 1.25 wt%	10	16	44	65
PLGA 2 wt% + chitosan 1.5 wt%	5	14	46	65
Uncoated PLGA 5wt%	38	54	-----------------	68

---

[5] continued on the next page

PLGA 5 wt% + chitosan 0.25 wt%	34	50	4	68
PLGA 5 wt% + chitosan 0. 5 wt%	31	46	8	68
PLGA 5 wt% + chitosan 0.75 wt%	22	36	18	68
PLGA 5 wt% + chitosan 1 wt%	10	22	32	68
PLGA 5 wt% + chitosan 1.25 wt%	8	17	37	68
PLGA 5 wt% + chitosan 1.5 wt%	4	11	43	68
Uncoated PLGA 10wt%	30	50	-----------------	75
PLGA 10 wt% + chitosan 0.25 wt%	26	46	4	75
PLGA 10 wt% + chitosan 0. 5 wt%	21	41	9	75
PLGA 10 wt% + chitosan 0.75 wt%	15	37	13	75
PLGA 10 wt% + chitosan 1 wt%	9	29	21	75
PLGA 10 wt% + chitosan 1.25 wt%	7	12	38	75
PLGA 10 wt% + chitosan 1.5 wt%	3	10	40	75

Six concentrations (0.25 wt%, 0.5 wt%, 0.75 wt%, 1 wt%, 1.25 wt% and 1.5 wt%) of chitosan solution were prepared for coating the PLGA particles with different sizes (**Fig. 5.16**). It was observed that as the concentration of chitosan increased, the burst release rate and the initial release rate of estradiol became lower in the first 24 and

72 hours, respectivly. However, samples coated with more concentrated chitosan solution (more than 1 wt%) were agglomereted together. For instance, in samples coated with 1.5 wt% chitosan solution, the release rate decreased even after 72 hours, this may be attributed to agglomeration even in the presence of stiring the particle solutions throughout the release profile determination. This problem was not observed in the samples coated with 1 wt% chitosan solution. For instance, the burst release from PLGA 2 wt% samples coated with 1 wt% chitosan solution was 15 % in the first 24 hours which followed by 23 % release within 3 days. These results showed reductions of 34% and 37% in the drug release over the first 24 and 72 hours, respectively.

(a)

(b)
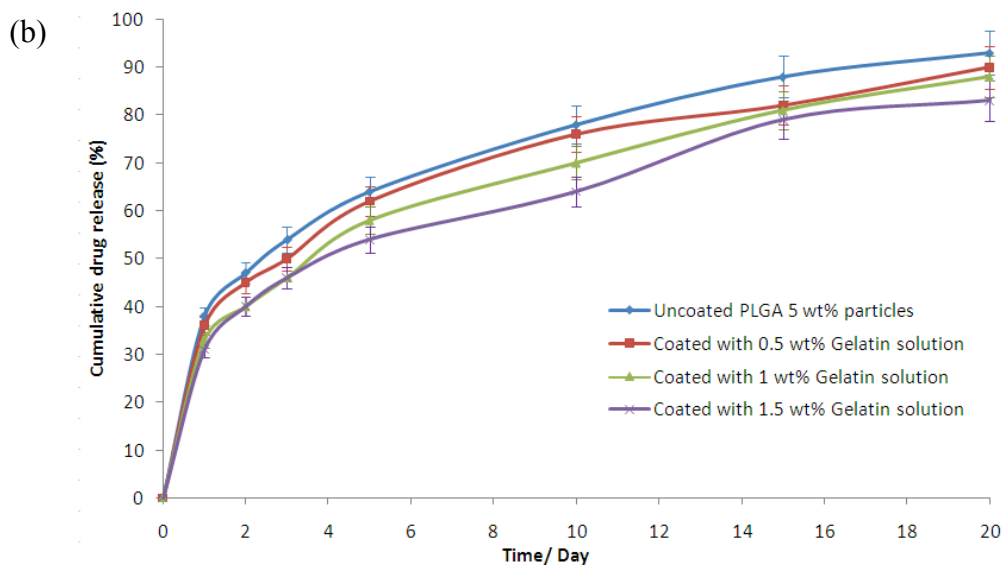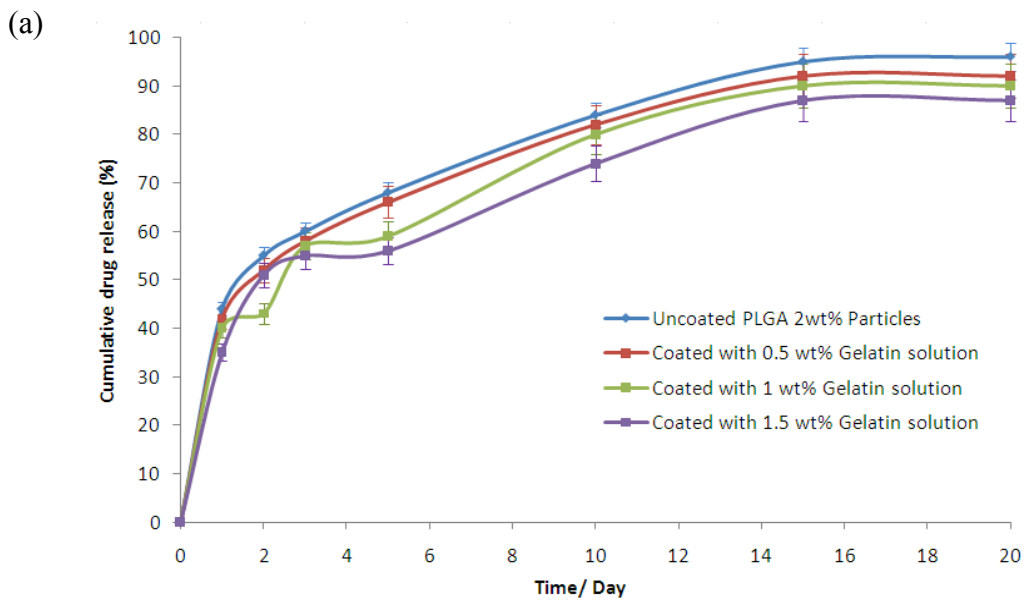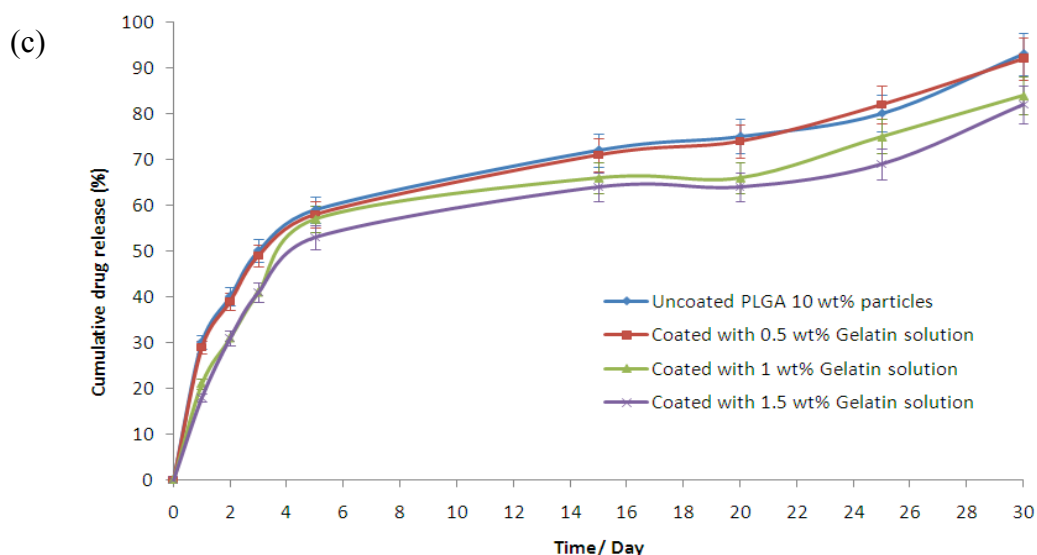
Figure 5.17 Estradiol release profile from PLGA particles with various sizes coated with gelatin solution (a) PLGA 2 wt%, (b) PLGA 5 wt%, (c) PLGA 10 wt%.

The total amount of estradiol released from the chitosan coated PLGA particles in 72 hours was reduced compared to the drug released from uncoated PLGA particles. In all samples (PLGA 2wt%, PLGA 5wt% and PLGA 10 wt% samples) coated with 1 wt% chitosan solution the initial release was reduced by 37%, 32% and 21 %, respectivley, for the first 72 hour. This was then followed by controlled and sustained estradiol release over 30 days (**Table 5.5**).

The smaller amount of estradiol released from chitosan coated PLGA particles might be explained by the fact that there are strong interactions between the polymers (chitosan and PLGA) and estradiol. The initial release is also reduced because now the surface region contains less drug since the coated chitosan layer is devoid of drug. Additionally, the presence of the chitosan layer could slow down the diffusion of estradiol from the polymeric carrier, which also prolongs the release time of estradiol. The release studies indicated that coating of chitosan onto PLGA encapsulate estrodiol particles could improve the release of the drug.

Table 5.6 Estradiol release data for gelatin coated PLGA particles and the effect of coating on burst and initial release.

Sample	Burst release % (released between 0 to 24)	Initial release % (released between 0 to 72)	Drug released reduction in 72 hr (%)	Encapsulation efficiency (%)
Uncoated PLGA 2wt%	44	60	-----------------	65
PLGA 2 wt% + gelatin 0. 5 wt%	42	58	2	65
PLGA 2 wt% + gelatin 1 wt%	40	57	3	65
PLGA 2 wt% + gelatin 1.5 wt%	35	55	5	65
Uncoated PLGA 5wt%	38	54	----------------	68
PLGA 5 wt% + gelatin 0. 5 wt%	36	50	4	68
PLGA 5 wt% + gelatin 1 wt%	33	46	8	68
PLGA 5 wt% + gelatin 1.5 wt%	31	46	8	68
Uncoated PLGA 10wt%	30	50	---------------	75
PLGA 10 wt% + gelatin 0. 5 wt%	29	49	1	75
PLGA 10 wt% + gelatin 1 wt%	21	41	9	75
PLGA 10 wt% + gelatin 1.5 wt%	18	41	9	75

Release profiles of estradiol from gelatin coated PLGA particles are shown in **Fig. 5.17**. As a biomaterial, gelatin has several advantages: it is a natural polymer that has

not shown antigenicity [Young *et al.* 2005] and it is completely resorbable *in vivo*. However, the *in vitro* release profile of the gelatin coated samples proved that gelatin did not last for 72 hours on the surface of the PLGA particles. The gelatin coating did not have a noticeable influence on the estradiol release profiles. This could be attributed to its lower stability at body temperature [Curcio *et al.* 2010]. Gelatin acts as a hydrophilic moiety on the surface morphology of the PLGA particles and it is soluble in the human body enviroment. The release profiles of the samples showed initial release reductions of 3, 8 and 9 percent in samples made from 2wt%, 5 wt% and 10 wt% PLGA solutions in the first 72 hours (**Table 5.6**).

In terms of effectiveness as a coating material, chitosan controlled both burst and initial release more effectively than gelatin. A number of –OH and – NH groups in chitosan, provide more opportunities for intermolecular hydrogen bonding with the surface of PLGA partcles. Chitosan forms an entangled network layer on the particle surface and limits the infiltration and diffusion of water into the drug carrier. Therefore, the diffusion of drug molecules from the particles surface to the release medium is restricted by the entanglements caused by the chitosan layer, which reduces the burst and initial release.

Summary

This study showed that drug loaded polymeric particles fabricated in previous studies (described in **Chapter 4**) are able to release their payload in a controllable manner. Furthermore, two strategies were applied in order to achieve more regulated and sustained drug release profiles: first, using ultrasound as a potentially extracorporeal stimulus to enhance the drug release when required; second, changing the surface properties of the particles via a coating method, in order to control the burst release phase.

In **Section 5.1**, it was shown that evans blue and estradiol loaded PLGA particles had release profiles which began with a burst release phase followed by a period of sustained release. The amount of drug released from the particles produced from the more concentrated solution was lower than that for those produced from the less concentrated solutions. In **Section 5.2**, the feasibility of ultrasonically augmenting drug release and polymer degradation was demonstrated. The amount of drug released increased as the power of the ultrasound increased, whereas, the active-period of the drug carriers was shortened. In **Section 5.3**, it was found that particle size and the surface properties of the carriers have a key role in controlling the burst release phase. Smaller particles showed more pronounced burst release which was due to the fact that the total surface area of a constant weight of particles increases. An efficient coating method was demonstrated to prevent the burst release. Coating the particles provides an additional layer with no drug on the surface which increases the diffusional resistance to the drug. For instance, 37 % reduction in drug released in the first 72 hours was observed with the chitosan coated PLGA particles fabricated using 2 wt% solution and coated with 1 wt% chitosan solution.

Chapter 6

Conclusions and future work

6.1 Conclusions

The main contribution of the research described in this thesis is the demonstration of electrohydrodynamic processing as an alternative and viable technique for preparing micro and nano size particles with narrow size distributions, and which satisfy the requirements for particles used in controlled release systems. The ultimate objective for the fabricated drug-loaded polymeric carriers was to have a regulated release profile so that they would release their payload in the correct quantity at the correct time. This objective was fulfilled via two approaches including ultrasound stimulated drug release and controlling the burst release phase using a coating technique. The following conclusions are drawn from the extensive investigations carried out to achieve this objective.

6.1.1 On size mapping of polycaprolactone particles using single needle EHDA processing

Biodegradable polycaprolactone polymer particles with different sizes were prepared using a single needle EHDA technique. A method of particle production providing systematic variation of size and size distribution has been demonstrated at ambient temperature and pressure, with adjustable applied voltage and flow rate serving as the process control parameters. The range of operating parameters in terms of flow rate (2-50 µl/min), applied voltage (0-15 kV) and the inherent properties of the processed solutions such as viscosity and electrical conductivity were identified for the ideal processing window of stable jetting (cone-jet). An increase in the applied voltage (~15kV) resulted in a reduction in particle size and this was more

pronounced at high flow rates (such as; 30, 40 & 50 µl/min) in the same region. The size distribution in more cases was monomodal but the carrier particles were more polydisperse at the peripheral regions of the stable cone-jet mode, as defined in the applied voltage-flow rate parametric map. It was found that in more viscous solutions the upper and lower limits of the required voltage for forming the stable cone-jet increased from 7.5 kV to 11 kV. The size of the particles obtained within the stable cone-jet mode window was found to decrease as the applied voltage increased, but this phenomenon was more noticeable at higher flow rates. Particle diameter was greatly influenced by viscosity. The mean size of the particles changed from 310 nm to 4.4 µm as the viscosity increased from 2.5 mPa s to 11 mPa s. It was observed that adding 15 wt % estradiol as a model drug to the PCL solutions, changed the electrical conductivity of the solutions and increased the size of the particles but did not have a significant impact on the morphology of the particles.

This study demonstrates electrohydrodynamic atomization method has a definite clear advantage over conventional methods for the fabrication of the polymeric particles (such as emulsion-solvent evaporation and spray drying) as it both provides control over particle size and size distribution; and avoids the use of elevated temperatures and pressures. Previous studies in the literature on electrohydrodynamic atomization have mostly focused on one fixed applied voltage and flow rate. This study investigated a wide range of operating parameters (applied voltage, flow rate and solution properties) to provide a more comprehensive view on the effect of processing parameters on EHDA mode mapping and size distribution.

6.1.2 On preparing polymeric carriers with different shape and size using single needle EHDA processing

Simple manipulations of the electric-field, flow rate and collecting distance, and varying the polymer concentration during electrohydrodynamic jetting were shown to provide a means of producing biodegradable PLGA and PCL drug carriers with different sizes, shapes and surface morphologies. It was shown that, in addition to the solution properties, applied voltage and flow rate, the collecting distance has a significant impact on the size of the generated structures. When the collection

distance was changed from 100 mm to 400 mm, a dramatic reduction in the particle size by at least an order of magnitude (10μm-200nm) was observed accompanied by a change from a crinkled surface to a smooth surface.

Increasing the viscosity of the solution was found to be essential in order to obtain shape changes. In contrast to the low concentration polymer solutions used to generate particles, the more concentrated PCL polymer solution (30 wt%) was found to be ideal for promoting chain entanglement and the corresponding shape change observed was a transition from spherical to oblong to a more needle-like shape. It was also observed that another key factor that can determine the shape of the particle is voltage. As it was increased, the particle shape could again be changed from a spherical to a needle-like structure. However, the exact applied voltage needed for change in shape depended on the polymer concentration and properties of the solution such as viscosity. Also, the aspect ratio of the needle-like shape particles was found to be reduced when the flow rate decreased from 5 μl/min to 2 μl/min, as there is a reduction in the particle length. This ratio could be reduced further by increasing the applied voltage to 16 kV and preparation of rod-like particles was achieved with a particle length ≥ 1μm. Available techniques to produce non-spherical polymer particles are limited and complicated, usually involving multiple processing stages, often using combinations of techniques, such as lithography, microfluidic processing and photopolymerisation. This study demonstrated for the first time that EHDA, which is less complicated and easier to control compared to the current methods, can be used to fabricate non-spherical (needle-like shape) particles in a single step.

6.1.3 On co-axial electrohydrodynamic production of drug-loaded micro- and nano-particles

In this part of the study, a co-axial EHDA system was utilised instead of a single needle. The aim was to directly encapsulate a second material in the polymeric carrier. In the preliminary study, a dye (EB) was encapsulated in the PLGA particles. The mean diameters of the particles fabricated from 2, 5 and 10wt% PLGA polymer

solutions were 110, 120 and to 2.5 μm, respectively. It was shown that the encapsulation of a second material (the EB dye solution) into the polymeric carrier was feasible via co-axial EHDA. A colorimetric *in vitro* release method confirmed that the produced PLGA carriers were able to release the loaded EB dye in a sustained manner.

In the next part of this study, estradiol which represents the major estrogen in humans was used as the model therapeutic agent. The PLGA solutions and the estradiol solution were pumped individually through the outer and inner needle of the co-axial EHDA setup, respectively. Estradiol loaded PLGA particles with a mean size ranging from 100 nm to 2.5 μm and corresponding polydispersivity of 11% to 38% were produced with encapsulation efficiency ranging between 65% and 75%. Detailed analysis using SEM showed that all particles were spherical with a smooth outer surface. Particles prepared from 2 wt% PLGA had a bimodal size distribution with two peaks. 70 % of the particles were <120 nm in diameter and 20 % of them were >500 nm. In this case the wider variation in particle size can be attributed to the generation of different types of droplets ("primary" and "satellite") during the processing. More than 90% of the particles prepared using 5 wt% PLGA were <120 nm in diameter. The particles produced from the 10 wt% PLGA, 95% had diameters >2 μm.

Encapsulation is a method of enclosing the therapeutic agent in individual and protective polymeric carriers. This study confirmed the successful encapsulation of a drug, estradiol, in different size ranges of PLGA particles. A few studies have reported the encapsulation of estradiol in PLGA particles and most of the cases employed the solvent evaporation method as the fabrication technique, which has some disadvantages such as relatively low encapsulation efficiency specifically in preparation of drug loaded particles in nano scale, defunctionalisation of drugs under extreme processing conditions and multisteps processing (see **Section 2.7.1**).

6.1.4 On *in vitro* release study of micro- and nano-particles produced via co-axial electrohydrodynamic processing

The *in vitro* release profiles from estradiol loaded PLGA particles were studied. It was observed that estradiol release was time-dependent and all the release profiles start with an initial "burst" release followed by a period of sustained release. In the last stage, the release rate for all the samples increased significantly as degradative hydrolysis of the polymer particles took place and the central region which would be expected to contain a higher concentration of drug was exposed. The release rate from particles produced from PLGA:DMAC 10 wt% solution was markedly slower than from particles produced from PLGA:DMAC 2 & 5 wt% solutions. This could be explained by the fact that the particles fabricated from the more dilute solutions were smaller in size and, with a decrease in particle size, the surface area to volume ratio increases leading to increased buffer penetration and faster drug diffusion. Release of the entrapped therapeutic agent from PLGA matrix occurs through diffusion and degradation mediated processes. During the early phases, release occurs mainly through diffusion in the polymer matrix; while during the later phases, release is mediated through both diffusion of the therapeutic agent and degradation of the polymeric carrier itself. It was confirmed that the encapsulated drug was released in a sustained manner over 30 days. However, the release profiles still suffered from the undesirable burst release phase, which is addressed in the final section of this thesis.

6.1.5 On studying the effect of ultrasound exposure on the release profile

Most studies in the literature have investigated the effect of ultrasound on the stimulation of the drug release from lipid-based drug delivery vehicles such as micelles and liposomes. This study, investigated ultrasound exposure on biodegradable particulate carriers. The release profile of the drug from PLGA carriers was clearly affected by exposing the particles to ultrasound in the preliminary studies. An increase in the rate of drug release was observed for all the samples exposed to ultrasound with a greater increase obtained for longer exposures. It was found that ultrasound had a slightly greater effect on the larger particles. Exposing the PLGA particles to 22.5 kHz ultrasound for 30s enhanced the rate of

release by 7.8% and was also seen to increase the porosity of the particles' surface. Both effects were thought to be related to cavitation activity.

Further investigations were then carried out to study the effect of the different ultrasound parameters (such as duty cycle, intensity, and exposure time) on the release profile. Estradiol loaded PLGA particles with a mean size ranging from 100 nm to 2.5 μm were produced with encapsulation efficiencies ranging from 65% to 75%. Samples were exposed to ultrasound at a range of powers, duty cycles and exposure times and the rate of drug release, acoustic emissions during exposure and effect upon particle surface morphology were all examined. All three exposure parameters were seen to have a significant enhancing effect upon the drug release rate. Only output power, however, had a discernable effect upon the energy of the acoustic emissions and the appearance of the particles. The former increased linearly with output power, whilst the surface of the particles showed an increasing number of pores. Both of these observations may be attributed to increasing cavitation activity and indicate that cavitation-mediated degradation is an important contributor to drug release enhancement. The lack of correlation between the energy of the acoustic emissions or changes in the particle appearance with duty cycle and exposure time, however, indicates that there may be an additional mechanism relating to the energy of the incident ultrasound field, which requires further investigation. Nevertheless, this investigation further demonstrates a promising biomedical application of ultrasound: controlling and regulating the release profiles of a therapeutic agent where diffusion and degradation rates are the main limiting factors, and currently restrict the efficiency of the process.

6.1.6 On modification of the initial release characteristics of estradiol encapsulated in PLGA particles

The main objective in developing drug delivery systems is to achieve an effective therapeutic administration via a sustained drug release over an extended period of time with a minimum dosing frequency. The release profile was modified by manipulating the characteristics of the polymeric carriers with the aim of achieving

an ideal controlled drug release system, i.e. one which operates as a steady state system, capable of keeping the drug dosage within the therapeutic window for the vast majority of the treatment with minimum burst release.

Estradiol loaded PLGA particles were produced by co-axial electrohydrodynamic processing. The three most important factors affecting drug release were identified as: particle size, type and concentration of the coating agent. The drug release profiles for particles with the size range 100 nm to to 4.5 μm were studied. The 'burst release' defined as the amount of drug released between 0-24 hours, was lower for the larger particles. Furthermore, the initial release, defined as the amount of drug released between 0-72 hours, was also studied. The initial release was lower for the larger particles. This was because the total surface area of a constant weight of particles decreases when the size of the particles increases. Also, in larger particles the diffusion pathways were longer which leads to a lower release rate and lower initial release.

Two different biocompatible coating agents (chitosan and gelatin) were studied. Chitosan was found to control the burst and initial release more effectively compared to gelatin. The FTIR stability results confirmed that chitosan was stable on the surface structure of the PLGA particles for approximately 3 days. It acts as a rate-limiting layer, which controls the diffusion rate and protects the drug from the living environment. Also, it was observed that as the chitosan concentration increased, the coating tickness increased from 20 nm to 70 nm. Coating the particle surface with chitosan considerably reduces the burst and initial release, without significantly affecting the release rate. For instance, in all samples (PLGA 2wt%, PLGA 5wt% and PLGA 10 wt% samples) coated with 1 wt% chitosan solution the initial release were reduced by 37%, 32% and 21 %, respectivly in the first 72 hours. While, the release profiles of the gelatin coated particles showed initial release reductions of 3%, 8% and 9% in samples made from 2 wt%, 5 wt% and 10 wt% PLGA solutions in the first 72 hours.

These results showed a great improvement in controlling the burst release phase as the coating technique reduces the burst without changing the rest of the release

profile. For instance, in previous literatures the minimum burst from chitosan coated PLGA (50:50) nanoparticles were aproximatly 36%; while in this study, 15% burst release was achieved. Both particle size and surface coating were found to have a significant effect on the release profile. The release profile from estradiol loaded PLGA particles can be tailored to achieve the desired characteristics by selective manipulation of particle properties. These principles can be applied to a general drug-polymer system after taking into account the specific interactions involved in the system.

6.2 Future work

Ideally, synthesised particulate capsules should possess the following features: high loading efficiency, controlled drug distribution and release characteristics, uniform size and shape. The processing technique should be able to generate these features, be efficient in terms of time and material usage, convenient and easily scalable. EHDA processing techniques have shown great promise in terms of these criteria offering a versatile tool for the generation of uniform particles and encapsulated structures. As it was shown in this thesis, EHDA techniques can achieve uniform dispersion of drug within a polymeric matrix with high loading capacity and minimal drug loss. However there are still several aspects of future work recommended as follows:

6.2.1 Encapsulation of different therapeutic agents

Effective drug delivery strategies are becoming more significant as more specific drugs become available with increasing knowledge about diseases from the human genome project. All therapeutic agents would optimally require tailored drug delivery systems and targeting mechanisms to deliver them to their specific target tissues without reducing their therapeutic efficacy. In this research, it was shown that biodegradable particles could be prepared with high encapsulation efficiency for estradiol, which is a hydrophobic drug. Particles formulated from PLGA should also be investigated for sustained and targeted/localized delivery of other ranges of therapeutic agents including cells, plasmid DNA, proteins and peptides.

6.2.2 Cell study for nanoparticles

Nanoparticles are a potentially useful drug delivery system capable of delivering a therapeutic agent by sustained delivery. Also, the nanoparticle size is very important for their great efficiency of arterial uptake [Song *et al.* 1998] and cellular entry [Desai *et al.* 1997] and preventing inflammatory tissue responses usually associated with larger size microparticles [Dev *et al.* 1997]. In this study, PLGA nanoparticles

with the size of ~100 nm were produced successfully. The *in vitro* release study showed an efficient drug release profile. However the mechanism of enhanced therapeutic efficacy of estradiol loaded nanoparticles at cellular level should be addressed. For instance, further research can be conducted on the mechanism of intracellular uptake of the nanoparticles, their trafficking and sorting into different intracellular compartments.

6.2.3 The effect of shape on various *in vivo* and *in vitro* parameters

Recently, there has been growing recognition that particle properties other than size and surface chemistry influence the effectiveness of drug delivery systems, in particular, shape. In this thesis, it was shown that carriers of different shapes could be obtained through different combinations of processing parameters. However, more studies should be carried out to fully understand how to control all EHDA processing parameters to obtain both the desired size distribution and shape, e.g. aspect ratio in needle-like shape particles. Also, *in vivo* and *in vitro* investigations of release profile, biocompatibility, clearance, and targeting of these particles are required to fully understand the factors determining the effectiveness of these particles. For instance, the dependence of phagocytosis by macrophages on shape and aspect ratio, the internalisation of needle-like shape particles and the biodistribution should be studied.

6.2.4 Micro and nanoparticles in tissue engineering

Tissue engineering has emerged as a viable alternative to the problem of organ and tissue shortage. The use of microspheres as scaffold materials for the growth of cells for tissue engineering is an emerging area of application in medical engineering [Botchwey *et al.* 2004]. Further research in this area could open up a new branch of applications for the micro and nanoparticles prepared by EHDA processing.

6.2.5 Preparation of multilayer particles

Further structures that can potentially be prepared using EHDA processing are multi-layered micro- and nano-particles capable of successfully penetrating the body's immune system and efficiently carrying therapeutic agents to their intended sites. Each layer can be systematically designed for a specific reason, which can meet and overcome each physiological barrier encountered as it moves through the body. Therefore, this technique is a significant progression which would lead to multilayered structures that could then have the potential for multilayer particles, multiple loading of drugs, prodrugs or other active agents required at a different time. This leads to greater efficiency and reduces the required dosage.

These multilayered structures can be produced via two methods. First, drug loaded nano/microparticles could be prepared using single or co-axial EHDA systems and subsequently they could be sent through the inner needle of the co-axial EHDA while sending an encapsulating polymer through the outer. This technique can be classed as a multi-step technique while there is a second method which is a simpler single-step technique. In this method, a co-axial tri-needle device can be designed to generate a variety of multilayer encapsulated structures using a range of materials. This would show major improvement on co-axial work and suggests considerable benefits, particularly in the healthcare area with potential applications within biomedical and pharmaceutical fields, for the preparation of encapsulated carriers and multilayered micro or nanoparticles.

6.2.6 Preparation of nanoparticles with low polydispersivity

As mentioned, nanoparticles are very much in need for drug delivery, particularly to the central nervous system [Blasi *et al.* 2007]. Since nanoparticles with a size and polydispersivity index of 100 nm and 11%, have been prepared with existing facilities in the EHDA set-up, it may be possible to prepare nanoparticles with a diameter < 100 nm. As various parameters (processing parameters and properties of the solution) are involved in the EHDA technique, modifying the processing parameters such as varying the collection distance, narrowing the gap between the

tip of the outer needle and varying the concentration of the solution may help in reducing the size to less than 100 nanometres with lower polydispersivity.

6.2.7 The effect of needle geometry on the EHDA processing

The geometry of the needle used in EHDA processing, is an important factor for the electric field. However, to the best of the author's knowledge, within the research work of EHDA spraying in the past few years, there are few documents to systematically demonstrate the influence of needle geometry, a vital factor for electric field which actually is the driving force for the liquid to form cone-jet mode in EHDA spraying. Almost all the previously discussed studies and investigations are based on the capillary with regular geometry. It was only briefly mentioned that 'the geometry of the nozzle influences the cone-jet domain drastically' without giving any explanation on the influence phenomena and mechanism [Chen *et al.* 1999]. Therefore, further investigations need to be conducted on studying the effects of the needle geometry (such as tip angle, tip length and shape) on the stable cone-jet domain, in which the cone-jet mode can only be achieved and maintained.

6.2.8 Targeted drug delivery via bioconjugation

EHDA method can be used to produce bioconjugated polymeric particles for targeted drug delivery. One of the most significant applications of targeted drug delivery is for cancer therapy. Cancer drug delivery is no longer simply encapsulating the drug in formulations for different routes of delivery. Experience, skill and knowledge from various technologies such as nanotechnology and advanced polymer chemistry need to bring together new ways of developing novel drug delivery system. One of the methods that can be applied is using monoclonal antibodies (MAbs). These are used both for diagnosis and therapy in cancer. PLGA polymeric particles can be used for site-specific drug delivery by incorporation of appropriate targeting groups of antitumor monoclonal antibodies. They can deliver anticancer payloads such as radionucleotides, toxins and chemotherapeutic agents to the tumors. Therefore, it prevents damage to the normal surrounding tissues.

6.2.9 Microbubbling

In all the experiments carried out via co-axial EHDA in this research, the encapsulated material was a dye or drug solution. However, this solution can be replaced with air to produce bubbles. In medical and pharmaceutical applications, there is rapidly growing interest in the use of microbubbles as ultrasound contrast agent particles, drug delivery systems and in the synthesis of artificial cell structures [Bertling *et al.* 2004, Botchwey *et al.* 2004]. A prerequisite for using microbubbles as contrast agent particles in ultrasound radiography is that they degrade *in vivo* within hours and that the largest particle should not exceed 8 μm diameter, in order to avoid capillary blockage [Raisinghani and DeMaria 2002]. In 2009, Farook *et al.* first developed the technique using co-axial EHDA to prepare microbubbles [Farook *et al.* 2009a]. They found EHDA microbubbling as a promising method to prepare microbubbles with specific size and size distribution. However, they have used polymethylsilsesquioxane biopolymer in their experiments which is not a degradable polymer. Therefore, it could be potentially beneficial to fabricate microbubbles from biodegradable and bioerodible polymers such as PLGA to improve the degradation properties of the microbubbles.

6.2.10 Ultrasound safety

Ultrasound has a long history of use in biomedical fields. In this study ultrasound was used in combination with estradiol drug. It was shown that ultrasound (range of applied frequencies were 20 to 22.5 kHz), enhanced the drug release. However, understanding the safety of therapeutic ultrasound and the development of generalised rules that account for ultrasound safety is an important topic for future research activities [Nyborg 2001, Madersbacher *et al.* 2003].

The issue of biological response in the use of ultrasound to stimulate drug release should be addressed. It is very probable that ultrasound frequencies which optimise membrane permeability are different to the frequencies which optimise drug release. Thus the response of cells and their membranes to ultrasound must be considered and damages to the target or adjacent tissues should be avoided or minimised.

Ultrasound frequencies used for medical applications is ranged from 19.5 kHZ to 10 MHz. Some examples of the applications of low frequency ultrasound are; angioplasty (19.5 kHz), ocular drug delivery (20 kHz), lipoplasty (20–50 kHz) and transdermal delivery of insulin, low-molecular weight heparin, vaccines (20-100 kHz) [Mitragotri 2005]. However, the significant clustering of applications is found around frequency of 1 to 3 MHz. For instances, the frequencies used for imaging and thus readily available to clinicians are 1MHz and above. At these frequencies, focusing and therefore targeting of treatments is better. Therefore, it is beneficial to look at exposing the particles at higher frequencies and study their release characteristics.

6.2.11 Commercial viability

A full assessment of commercial and clinical viability of the utilised techniques in this study is an important issue which should be addressed in future. EHDA technique has some clear advantages in terms of simplicity, efficiency, cleanliness and ambient operation. However there is the issue of scaling up and associated cost to address. It should be noted that EHDA with a single nozzle is a low-volume throughput process and it is not suitable or efficient for traditional industrial spraying processes. Approaches that address this problem are to use multi-nozzle or slit-nozzle systems [Snarski *et al.* 1991, Almekinders and Jones. 1999, Regele *et al.* 2002]. Therefore, more investigation can be conducted on scaling up and commercialising this technique via two methods: first, scaling up for mass production through the use of multiplexed microfabricated sources of spraying, second, fabrication of miniaturised portable devices for encapsulation and delivery of drugs for patient-specific needs.

References

Ahmad Z., Zhang H.B., Farook U., Edirisinghe M., Stride E., Colombo P., (2008), Generation of multilayered structures for biomedical applications using a novel tri-needle co-axial device and electrohydrodynamic flow. *J. R. Soc. Interface*, **27**, 1255-1261.

Almekinders J.C., Jones C., (1999), Multiple jet electrohydrodynamic spraying and applications, *J. Aerosol Sci.,* **30** (7), 969–971.

Amsden B.G., Gossen M.F.A., (1997), An examination of factors affecting the size, distribution and release characteristics of polymer microbeads made using electrostatics. *J. Control. Releas.,* **43**,183–196.

Armani D.K., Liu C., (2000), Microfabrication technology for polycaprolactone, a biodegradable polymer. *J. Micromech. Microeng.*, **10,** 80-84.

Arshady R., (1989), Microspheres and Microcapsules: A Survey of Manufacturing techniques, part 1: Suspension cross-linking. *Polym. Eng. Sci.,* **29,** 1746-1758.

Arshady R., (1990), Microspheres and Microcapsules: A Survey of Manufacturing techniques, part III: Solvent evaporation. *Polym. Eng. Sci.,* **30**, 905-914.

Arshady R., (1991), Preparation of biodegradable microspheres microcapsules: 2. Polylactides and related polyesters. *J. Control. Release*, **17**, 1-22.

Arya N., Chakraborty S., Dube N., Katti D.S., (2009), Electrospraying: a facile technique for synthesis of chitosan-based micro/nanospheres for drug delivery applications. *J. Biomed. Mater. Res. B Appl. Biomater.,* **31**, 17-31.

Avgoustakis K., (2004), Pegylated poly(Lactide) and poly(lactide-co-glycolide) nanoparticles: preparation, properties and possible applications in drug delivery. *Curr. Drug Deliv.,* **1**, 321-333.

Bangham A.D., Standish M.M., Watkins J.C., (1965), Diffusion of univalent ions across the lamellae of swollen phospholipids. *J. Mol. Biol*., **13**, 238-252.

Barisci J., Liu L., Strounina E., Wallace G., (2000), Factors affecting the yield of polypyrrole colloids produced under electrohydrodynamic conditions, *Colloid Surface A,* **167**, 201-208.

Barnett S.B., Ter H., Ziskin M.C., Nyborg W.L., Maeda K., Babg J.J., (1994), Current Status of Research on Biophysical Effects of Ultrasound. *Ultrasound Med. Biol.,* **20**(3), 205–218.

Batycky R.P., Hanes J., Langer R., Edwards D.A., (1997), A theoretical model of erosion and macromolecular drug release from biodegrading microspheres, *J. Pharm. Sci.,* **86,** 1464–1477.

Benoit M.A., Baras B., Gillbard J., (1999), Preparation and characterization of protein-loaded poly(ε-caprolactone) microparticles for oral vaccine delivery. *Int. J. Pharm.,* **184**, 73–84.

Berkland C., Packa D.W., Kim K.K., (2004), Controlling surface nano-structure using flow-limited field-injection electrostatic spraying (FFESS) of poly (d,l-lactide-co-glycolide). *Biomaterials*, **25**, 5649-5658.

Bertling J., Blomer J., Kummel R., (2004), Hollow microspheres. *Chem. Eng. Technol.,* **27**, 829-837.

Blanco-Prieto M.J., Campanero M.A., Besseghir K., Heimgatner F., Gander B., (2004), Importance of single or blended polymer types for controlled in vitro release and plasma levels of a somatostatin analogue entrapped in PLA/PLGA microspheres. *J. Control. Release*, **96***,* 437-448.

Blasi P., Giovagnoli S., Schoubben A., Ricci M., Rossi C., (2007), Solid lipid nanoparticles for targeted brain drug delivery. *Adv. Drug Delivery Rev.,* **59**, 454-477.

Boas U., Heegaard P.M.H., (2004), Dendrimers in drug research. *Chem. Soc. Rev.* **33**(1), 43–63.

Borra J.P., Camelot D., Marijnissen J.C.M., Scarlett B., (1997), A new production process of powders with defined properties by electrohydrodynamic atomization of liquids and post-production electrical mixing. *J. Electrostatics*, **40**, 633-638.

Botchwey E.A., Pollack S.R., Levine E.M., Johnston E.D., Laurencin C.T., (2004), Quantitative analysis of three-dimensional fluid flow in rotating bioreactors for tissue engineering. *J. Biomed. Mater. Res. Part A*, **69A**(2), 205-215.

Brannon-Peppas L., (1997), Polymers in controlled drug delivery. *Medical plastics Magazine*, November, 34-45.

Brazel C.S., Peppas N.A., (1999), Recent studies and molecular analysis of drug release from swelling-controlled devices, *STP Pharma Sci.,* **9**, 473-485.

Brennen C.E. (1995), Cavitation and Bubble Dynamics. Oxford University Press; New York. 282-300.

Brocchini S., Duncan R. (1999), Pendant drugs release from polymers. In Encyclopaedia of Controlled Drug Delivery, Vol 2. Edited by Mathowitz E. New York: John Wiley and Sons; 786-816.

Bungenburg de Jong H. G., Kaas A. J., (1931), Zar Kennetus komplex koazeration, V. Mitteilung: relative verschiebumer im elektrischen gleichstromfeide von fllussigkeits-einschliebungen in komplex-kooazervat-tropfehen, *Biochem. Z.,* **232**, 338-345.

Burlak G., Koshevaya S., Sanchez-Mondragon J., Grimalsky V., (2001), Electromagnetic eigenoscillations and fields in a dielectric microsphere with multilayer spherical stack, *Opt. Commun.*, **187**, 91-105.

Burke P.A., Klumb L.A., Herberger J.D., Nguyen X.C., Harrell R.A., Zordich M., (2004), Poly(lactide-co-glycolide) microsphere formulations of darbepoetin alfa: spray drying is an alternative to encapsulation by spray-freeze drying. *Pharm. Res.*, **21**, 500-506.

Burton K.W., Shameem M., Thanoo B.C., Deluca P.P., (2000), Extended release peptide delivery systems through the use of PLGA microsphere combinations. *J. Biomater. Sci.*, **11**, 715-729.

Cai Q., Bei J.Z., Wang S.G., (2000), Study on the biocompatibility and degradation behaviour of poly(l-lactide-co-glycolide) *in vitro* and in vivo. *Chin. J. Funct. Polym.,* **13**, 249–54.

Calloway D., (1997), Beer-Lambert Law. *J. Chem. Educ.*, **74** (7), 744.

Carrasquillo K.G., Stanley A.M., Aponte-Carro J.C., De Jesus P., Costantino H.R., Bosques C.J., Griebenow K., (2001), Non-aqueous encapsulation of excipient-stabilized spray-freeze dried BSA into poly(lactide-co-glycolide) microspheres results in release of native protein. *J. Control. Release*, **76,** 199-208.

Cavrini V., Di Pietra A.M., Gatti R., (1989), Analysis of miconazole and econazole in pharmaceutical formulations by derivative UV spectroscopy and liquid chromatography (HPLC)*, J. Pharma. Biomed. Analy.*, **7** (12), 1535-1543.

Champion J.A., Mitragotri S. (2006), Role of target geometry in phagocytosis. *Proc. Natl. Acad. Sci. USA,* **103**(13), 4930-4934.

Chang M.W., Stride E., Edirisinghe M., (2010), A New Method for the Preparation of Monoporous Hollow Microspheres. *Langmuir*, **22**, 234-245.

Chang M.W., Stride E., Edirisinghe M., (2009), A novel process for drug encapsulation using a liquid to vapour phase change material. *Soft Matter*, **5**, 5029-5036.

Chang R.K., Price J.C., Whitworth C.W., (1986), Dissolution characteristics of poly (ε-carolactone)-polylactide microspheres of chlorpromazine. *Drug Dev. Ind. Pharm.*, **12**, 2355-2380.

Chen C.H., Emond M.H J., Kelder E.M., Meester B., Schoonman J. (1999), Electrostatic sol-spray deposition of nanostructured ceramic thin films. *J. Aerosol. Sci.* **30**, 959-967.

Chen X., Jia L., Yin X., Cheng J., (2005), Spraying modes in coaxial jet electrospray with outer driving liquid, *Phys. Fluids.*, **17,** 2101-2108.

Chiellini , Piras A.M., Errico. Chiellini E., (2008), Micro/nanostructured polymeric systems for biomedical and pharmaceutical applications, *Nanomedicin*, **3** (3), 367-393.

Ciach T., (2007), Encapsulation of proteins by Electro Hydro Dynamic Atomization. *Macromol. Symp.*, **253**, 98-102.

Clark A.R., (1995), Medical aerosol inhalers. Past, present and future. *Aerosol. Sci. Technol.,* **22**, 374-391.

Cloupeau M.P.F., Prunet-Foch, B., (1990), Electrostatic Spraying of Liquids: Main Functioning *Modes, J. Electrostat.*, **25**, 165-184.

Cloupeau M.P.F., Prunet-Foch B., (1994), Electrohydrodynamic spraying functioning modes, A critical review. *J. Aerosol Sci.* **25**, 1121-1136.

Cohen S., Yoshioka T., Lucarelli M., Hwang L. H., Langer R., (1991), Controlled delivery systems for proteins based on PLGA microspheres. *Pharm. Res.,* **8**, 713-720.

Coopman V.A., Cordonnier J.A., De Meyere C.A. (2005), Fatal workplace accident involving ethyl acetate: a distribution study. *Forensic Sci. Int.*, **154**(2-3), 92-95.

Crotts G., Park T.G., (1998), Protein delivery from poly(lactic-co-glycolic acid) biodegradable microspheres: release kinetics and stability issues, *J. Microencapsul.,* **15**, 699-713.

Curcio M., Spizzirri U.G., Iemma F., Puoci F., Cirillo G., Parisi O. I., Picci N., (2010), Grafted thermo-responsive gelatin microspheres as delivery systems in triggered drug release, *Eur. J. pharm. Biopharm*, **76**, 48-55.

Dalecki D., (2004), Mechanical bioeffects of ultrasound. *Annu. Rev. Biomed. Eng.*, **6**, 229-248.

Demir H., Menku P., Kirnap M., Calis M., Ikizceli I., (2004), Comparison of the effects of laser, ultrasound, and combined laser ultrasound treatments in experimental tendon healing. *Lasers Surg. Med.,* **35**, 84-89.

Deng W.W., Klemic J.F., Li X., Reed M.A., Gomez A., (2006), Increase of electrospray throughput using multiplexed microfabricated sources for the scalable generation of monodisperse droplets. *J. Aerosol Sci.*, **37**(6), 696-714.

Desai M.P., Labhasetwar V., Walter E., Levy R.J., Amidon G.L., (1997), The mechanism of uptake of biodegradable microparticles in Caco-2 cells is size dependent, *Pharm. Res.,* **14**, 1568-1573.

Dev V., Eigler N., Fishbein M.C., Tian Y., Hickey A., Rechavia E., Forrester J.S., Litvack F., (1997), Sustained local drug delivery to the arterial wall via biodegradable microspheres. *Catheter. Cardio. Diag.***,** **43** (4), 324-332

Ding L., Lee T., Wang C., (2005), Fabrication of monodisperse Taxol loaded particles using electrohydro dynamic atomization. *J. Control. Release,* **102**, 395-413.

Edwards D.A., Hanes J., Caponetti G., Hrkach J., Ben-Jebria A., Eskew M.L., Mintzes J., Deaver D., Lotan N., Langer R., (1997), Large porous particles for pulmonary drug delivery. *Science.*, **276**, 1868-1871.

Farook U., Stride E., Edirisinghe M.J., (2009a), Controlling the size and size distribution of electrohydrodynamically prepared microbubbles. *Bubble Sci. Eng. Tech.,* **1**(1-2), 53-57.

Farook U., Stride E., Edirisinghe M.J., (2009b), Preparation of suspensions of phospholipid-coated microbubbles by coaxialelectrohydrodynamic atomization. *J. R. Soc. Interface*, **6**, 271-277.

Farook U., Stride E., Edirisinghe M.J., Moaleji R., (2007a), Microbubbling by co-axial electrohydrodynamic atomization *Med. Biol. Eng. & Comp.*, **45**, 781-789.

Fatemi M., Greenleaf J.F., (1998), Ultrasound-stimulated vibro-acoustic spectrography. *Science.*, **280**, 82-85.

Felt O., Buri P., Gurny R., (1998), Chitosan: a unique polysaccharide for drug delivery. *Drug Dev. Ind. Pharm.* **24**, 979-993.

Ferrara K.W., (2008), Driving delivery vehicles with ultrasound. *Adv. Drug Deliv. Rev.*, **60**, 1097-1102.

Folkman J., Long DM., (1964), The use of silicone rubber as carrier for prolonged drug therapy. *J. Surg. Res.*, **4**, 139-142.

Freitas S., Merkle H.P., Gander B., (2005), Microencapsulation by solvent extraction/evaporation: Reviewing the state of the art of microsphere preparation process technology. *J. Control Release.*, **102**, 313-332.

Fu K., Pack D.W., Kilbanov A.M., Langer R., (2000), Visual evidence of acidic environment within degrading poly(lactic-co-glycolic acid)(PLGA) microspheres, *Pharm. Res.*, **17**, 100-106.

Fukushima S., Kishimoto S., Takeuchi Y., Fukushima M., (2000), Preparation and evaluation of o/w type emulsions containing antitumor prostaglandin. *Adv. Drug. Deliv. Rev.*, **45**, 65-75.

Ganan-Calvo, (1997a), On the theory of electrohydrodynamically driven capillary jets. *J. Fluid Mech.*, **335**, 165-188.

Ganan-Calvo A.M., Davila J., Barrero A., (1997b), Current and droplet size in the electrospraying of liquids. Scaling laws. *J. Aerosol Sci.*, **28** (2), 249-275.

Gaumet M., Vargas A., Gurny R., F. Delie, (2007), Fluorescent biodegradable PLGA particles with narrow size distributions: preparation by means of selective centrifugation. *Eur. J. pharm. Biopharm*, **342**(1), 222-230.

Gilbert W., (1600), De Magnete, Magneticisque Corporibus, et de Magno Magnete Tellure (On the Magnet and Magnetic Bodies, and on That Great Magnet the Earth), 1st Edition. London: Peter Short, 1544-1603.

Gopferich A., (1996), Mechanisms of polymer degradation and erosion. *Biomaterials,* **17**(2), 103-114.

Gaponik N., Radtchenko I.L., Sukhorukov G.B., Rogach A.L., (2004), Luminescent Polymer Microcapsules Addressable by a Magnetic Field. *Langmuir.*, **20,** 1449-1452.

Gratton S.E.A., Pohlhaus P.D., Lee J., Guo J., Cho M.J., desimone J. M., (2007), Nanofabricated particles for engineering drug therapies: A preliminary biodistribution study of PRINT nanoparticles. *J. Control. Release.,* **121**(1-2)**,** 10-18.

Gregoriadis G., (1977), Targeting of Drugs. *Nature.,* **165**, 407-411.

Grossman J., (1994), The evolution of inhaler technology. *J. Asthma.*, **31**, 55-64.

Guan G., Zhang Z., Wang Z., Liu B., Gao D., Xie C., (2007), Single-Hole Hollow Polymer Microspheres toward Specific High-Capacity Uptake of Target Species. *Adv. Mater.*, **19**, 2370-2374.

Hartman R.P.A., Brunner D.J., Marijnissen J.C.M., Scarlett b., (1998), Scaling laws for droplet size and current produced in the cone-jet mode. *J. Aeorosol Sci.*, **29**(1), 977-978.

Hartman R.P.A., Borra J.P., Brunner D.J., Marijnissen J.C.M., Scarlet B., (1999), The evolution of electrohydrodynamic sprays produced in the cone-jet mode: a physical model. *J. Electrostat.,* **47,** 143-170.

Hartman R.P.A., Brunner D.J., Camelot D.M.A., Marijnissen J.C.M., Scarlett B., (2000), Jet Break-Up in electrohydrodynamic atomization in the cone-jet mode. *J. Aerosol. Sci.*, **31**(1), 65-95.

Hayati I., Bailey A. I., Tadros T. F., (1987a), Investigations into the mechanisms of electrohydrodynamic spraying of liquids. Pt. I. Effect of electric field and the environment on pendant drop and factors affecting the formation of stable jets and atomisation. *J. Colloid Interface Sci.*, **117**, 205-221.

Hayati I., Bailey A. I., Tadros T. F., (1987b), Investigations into the mechanisms of electrohydrodynamic spraying of liquids. Pt. II. Mechanism of stable jet formation and electrical forces acting on a liquid cone. *J. Colloid Interface Sci.*, **117**, 222-230.

Hed J., Dahlgren C., Rundquist I., (1983), A Simple Fluorescence Technique to Stain the Plasma Membrane of Human Neutrophils. *Histochemistry.*,**79**(1), 105-110.

Hodnett M., Chow R., Zeqiri B., (2004), High-frequency acoustic emissions generated by a 20 kHz sonochemical horn processor detected using a novel broadband acoustic sensor: a preliminary study, *Ultrason. Sonochem.*, **11**, 441-454.

Hombreiro P.M., Zinutti C., Lamprecht A., Ubrich N., Astier A., Hoffman M., Bodmeier R., Maincent P., (2000), The preparation and evaluation of poly(epsilon-caprolactone) microparticles containing both a lipophilic and a hydrophilic drug. *J. Control. Release.*, **65**, 429-438.

Huang X., Brazel C.S., (2001), On the importance and mechanisms of burst release in matrix-controlled drug delivery systems, *J. Control. Release.*, **73,** 121-136.

Iglesias R.B., Lorenzo C.A, ConcheiroA., (2003), Controlled release of estradiol solubilized in carbopol/surfactant aggregates. *J. Control. Release.*, **93** (3), 319-330.

Ijsebaert J.C., Geerse K.B., Marijnissen J.C.M., Scarlett B., (1999), Electrohydrodynamic spraying of inhalation medicine. *J. Aerosol Sci.*, **30**, 825-826.

Ikada Y., Tabata Y., (1998), Protein release from gelatin matrices, *Adv. Drug Delivery Rev.*, **31**, 287-301.

Jain RA., (2000), The manufacturing techniques of various drug loaded biodegradable poly(lactide-co-glycolide) (PLGA) devices. *Biomaterials.*, **21**(23), 2475-2490.

Jalil R., Nixon J.R., (1990), Biodegradable poly(lactic acid) and poly(lactide-co-glycolide) microcapsules: problems associated with preparative techniques and release properties. *J. Microencapsul.*, **7**, 297-325.

Jamshidi K., Hyon S.H., Ikada Y., (1988), Thermal characterization of polylactides. *Polymer.*, **29**, 2229-2234.

Jaworek A., Krupa A., (1999a), Classification of the modes of EHD spraying. *J. Aerosol. Sci.*, **30**(7), 873-893.

Jaworek A., Krupa A., (1999b), Jet and drops formation in electrhydrodynamic spraying of liquids. A system approach, *Exp. in Fluids*, **27,** 43-52.

Jaworek A., Sobczyk A.T. (2008), Electrospraying route to nanotechnology: An overview, *J. Electrostat.,* **66,** 197–219.

Jaworek A. Krupa A. Sobczyk A.T., Lackowski M., Czech T., Ramakrishna S., Sundarrajan S., Pliszka D., (2008), Electrospray nanocoating of microfibers. *Solid State Phenom.*, **140,** 127-13.

Jayasinghe S.N., Edirisinghe M.J., (2002), Effect of Viscosity on the Size of Relics Produced by Electrostatic Atomization. *J. Aerosol. Sci.*, **33**(10), 1379-1388.

Jayasinghe S.N., Edirisinghe M.J., (2004), Electrostatic atomization of a ceramic suspension. *J. Eur. Ceramic Soc.*, **24**, 2203-2213.

Jayasinghe S.N., Edirisinghe M.J., Wilde T., (2002), A novel ceramic printing technique based on electrostatic atomization of a suspension. *Mater. Res. Innovations.*, **6**, 92-95.

Jenne J., (2001), Cavitations in Biological Tissues. *Ultras. chall. in Med.*, **22**, 200-207.

Johansen P., Moon L., Tamber H., Merkle H.P., Gander B., Sesardic D., (1999), Immunogenicity of single-dose diphtheria vaccines based on PLA/PLGA microspheres in guinea pigs. *Vaccine.*, **18**, 209-215.

Jiang P., Hwang K.S., Mittleman D.M., Bertone J.F., Colvin V.L., (1999), Template-directed preparation of macroporous polymers with oriented and crystalline arrays of voids. *J. Am. Chem. Soc.*, **121**, 11630-11637.

Kalra V., Lee J.H., Park J.H., Marquez M., Joo Y.L., (2009), Confined Assembly of Asymmetric Block-Copolymer Nanofibers via Multiaxial Jet Electrospinning. *Small.*, **5**, 2323-2332.

Kaparissides C., Alexandridou S., Kotti K., Chaitidou S., (2006), Recent Advances in Novel Drug Delivery Systems, *J. Nanotech. Online.*, **2**, 1-11.

Kawaguchi H. (2000), Functional polymer microspheres. *Prog. Polym. Sci.*, **25**, 1171-1210.

Kawashima Y., Serigano T., Hino T., Yamamoto H, Takeuchi H., (1988), A new powder design method to improve inhalation efficiency of pranlukast hydrate dry powder aerosols by surface modification with hydroxypropylmethylcellulose phthalate nanospheres. *Pharmaceut. Res.*, **15**, 1748-1752.

Kim S., Kim JH., Jeon O., Kwon IC, Park K., (2009), Engineered polymers for advanced drug delivery, *Eur. J. Pharm. Biopharm.*, **71**, 420-430.

Kishida A., Murakami K., Goto H., Akashi M., Kubita H., Endo T., (1998), Polymer drugs and polymeric drugs X: slow release of 5-fluorouracil from biodegradable poly(g-glutamic acid) and its benzyl ester matrices, *J. Bioact. Compat. Polym.*, **13**, 270-278.

Kissel T., Li Y.X., Volland C., Görich S., Koneberg R., (1995), Parenteral protein delivery systems using biodegradable polyesters of ABA block structure, containing hydrophobic poly(lactide-co-glycolide) A blocks and hydrophilic poly(ethylene oxide) B blocks. *J. Control. Release.*, **39**, 315-326.

Kohane D.S., Tse J.Y., Yeo Y., Padera R., Shubina M., Langer R., (2006), Biodegradable polymeric microspheres and nanospheres for drug delivery in the peritoneum. *J. Biomed. Mater. Res. A.*, **77A**, 351-361.

Kokubo T., Kushitani H., Sakka S., Kitsugi T., Yamamuro T., (1990), Solutions able to reproduce *in vivo* surface-structure changes in bioactive glass-ceramic A-W, *J. Biomed. Mater. Res.*, **24**, 721-734.

Kost J., Leong K., Langer R., (1989), Ultrasound-enhanced polymer degradation and release of incorporated substances (controlled release/drug delivery systems). *Proc. Nati. Acad. Sci.* **86**, 7663-7666.

Ku B.K., Kim S.S., (2002), Electrospray characteristics of highly viscous liquids. *J. Aerosol. Sci.*, **33**, 1361-1378.

Kuijpers A.J., van Wachem P.B., van Luyn M.J., Plantinga J.A., Engbers G.H., Krijgsveld J., Zaat S.A., Dankert J., Feijen J., (2000a), *In vivo* compatibility and degradation of crosslinked gelatin gels incorporated in knitted Dacron, *J. Biomed. Mater. Res.*, **51**, 136-145.

Kuijpers A.J., Engbers G.H., Krijgsveld J., Zaat S.A., Dankert J., Feijen J., (2000b), Cross-linking and characterisation of gelatin matrices for biomedical applications, *J. Biomater. Sci., Polym. Ed.*, **11**, 225-243.

Kwon IC., Bae YH., Kim SW., (1991), Electrically erodible polymer gel for controlled release of drugs. *Nature.*, **354**, 291-293.

Langer G., Yamate G., (1969), Encapsulation of liquid and solid aerosol particles to form dry powders. *J. Coll. Interface. Sci.*, **29**, 450-455.

Langer R., Folkman J., (1976), Polymers for the sustained release of proteins and other macromolecules. *Nature.*, **263**, 797-800.

Langer R., (1990), New methods of drug delivery. *Science.*, **249**, 1527-1533.

Langer R., (1998), Drug delivery and targeting. *Nature.*, **392**, 5-10.

Lanza G.M., Yu, X., Winter P.M., Abendschein D.R., Karukstis K.K., Scott M.J., Chinen L.K., Fuhrhop R.W., Scherrer D.E., Wickline S.A., (2002), Targeted antiproliferative drug delivery to vascular smooth muscle cells with a magnetic resonance imaging nanoparticle contrast agent: implications for rational therapy of restenosis. *Circulation.*, **106**(22), 2842–2847.

Larina I.V., Evers B.M., Ashitkov T.V., Bartels C., Larin K.V., Esenaliev R.O., (2005), Enhancement of drug delivery in tumors by using interaction of nanoparticles with ultrasound radiation. *Technol. Cancer Res. Treat.*, **4**, 217-226.

Lazar D.A., Curra F.P., Mohr B., McNutt L.D., Kliot M., Mourad P.D., (2001), Acceleration of recovery after injury to the peripheral nervous system using ultrasound and other therapeutic modalities. *Neurosurg. Clin. N. Am.*, **12**, 353-357.

Lee C.C., MacKay J.A., Frechet J.M.J., Szoka F.C., (2005), Designing dendrimers for biological applications. *Nat. Biotechnol.*, **23**(12), 1517-1526.

Lee J.S., Chae G.S., Kim M.S., Cho S.H., Lee H.B., Khang G., (2004), Degradation behaviour *in vitro* for poly(D,L-lactide-co-glycolide) as drug carrier. *Biomed. Mater. Eng.,* **14**(2), 185-192.

Lee Y.H., Kim C.A., Jang W.H., Choi H.J., Jhon M.S., (2001), Synthesis and electrorheological characteristics of microencapsulated polyaniline particles with melamine-formaldehyde resins, *Polymer.*, **42**, 8277-8283.

Lentacker I., Geers B., Demeester J., De Smedt S.C., SandersnN.N., (2010), Design and Evaluation of Doxorubicin-containing Microbubbles for Ultrasound-triggered Doxorubicin Delivery: Cytotoxicity and Mechanisms Involved. *Molecular Therapy.*, **18**, 101-108.

Li S., Vert M., (1999), Biodegradable polymers: polyesters. In *Encyclopaedia of Controlled Drug delivery,* Vol 1. Edited by Mathowitz E. New York: John Wiley and Sons, 71-93.

Li F., Yin X.Y., (2006), Linear instability of a co-flowing jet under an axial electric field. Phys. Rev. E Stat. Nonlin. *Soft Matter. Phys.*, **74**(3), 36304-36307.

Lim D., Hwang S., Uzun O., Stellacci F., Lahann J., (2010), Compartmentalization of Gold Nanocrystals in Polymer Microparticles using Electrohydrodynamic Co-Jetting, *Macromol. Rapid Commun.*, **31**, 76-182.

Loo S.C.J., Ooi C.P., Boey F.Y.C., (2005), Influence of electron beam radiation on the hydrolytic degradation behaviour of poly(lactide-co-glycolide) (PLGA). *Biomaterials.*, **26**, 3809-3817.

Lopez-Harrera J.M., Barrero A., Lopez A., Loscertales I.G., Marquez M., (2003), Coaxial jets generated from electrified Taylor cones. Scaling laws. *J. Aerosol. Sci.*, **34**, 535-552.

Loscertales I.G., Barrero A., Guerrero I., Cortijo R., Marquez M., Ganan C.A.M., (2002), Micro/Nano Encapsulation via Electrified Coaxial Liquid Jets. *Science.*, **295**, 1695-1698.

Luan X., Skupin M., Siepmann J., Bodmeier R., (2006), Key parameters affecting the initial release (burst) and encapsulation efficiency of peptide-containing poly (lactide-co-glycolide) microparticles. *Int. J. Pharm.*, **324,** 168-175.

Madan P. L. (1978), Microencapsulation I. Phase Separation or Coacervation. *Drug dev. Ind. Pharm.*, **4**, 95-116.

Madersbacher S., Marberger M., (2003), High-energy shockwaves and extracorporeal highintensity focused ultrasound. *J. Endourol.*, **17**(8), 667–672.

Mainardes R.M, Urban C.C.M., Priscila O.C., Marco V.C., Raul C.E., Maria P.D.G., (2006), Liposomes and Micro/Nanoparticles as Colloidal Carriers for Nasal Drug Delivery. *Curr. Drug Targets.*, **3**(3), 275-285.

Mallapragada S.K., Peppas N.A., Colombo P., (1997), Crystal dissolution-controlled release systems. II. Metronidazole release from semicrystalline poly (vinyl alcohol) systems, *J. Biomed. Mater. Res.*, **36**, 125-130.

Mallarde D., Boutignon F., Moine F., Barre E., David S., Touchet H., Ferruti P., Deghenghi R., (2003), PLGA-PEG microspheres of teverelix: influence of polymer type on microsphere characteristics and on teverelix *in vitro* release. *Int. J. Pharm.*, **261**, 69-80.

Marmottant P., Hilgenfeldt S., (2003), Controlled vesicle deformation and lysis by single oscillating bubbles. *Nature.*, **423**, 153-156.

Mathiowitz E., Jacob J.S., Jong Y.S., Carino G.P., Chickering D.E., Chaturvedi P., Santos C.A., Vijayaraghavan K., Montgomery S., Bassett M., Morrell C., (1997), Biologically erodable microsphere as potential oral-drug delivery system. *Nature.*, **386**, 410-414.

Mei F., Chen D., (2007), Investigation of compound jet electrospray: Particle encapsulation. *Phys. Fluids.*, **19**, 103303-103313.

Mitragotri S, Blankschtein D, Langer R., (1995), Ultrasound-mediated transdermal protein delivery. *Science.*, **269**, 850-853.

Mitragotri S., (2005), Healing sound: the use of ultrasound in drug delivery and other therapeutic applications. *Nat. Rev. Drug. Discov.*, **4**, 255-60.

Mitragotri S., Lahann J., (2009), Physical approaches to biomaterial design. *Nat. Mater.*, **8**, 15-23.

Mitschele J., (1996), Beer-Lambert Law, *J. Chem. Educ.*, **73**(11), 260-261.

Mittal G., Sahana D.K., Bhardwaj V., Ravi Kumar M.N.V., (2007), Estradiol loaded PLGA nanoparticles for oral administration: Effect of polymer molecular weight and copolymer composition on release behavior *in vitro* and *in vivo. J. Control. Release.*, **119**, 77-85.

Miyazaki S., Yokouchi C., Takada M., (1988), External control of drug release: controlled release of insulin from a hydrophilic polymer implant by ultrasound irradiation in diabetic rats, *J. Pharm. Pharmacol.*, **40**, 716-717.

Mizushige K., Kondo I., Ohmori K., Hirao K., Matsuo H., (1999), Enhancement of ultrasound-accelerated thrombolysis by echo contrast agents: dependence on microbubble structure. *Ultrasound in Med. & Biol.*, **25**(9), 1431-1437.

ModiS., Jain J.P., Kumar N., (2005), Synthesis, characterization, and degradation of poly(ester-anhydride) for particulate delivery, *Isr. J. Chem.,* **45**(4),401-409.

Monsky, W.L., Fukumura, D., Gohongi, T., Ancukiewcz, M., Weich, H.A., Torchilin, V. P., Yuan, F., Jain, R. K., (1999), Augmentation of transvascular transport of macromolecules and nanoparticles in tumors using vascular endothelial growth factor. *Cancer Res*., **59**(16), 4129-4135.

Moore C., Promes S.B., (2004), Ultrasound in pregnancy. *Emerg. Med. Clin. North Am.*, **22**, 697-722.

Mora D.J. F., Loscertales I., (1994), The current emitted by highly conduction Taylor cones. *J. Fluid Mech.,* **260**, 155-184.

Morota K., Matsumoto H., Mizukoshi T., Konosu Y., Minagawa M., Tanioka A., Yamagata y., Inoue K., (2004), Poly(ethylene oxide) thin films produced by electrospray deposition: morphology control and additive effects of alcohols on nanostructure. *J. Colloid Interface Sci.*, **279**(2)**,** 484-492.

Murillo M., Gamazo C., Goni M., Irache J., Blanco-Prieto M., (2002), Development of microparticles prepared by spray-drying as a vaccine delivery system against brucellosis. *Int. J. Pharm.*, **242**, 341-344.

Murthy R.S.R., (1997), Biodegradable polymers. *Controlled and Novel Drug Delivery*. CBS Publisher, New Delhi, 27-51.

Musante C.J., Schroeter J.D., Rosati J.A., Crowder T.M., Hickey A.J., Martonen T.B., (2002), Factors affecting the deposition of inhaled porous drug particles. *J. Pharm. Sci*., **91**, 1590-1600.

Nishiyama N., Kataoka K., (2003), Polymeric micelle drug carrier systems: PEG-PAsp(Dox) and second generation of micellar drugs. *Adv. Exp. Med. Biol*., **519**, 155-177.

Nyborg W., (2001), Biological Effects of Ultrasound: Development of Safety Guidelines. Part II:General Review. *Ultrasound Med. Biol.*, **27**, 301-333.

O'Donnell P.B., Mcginity J.W., (1997), Preparation of microspheres by the solvent evaporation technique. *Adv. Drug Deliver. Rev.*, **28**, 25-42.

Ohtsuki C., Aoki Y., Kokubo T., Bando Y., Neo M., Nakamura T., (1995), Transmission electron microscopic observation of glass-ceramic A-W and apatite layer formed on its surface in a simulated body fluid, *J. Ceram. Soc. Japan.*, **1039** (5), 449-454.

Okada H., Toguchi H., (1995), Biodegradable microspheres in drug delivery. *Crit. Rev. Ther. Drug Carrier Syst.,* **12**(1), 1-99.

Okochi H., Nakano M., (2000), Preparation and evaluation of w/o/w type emulsions containing vancomycin. *Adv. Drug Deliv. Rev.*, **45**, 5-26.

Oyane, Kim H.M., Furuya T., Kokubo T., Miyazaki T., Nakamura T., (2003), Preparation and assessment of revised simulated body fluid, *J. Biomed. Mater. Res.*, **65A**, 188-195.

Paik N.J., Cho S.H., Han T.R., (2002), Ultrasound therapy facilitates the recovery of acute pressure-induced conduction block of the median nerve in rabbits. *Muscle Nerve.*, **26**, 356-361.

Paine M.D., Alexander M.S., Stark J.P.W., (2007), Nozzle and liquid effects on the spray modes in nanoelectrospray. *J. Colloid Interface Sci.*, **305**, 111-123.

Pareta R., Edirisinghe M.J., (2006), A novel method for the preparation of biodegradable microspheres for protein drug delivery. *J. R. Soc. Interface.*, **3**, 573-582.

Pareta R., Brindley A., Edirisinghe M.J., Jayasinghe S.N., Luklinska Z.B., (2005), Electrohydrodynamic atomization of protein (bovine serum albumin). *J. Mater. Sci.: Mater. Med.*, **16**, 919-925.

Park T.G., Lee H.Y., Nam Y.S., (1998), A new preparation method for protein loaded poly(,-lactic-co-glycolic acid) microspheres and protein release mechanism study. *J. Control. Release.*, **55**, 181-191.

Pancholi K.P., Farook U., Moaleji R., Stride E., Edirisinghe M., (2007), Novel methods for preparing phospholipid coated microbubbles. *Eur. Biophys. J.*, **37**, 515-520.

Pancholi K.P., Stride E., Edirisinghe M., (2008), Generation of microbubbles for diagnostic and therapeutic applications using a novel device. *J. Drug Target.*, **16**(6), 494-501.

Panyam J., Labhasetwar J., (2003), Biodegradable nanoparticles for drug and gene delivery to cells and tissue. *Adv. Drug Deliv. Rev.*, **55**(3), 329-347.

Pham Q. P., Sharma U., Mikos A. G., (2006), Electrospinning of polymeric nanofibers for tissue engineering applications: A review. *Tissue Eng.*, **12**(5), 1197-1211.

Pilcer G., Vanderbist F., Amighi K., (2009), Preparation and characterization of spray-dried tobramycin powders containing nanoparticles for pulmonary delivery. *Int. J. Pharm.*, **365**(1-2), 162-169.

Pitt C.G., (1990), The controlled parenteral delivery of polypeptides and proteins. *Int. J. Pharm.*, **59**, 173-196.

Pitt W.G., Husseini, G.A., Staples B.J., (2004), Ultrasonic Drug Delivery-A General Review, *Expert Opin. Drug Deliv.*, **1**(1), 37-56.

Pohanish, R.P., Ethyl Acetate. In, Sittig's Handbook of Toxic and Hazardous Chemicals and Carcinogens, Fourth Ed., Vol. 1. Norwich, NY: Noyes Publications, William Andrew Publishing, 2002, 1039-1041.

Poliachik S.L., Chandler W.L., Mourad P.D., Bailey M.R., Bloch S., Cleveland R.O., Kaczkowski P., Keilman G., Porter T., Crum L.A., (1999), Effect of high intensity focused ultrasound on whole blood with and without microbubble contrast agent. *Ultrasound in Med. & Biol.*, **25**, 991-998.

Prausnitz M.R., Mitragotri S., Langer R., (2004), Current status and future potential of transdermal drug delivery. *Nat. Rev. Drug Discov.,* **3**, 115-124.

Pushkar S., Philip A., Pathak K., Pathak D., (2006), Dendrimers: Nanotechnology Derived Novel Polymers in Drug Delivery, *Indian J. Pharm. Educ. Res.*, **40**(3), 153-158.

Raisinghani A., DeMaria A.N., (2002), Physical principles of microbubble ultrasound contrast agents. *Am. J. Cardiol.*, **90**, 3J-7J.

Rasiel A., Sheskin T., Bergelson L., Domb A.J., (2002), Phospholipid Coated Poly(lactide acid) Microspheres for the Delivery of LHRH Analogues. *Polym. Adv. Technol.*, **13**, 127-136.

Ravivarapu H.B., Lee H., DeLuca P.P., (2000), Enhancing initial release of peptide from poly(D,L-lactide-co-glycolide) (PLGA) microspheres by addition of a porosigen and increasing drug load, *Pharm. Dev. Technol.*, **5**, 287-296.

Rayleigh J.W.S., (1882), On the Equilibrium of a Liquid Conducting Masses charged with Electricity. *Philosophical Magazine.*, **14**, 184-186.

Regele J.D., Papac M.J., Rickard M.J.A., Dunn-Rankin D., (2002), Effects of capillary spacing on EHD spraying from an array of cone jets, *J. Aerosol Sci.*, **32**(11), 1471-1479.

Roh K.H., Martin D.C., Lahann J., Triphasic Nanocolloids. (2006), *J. Am. Chem. Soc.*, **128**, 6796-679.

Rooney J.A., (1970), Hemolysis Near an Ultrasonically Pulsating Gas Bubble. *Science.*, **169**, 869-871.

Samarasinghe S.R., Balasubramanian K., Edirisinghe M.J., (2008), Encapsulation of silver particles using co-axial jetting. *J. Mater. Sci. Mater. Elect.*, **19**, 33-38.

Savic R., Luo L., Eisenberg A., Maysinger D., (2003), Micellar nanocontainers distribute to defined cytoplasmic organelles, *Science.*, **300**, 615-618.

Schliecker G., Schmidt C., Fuchs S., Wombacher R., Kissel T., (2003), Hydrolytic degradation of poly(lactide-co-glycolide) films: Effect of oligomers on degradation rate and crystallinity. *Int. J. Pharm.*, **266**, 39-49.

Schmidt W., Roessling G., (2006), Novel manufacturing process of hollow polymer microspheres. *Chem. Eng. Sci.*, **61**, 4973-4981.

Schreier H., Gonzalez-Rothi R.J., Stecenko A.A., (1993), Pulmonary delivery of liposomes. *J. Control. Release.*, **24**, 209-223.

Setterstrom J.A., Tice T.R., Meyers W.E., Vincent J.W., Development of encapsulated antibiotics for topical administration to wounds, in: *Second World Congress on Biomaterials 10th Annual Meeting of the Society for Biomaterials*, Washington, DC, 1984, 4.

Shive M.S., Anderson J.M., (1997), Biodegradation and biocompatibility of PLA and PLGA microspheres. *Adv. Drug Deliv. Rev.*, **28**, 5-24.

Singh J., Roberts M.S., (1989), Transdermal delivery of drugs by iontophoresis: a review. *Drug Des. Deliv.*, **4**(1), 1-12.

Sinha V.R., Trehan A., (2003), Biodegradable microspheres for protein delivery. *J. Control. Release.*, **90**(3), 261-280.

Sinha V.R., Trehan A., (2005), Biodegradable microspheres for parenteral delivery. *Crit. Rev. Thera. Drug.*, **22**(6), 535-602.

Smith D.P.H., (1986), The electrodynamic atomization of liquids. *IEEE Trans. Ind. Appl. IA.*, **22**, 527-535.

Snarski S.R., Dunn P.F., (1991), Experiments characterizing the interaction between two sprays of electrically charged liquid droplets, *Exp. Fluids.*, **11**(4), 268–278.

Song C., Labhasetwar V., Cui X., Underwood T., Levy R.J., (1998), Arterial uptake of biodegradable nanoparticles for in- travascular local drug delivery: results with an acute dog model, *J. Control. Release.*, **54**, 201-211.

Suzuki R., Takizawa T., Negishi Y., Utoguchi N., and Maruyama K., (2007), Effective gene delivery with liposomal bubbles and ultrasound as novel non-viral system. *J. Drug Target.*, **15**, 531-537.

Swain B. P., Pattanayak D. K., (2008), Simulated body fluid (SBF) adsorption onto a-SiC:H thin films deposited by hot wire chemical vapor deposition (HWCVD), *Mater. Letter.*, **62**, 3484-3486.

Tamada J, Langer R., (1990), Erosion mechanism of hydrolytitally degradable polymers. *Proc. Nat. Acad. Sci. USA.*, **90**, 552-556.

Tang K., Gomez A., (1994), On the structure of an electrostatic spray of monodisperse droplets. American Institute of Physics, *Phys. Fluids.*, **6**(7), 2317-2332.

Tang K., Gomez A., (1995), Generation of monodisperse water droplets from electrospray in a corona-assisted cone-jet mode. *J. Coll. Interface Sci.,* **175**, 326-332.

Tang K., Gomez A., (1996), Monodisperse elctrosprys of low electric conductivity liquids in the cone-jet mode. *J. Coll. Interface Sci.*, **184**, 500-511.

Taylor G., (1964), Disintegration of Water Drops in an Electric Field. *Pro. Royal Soc. Series A Mathemat. Phys. Sci.*, **20**, 383-397.

Thompson D.R., Kougoulos E., Jones A.G., Wood-Kaczmar M.W., (2005), Solute concentration measurement of an important organic compound using ATR-UV spectroscopy. *J. Cryst. Growth*, **27**(1-2), 230-236.

Uhrich K.E., Cannizzaro S.M., Langer R.S., Shakesheff K.M. (1999), Polymeric systems for controlled drug release. *Chem. Rev.*, **99**, 3181-3198.

Unger E.C., Hersh E., Vannan M., Matsunaga T.O., McCreery T., (2001), Local drug and gene delivery through microbubbles. *Prog. Cardiovasc. Dis.*, **44**, 45-54.

US Pat. 2,712,507, Pressure sensitive record material, BK Green (1955).

US Pat. 2,800,457, Microscopic capsules containing oil. BK. Green and L. Schleicher (1957).

Valles S.L., Dolz-Gaiton P., Gambini J., Borras C., Lloret A., Pallardo F.V., Viña J., (2010), Estradiol or genistein prevent Alzheimer's disease-associated inflammation correlating with an increase PPAR gamma expression in cultured astrocytes. *Brain Res.*, **1312**, 138-144.

Valo H., Peltonen L., Vehvilalnen S., Karjalainen M., Kostiainen R., Laaksonen T., Hirvonen J., (2009), Electrospray Encapsulation of Hydrophilic and Hydrophobic Drugs in Poly (L-lactic acid) Nanoparticles. *Small.*, **5**, 1791-1798.

Vert M, Feijen J, Albertson A, Scott G, Chiellini E. (1992), Degradable Polymers and Plastics. *Melksham Redwood Press Ltd.*, 73-92.

Vonarbourg A., Passirani C., Desigaux L., Allard E., Patrick Saulniera O. L., Benoit J.P., Pitard B., (2009), The encapsulation of DNA molecules within biomimetic lipid nanocapsules. *Biomaterials.*, **30**, 3197-3204.

Wang J., Wang B. M., Schwendeman S. P., (2002), Characterization of the initial burst release of a model peptide from poly(D,L-lactide-co-glycolide) microspheres . *J. Control. Release.*, **82**, 289-307.

Warden SJ., (2003), A new direction for ultrasound therapy in sports medicine. *Sports Med.*, **33**, 95-107.

Weber C., (1931), On the breakdown of a fluid jet. *J. Mech.Appl. Math.*, **11**, 136-159.

Wheatley M.A., Chang M., Park E., Langer R., (1991), Coated alginate microspheres: factors influencing the controlled delivery of macromolecules, *J. Appl. Polym. Sci.*, **43,** 2123-2125.

Witschi C., Doelker E., (1998), Influence of the microencapsulation method and peptide loading on poly(lactic acid) and poly(lactic-co-glycolic acid) degradation during in vitro testing. *J. Control. Release.*, **51**, 327-341.

Wu Y., Yang W., Wang C., Hu J., Fu S., (2005), Chitosan nanoparticles as a novel delivery system for ammonium glycyrrhizinate, *Int. J. Pharm.*, **295**(1-2), 235-245.

Wu J.R., Nyborg W.L., (2008), Ultrasound cavitation bubbles and their interaction with cells. *Adv. Drug Deliv. Rev.*, **60,** 1103-1116.

Wu Y., Clark R.L., (2007), Controllable porous polymer particles generated by electrospraying. *J. Colloid Interface Sci.*, **310**, 529-535.

Wu Y., Mackay J.A., Mcdaniel J.R., Chilkoti A., Clark R.L., (2009a), Fabrication of elastin-like polypeptide nanoparticles for drug delivery by electrospraying. *Biomacromolecules.*, **10**,19-24.

Wu Y., Yu B., Jackson A., Zha W., Lee L.J., Wyslouzil B.E., (2009b), Coaxial Electrohydrodynamic Spraying: A Novel One-Step Technique To Prepare Oligodeoxynucleotide Encapsulated Lipoplex Nanoparticles. *Mol. Pharm.*, **6**, 1371-1379.

Xie J., Marijnissen J.C.M., Wang C.H., (2006a), Microparticles developed by electrohydrodynamic atomization for the local delivery of anticancer drug to treat C6 glioma in vitro. *Biomaterials.,* **27**, 3321-3332.

Xie J., Lim L.K., Phua Y.Y., Hua J.S., Wang C.H., (2006b), Electrohydrodynamic atomization for biodegradable polymeric particle production. *J. Colloid Interface Sci.*, **302**, 103-112.

Xie J., Ng W.J, Lee L.Y., Wang C., (2008), Encapsulation of protein drugs in biodegradable microparticles by co-axial electrospray. *J. Colloid Interface Sci.*, **317**, 469-476.

Xu Y., Skotak M., Hanna M., (2006), Electrospray encapsulation of water-soluble protein with polylactide. I. Effects of formulations and process on morphology and particle size. *J. Microencapsul.*, **23**, 69-78.

Xu Y., Hanna M.A., (2007), Electrosprayed bovine serum albumin-loaded tripolyphosphate cross-linked chitosan capsules: synthesis and characterization. *J. Microencapsul.*, **24**, 143-151.

Yamaguchi Y., Takenaga M., Kitagawa A., Ogawa Y., Mizushima Y., Igarashi R., (2002), Insulin-loaded biodegradable PLGA microcapsules: initial burst release controlled by hydrophilic additives. *J. Control Release*, **81**, 235-249.

Yamamoto M., Ikada Y., Tabata Y., (2001), Controlled release of growth factors based on biodegradation of gelatin hydrogel, *J. Biomater. Sci., Polym. Ed*., **12,** 77-88.

Yang Y.Y., Chung T.S., Ng N.P., (2001), Morphology drug distribution and in vitro release profiles of biodegradable polymeric microspheres containing protein fabricated by double-emulsion solvent extraction/evaporation method. *Biomaterials.*, **22**(3), 231-241.

Yao C.H., Liu B.S., Hsu S.H., Chen Y.S., Tsai C.C., (2004), Biocompatibility and biodegradation of a bone composite containing tricalcium phosphate and genipin crosslinked gelatin, *J. Biomed. Mater. Res*., **69A,** 709-717.

Yao J., Lim L.K., Xie J., Hua J., Wang C.H., (2008), Characterization of electrospraying process for polymeric particle fabrication. *J. Aerosol Sci.*, **39**, 987-1002.

Young S., Wong M., Tabata Y., Mikos A.G., (2005), Gelatin as a delivery vehicle for the controlled release of bioactive molecules, *J. Control. Release.*, **109**, 256-274.

Yoshida M., Roh K.H., Lahann J., (2007), Short-term biocompatibility of biphasic nanocolloids with potential use as anisotropic imaging probes. *Biomaterials.*, **28**, 2446-2456.

Yoshii H., Soottitantawat A., Liu X.D., Atarashi T., Furuta T., Aishima S., Ohgawara M., Linko P., (2001), Flavor release from spray-dried maltodextrin/gum arabic or soy matrices as a function of storage relative humidity, *Int. J. Food Sci. Technol.*, **2**, 55-61.

Zbicinski I., Smucerowicz I., Strumillo C., Crowe C., (2000), Application Of Pulse Combustion Technology In Spray Drying Process, *Braz. J. Chem. Eng*., **17**, 4-7.

Zhang H., Zhang J., Streisand J.B., (2002), Oral mucosal drug delivery - Clinical pharmacokinetics and therapeutic applications. *Clin. Pharmacokinet.*, **41**(9), 661-680.

Zhang H.B., Jayasinghe S.N., Edirisinghe M.J., (2006), Electrically-forced Microthreading of Highly Viscous Dielectric Liquids. *J. Electrostatics.*, **64**(6), 355-360.

Zhang H., Lu Y., Zhang G., Gao S., Sun D., Zhong Y., (2008), Bupivacaine-loaded biodegradable poly(lactic-co-glycolic) acid microspheres I. Optimization of the drug incorporation into the polymer matrix and modelling of drug release. *Int. J. Pharm.*, **351**, 244-249.

Zhang J. X., Chen D., Wang S. J., Zhu K. J., (2005), Optimizing double emulsion process to decrease the burst release of protein from biodegradable polymer microspheres. J. *Microencapsul.*, **22**(4), 413-422.

Zhu G.Z., Mallery S.R., Schwendeman S.P., (2000), Stabilization of proteins encapsulated in injectable poly (lactide-co-glycolide). *Nat. Biotechnol.*, **18**, 152-157.

Zeleny J., (1917), Instability of electrified liquid surfaces. *Phys. Rev.*, **10**(1), 1-7.

Zimlich W.C., Ding J.Y., Busick D.R., Moutvic R.R., Placke M.E., Hirst P.H., Pitcairn G. R., Malik S., Newman S.P., Macintyre F., Miller P.R., Shepherd M.T., Lukas T.M., (2000), The development of a novel electrohydrodynamic pulmonary drug delivery device. In: *Proceedings of Respir. Drug Deliv VII*, 241-246.